AD NUMBER

AD867045

NEW LIMITATION CHANGE

TO

Approved for public release, distribution unlimited

FROM

Distribution authorized to U.S. Gov't. agencies and their contractors; Critical Technology; FEB 1970. Other requests shall be referred to Air Force Propulsion Laboratory, Wright-Patterson AFB, OH 45433.

AUTHORITY

AFAPL ltr., 12 Apr 1972

REPRODUCTION QUALITY NOTICE

This document is the best quality available. The copy furnished to DTIC contained pages that may have the following quality problems:

- Pages smaller or larger than normal.
- Pages with background color or light colored printing.
- Pages with small type or poor printing; and or
- Pages with continuous tone material or color photographs.

Due to various output media available these conditions may or may not cause poor legibility in the microfiche or hardcopy output you receive.

☐ If this block is checked, the copy furnished to DTIC contained pages with color printing, that when reproduced in Black and White, may change detail of the original copy.

AFAPL-TR-67-114
Part III, Volume I

VAPORIZING AND ENDOTHERMIC FUELS FOR ADVANCED ENGINE APPLICATION

Part III. Studies of Thermal and Catalytic Reactions, Thermal Stabilities, and Combustion Properties of Hydrocarbon Fuels

A.C. Nixon, G.H. Ackerman, L.E. Faith, H.T. Henderson, A.W. Ritchie, L.B. Ryland, T.M. Shryne

Shell Development Company,
A Division of Shell Oil Company

TECHNICAL REPORT AFAPL-TR-67-114, Part III, Volume I

February 1970

Air Force Aero Propulsion Laboratory
Air Force Systems Command
Wright-Patterson Air Force Base, Ohio

PAGES _____

ARE

MISSING

IN

ORIGINAL

DOCUMENT

FOREWORD

This report was prepared by Shell Development Company, Emeryville, California, under U.S. Air Force Contract No. AF 33(615)-3789. The contract was initiated under Project No. 3048, Task No. 304801. The work was administered under the direction of the Aero Propulsion Laboratory, Mr. H. R. Lander, Project Engineer, AFPL.

This report covers work for June 1968 to September 1969.

A. C. Nixon was principal investigator and project supervisor for Shell Development Company. The professional staff participating in the investigation was comprised of: G. H. Ackerman, L. E. Faith, H. T. Henderson, A. W. Ritchie, L. B. Ryland, and T. M. Shryne.

This report was submitted by the authors on November 7, 1969.

This technical report has been reviewed and is approved.

Arthur V. Churchill

ARTHUR V. CHURCHILL, Chief Fuel Branch
Fuel, Lubrication and Hazards Division

ABSTRACT

The investigation of the feasibility of utilizing the endothermic and enthalpic capacity of hydrocarbons to fuel and cool high speed aircraft is continued. [illegible] survey, the literature and present performance of interest in this area of application. Calculation of the cooling requirement for a Mach 8 supersonic combustion ramjet engine under standard conditions indicate that this would be about 1900 Btu per pound of fuel.

The possibility of utilizing the dehydrogenation of bridged-ring naphthenes for providing additional heat sink has been studied but no suitable catalysts have been found for this reaction. Studies on methods accelerating the thermal cracking of paraffins by means of additives has shown some promise. In the dehydrogenation of naphthenes over supported platinum catalysts the stability of the catalyst was found to be inversely proportional to the pore size of the support, and is also affected by the composition of the support. Efforts to induce the dehydrogenation of methylcyclohexane using dispersed catalysts has met with some success. Also quite marked variations in the rate and type of reaction have been observed depending on the type and source of the metal used for the reactor tube.

A large number of additional granular catalysts have been tested for their activity in dehydrogenation of MCH. Although about one third of these are superior in activity and/or stability to our standard laboratory catalysts none of outstanding activity has been discovered. The attractive concept of emplacing a catalyst on a reactor wall has continued to be studied with considerable success. Calculations showed that diffusion limitations could be avoided if a wall coating thickness of no more than 3 mils was maintained. Testing of wall catalyst of about this dimension in the FSSTR resulted in satisfactory operation with high utilization of the catalyst and no pressure drop. Also for the first time in the FSSTR an improved catalyst from the catalyst development program has been tested and found indeed to be superior to the standard R-8 catalyst. Decalin has also been dehydrogenated over the same catalyst. Heat transfer studies have been carried out with MCH, Decalin, SHELLDYNE-H,® and JP-7 fuel in small diameter test sections under heat fluxes up to 8 x 10^6 Btu per hour per square foot. Studies on the effect of high temperatures of the thermal stability of various fuels of interest have been continued with emphasis on methods of measuring the deposit left on tube surfaces. Combustion and electron back-scattering are the methods of present choice and an instrument based on a latter principle has been designed. Construction of mathematical models to represent the various portions of an endothermic fuel system has been continued with the development of heat transfer correlations and a model for the reaction kinetics of Decalin dehydrogenation. Physical properties for Decalin and JP-5 are included. Calculation of the rates of oxidation of normal octane and SHELLDYNE-H from shock tube studies indicates similar rates of reaction and a similar low response to the effect of temperature.

TABLE OF CONTENTS

TABLE OF CONTENTS (Contd)

TABLE OF CONTENTS (Contd)

TABLE OF CONTENTS (Contd)

TABLE OF CONTENTS (Cont'd)

ILLUSTRATIONS

ILLUSTRATIONS (Cont'd)

ILLUSTRATIONS (Contd)

ILLUSTRATIONS (Contd)

ILLUSTRATIONS (Contd)

TABLES

TABLES (Contd)

TABLES (Cont'd)

TABLES (Cont'd)

TABLES (Contd)

TABLES (Contd)

TABLES (Contd)

TABLES (Contd)

VAPORIZING AND ENDOTHERMIC FUELS FOR ADVANCED ENGINE APPLICATION

Introduction

As airbreathing-engine-propelled vehicle speeds increase thermal problems multiply due to the effect of stagnation temperature. While total cooling needs increase, the most critical regions are the leading edges and the engines. Although thermal effects can be somewhat accommodated by improved materials and passive cooling, sustained hypersonic flight in the atmosphere requires a substantial heat sink. Compared to a mechanical refrigeration system or a non-combustible coolant the fuel is the best source of cooling.

The objective of this study is to provide the information necessary for specifying fuels which will be capable of providing cooling and propulsion for engines powering aircraft in the speed range above Mach 3. Such a fuel will provide cooling by giving up its latent and sensible heat and by undergoing endothermic reactions before it is fed into the engine. Practically, this could be in the temperature range up to about 1400°F. In order for the fuel to function in this manner, it must have excellent thermal stability up to the temperature at which reaction occurs and also it and its reaction products must be stable to any post-reaction heating avoid fouling problems.

Fuel must react cleanly and rapidly under the temperature and pressure conditions prevailing in the heat exchanger-reactor, must provide sufficient heat sink to absorb the amount of heat required to preserve the integrity of the engine or other parts being cooled and finally it and its reaction products must be suitable fuels for providing propulsion for the aircraft.

This report details results obtained over the past 15 months in a continuing effort of research in this area. Results of previous work are given under the annual quarterly reports under the appropriate contract.[a] In order to allow precise definition of fuel required for such service, its behavior in various parts of fuel combustion system has to be determined. In order to achieve this we have, in general, examined various problems that might arise under application conditions. We have studied thermal stability problems that could originate in fuel tanks and various metering devices and fuel lines, deposition or coking problems that could affect the efficiency of the heat exchanger-reactor devices and catalysts or plug fuel nozzles, and have determined combustion parameters which will be useful in the specification, design or operation of the combustion chambers. In order to provide specific interpolation or extrapolation of experimental data or to develop generalized correlations amongst various fuels, we have been endeavoring to assemble all pertinent physical and thermochemical data for the fuels studied and utilize available proprietary or literature methods of correlation.

Fuels have been selected on the basis of their general suitability as fuels and particularly, on the basis of the amount of heat sink that they provide. Both catalysts and fuels in specific combinations have been tested in laboratory equipment to determine reaction rates and activities and

a) See References.

stabilities of catalysts. Following the obtaining of this basic data, in order to subject the heat sink system to conditions more nearly approaching those that prevail under application conditions, the final step in the evaluation of the reacting systems involves the use of the fuel system simulation test reactor (FSSTR) which is a heat compensated flow calorimeter, instrumented to allow the determination of heat flux, heat transfer coefficients and pressure drops, as well as degree of reaction. Information generated in this way is utilized in the construction of a mathematical model of the system which can be utilized by engine designers and airframe manufacturers for systems designs.

Studies done to date indicate that the best chance of success for application of the heat sink endothermic reaction principle will be via the catalytic dehydrogenation of naphthene hydrocarbons. The most extensively studied system, and the only one that has been carried through the FSSTR stage of experimentation completely, is the methylcyclohexane - Pt/Al_2O_3 combination. Good representation of this system by the mathematical model has been achieved. The necessity for more active and more stable catalysts has been indicated by experimentation in this unit. The importance of restricting the oxygen content of the fuel under severe conditions has also been demonstrated. Combustion studies have indicated that no unique limitations on either subsonic or supersonic combustion burning should exist in a practical system.

In early work a limited number of readily available catalysts were tested with a variety of possible fuel materials. Reactions of interest which have been studied include dehydrogenation, dehydrocyclozation and depolymerisation. We found that reasonably promising catalysts existed for the first reaction but no existing catalysts were sufficiently active or stable to allow utilization of the other two. Based on the amount of heat sink available and existing kinetic considerations we have emphasized mainly the development of better catalysts for the dehydrogenation reaction, since high heat fluxes demand high fuel flows and short contact times. Accordingly we have been conducting an extensive catalyst development program aimed at producing more active, more stable and cheaper catalysts. This involves a small scale preparation of a wide variety of catalysts in which catalytic elements (e.g., transition metals) are deposited on a variety of substrates, such as alumina, which can be modified by the introduction of ancillary elements. Such catalysts are always tested under standardized conditions in a small scale laboratory unit (the micro catalyst test reactor, MICTR) for preliminary screening. The best ones are then subjected to more extensive tests in larger laboratory (bench scale) equipment. In order to minimize pressure drop and the possibility of coking we have been studying the concept of applying the catalyst either as a thin film on the wall of tubes or as soluble or dispersed integral catalysts with the fuel which will be consumed with the fuel in the engine.

On the basis of work already done on combustion problems with hydrocarbon systems and because of the possibility of the application of higher molecular weight fuels, more work must be done on the supersonic combustion aspects of endothermic fuels and reaction products. On this basis we have recently modified our shock tube equipment to allow us to operate at higher temperatures and pressures.

In order to evaluate, in a short length of time, the behavior of an endothermic fuel under conditions simulating those of probable actual use, a device was built for measuring the thermal stability and plugging tendencies of fuels in such fuel-catalysts systems under standardized conditions. This device, called the catalyst and fuel system test reactor (CAFSTR), has performed, operationally, very satisfactorily but a major problem is the evaluation of the degree of fouling of the heating tubes. This is similar to the problem encountered with the Erdco coker but is more severe in this case because of the high temperatures involved and the fact that the high temperature alloys used change color on heating. We originally intended to measure the change in heat transfer but this proved to be unreliable at low deposit levels. More recent studies have been directed towards devising a method of evaluating the amount of deposit on the tube. Presently we favor either removing the deposit quantitatively by combustion or measuring the thickness by beta ray back scattering, which seem to give comparable results.

Studies have also been undertaken to support contractors working on the development of missiles which will utilize enthalpic fuel cooling. These involve developing physical and thermochemical properties for fuels of interest as well as studying the behavior of such fuels in the FSSTR at heat fluxes up to 8×10^6 Btu/hr/sq ft in a variety of tube sizes ranging down to an internal diameter of 0.026 in. This involves studies with conventional advanced jet fuels as well as the high density fuel, SHELLDYNE-H.

More recently renewed interest has developed in the greater utilization of fuel cooling for improving the thermal efficiency of turbine engines by increasing cycle temperatures through fuel cooling (either, direct or indirect) of combustors and turbine blades. This system can be useful even for engines for subsonic aircraft. We have been cooperating with such efforts by supplying information and opinions regarding the interaction of the fuel with the system.

Some idea of the extent of our interaction with other contractors in the general area of advanced fuels and propulsion systems is indicated in Figure 1.

Summary

A number of papers have been noted which are of interest in connection with the general problem. They involve shock relaxation in a particle gas mixture with mass transfer between phases, a study of liquid jet penetration in a hypersonic stream, ignition delay in diffusive supersonic combustion, optimum body geometries of minimum heat transfer at hypersonic speeds, an equation for stagnation point radiative heat transfer, design of a leading edge for a hypersonic inlet, and consideration of turbine cooling systems. These are reviewed and commented upon briefly. In addition, we have done a straight forward calculation on the amount of heat sink required by Mach 8 supersonic combustion ramjet engine. For the rather simplified assumptions that were made, the heat sink comes out almost equal to that which could be provided by the complete dehydrogenation and heating of MCH to about 1200°F, namely 1900 Btu/lb fuel.

Laboratory studies of candidate fuels and some catalyst systems were continued. In order to extend the scope of the laboratory data on

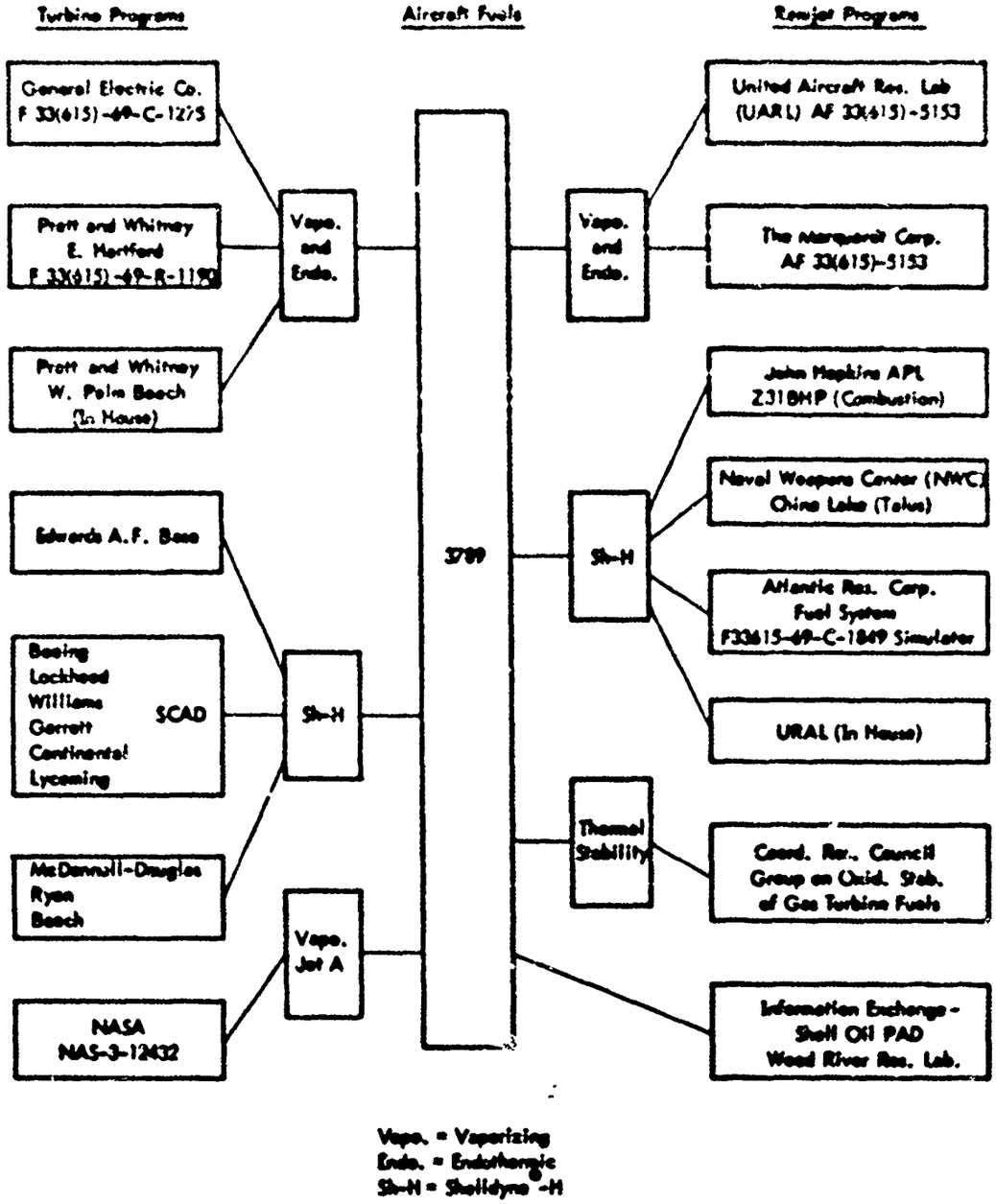

Vapo. = Vaporizing
Endo. = Endothermic
Sh-H = Shelldyne -H

Figure 1. INTERACTION BETWEEN SHELL DEVELOPMENT CONTRACT AF 33(615)-3789 AND OTHER ACTIVITIES

thermal reaction for MCH and Decalin the pressure rating of the bench scale system was increased to 1000 psi and thermal reaction studies were conducted under these conditions at temperatures to 1292°F. Compared to information obtained at lower pressures, it appears that the first order rate constants were indifferent to pressure indicating a true first order kinetic scheme. Gas and liquid product composition were not effected as much with Decalin as MCH. Coke formation was higher in both cases with higher pressure but this may be an effect of increased contact time. Generally, the increased pressure gave more hydrogen, CH_4 and saturated hydrocarbons.

The effect of various additives, capable of producing free radicals, on the rate of thermal cracking of n-dodecane has been investigated to determine if the rate and specificity of this reaction could be enhanced enough to make it useful for endothermic cooling. Some success has been achieved in that the rate has been increased sixfold at ca 1000°F, although the effect decreases at higher temperatures. Product distribution is about the same as without catalyst. This approach looks promising and the study will be continued.

We have recently constructed a pulse reactor for investigating the reactivity of various fuel/catalyst combinations under this mode of reaction. The pulse reactor has the advantage of requiring only about 1 microliter of fuel per experiment with the products of the reaction being led directly to a gas chromatographic analyzer. This allows rapid completion of the experiment. Many of the reaction studies reported were carried out in the pulse reactor. Six catalysts developed under our catalytic development program and indicated to be superior to the reference catalyst were examined in the pulse reactor using MCH as the test fuel. Two characteristics were noted with this series of experiments. First, all the catalysts showed a much enhanced reactivity in the pulse reactor compared to their behavior in the standard bench scale equipment by a factor of about 200 fold. This is probably due to the absence of diffusion limitations because of the small volume ratio of the charge to catalyst pore volume and to the very small temperature drop resulting from reaction. Second, the catalysts did not display as great differences in behavior under pulse reactor conditions and, third, more hydrocracking leading to benzene was evident. Also, deactivation was more prominent when helium carrier gas was used. Similar results were observed when Decalin was tested in the pulse reactor, although some differences in detail exist for the thermal reaction between the pulse and bench scale reactors, probably due to differences in the effect of contact time in the two types of equipment. Dimethanoldecalin, a possible high density fuel component, which is capable of undergoing catalytic endothermic dehydrogenation, was also tested at both the thermal and catalytic dehydrogenation conditions in the pulse reactor. Thermally, it reacted more slowly than DHN but catalytically it did not appear to give a clear dehydrogenation reaction. Considerable cracking occurred accompanied by catalyst deactivation and the total conversion was less than 1/3 that displayed by DHN. This suggests that this strained type of molecule, which contains cyclopentane rings in its structure, behaves on dehydrogenation somewhat like cyclopentane which is very prone to dehydrogenate to coke as well as other side reactions. In experiments with bicycloheptane in the pulse reactor, it appeared that the reaction tube was catalyzing the reaction. This was investigated more extensively using Decalin as the feed material. Comparison of different tubes from different manufacturers of 304 stainless steel and one tube of 316 stainless steel from

a still different manufacturer indicated that they all apparently catalyzed the reaction to different degrees and in different ways. The 316 stainless steel appeared to act as a rather poor dehydrogenation catalyst.

Experiments with BCH indicated that it was also less reactive both thermally and catalytically than Decalin. It was quite similar in its reactions to dimethanoldecalin. Catalytic reaction even in the presence of catalyst seem to be mainly in the direction of thermal decomposition. The rate of catalyst deactivation was quite high. It appears that for these bridged ring compounds the present platinum on alumina catalysts we are using are not effective. Experiments on the use of integral catalysts with MCH have also been continued in the pulse reactor. Positive indications of catalysis have been observed although none of the catalysts has been as active or as selective as the Pt/Al_2O_3 catalyst in either the bed or wall form. At 1022°F the most active material gave 32% conversion and the most selective gave 80% selectivity for aromatics. Generally, conversions were less than 10% and selectivities were 15 to 30%. Indications are that the structure of the additive molecule had a considerable affect on the activity of the material as a catalyst.

The effort to produce improved granular catalysts has continued. Up to date 827 different catalysts have been obtained or prepared and most of these have been tested for MCH dehydrogenation. We have finally succeeded in preparing a non-platinum containing catalyst with properties practically equivalent to the reference catalyst, by improving the performance of a previously prepared promising catalyst, which however had poor temperature and conversion stability, by pretreating the support before inpregnation. Several platinum containing catalysts have been improved in performance by the addition of non-reducible oxides in low concentration to the support. Five platinum catalysts on a specific support have been improved in performance over that of the reference catalyst by ion exchange of selected elements. About 35% of all catalysts prepared have had greater activity than the reference catalyst. However, in no case was the improvement in activity spectacular. We found it possible to promote an inactive metal on alumina catalyst by the addition of other metals, in all cases to a greater extent that could have been achieved with the added metal separately. The effect of emplacing the metal in the form of a chelate did not offer any advantages over using the older metalizing salt solution and in fact had a tendency to promote cracking of toluene to benzene.

The effect of the catalyst pore size on catalyst stability for the dehydrogenation of MCH was determined. We had previously shown that in the dehydrogenation of Decalin over the same group of Pt/Al_2O_3 catalysts, the stability was an inverse relation of the average pore diameter. Similar relationship was found for MCH except that this system was more tolerant to reduced pressure. Similar rates of poisoning occurred at 1 atm compared to 10 atm for Decalin. This phenomenon has previously been explained on the basis of the variation of hydrogen partial pressure within the pores with the small pores favoring higher partial pressures and thus lower rates of poisoning. The same explanation seems to hold in this case. The one exception to the correlation seems to be explicable either on the basis of partial platinization or on a higher than first order correlation with pore diameter.

Efforts to develop a satisfactory wall catalyst in order to minimize pressure drop have continued with encouraging indications of success. Calculations indicate that such a system should not be heat transfer limited provided fluid flow through the system is in a highly turbulent condition. Diffusion limitation can be avoided by keeping the thickness of catalyst layer below about 5 mils. Effort in the laboratory has been directed mainly to improving adhesion to stainless steel surfaces. Carbonizing an epoxy coating or decomposing a metal salt did not provide a good base for a wall catalyst but one undercoating material was found which promoted good adherence of the catalyst to stainless steel. Pretreatment with hot nitric or hydrochloric acid did not improve adherence although sand blasting did.

Two 1/8" dia x 2' long tubes coated with wall catalysts containing a Pt/Al_2O_3 catalyst have been examined in the FSSTR with generally encouraging results. In the first series of experiments, in which no power was applied to the catalyst section but the feed was preheated to as high as 1000°, cracking as well as dehydrogenation occurred. In the second series with a different catalyst, no cracking occurred either when no power was applied to the catalyst section or when it was. At the highest power level up to 36% conversion to toluene occurred at an LHSV of 8,600 with no significant pressure drop. However, on increasing the power to the section, some deactivation of the catalyst occurred which reduced the efficiency of the catalyst on returning to lower power inputs. However, during the period of satisfactory operation, the efficiency of the catalyst in terms of weight of toluene produced per unit weight of platinum per hour was about 4 times that experienced in a 2' long packed bed type reactor.

Investigation of the cooling capacity of various possible missile fuels under non-reactive conditions was continued using the miniature tubes in the FSSTR unit. The fuels being studied for this application are MCH, Decalin, SHELLDYNE-H, and F-71 (JP-7). These are being studied in the first instance under conditions where tube burn out or coke formation is unlikely, that is, relatively low fluid temperatures. Heat transfer to Decalin and F-71 have been studied at heat fluxes up to 8×10^6 Btu/hr/sq ft and with SHELLDYNE-H at a heat flux up to 4×10^6 Btu/hr/sq ft. Correlative studies have also been carried out on the information obtained from this unit at values of heat fluxes up to 6×10^6 Btu/hr/sq ft. Good correlation was obtained using MCH as fuel with the equation $Nu = 0.000595\ Re^{1.091} \times Pr^{0.786}$. Much better correlation was obtained with this equation than with Dittus-Boelter or the Sieder-Tate equations. The applicability of this particular correlation for other fuels in the study and under more severe temperature conditions will be determined in the future.

One of the best catalysts for MCH for the development program (Shell 113) has been run in the FSSTR with both MCH and Decalin as feeds. With MCH in a 2' reactor at LHSV = 1550 in comparison with R-8 catalyst, excellent results were obtained with 3.5% greater conversion at 30°F lower exit temperature. Some deactivation occurred at the highest heat flux but the catalyst could be regenerated by H_2 treatment. The Decalin runs in the 10' reactor at 118 LHSV were the first attempted with this feed in the FSSTR and no problems are encountered. Reactivity with Decalin was comparable to that with MCH although deactivation occurred more rapidly at the highest heat flux, as would be predicted from bench scale results.

Investigations into the thermal stability of fuels of interest were continued. Statistical treatment of SD Coker data for Decalin, SHELLDYNE and SHELLDYNE-H has been applied and correlative equations have been derived expressing the maximum code and total code rating in terms of temperature. In general the equations represent the experimental values to within one number for maximum code ratings. Pressure over the range 150-600 psig had no significant effect on coker ratings. It was found also that titanium as a coker tube material seemed to promote a heavier deposit than did aluminum. However, this evaluation suffers from the subjective nature of the rating method.

A brief study has been conducted in the SD Recycle Coker with a thermally stable fuel to determine the trade off aspects of time and temperature on thermal stability in this coker. Time was varied from 1-6 hours, temperatures from 600-675° and the pressure was held constant. The data obtained was treated by regression analysis and equations relating the maximum tube and total tube rating to time and temperature were developed. Coker ratings increased with both time and temperature but an interaction effect was evident. Results indicate that it would be possible (with this fuel) to reduce the test time from 5 to 2 hours by increasing the temperature by about 20°. A short study was also made on the effect of different polishing agents on the results obtained in this coker. Using Decalin as a test fluid, several different polishing agents were used in the preparation of the tubes with a small but measurable effect on maximum code rating but a rather greater effect on total rating. With the specification (A-1) polish, the effect of achieving a 0.5 rather than 0 fresh tube rating had no significant effect in the case of Decalin, but had a considerable effect in the case of SHELLDYNE-H. Thermal stability values have also been determined in the SD Coker for dimethanodecalin and RJ-4 fuel. Estimated break points for these fuels are respectively 575 and 625°F.

In the determination of thermal stability in the SD Coker, a number of different solvents have been used in order to ensure clean liners before beginning the next run. Since the possibility existed that some of the solvent could be left in the system accidentally, the effect of 1% of a number of ordinary solvents has been checked using Decalin as a substrate. Of the dozen or so checked, dimethylsulfoxide, methylene dichloride and perchloroethylene were found to have a markedly adverse effect on the measured thermal stability. A previous result which indicated that a high surface area of iron in contact with Decalin could have a negative effect on the thermal stability of the Decalin, has been disproved by subsequent experimentation. Rechecking the results with copper, however, confirmed the susceptibility of Decalin to this contaminating surface.

Investigation of better methods of determining the thickness or amount of deposit found on a surface by a heated fuel has been continued and a comparison of different methods is given. On the basis of such a comparison a "bread-board" model of a β ray backscattering device was assembled and the deposits on a number of Alcor JFTOT tubes were compared with visual ratings and combustion determined values. Generally, good agreement was obtained between the combustion and β ray backscattering results but in some instances the visual ratings deviated markedly. As a result, a prototype model of a β ray backscattering device has been designed and authorization for construction obtained.

We reported previously that a shipment of Decalin from the fuel bank (RAF-bbl-oC) had very poor thermal stability which could be improved by a silica gel treatment. The brown-black adsorbate was removed from the silica gel by acetone elution and was separated into two phases - a liquid and a crystalline phase. The separated phases had little effect on thermal stability when added back to the purified Decalin separately but when added in combination they do have a markedly deleterious effect. No reason for this behavior has been adduced as yet. Additions and modifications to our equipment for determining thermal stability are described in this report. The results of electron microscope examination of a filter from a thermal stability run with SKELLYTHE at 625°F where extensive plugging of the filter occurred show that the material on the filter in the main resembles chunks of resin which are probably somewhat plastic at high temperature.

The physical properties calculation was expanded to permit simulation of the properties of the mixtures of the two Decalin isomers. The calculation is consistent with and incorporates previous methods for determining the properties of the pure isomers. The results are given in the Appendix. The gas phase properties were generally estimated by pseudo-critical methods and liquid phase properties generally determined by mol fraction averaging of the pure component properties. Actual methods used are described in the body of the report.

Although the two dimensional mathmodel developed for representing the dehydrogenation of MCH over Pt/Al_2O_3 catalyst in a cylindrical packed bed reactor has performed excellently well, we have had difficulties extending the same type of treatment to the Decalin dehydrogenation system. This is thought to be previously due to the far larger number of reactions involved. Our attempts to do this and a discussion of the development of a simpler but probably adequate first order model are included in the report.

Considerations Affecting Applications

Literature

Grenleski and Billig[1]) have recently reported on the engineering problems associated with the design of a water cooled tubular nickel leading edge for a hypersonic inlet. Although water was used as the coolant in this case, it appears likely that their results could be duplicated by use of the fuel as coolant. Design analysis was intended to apply to conditions of Mach 6.5, total temperature 3400°F, total pressure 450 psi. It appears that the fabrication techniques for forming the leading edge and the method of introducing cooling could be used in a fuel cooling application. The maximum heat flux studied was 2×10^6 Btu/hr/sq ft. It is particularly encouraging that conventional correlative methods yielded satisfactory design parameters. Heat transfer values were calculated by means of the Dectra and Hidalgo[2]) correlation and pressure drop with the Darcy equation.[3])

An interesting study appeared recently on the "Considerations of Turbine Cooling Systems for Mach 3 Flight" by Francis S. Stepka.[4]) The study presents a method for determining the approximate average midspan metal temperatures and cooling flow requirements of turbine air foils cooled by

1) See References.

compressor exit bleed air. The indication is that reduction of the temperature of the cooling air by means of heat exchange with the fuel is the best method for reducing air foil metal temperatures or cooling flow requirements. The author considers the use of jet A fuel and liquid methane. Even cursory examination of the curves presented in the paper indicates that substantially enhanced benefits could be obtained by using reactive cooling such as dehydrogenation of MCH in a heat exchanger-reactor. We intend to use the author's method to make some approximate comparisons for this system.

A number of papers have appeared recently which are of interest in connection with the overall problem of containment of heat in aircraft at hypersonic speeds. One is by Y. Aihara,[5] on the "Optimum Body Geometries of Minimum Heat Transfer at Hypersonic Speeds". This is a theoretical analysis of a minimum heat transfer body at hypersonic speeds, i.e., a body for which the total laminar convective heat transfer rate is minimized. The author derives equations by which the minimum heat transfer can be calculated as a function of flight conditions. Another paper by I. Da-Riva and J. L. Urrutia[6] is entitled the "Ignition Delay in Diffusive Supersonic Combustion". This paper deals with the study of the zone located near the injector exit of an idealized supersonic combustion burner using hydrogen as fuel. A simplified kinetic scheme is assumed and the presence of radicals is considered to be due to the dissociation at the injector outer boundary layer. It is shown that the temperature of the injector outer wall and to a lesser extent pressure, injector length and the conditions outside of the boundary layer control the ignition process. Another paper is entitled the "Study of Liquid Jet Penetration in a Hypersonic Stream" by I. Catton, D. E. Hill, and R. P. MacRae.[7] The authors develop a single expression for predicting the depth of injection of a liquid jet into a hypersonic stream for arbitrary injection angle and dynamic pressure ratio. The developed equation shows an excellent correlation with experimental data. Still another paper in the same issue is on "Shock Relaxation in a Particle-Gas Mixture With Mass Transfer Between Phases" by R. Panton and A. K. Oppenheim.[8] The authors studied the structure of the relaxation zone behind the shock front propagating into a particle-gas mixture where the particles are liquid drops and mass transfer therefore had to be taken into account. Finally, J. D. Anderson, Jr. presented a note on "An Equation for Stagnation Point Radiative Heat Transfer".[9] The author develops an equation for radiative heat transfer as a function of the radius of curvature of the radiating surface. Good agreement was found between experimental data and the equation, for example, at a velocity of 50,000 ft/sec and 200,000 ft altitude. Interestingly, the equation also represents fairly well the radiative intensity at a shock tube end wall as a function of time after shock reflection.

Heat Sink Requirements at Mach 8[a)]

Calculations have been made in the past of the relation between aircraft speed and engine heat sink requirements and these have been reported previously.[3,4] However, a very wide spread of values has resulted due to variations in operating conditions and basic assumptions. When an opportunity arose to do an independent evaluation of this problem advantage was taken of it. The conditions chosen were to involve a speed of Mach 8 with supersonic

a) This analysis was done and the report prepared by Dr. R. A. Brown as part of a training assignment.

combustion and assumed a typical hypersonic engine. Thus, this analysis makes a rough estimate of this heat load for such an engine. Methods and data available here and the literature were used.[12)13)14)15)16)17)18)] A 450,000 lb aircraft is assumed to be flying at Mach 8 and 100,000 ft altitude using a single supersonic combustion ramjet engine. Figure 2 is a longitudinal section of the engine. The engine consists of three parts: (1) the diffuser where the incoming air increases its static temperature and pressure; (2) the combustor where fuel is added, burned and the temperature and pressure further increases and (3) the nozzle where the gases are expanded. Ideally, (1) to (3) is an isentropic compression, (3) to (5) Rayleigh line process (heat addition in a constant area duct with no friction) and, (5) to (6) an isentropic expansion assignment. In this analysis this ideal cycle is modified by calculating a total pressure drop from (1) to (3) using an expression by Dugger for a 3 shock inlet. Otherwise, the analysis follows this ideal cycle.

Heat transfer requirements for the diffuser are assumed to be negligible as the engine surface will be exposed to space and therefore free to radiate heat away. In the combustion region heat transfer is calculated using turbulent flow theory in an annulli with corrections for high speed flow. No attempt has been made to account for radiative heat transfer from the flame. Heat transfer in the nozzle is based on a turbulent flat plate relation, the leading edge at the nozzle inlet. Again no flame radiation has been figured. In addition, no attempt has been made to account for the effects of shocks. Temperatures at the combustor exit are in the range where air begins to dissociate and therefore the physical properties have been extrapolated into a region where they are not valid. In all cases a wall temperature of 2000°R has been assumed. Although this is rather low and could perhaps be legitimately extended to 2460°R it will result in conservative answers.

The results are summarized in Tables 1 and 2. The detailed calculations are given in the Appendix.

It will be noted that the cooling required comes to 1867 Btu/hr per pound of fuel. By coincidence this is just about the amount of heat sink that would be provided by MCH being reacted completely to toluene and hydrogen and heated to 1500°F. While this is not claimed to be a particularly sophisticated analysis the magnitude of the heat sink required indicates the sort of bounds that can be expected to prevail.

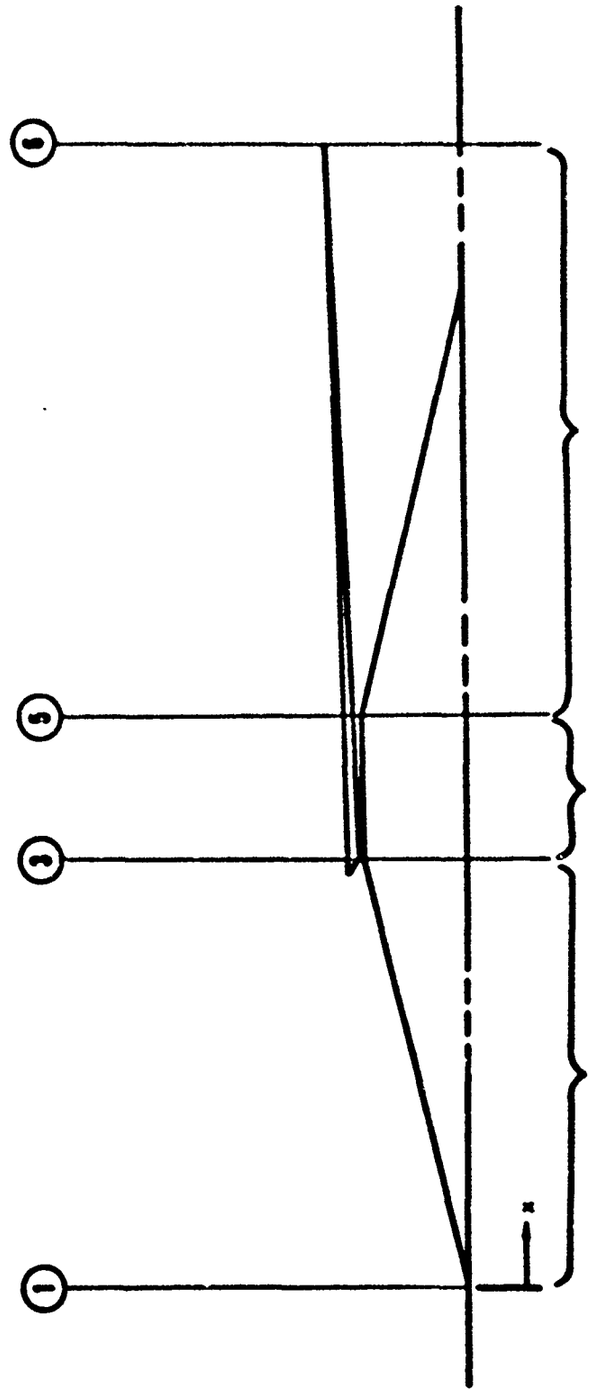

Figure 2. SECTION OF SUPERSONIC COMBUSTION RAMJET ENGINE

Table 1 SUMMARY OF RESULTS FOR MACH 8 ENGINE

Assumed Values:

Speed of Vehicle: Mach Number = 8 at 100,000 ft Altitude
Weight of Vehicle: 450,000 lb (including fuel)
L/D: 5.24
Fuel: MCH converted to 75 H_2 + 25 toluene by volume
E. R. = 1.0
Diffuser Efficiency: η_d = .959
Nozzle Efficiency: η_n = .95
Mach Number at Combustor Inlet: M_4 = 2.5
Length of Nozzle: 40 ft
Engine Wall Temperature: 2000°R
Fuel Temperature: 900°F
Combustion and Mixing Accomplished in 2 msec

Calculated Values:[a]

F/A = .0698 lbm Air/lbm Fuel
Thrust: 85833 lb
Specific Impulse: I_f = 852 sec
Overall Efficiency: η_o = .424
Heat Transferred From Combustor: 1727 Btu/lbm Fuel
Heat Transferred From Nozzle: 140 Btu/lbm Fuel
Total Heat Transferred to Fuel: 1867 Btu/lbm Fuel

a) See Table 2 for tabulated station results

Table 2. STATION VALUES

Mach 8 Engine

Station	Distance, x (ft)	Area, A (ft^2)	Pressure, P ($lb/in.^2$)	Temp, T (°R)	Mach No., M
1	0	139 23	C.155	420 1	8 0
3	30	10.03	20 4	2500.0	2 5
5	40	10.03	51.3	5791.0	1.265
6	80	323.58	0.250	1177.9	5.28

Laboratory Studies

Laboratory studies of candidate endothermic fuels and their catalyst systems were continued. The thermal reaction of n-dodecane using additives; of methylcyclohexane and Decalin at elevated pressures; and of rocket fuel RJ-4 (tetrahydrocyclopentadiene dimer) were studied. Using a pulse reactor system, the dehydrogenation of methylcyclohexane with dispersed catalysts and over various supported catalysts was investigated; and the reactivities of Decalin, dimethanodecalin, and bicycloheptane were determined. A few catalysts were evaluated for the dehydrogenation of methylcyclohexane in the bench-scale reactor.

Catalyst Stability for Dehydrogenation of Naphthenes

Previous studies with platinum on alumina catalysts showed that for the dehydrogenation of Decalin (DHN), catalyst stability was affected by the pore structure of the catalyst support; and that greater stabilities were obtained with supports of small pore diameters. This work now has been extended and stability in relation to pore size has been studied for the dehydrogenation of methylcyclohexane (MCH). Further, the influence of chemical composition of the support and the catalyst metal composition on stability have been examined for dehydrogenation of both MCH and DHN.

The tests were done in our bench-scale laboratory reactor system which was a tubular flow reactor equipped with conventional devices for measuring feed flow rates and for collecting liquid and gas products. The reactor was a stainless steel tube (No. 347, 1/2-in. IPS) 32-in. long, 5/8-in. ID, and was heated by an electric furnace. The catalyst was contained in the annular space between the thermowell and the reactor wall. In order to supply heat rapidly to the catalyst bed, the annular distance between the thermowell and the reactor wall was made about 1/16 in. which was about one pellet diameter. The catalyst bed was about 4-1/2-in. long and had a volume of 7 ml. Prior to carrying out the experiments, the catalysts were reduced in situ with hydrogen for 30 minutes at 572°F (300°C) and then for one hour at the reaction temperature. The complete apparatus was described in detail in a previous report.[11]

The reactor wall temperature was measured by a thermocouple pressed against the outside reactor wall by the furnace block and located about 1 in. below the top of the catalyst bed. The catalyst bed temperatures were measured by thermocouples contained in the thermowell. The thermocouples were 1 in. apart and the top thermocouple was about 1/2 in. below the top of the catalyst bed. The "effective" catalyst temperature was somewhere between the reactor wall temperature and the catalyst bed temperature.

During reaction the catalyst bed temperature (thermocouple measurements) was considerably lower than the furnace block temperature due to the endothermic heat of reaction. As the catalyst deactivated the catalyst bed, temperature increased and the magnitude of the temperature increase was taken as a measure of catalyst deactivation. Another quatitative indication of catalyst deactivation was the movement of the "cold spot" down the catalyst bed.

Product analyses were done by GLC from which conversions and selectivities were calculated.

Effect of Pore Size

In previous work on the dehydrogenation of Decalin (DEH),[16] it was observed that catalyst deactivation occurred when the reaction was carried out at 10 atm pressure and moderate conversion. Subsequently it was shown that the deactivation rate varied generally directly with catalyst pore size. A similar catalyst deactivation was observed with MCH at 1 atm pressure (but not at 10 atm),[3] and it was of interest to study the effect of pore size on catalyst stability with this feed.

The tests were done at 1 atm pressure and a block temperature of 842°F. Each catalyst was tested in a series of 30 minute runs at LHSV's of 5, 15, 30, 50, 80 and 100 or until the catalyst became inactive. The increase in catalyst bed temperature (ΔT max) during the run was taken as a measure of catalyst deactivation. Seven ml of catalyst were used for each test.

The catalysts used in this study were the same as were used for the dehydrogenation of Decalin.[16] These were:

1% Pt on Harshaw Alumina (Standard Laboratory Catalyst)

Shell 108 (1% Pt on Alumina A; 10280-108)

Shell 45 (10280-45, 5% Pt on non-alumina support)

Aeroform PHF-4 (0.8% Pt; American Cyanamid)

RD-150 (0.65% Pt, Sinclair-Baker)

UOP-R8 (0.76% Pt, Universal Oil Products)

The pertinent physical properties of these catalysts are shown in Table 3.

At low space velocity (LHSV = 5), high conversions were obtained and all of the catalysts were stable. With increased space velocity conversion declined and stability varied (Figure 3). For example, at LHSV of 30, all catalysts were active, but at LHSV of 100 only Shell 45 and Shell 108 were active. The complete test data for the six catalysts are tabulated in Tables 119 to 124, Appendix.

Presumably hydrogen generated during the run acts to remove coke precursors from the catalyst surface. At high conversion the partial pressure of hydrogen is high and the catalyst is stable. As conversion declines, the partial pressure of hydrogen is lower, hence the rate of poison removal is lower and the catalyst deactivates. As reaction occurs in the catalyst pores, the conversion per unit pore volume and hence the hydrogen partial pressure in the pore will be greater in the smaller diameter pores (for a given set of conditions) as the surface to volume ratio is greater in smaller pores. Thus, catalysts with smaller pores should be more stable.

Catalyst deactivation (ΔT max) as a function of average pore diameter for the five platinum on alumina catalysts is shown in Figure 44 (LHSV = 30). The pertinent data are summarized in Table 4. Indeed, the catalysts with the smaller pore diameter were more stable. Similar results were obtained with Decalin at 10 atm pressure (LHSV = 100, 1022°F)[16] and these data are also shown in Figure 4. The fact that the catalysts were more stable with MCH than

Table 5. PHYSICAL PROPERTIES OF VARIOUS CATALYSTS

Catalyst		1% Pt on 0104 Al_2O_3 (Standard Catalyst)	American Cyanamide Aerofore PHF-4; 0.8% Pt	Sinclair-Baker BP-150; 0.65% Pt		Shell 108 1% Pt on Al_2O_3 A	Shell 65 (0208-45 3% Pt[b])		BDP-88;[a] 1% Pt on Al_2O_3 B
Surface Area, m^2/g		103	220	480		237	145		154
Bulk Density, g/cc (18-20 mesh size)		0.86	0.89	0.93		0.98	0.88		0.83
Total Pore Volume, cc/g		0.286	0.807	0.402		0.251	0.377		0.719
Pore Size Distribution	Pore Diameter, A	Cumulative Volume, cc/g			Pore Diameter, A	Cumulative Volume, cc/g		Pore Diameter, A	Cumulative Vol, cc/g
	16	0.000	0.000	0.042	18	0.015	-	24	0.003
	17	0.010	0.000	0.061	24	0.027	0.016	35	0.024
	18	0.000	0.000	0.078	50	0.177	0.013	52	0.050
	24	0.001	0.016	0.141	97	0.206	0.075	82	0.081
	50	0.013	0.042	0.173	185	0.219	0.342	147	0.188
	102	0.085	0.193	0.255	354	0.233	0.337	235	0.328
	204	0.192	0.528	0.315	723	-	0.370	419	0.569
	454	-	-	0.371	850	0.251	0.337	850	0.719
	850	0.266	0.807	0.402					

a) Pore distribution determined on B-S alumina base.
b) On nonalumina support.

Table 4. DEHYDROGENATION OF MCH OVER VARIOUS CATALYSTS

Summary Table

Feed: Pure MCH Reaction Time: 30 Minutes
Catalyst Volume: 7 ml
Pressure 1 atm
LHSV: 30

Catalyst	Conv., % @ 842°F	Total Pore Volume, cc/g	ΔT max, °F, Catalyst Bed at 842°F Block Temp.	Average Pore Diameter, A	Pore Volume - Diameter Factor cc-A/g
Standard Catalyst	37.2	0.266	50	106	28
Sinclair-Baker RD-150; 0.65%	72.5	0.402	14	35	14
Shell 108	69.6	0.251	4	42	11
Shell 45	80.7	0.357	0	95	31
American Cyanamide Aeroform PHF-4; 0.8% Pt	58.4	0.607	135	111	67
UOP-88; 0.76% Pt	15.3	0.719	162	175	126

a) Standard laboratory catalyst.

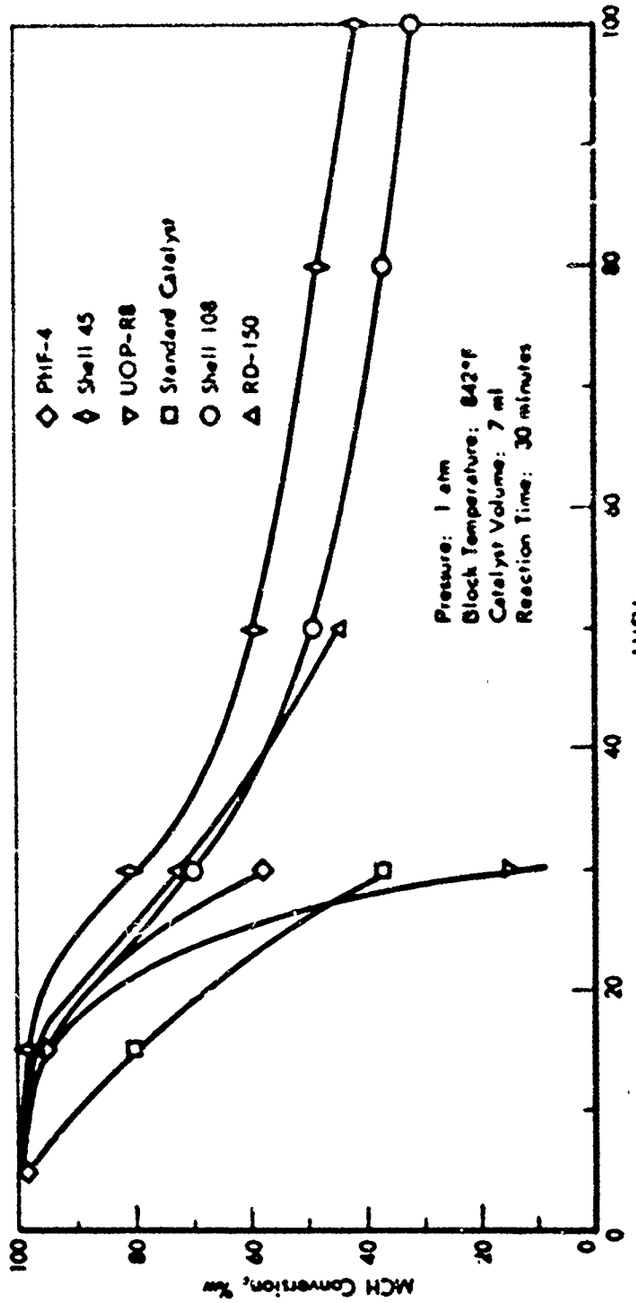

Figure 3. DEHYDROGENATION OF MCH OVER VARIOUS CATALYSTS

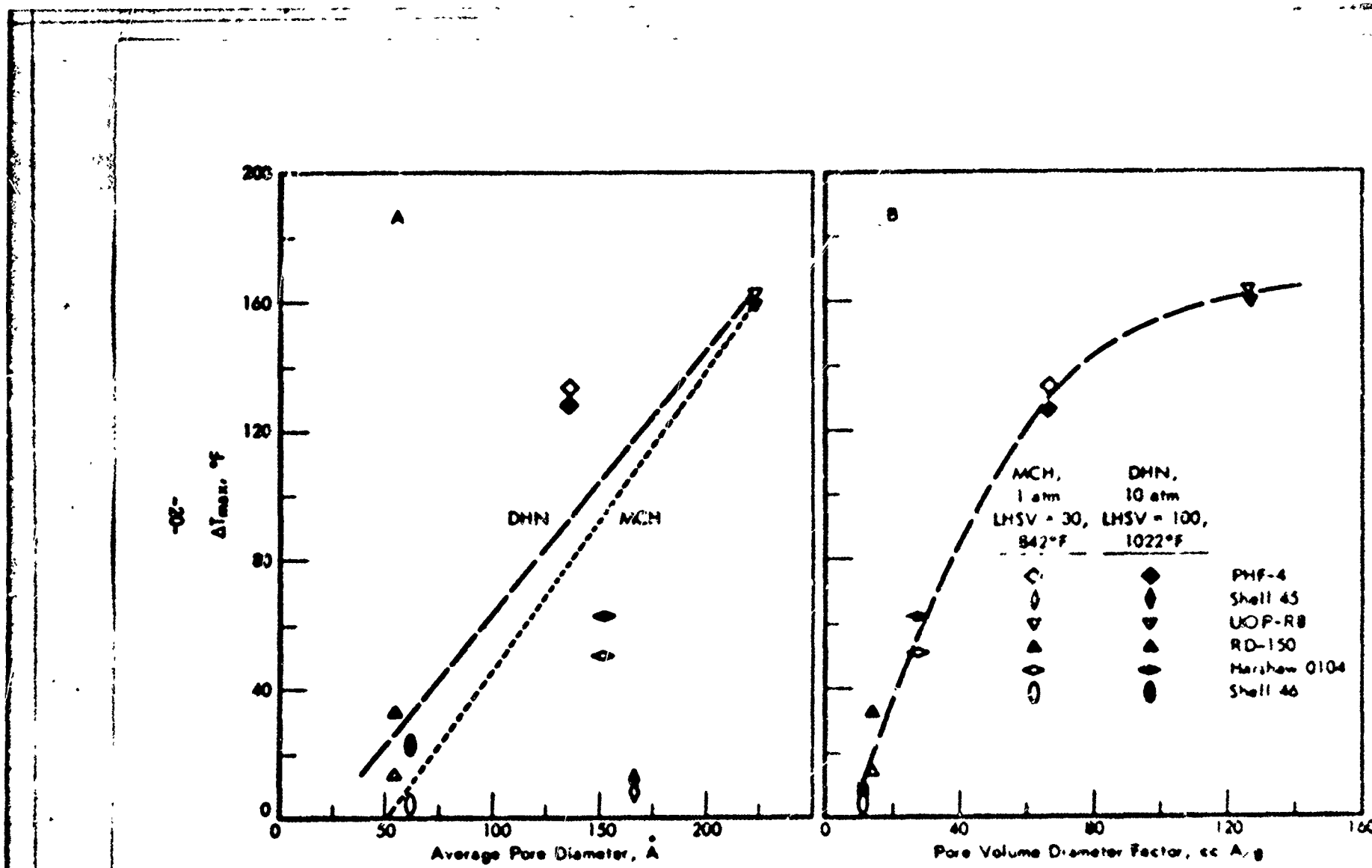

Figure 4. DEHYDROGENATION OF MCH AND DHN WITH VARIOUS CATALYSTS
Effect of Pore Size on Catalyst Stability

with Decalin suggests that the coke precursors or poisons formed during dehydrogenation of a monocyclic naphthene are a different species and are more readily removed by hydrogen than those formed during dehydrogenation of a dicyclic naphthene. (Shell 45 was not included as the chemical composition of this catalyst was quite different from that of the other five catalysts.)

While the least stable catalyst had the largest average pore diameter and the most stable catalyst had the smallest pore diameter, there is an anomaly in the region of about 100Å pore diameter. Thus the PHF-4 and the standard laboratory catalyst have about the same average pore diameter, but the catalyst bed temperature increase with the former was about twice that observed with the latter catalyst. As the pore distributions for these two catalysts were about the same, it appears that pore size is not the only factor in controlling catalyst stability.

Visual examination of PHF-4 showed that the platinum was concentrated on the periphery of the catalyst pellets (1/16-in. extrudate). Thus this catalyst was different from the other catalysts in that: a) the effective pore length was less as the pores were only partially covered by platinum; and b) the platinum was concentrated closer to the pore mouth. Conceivably for a given conversion this could result in lower hydrogen pressure in the catalyst pores as hydrogen would tend to diffuse out of the pore more readily in the region closer to the pore mouth.

Table 5 shows hydrogen partial pressures at the pore mouth and pore centerline for various pore diameters and reactor conversions. These values were calculated[a] for 1/16-in. diameter pellets at 842°F, 1 atm pressure using the pore model of Wheeler,[22] (i.e., open ended, straight cylindrical pores). While this model is not necessarily representative of the pores in our catalyst pellets, nevertheless the calculations serve to illustrate that there can be considerable difference in pressure at the centerline and at the pore mouth. Thus the observed difference in stability between catalysts PHF-4 and our laboratory catalyst may well be a diffusion effect.

An interesting correlation was obtained when the increase in catalyst bed temperature was plotted as a function of the product of pore volume times pore diameter ("pore volume-diameter" factor, Table 4. Figure 4 shows such a plot and no anomaly exists for the two catalysts. The physical significance of this correlation is being considered.

In summary then, our work shows that for the dehydrogenation of naphthenes without added hydrogen catalyst stability varies inversely as the pore size and that good stability is favored by smaller pore diameter. Further, it implies that longer pores will improve stability but that smooth nonporous catalysts will be highly unstable.

Effect of Catalyst Support and Catalyst Composition

In the previous section[b] it was shown that catalyst pore size was an important factor in determining the stability of a catalyst. However, other factors can also effect stability and this section presents a

a) The calculations were made by Dr. J. E. Bailey, Chemical Engineering Dept.
b) See page 16.

Table 5. DEHYDROGENATION OF METHYLCYCLOHEXANE

Calculated H_2 Partial Pressure in Catalyst Pores for Various Pore Diameters

Feed: Pure MCH
Temperature: 846°F
Pressure: 1 atm

Reactor Conversion, %	H_2 Pressure, atm, at:							
	Pore Mouth	Pore Centerline						
		Pore Diameter, Å						
		50	100	150	200	250	400	850
0.1	0.000	0.431	0.427	0.408	0.374	0.333	0.221	0.073
15	0.310	0.563	0.560	0.549	0.530	0.507	0.441	0.354
30	0.474	0.632	0.631	0.624	0.612	0.597	0.556	0.502
50	0.600	0.686	0.685	0.682	0.675	0.667	0.645	0.615
75	0.692	0.725	0.725	0.724	0.721	0.718	0.710	0.698
90	0.739	0.741	0.741	0.741	0.740	0.739	0.736	0.732

preliminary study of the effect of catalyst support composition, and catalyst metal composition on stability. Two supports other than alumina were tested; all of the catalysts contained platinum metal only except for one, which had a "metal activator" added.

Two commercial and four laboratory catalysts (prepared under our catalyst development program) were tested. These were:

Houdry 200-SR (0.5% Pt on alumina)
UOP R-16Z (Pt plus a "metal activator" on alumina)
Shell 10280-44 (our standard 1% Pt on alumina)
Shell 10860-114B (Pt on support No. 6)
Shell 10860-114C (Pt on support No. 6)
Shell 10860-113A (Pt on support No. 5)

R-16Z was a Universal Oil Products high stability Platforming catalyst, containing a "metal activator" but whose composition was not determined, as per our agreement with UOP. As R-16Z represents an improvement over UOP-R8 Platforming catalyst, our test data for R-8 obtained earlier is included in this work for comparison. No H_2 was added to the feed during these tests.

Decalin

With Decalin the catalysts were tested at 10 atm pressure and LHSV of 100. Each catalyst was tested initially at 842°F and then at successively higher temperature (in 90°F increments) through 1202°F, or until the catalyst became inactive. The test period was 30 minutes at each temperature. The feed (F-113 DHN) had the following composition:

25.0% trans-DHN
74.6% cis-DHN
0.4% tetralin (THN)

The data are presented in Tables 6 and 7.

Activities and stabilities varied greatly between catalysts. Of those evaluated in this series of tests, 114C was the most active and the most stable, while 113A was the least active and the least stable. At the lowest test temperature (842°F) catalyst bed temperature (ΔT max) increases varied from 5°F (114C) to 38°F (113A) (Figure 5). With increased temperature 113A and 200-SR were almost completely deactivated at 1022°F (ΔT max = 235°F and 178°F, respectively), while at 1112°F bed temperature increases of over 100°F were observed for 114B and R-16Z, signifying considerable deactivation at this temperature. 114C showed little or no deactivation at 1022°F and lower and bed temperature increases of only 16°F and 67°F were observed at 1112°F and 1202°F, respectively (Figure 5). Based on the increase in catalyst bed temperature at 1022°F (ΔT max) relative catalyst stabilities were:
114C > R-16Z > 114B > 44 >> R-8 > 200-SR >> 113A.

Table 6. DEHYDROGENATION OF DECALIN: TYPE 6 CATALYST SUPPORTS

Pressure: 10 atm
LHSV: 100
Catalyst Volume: 7 ml
Reaction Time: 30 min
Feed: [illegible] Decalin
25.0% trans-DHN
74.8% cis-DHN
0.4% THN

Catalyst Number	← 12860-11C →									← 10660-11C →				
Run No. 11325-	24	25	26-1	26-2	28-1	28-2	28-3[a]	29-1[b]	29-2	30	31	32-1	32-2	33
Temperature, °F														
Block	842	932	1022	1112	← 1202 →					842	932	1022	1112	1202
Wall	704	755	831-29	894	966-8	970	998	787-837	866	711-14	777-81	851-55	925-30	1045-72
Catalyst Bed	803-08	841-44	887-71	700-18	838-905	923	950	734-47	750	828-42	871-87	772-85	783-891	1022-1112
	509-801	871	860-58	889-83	770-79	772	788	758-54	752	814-21	851-55	889-94	729-48	864-941
	804-06	844-41	869-67	704-05	780-72	765	770	786-84	779	815-21	853-55	891-84	732-41	842-71
	814-15	853-51	886-84	729	815-797	786	788	761-63	963	832-33	871	7.8	766-68	960-66
ΔT_{max}	5	3	4	16	67	-	-	40	29	14	16	43	108	90
Product Analysis, %														
Cracked, liquid	0.0	0.0	0.1	0.7	4.5	3.1	2.8	2.7	2.4	0.0	0.1	0.2	0.7	3.0
trans-DHN	36.8[d]	31.6[d]	26.5[d]	20.8	12.1	14.1	14.7	12.8	13.2	36.4	30.8	25.1	21.0	15.3
cis-DHN	20.8	17.5	18.9	8.9	4.3	8.2	7.3	6.5	5.3	28.8	23.7	21.1	17.8	13.6
THN	22.0	17.8	13.3	7.8	3.4	4.1	4.4	3.7	3.9	15.7	12.5	8.0	5.3	6.4
N	20.3	33.4	48.8	63.8	75.1	72.2	70.4	76.0	75.7	20.5	32.8	45.4	54.8	54.4
Others[c]	0.1	0.1	0.1	0.2	0.4	0.3	0.4	0.5	0.4	0.1	0.1	0.2	0.4	0.5
DHN Conversion, %	41.8	50.5	67.0	71.7	83.0	79.1	77.4	82.3	80.9	33.1	44.9	53.2	60.8	64.1

a) Reaction time 15 minutes.
b) Catalyst treated with H_2 for 60 min at 1202°F before this run.
c) Emerged after cis-DHN and after N in GLC analysis.
d) cis- to trans-isomerization.

Table 7. DEHYDROGENATION OF DECALIN: VARIOUS CATALYST SUPPORTS

Pressure: 10 atm
LHSV: 100
Catalyst Volume: 7 ml
Reaction Time: 30 min

Feed: F-115 Decalin
25.0% trans-DHN
74.6% cis-DHN
0.4% THN

Run No. 11525-	21	22	23	50	51	52	60	61	62-1	62-2	63-1	64	65	66	67
Catalyst	1% Pt on Al_2O_3 [a]			Houdry [illegible]			Girdler G-58						[illegible]		
Temperature, °F															
Block	842	932	1022	842	932	1022	842	932	1022	1112	1022	1112	842	932	1022
Wall	716-8	772-83	849-51	711-14	772-88	878-913	724-30	788	845-53	932-45	836-845	1026-1035	716-8	816-848	894-898
Catalyst Bed	642-58	680-709	725-88	669-91	734-817	836-77	648-53	676-97	714-36	774-[illegible]	693-[illegible]	[illegible]	642-58	772-[illegible]	[illegible]
	621-30	658-66	696-707	655-64	670-734	742-[illegible]	655-59	662-66	694-[illegible]	734-63	728-[illegible]	[illegible]	621-30	677-[illegible]	774-[illegible]
	650-55	668-73	707-12	655-57	673-78	734-[illegible]	646-48	673	724-31	754-63	736-[illegible]	[illegible]	650-55	717-[illegible]	794-[illegible]
	639-44	676-82	723-25	644	617-807	745-806	653	680	716-18	765-75	765 774	854-[illegible]	644-[illegible]	746-[illegible]	765 83
ΔT_{max}, °F	16	27	63	22	83	178	5	11	22	[illegible]	112[d]	[illegible][d]	38	133	233
Product Analysis, %w															
Cracked, liquid	0.0	0.0	0.1	0.1	0.1	1.1	0.0	0.0	0.1	0.6	0.5	3.4	0.3	0.1	0.3
trans-DHN	29.7[b]	26.7[b]	22.5	30.4	26.7	22.0	30.7[b]	26.06[b]	24.4	19.3	24.8	18.6	29.7	23.1	21.6
cis-DHN	55.0	57.7	49.7	55.4	51.8	37.7	57.7	51.7	45.5	42.8	48.7	44.4	54.5	48.2	42.4
THN	12.0	8.	6.1	12.9	9.3	5.7	11.0	11.0	9.2	5.3	5.7	3.6	8.9	7.4	5.1
N	23.2	36.4	47.3	20.7	31.9	20.8	20.8	34.1	43.3	32.0	26.4	20.3	17.6	23.2	28.0
Others[c]	0.1	0.1	0.2	0.5	0.6	2.0	0.0	0.2	0.5	1.2	5.7	11.2	3.1	1.1	1.1
DHN Conversion, %w	54.7	43.0	53.2	53.8	40.3	54.7	51.1	42.0	52.3	67.3	58.3	61.0	26.1	34.2	55.1

a) Standard Catalyst No. 13200-44.
b) Cis to trans isomerization during the run.
c) Emerged after naphthalene and after cis-DHN.
d) H_2 treated at 1022°F for 3 hrs at 1 atm before this run.
e) Cold spot moved down the catalyst bed.

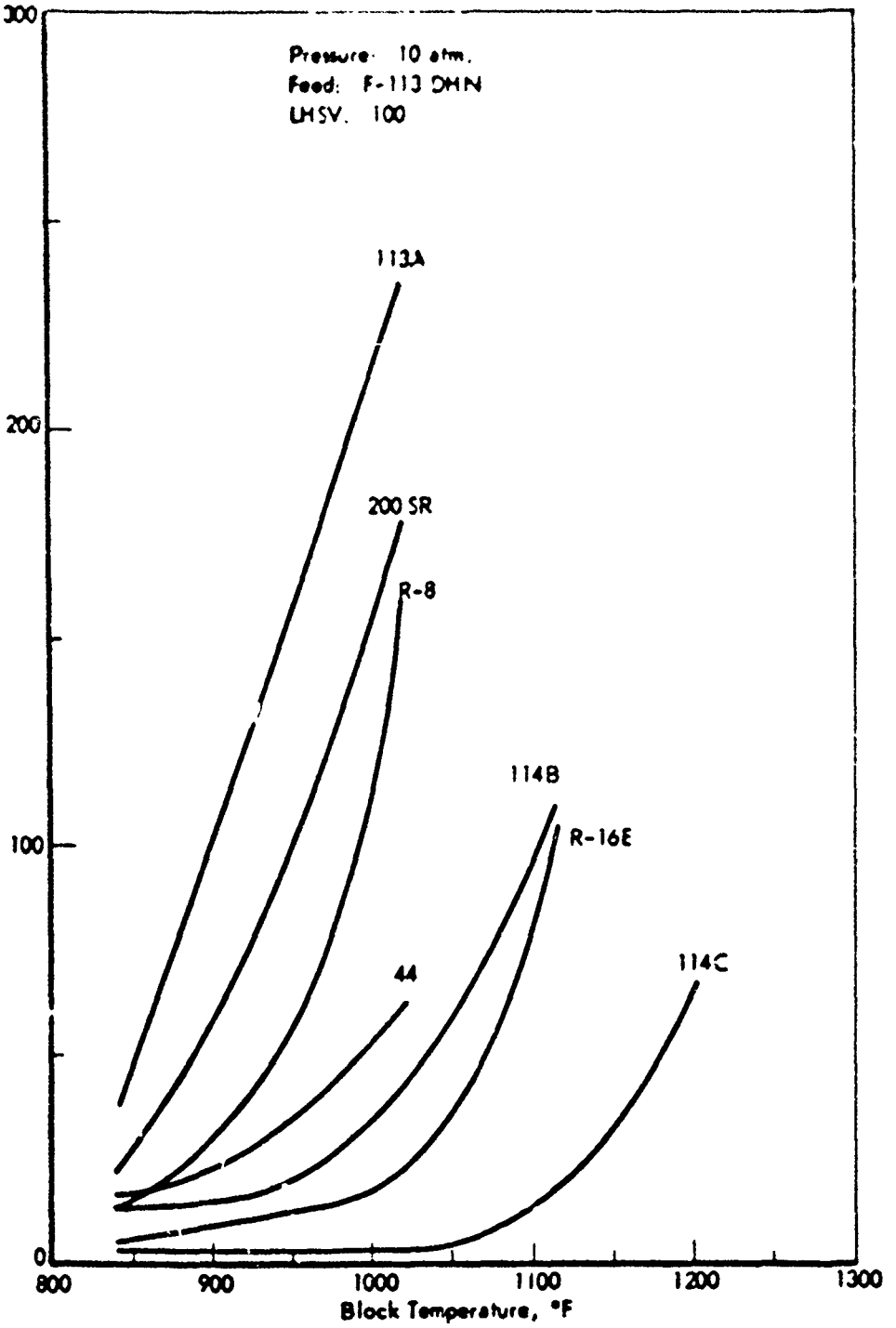

Figure 5. DEHYDROGENATION OF DECALIN OVER VARIOUS CATALYSTS
EFFECT OF TEMPERATURE ON CATALYST STABILITY

Conversion increased with increased temperature but declined when the catalyst became deactivated (Figure 6). At the lowest test temperature where deactivation was the least, relative activities based on DHN conversions were: 114C > R-8 ≈ 44 ≈ 200SR ≈ 114B > R-16E > 113A.

Product material was principally tetralin (THN) and naphthalene (N). At the highest test temperature (1202°F) some cracking occurred, possible due to thermal reaction (Tables 6 and 7). At the lower test temperatures some cis to trans-DHN isomerization was observed.

Methylcyclohexane

The MCH-catalyst system was considerably more stable than the decalin (DHN) system. Thus with our standard 1% Pt on Al_2O_3 catalyst, good stability was observed with MCH at 10 atm pressure[11] but not at 1 atm[11]; while with DHN good stability was observed at 30 atm[10] but not at 10 atm[10] pressure. Consequently in these studies with MCH, stability tests were done at 1 atm pressure. Each catalyst was tested at a single temperature, 842°F, in a series of successive runs with increasing space velocities from 5 to 100 LHSV. The test was terminated if the catalyst became inactive before reaching LHSV of 100. The complete data are presented in Tables 125 to 129 in the Appendix and are summarized in Figure I.

At low space velocity (LHSV = 5) high conversions were obtained and all of the catalysts were stable (i.e. little or no temperature change during the run). With increased space velocity conversion declined and catalyst stability varied (Figure 6). For example, at LHSV of 30 three of the seven catalysts were inactive at the end of the run, while at LHSV of 100 only one catalyst, 114C, had not deactivated. These conclusions were based on the increase in catalyst bed temperatures and the movement of the "cold spot" down the catalyst bed (Tables 125 to 129). Indeed with this latter catalyst there was only a 6°F increase in bed temperature during the run at LHSV of 100. Based on the bed temperature increases at LHSV of 50 the relative catalyst stabilities were: 114C > R-16E > 44 ≈ 114B ≫ R-8 ≈ 113A ≫ 200SR. As was observed with DHN catalyst 114C was the most active and the most stable catalyst.

Product material was primarily toluene at 90+% selectivity. At the lowest space velocity (i.e. longest contact time) some benzene was found with some of the catalyst. Presumably this was due to a hydro-dealkylation side reaction.

Summary and Conclusions

From the results obtained in the present series of tests, it was evident that both catalyst support and catalyst composition can effect stability. Thus, 114B and 113A contained the same amount of platinum but different supports and yet the former was much more stable than the latter. Further, R-16E catalyst was about like R-8 except that the former contained a "metal activator". Our tests showed that the Pt-alloy catalyst (R-16E) was much more stable than its counterpart R-8.

The most stable (and also the most active) catalysts tested thus far were 114C and Shell 46. Both catalysts gave about the same conversion and

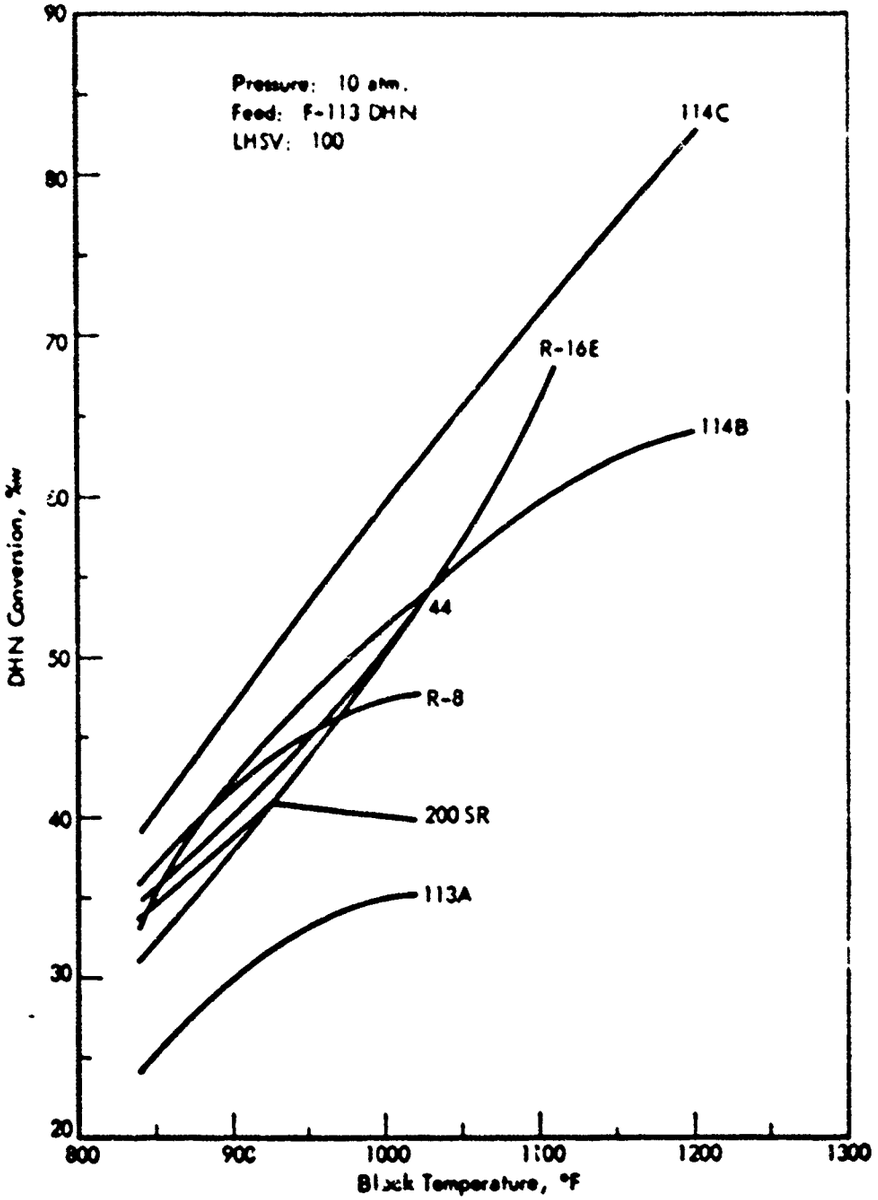

Figure 6. DEHYDROGENATION OF DHN OVER VARIOUS CATALYSTS
EFFECT OF TEMPERATURE ON CONVERSION

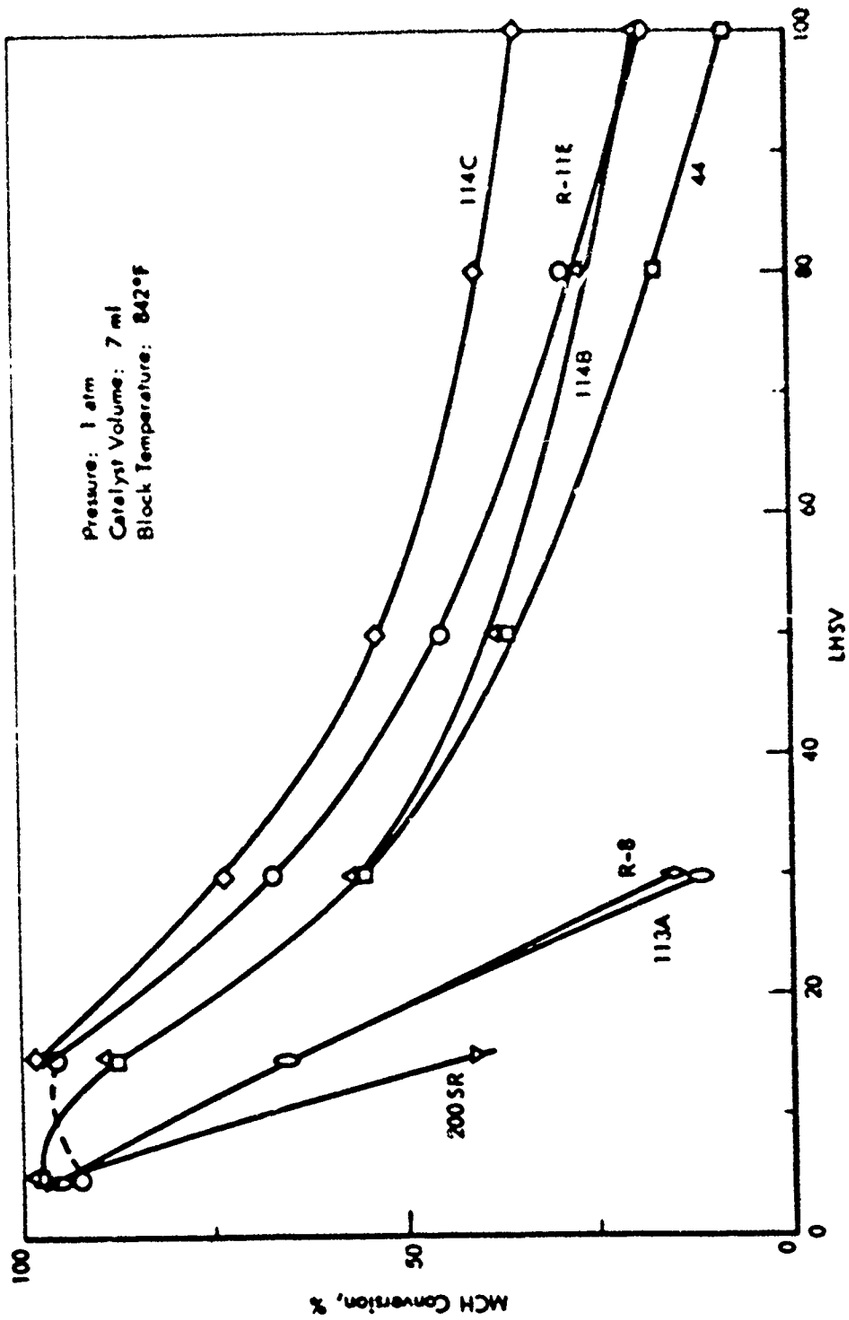

Figure 7. DEHYDROGENATION OF MCH OVER VARIOUS CATALYSTS

bed temperature increases when tested with DHN.[10] However, the bulk density of 114C was about 40% of that of Shell 46, hence the former appears to be a superior catalyst on the basis of conversion per unit weight of platinum.

We are continuing our study of factors effecting catalyst stability and will include testing other supports, other platinum-alloy combinations, and methods of improving metal dispersion (i.e. metal surface area) on various supports.

Thermal Reactions Studies

n-Dodecane Using Additives

There is considerable interest as to the maximum amount of heat sink that can be obtained with a paraffinic type jet fuel (JP-7). The latent and sensible heat obtainable from this material is about 1000 Btu/lb when heated to 1400°F. An additional 500 Btu/lb could be obtained by thermally cracking the fuel to about 50% conversion. However, under conventional cracking reaction conditions, some coke is produced, which is undesirable. Also the rate, at moderate temperatures, is too low. We are investigating the possibility of enhancing the rate of thermal reaction with concurrent reduction in coke made, using free radical initiating fuel additives.

These experiments were done in both the pulse reactor and the small bench-scale flow reactor (1/4" O.D. reactor tube). Both apparatii are described in detail in the Appendix. Tests were done at 10 atm pressure, over the temperature region of 1022° to 1202°F using n-dodecane as the test fluid. In these experiments the reactor tube was filled with quartz chips (10-20 mesh) and LHSV's were calculated based on the bulk volume of the quartz (i.e. volume of the empty tube) and the apparent contact time (ACT) was calculated based on the void volume in the tube (i.e. one-half the volume of the empty tube). This is close to the actual contact time and is different from our calculation of ACT for catalytic beds, which ignores catalyst volume.

Thirty-three different additives were screened in pulse reactor tests and then a solution of one of the more promising additives in n-dodecane was tested under both continuous flow and pulse reactor conditions.

In the pulse reactor tests, 3% or less additive (organometallics or organic compounds) in n-dodecane were tested at 1022°F and 1112°F. Some success was achieved and dodecane conversions were increased six-fold at 1022°F (from 3.5 to 18.5%) and two-fold at 1112°F (from 20% to 41%) by means of additives (Table 8). A few of the additives acted as inhibitors and declines in conversion were observed in some cases (cf Nos. 199-2, 5, 20, 22 Table 8). Generally, some functional groups were more effective than others, and where substitution in a functional group occurred, the type of substituted group appeared to influence the overall effectiveness of the functional group.

The reaction products were lighter than n-dodecane and presumably were cracked material (Table 9). From GLC emergence times the principal component appeared to be a C_8 hydrocarbon (peak No. 1, Table 9) and was not identified further. In calculating conversion it was assumed that each

Table 8. EFFECT OF ADDITIVES ON THE THERMAL REACTION OF [illegible]

Pulse Volume: 1 µl
Contact Time: 1 sec
Pressure: 10 atm

Additive No. 11325-	Additive, %w	C_{12} Conversion, %w		
		1022°F	1112°F	For 2%w Additive, 1112°F
None	-	3.5	20.1	20.1
199- 1	(<2.1)[a]	2.9	-	-
2	2.7	3.0	-	-
3	2.8	4.1	-	-
4	(<2.2)[a]	8.0	26.0	-
5	2.4	2.1	-	-
6	(<2.3)[a]	3.8	-	-
7	2.7	9.4	27.6	24.9
8	(<2.7)[a]	5.8	23.0	-
9	(<2.1)[a]	7.6	25.4	-
10	(<1.9)[a]	3.7	-	-
11	2.5	7.1	30.5	28.4
12	2.1	-	29.1	28.7
13	(<3.4)[a]	13.5	32.6	-
14	4.4	16.3	35.9	27.3
15	(<2.9)[a]	-	20.9	-
16	(<1.1)[a]	-	21.1	-
17	(<1.7)[a]	-	20.1	-
18	(<0.9)[a]	-	21.8	-
19	(<1.3)[a]	-	20.7	-
20	(<2.7)[a]	-	16.0	-
21	1.7	-	27.3	28.6
22	1.7	-	18.8	-
23	1.4	-	24.6	26.5
24	1.9	-	24.1	24.3
25	1.7	-	22.4	22.9
26	1.8	-	35.8	37.5
27	1.8	-	30.7	31.9
28	1.3	-	27.5	31.6
29	1.9	-	37.5	38.4
200- 1	2.6	-	41.2	36.3
2	1.7	-	32.8	34.8
3	1.3	-	22.4	23.6
4	1.7	-	33.3	35.6

a) Saturates.

Table 9. THERMAL REACTION OF n-DODECANE - PULSE REACTOR

Liquid Product Distribution

Pulse Volume: 1 µl
Contact Time: 1 sec
Pressure: 10 atm
He Flow Rate: 200 cc/min

Run No. 11325-	Feed	5-1	15-3	7-3	15-2	9-1	9-2	12-2	12-3	17-1	18-2	19-4
Additive No. 11325-	-	None	199-14	199-7	199-13	None	199-7	199-13	199-14	199-14a)	199-16	200-1
Temperature, °F	-	← 1022 →				← 1112 →						
Product Analysis, %w												
Peak 1	0.0	1.6	8.4	4.3	9.7	10.9	(18.2b)	18.9	21.3	20.4	(23.4b)	25.7
2	0.0	0.5	2.1	1.1	2.4	2.5		3.7	3.9	4.6		3.3
3	0.0	0.4	1.5	1.6	1.7	1.9	3.3	2.8	3.1	3.0	2.7	3.4
4	0.0	0.3	1.5	0.8	1.5	1.6	2.1	2.4	2.6	2.7	3.2	2.9
5	0.0	0.3	1.1	0.6	1.3	1.4	1.8	2.0	2.1	2.2	2.3	2.3
6	0.0	0.3	1.1	0.7	1.2	1.3	1.6	1.9	1.9	2.0	2.1	2.0
7	0.0	0.1	0.4	0.3	0.4	0.5	0.6	0.7	0.8	0.8	0.8	0.8
8	0.0	0.0	0.1	0.0	0.1	0.1	0.1	0.2	0.1	0.1	0.1	0.1
9	99.4	95.9	83.1	90.0	80.9	79.3	71.8	66.8	65.5	63.6	64.8	58.8
10	0.6	0.6	0.7	0.6	0.8	0.5	0.5	0.6	0.5	0.6	0.6	0.7
n-Dodecane Conv., %w	-	3.5	16.3	9.4	18.5	20.1	27.6	32.6	35.9	36.3	35.8	41.2

a) Repeat run.
b) Poor separation of peaks one and two in GLC analysis.

molecule of dodecane reacted gave one molecule of product, hence the conversions are maximum values. Product distributions did not appear to be affected by additives and analyses for several runs with different additives are presented in Table 9. No estimate of coke make could be made from the pulse reactor data.

The effectiveness of additive 200-2 was tested further under continuous flow conditions in our small bench-scale reactor. This apparatus had a 1/4-in. OD reactor tube and is described in detail in the Appendix. The tests were done at 10 atm pressure using pure n-dodecane and 2% of 200-2 in n-dodecane as test fluids. Two series of experiments were done, one series at 1022 and 1112°F and at LHSV of 12 to 143; and a second series at 1022°F; 1112 and 1202°F and at LHSV of 59 to 146. The complete data are shown in Table 10 and are summarized in Figure 8.

In this reactor system, at a given reaction temperature, the effect of additive on conversion was less with increased space velocity. As an example at 1112°F the enhanced conversion due to additive was 23.5% at LHSV of 12, but was only 16% at LHSV of 130 to 140 (cf runs 40-2 and 42; and Runs 39 and 43-1, Table 10). This suggests that free radical initiation by the additive was slower than radical initiation by purely thermal means. Further, the effect of additive on conversion (i.e., rate) was less as the temperature increased; and at 1202°F there was only a slight increase in conversion due to the presence of the additive (Table 10; Figure 8).

Product distributions were similar with both feedstocks. Liquid product analyses (GLC) are shown in Table 10; gas phase analyses (mass spec.) are shown in Table 11. Liquid phase product components have not been identified as yet. Gas phase products were a small amount of hydrogen and C_1 to C_5 hydrocarbons, with more olefin than the corresponding saturate and ethylene being the major component (Table 11).

Qualitatively the coke make appeared about the same with both feedstocks, although the coke appearance was different. Thus with pure dodecane the coke was dull black, while with the additive present the coke was shiney black. The coke formed a thin layer on the quartz chips.

In order to have comparable data from the pulse reactor, a few tests were run in this system with both feedstocks at 1022 and 1112°F. The data are shown in Table 12 and in Figure 8 by the solid points. Based on dodecane conversions the rate of cracking was enhanced by factors of 1.8 at 1022°F and 1.4 at 1112°F by the additive. This was only slightly greater than the rate enhancement observed in the flow system (cf Runs 43-1 and 39; and Runs 41 and 38-1; Table 10 and also Figure 8), and was considerably less than the sixfold enhancement of rate observed in the initial exploratory work in the pulse reactor (Table 11). As the additive used in the exploratory work came from a different source than that used in the 2% solution, this suggests that purity of additives may be an important factor in their effectiveness.

The results obtained thus far showed that indeed it was possible to enhance the rate of cracking by the use of additives. Thus far it has been shown that rate increases due to additives were appreciable at 1000°F (i.e., sixfold in the pulse reactor tests), but were only 20% or less at 1202°F. It is well accepted that thermal cracking reactions proceed via a free-radical mechanism. Thus the observed differences in rates at the two temperatures

Table 10. THERMAL REACTION OF n-DODECANE WITH FUEL ADDITIVE

Pressure: 10 atm
Reactor filled with quartz chips

Series	Plug										Recycle											
Run No. 11505-	35-1	35-2	49	50-1	50-2	51	52	53-1	53-2	54	55	56	57-1	57-2	58	59	60	61	62-1	62-2	63	64
Feed	pure n-dodecane					all 200-ml runs in n-dodecane					pure n-dodecane						all 200-ml runs in n-dodecane					
Temperature, °F																						
Bomb	1000		1112			1000		1112			1000						1000					
Wall	1000	1000	1150	1150	1137	1000	1000	1145	1150	1137	1000	1000	1145	1145	1000	1000	1000	1000	1145	1145	1145	1145
Reactor (Effective)	1075	1079	1148	1143	1121	1095	1055	1143	1141	1147	1055	1078	1141	1145	1078	1113	1055	1078	1143	1145	1145	1145
Flow Rate, cc/min	2.0	0.6	6.0	2.0	2.0	2.0	0.6	6.0	2.0	0.6	6.0	2.0	6.0	2.0	6.0	2.0	6.0	2.0	6.0	2.0	6.0	2.0
LHSV[1]	60	18	180	60	33	61	18	147	63	33	122	39	133	66	180	60	122	39	133	66	133	66
Δt, [2] sec	1.9	10.1	0.79	1.8	0.8	2.0	10.1	0.84	1.8	0.5	2.0	2.0	0.84	1.7	2.0	6	0.84	2.0	0.84	1.8	0.84	1.8
Reaction Period, min	15	15	15	15	30	15	30	15	15	30	15	15	15	15	15	15	15	15	15	15	15	15
Effective Reactor Volume, cc	1.35	0.98	1.66	1.89	1.85	1.97	0.98	1.84	1.1	1.95	0.98	0.98	1.84	1.81	1.68	1.35	1.84	0.98	1.84	1.84	1.84	1.84
Liquid Product Analysis, lb																						
Peak 1	2.5	1.6	5.0	2.1	3.4	2.8	5.1	4.7	6.4	5.8	1.3	0.6	6.1	6.1	5.1	4.5	1.7	2.0	3.0	3.7	5.9	5.7
2	1.0	2.6	2.4	3.4	4.8	1.8	3.9	4.7	4.4	7.0	0.6	1.2	2.3	3.9	5.8	1.0	1.0	1.1	2.0	4.2	1.3	6.7
3	0.8	2.4	1.0	2.7	3.8	1.5	3.1	4.1	3.4	3.8	0.3	1.0	1.8	3.0	3.8	0.7	0.8	1.2	4.1	3.6	6.2	4.1
After 3	0.0	0.0	0.0	0.0	0.8	0.0	0.1	0.0	0.1	1.0	0.0	0.0	0.1	0.2	3.6	0.0	0.0	0.0	0.2	0.4	0.4	0.4
4	0.8	2.0	1.6	2.4	4.1	1.3	4.7	1.9	4	6.1	0.3	0.7	1.4	0.7	3.5	0.7	0.8	1.1	1.5	1.1	1.1	1.1
After 4	0.0	0.0	0.0	0.0	0.3	0.0	0.0	0.0	0.0	0.3	0.0	0.0	0.0	0.0	1.1	0.0	0.0	0.0	0.0	0.0	0.0	0.0
5	0.7	1.9	1.5	2.3	3.3	1.2	2.3	1.7	2.3	3.4	0.3	0.8	1.5	2.3	2.7	0.8	0.7	1.6	1.8	1.6	1.6	1.6
After 5	0.0	0.0	0.0	0.0	0.1	0.0	0.0	0.0	0.0	0.1	0.0	0.0	0.0	0.0	0.0	0.0	0.0	0.0	0.0	0.0	0.0	0.0
6	0.6	1.7	1.2	2.1	3.0	1.1	2.1	1.6	2.3	2.5	0.3	0.7	1.0	2.1	2.3	0.7	0.6	1.4	1.6	1.4	1.4	1.4
After 6	0.1	0.0	0.0	0.0	0.0	0.0	0.0	0.0	0.1	0.0	0.0	0.0	0.0	0.0	0.0	0.0	0.0	0.0	0.0	0.0	0.0	0.0
7	0.2	0.3	0.0	0.7	1.4	0.3	0.8	0	0.8	1.0	0.1	0.2	0.0	0.2	1.2	1.0	0.2	0.1	0.3	0.4	0.4	0.4
After 7	0.1	0.1	0.1	0.0	0.0	0.0	0.0	0.1	0.0	0.0	0.0	0.0	0.0	0.0	0.0	0.0	0.0	0.0	0.0	0.0	0.0	0.0
8	0.0	0.1	0.1	0.2	0.2	0.1	0.1	0.1	0.2	0.1	0.0	0.0	0.1	0.2	0.3	0.0	0.0	0.0	0.1	0.1	0.1	0.1
9 (n-dodecane)	90.7	88.8	89.3	77.6	90.2	87.6	85.3	83.4	71.5	85.5	95.0	89.6	88.3	85.5	84.1	94.1	95.1	89.3	88.7	79.7	83.5	84.1
10	1.5	1.7	1.7	1.5	0.8	0.1	1.5	1.5	1.3	0.6	0.1	0.0	0.0	1.7	1.5	1.1	1.8	0.6	1.0	1.5	1.8	1.1
O_2 Converted to, lb																						
Light Gas	0.0	0.0	0.0	3.3	20.0	0.3	0.0	0.0	0.3	15.7	0.0	0.2	0.0	3.0	10.1	29.8	0.0	1.0	0.0	3.4	0.3	15.6
Total	7.3	10.8	10.5	18.6	49.8	13.6	21.5	16.9	25.6	51.3	4.0	11.0	12.3	23.1	37.3	37.8	7.0	10.3	12.3	25.3	18.4	34.1
First Order Rate Constant, sec^{-1}	0.030	0.036	0.08	0.16	0.079	0.073	0.035	.21	0.17	0.13	0.051	0.045	0.08	0.16	0.14	0.035	0.05	0.08	0.08	0.14	0.11	0.14

a) Based on quartz volume + effective volume of empty tube
b) Based on void volume + one half effective volume empty tube

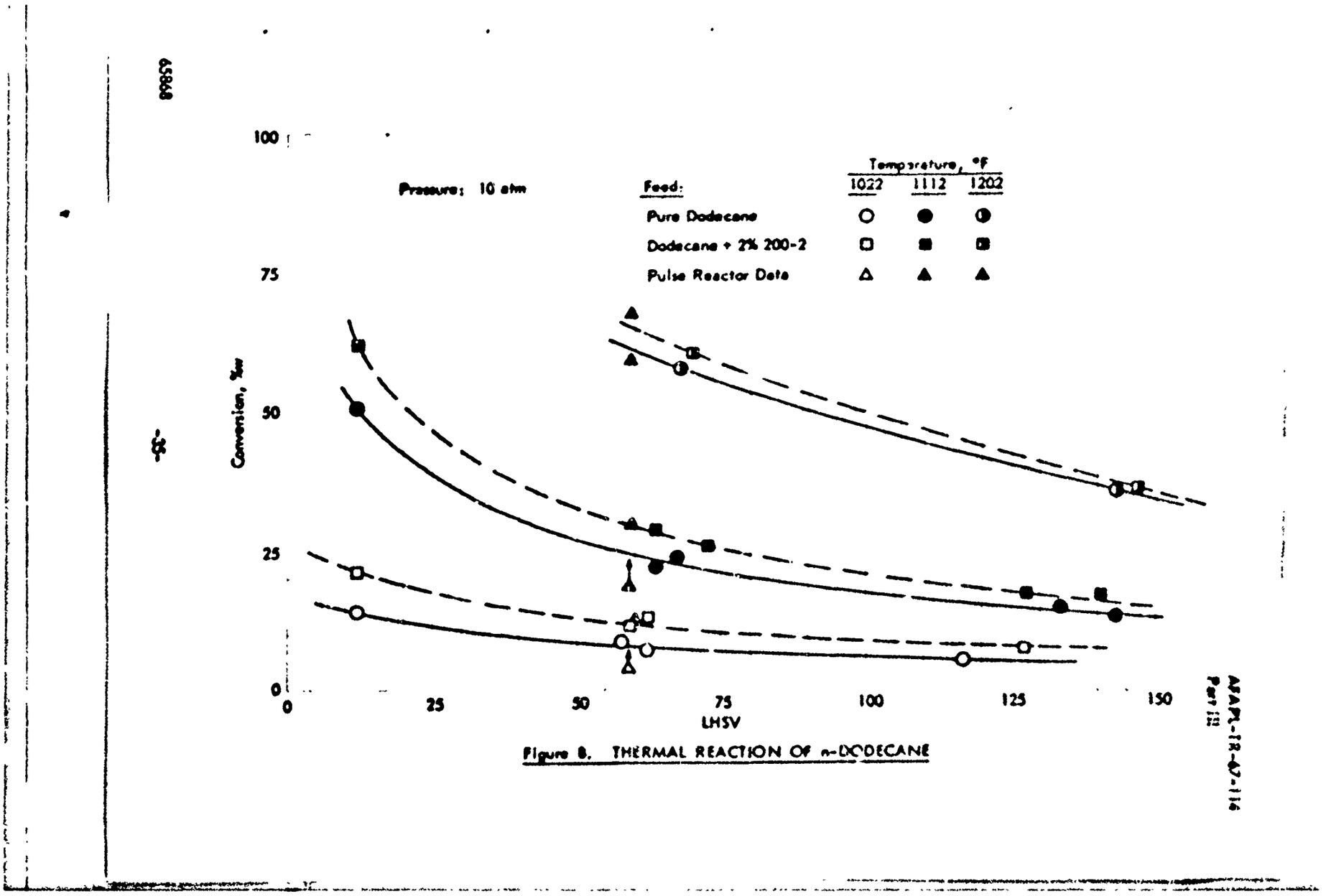

Figure 8. THERMAL REACTION OF n-DODECANE

Table 11. THERMAL REACTION OF DODECANE WITH HYDROGEN

Gas Phase Product Distribution

Pressure: 10 atm

Run No. 11325-	40-2	44
Feed	Pure n-dodecane	n-Dodecane plus 2% 200-2
Block Temperature, °F	1112	1112
C_{12} Conversion to, %w		
Light Gas	20.0	26.7
Total	49.8	61.5
Gas Product Analysis, %w		
H_2	2.4	2.3
CH_4	21.6	20.0
C_2H_4	32.8	32.9
C_2H_6	18.0	21.3
C_3H_6	14.9	12.5
C_3H_8	4.3	6.2
Butadiene	0.6	0.2
C_4H_8	3.3	3.0
C_4H_{10}	0.6	0.9
C_5H_{10}	0.9	0.8
Others[a]		

a) Isoprene + methylcyclopentene.

Table 12. THERMAL REACTION OF [illegible] WITH FUEL ADDITIVES, PULSE RUN B

Pulse Volume: 1 µl
He Flow Rate: About 1 sec
Contact Time: 200 cc/min

Run No. 11325-	45-1	45-2	45-3	[illegible]
Feed	Pure C_{12}	C_{12} + 2% 200-2	Pure C_{12}	C_{12} + 2% 200-2
Temperature, °F	← 1022 →		← 1112 →	
Product Analysis, %w				
Peak 1	3.1	7.1	14.7	21.8
2	0.[illegible]	1.6	2.8	4.1
3	0.6	1.2	2.0	2.7
4	0.5	1.0	1.5	2.0
5	0.4	0.9	1.4	1.9
6	0.3	0.8	1.2	1.8
7	0.1	0.2	0.5	0.6
8	0.2	0.0	0.4	0.3
9	92.3	85.9	74.1	63.7
10	1.8	1.3	1.4	1.1
n-Dodecane Conversion, %w	7.7	14.1	25.9	36.3

may be due to differences in activation energies for free radical production; or it may be that the free radical decomposition products at the higher temperature contain less free radicals than the products at the lower temperature. Experiments are being continued with other types of free radical initiators.

Methylcyclohexane and Decalin at Elevated Pressures

In conjunction with the possible utilization of endothermic fuels to missile application, it was of interest to extend our thermal reaction studies to pressures higher than 10 atm. Accordingly the thermal reaction of methylcyclohexane (MCH) and Decalin (DHN) were studied over the pressure range of 10 to 68 atm (1000 psig) at 1022 to 1292°F.

The reactor was a stainless steel tube (No. 304) 30 inches long, 1/4-in. OD with 0.035-in. wall thickness. Reaction was carried out in the lower part of the tube and the top part served as a feed preheater. The reactor was furnace-heated and a 13-in. long secondary furnace liner surrounded the reactor tube at the reaction zone. Figure 9 shows the secondary furnace liner and its position in the furnace. This reactor system was described in detail in the Appendix.

The reactor wall temperature was measured at seven points along the tube. The points were 1-1/2 inches apart and the top point was one inch below the top of the secondary liner (Figure 9). The temperature of the reactor wall varied down the tube and Figure 10 shows the temperature variation for a furnace block temperature of 1202°F.

The maximum reaction rate will occur in the region of maximum temperature. Presumably the rate in that portion of the tube whose temperature was 18°F (10°C) or more below the maximum temperature, did not contribute appreciably to the overall rate. Thus the "effective" volume of the tube was that portion of the tube whose temperature was within 18°F of the maximum wall temperature, and whose volume was determined from a plot such as Figure 10. The "effective" reactor temperature was taken as 9°F below the maximum temperature.

The reactor tube was packed with quartz chips (10-20 mesh). Space velocities (LHSV)[a] then were calculated from the "effective" tube volume (i.e., bulk volume of the quartz chips); apparent contact times (ACT) were calculated from the void volumes of the packed tube.

Liquid reaction products were analyzed by GLC and gas products by mass spectrometry. Some coke was formed but was not measured quantitatively. The difference in weight between the liquid feed and liquid products was taken as "light gas plus coke".

First order rate constants were calculated from the disappearance of starting material.

---

a) Liquid Hourly Space Velocity = volumes of feed per volume of catalyst (i.e., quartz) per hour.

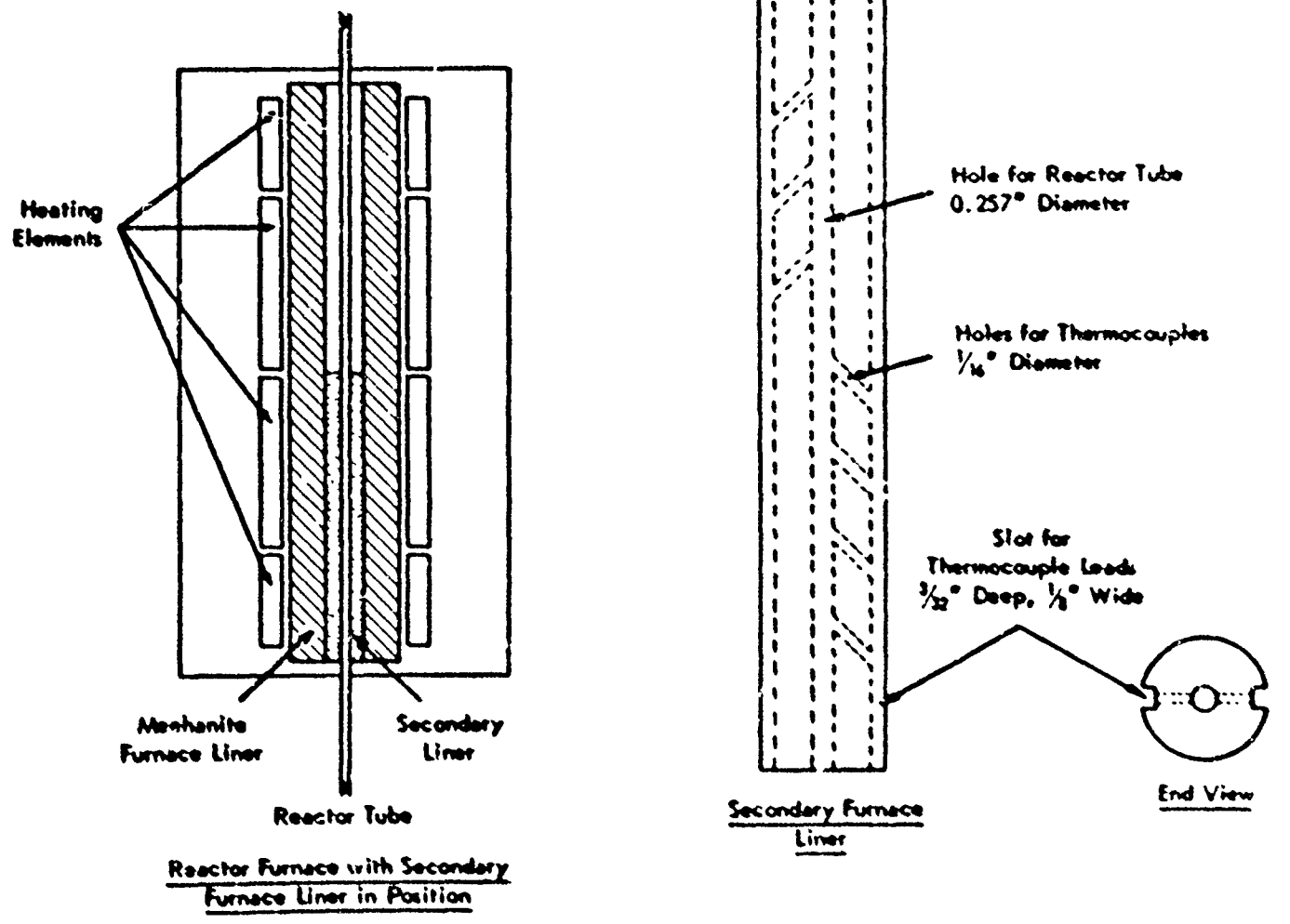

Reactor Furnace with Secondary Furnace Liner in Position

Figure 9. SECONDARY FURNACE LINER FOR 1/4" OD REACTOR TUBE

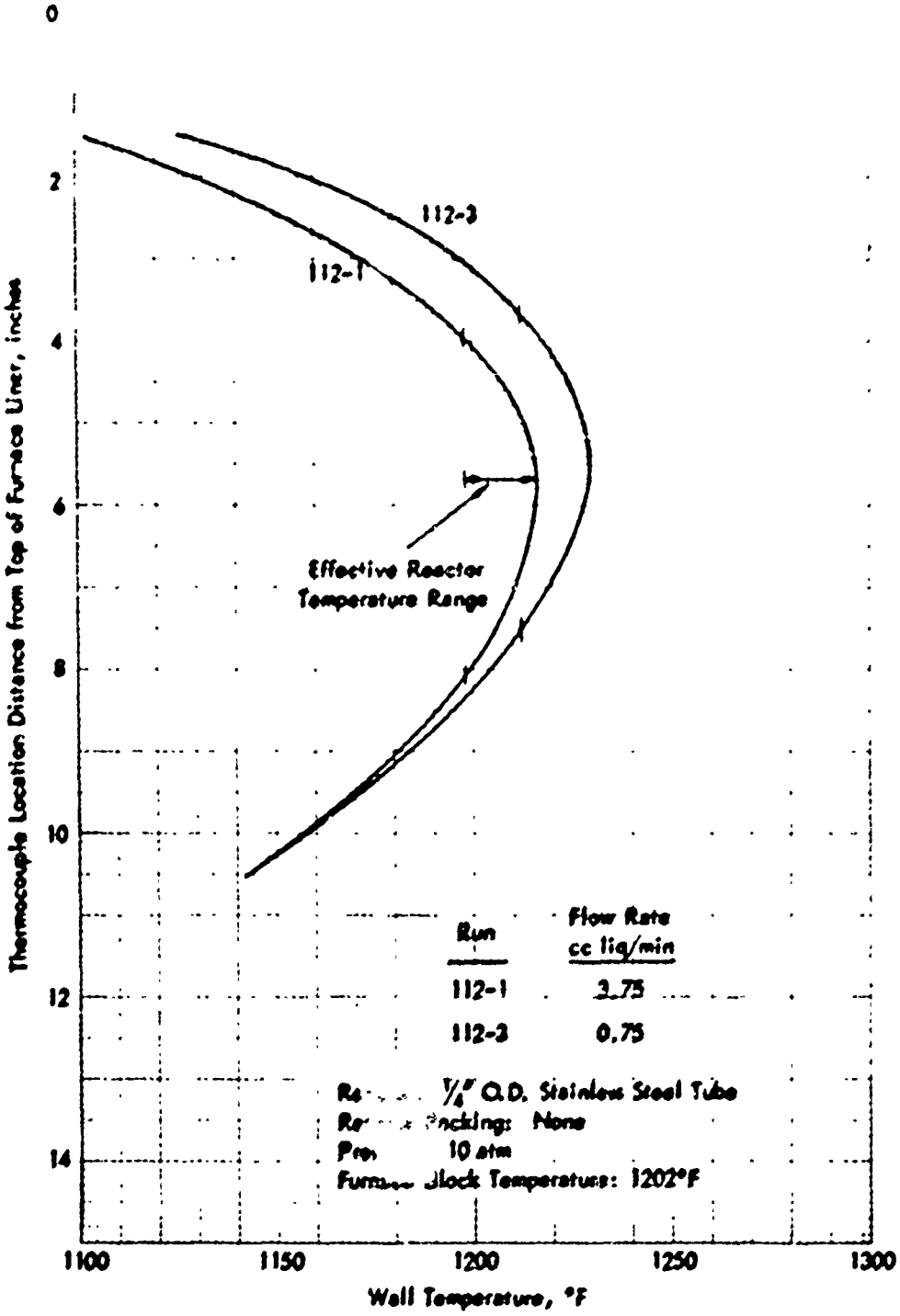

Figure 10. REACTOR TEMPERATURE PROFILE

64157

Methylcyclohexane

The complete data for the thermal reaction studies with MCH are presented in Tables 13 and 14 for 10, 30 and 68 atm, respectively. At constant space velocity, increased conversion was observed with increased pressure; presumably due to increased contact time. As an example at 1202°F and LHSV's of 65 to 75, conversions of 16.9%, 48.6% and 74.3% were observed at 10, 30 and 68 atm pressure. However, in these runs the first order rate constants varied only between 0.22 to 0.25 sec^{-1}, which suggests that the overall reaction rate was first order in MCH as found previously at the lower pressures.

At constant contact time, conversion appeared to be independent of pressure. This was concluded from the data of Figure 11 which shows conversion as a function of contact time (ACT) at three different pressures. Within the limits of experimental accuracy, the points for all three pressures fell on the same line at each temperature.

Liquid products were cracked liquids (several components lighter than benzene), benzene, toluene and three unidentified components that emerged on the GLC column before and after MCH and after toluene (Tables 13 and 14). Gas phase products were hydrogen and C_1 to C_4 hydrocarbons. Gas phase product distributions for a number of runs at various temperatures and pressures are tabulated in Table 15.

Pressure did effect the reaction product distribution. As an example, at 1202°F and constant conversion (i.e., same depth of cracking), increasing the pressure decreased the amount of cracked liquids and light gas plus coke; but increased the liquid components that emerged before and after MCH[a] (Table 16).

In the light gas fraction for these runs (Table 15), increased pressure increased the concentration of H_2, CH_4 and saturated hydrocarbons. Qualitatively more coke was formed at higher pressures as the reactor plugged in runs at 68 atm and 1252°F and LHSV of 150.

Decalin

Thermal reaction studies with Decalin were done at 10, 30 and 68 atm pressure. The complete data are tabulated in Tables 17 and 18 and are summarized in Figure 1. In general the results obtained with this naphthene were similar to those obtained with MCH. Thus at constant space velocity an increase in conversion was observed with increased pressure (cf Run 143 and 146-1, Table 17 and 107-3, Table 18), presumably due to increasing ACT. At comparable contact times (ACT) conversions and first order rate constants were essentially independent of pressure, signifying first order kinetics (Figure 12, cf Runs 154-2, 156-1, Table 17). Unlike MCH liquid product distribution did not appear to be effected by pressure.

Gas phase product distribution for a number of runs are shown in Table 19. As was observed with MCH increased pressure gave more H_2, CH_4 and saturated hydrocarbons, although the effect of pressure on product distribution

a) This material could well be paraffins and olefins formed by ring opening.

Table II. THERMAL REACTION OF MCH AT 10 ATM & ATM PRESSURE

Reactor filled with quartz chips
Reactor: 1/4" OD stainless steel; No. 304, Bishop and Co.
Reaction Time: 15 minutes
Feed: Pure MCH

10 atm Pressure

Run No. 10018-	115	117	120-1	120-2	121	123	124	125-1	135	136-1	136-2	172	173
Block Temperature, °F	1022		1112			1202			1252			1202	
MCH Flow Rate, cc/min	2.0	0.4	0.4	2.0	4.0	0.4	2.0	4.0	0.4	2.0	4.0	2.0	0.4
Effective Reactor Temp., °F	1035	1036	1126	1125	1123	1226	1218	1216	1276	1270	1270	1228	1230
LHSV[a]	88	12	16	82	168	16	75	154	16	37	168	82	11
ACT[b]	0.56	2.8	2.2	0.50	0.22	1.8	0.38	0.19	1.8	0.78	0.15	0.47	2.4
Product Analysis, %o													
Benzene	0.0	0.0	0.1	0.0	0.0	4.2	0.5	0.1	5.8	1.8	0.5	0.0	0.4
H_1	0.2	0.2	1.3	0.3	0.1	5.1	3.1	1.4	1.1	4.9	3.0	0.5	3.5
MCH	99.5	99.4	96.7	98.8	99.7	54.3	83.1	93.6	13.4	69.0	87.1	98.4	90.8
H_2	0.0	0.0	0.0	0.0	0.0	2.6	1.4	0.0	0.7	1.8	0.0	0.0	0.0
Toluene	0.1	0.1	0.1	0.1	0.0	3.1	0.6	0.0	3.0	1.5	0.7	0.0	0.7
H_3	0.0	0.1	0.6	0.2	0.0	2.7	1.4	0.8	1.8	2.1	1.4	0.5	1.4
Cracked Liquid	0.1	0.2	1.2	0.6	0.2	19.6	3.5	1.9	3.5	12.3	7.3	0.6	4.3
Light Gas and Coke	0.0	0.0	0.0	0.0	0.0	11.5	6.4	3.2	71.7	6.5	0.0	0.0	0.0
MCH Conversion, %o	0.5	0.6	3.3	1.2	0.3	48.7	16.9	6.4	86.6	31.0	12.9	1.6	20.0
First Order Rate Constant, sec^{-1}	-	-	0.0035	-	-	0.19	0.23	0.17	0.55	0.23	0.38	-	0.048

20 atm Pressure

Run No. 10018-	116	118	119-1	119-2	122-1	125-3	126-1	126-3	137	138-1	138-3	174	174-3
Block Temperature, °F	1022		1112			1202			1252			1202	
MCH Flow Rate, cc/min	2.0	0.4	0.4	2.0	4.0	0.4	2.0	4.0	0.4	2.0	4.0	2.0	0.4
Effective Reactor Temp, °F	1034	1033	1125	1125	1121	1222	1211	1208	1281	1283	1256	1128	1130
LHSV[a]	112	22	16	82	134	16	88	158	16	88	143	78	16
ACT[b]	1.8	9.8	6.7	1.5	0.78	5.5	1.3	0.58	5.3	1.3	0.88	1.3	6.8
Product Analysis, %o													
Benzene	0.0	0.0	2.3	0.3	0.0	17.2	6.6	1.1	6.6	18.2	2.7	0.2	6.5
H_1	0.6	1.6	7.4	2.0	1.7	7.6	10.0	6.6	0.6	5.3	0.0	2.7	19.7
MCH	98.0	97.6	80.2	94.7	96.7	37.6	54.6	79.5	21.3	25.3	85.3	82.5	50.6
H_2	0.0	0.0	2.1	0.0	0.0	0.0	2.2	2.0	0.0	2.2	2.6	0.0	5.6
Toluene	0.1	0.1	1.7	0.3	0.0	11.0	3.0	0.0	4.0	0.1	1.0	0.0	3.6
H_3	0.0	0.6	2.1	1.0	0.3	5.7	3.5	1.0	2.3	3.0	2.5	0.0	2.7
Cracked Liquid	0.3	0.6	5.7	2.0	1.3	11.2	15.0	8.1	1.5	16.6	13.0	2.7	11.2
Light Gas and Coke	0.0	0.0	17.4	0.0	0.0	12.0	0.2	0.0	63.6	30.7	4.1	0.0	12.0
MCH Conversion, %o	1.4	2.4	20.0	6.3	3.3	62.4	46.6	20.5	78.7	74.7	34.7	20.2	60.5
First Order Rate Constant, sec^{-1}	-	0.0027	0.037	0.028	0.025	0.086	0.25	0.10	0.14	0.53	0.24	0.082	0.205

a) Based on quartz volume.
b) Based on void volume.

Table 14. THERMAL REACTION OF MCH AT 68 ATM PRESSURE

Reactor filled with quarts chips
Reactor: 1/4" OD stainless steel; Bishop and Co.
Reaction Time: 15 minutes
Feed: Pure MCH

Run No. 11018-	164	165	166-1	166-2	167	168	169	170-1	170-2	175-1	175-2
Block Temperature, °F	←1022→		←1112→				←1202→			←1112→	
MCH Flow Rate, cc/min	4.0	2.0	0.4	4.0	2.0	0.4	4.0	2.0	0.4	2.0	0.4
Effective Reactor Temp, °F	1031	1035	1036	1123	1125	1128	1208	1213	(c)	1125	1128
LHSV[a]	123	61	12	138	64	12	150	67		65	14
ACT[b]	1.8	3.7	18.7	1.4	3.3	17.6	1.3	3.0		3.9	12.6
Product Analysis, %w											
Benzene	0.0	0.0	0.3	0.3	1.4	5.7	3.6	8.7		1.2	10.5
U_1	0.8	1.9	6.8	5.7	10.6	6.3	13.6	10.0		11.0	9.9
MCH	99.1	97.5	88.6	90.3	74.7	54.6	51.4	25.7		79.8	31.5
U_2	0.0	0.0	0.0	0.0	5.5	0.0	5.8	3.4		0.0	3.9
Toluene	0.0	0.0	0.8	0.5	0.5	4.9	2.9	7.2		1.0	9.4
U_3	0.0	0.4	1.0	1.2	1.7	9.4	3.4	5.8		1.8	1.9
Cracked Liquid	0.1	0.2	2.0	2.0	5.6	5.8	12.3	16.4		5.2	13.5
Light Gas and Coke	0.0	0.0	0.0	0.0	3.0	21.7	7.0	22.9		0.0	19.6
MCH Conversion, %w	0.9	2.5	11.4	9.7	25.3	45.4	48.6	74.3		20.2	68.5
First Order Rate Constant, sec^{-1}	-	0.0033	0.0032	0.032	0.043	0.017	0.24	0.22		0.034	0.037

a) Based on quarts volume.
b) Based on void volume.
c) Reactor plugged.

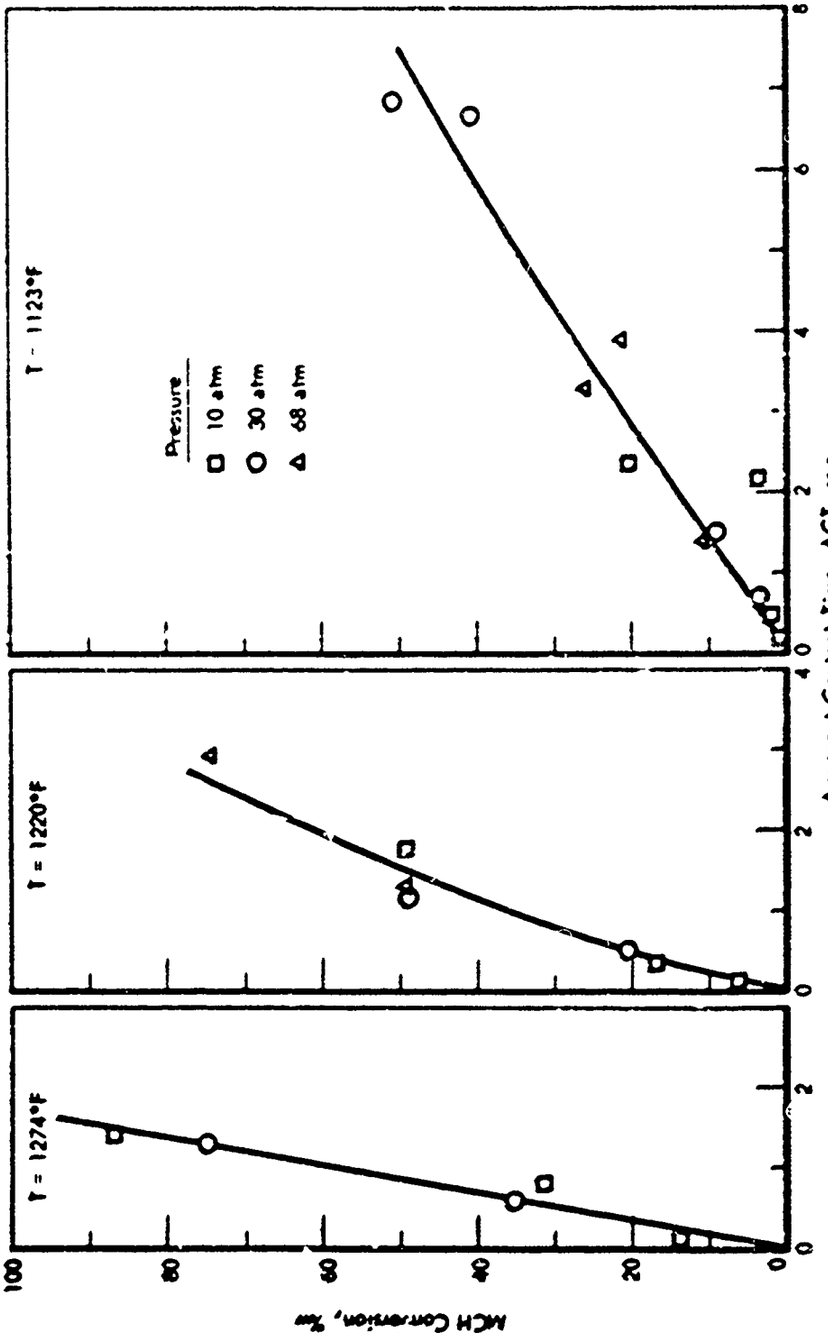

Figure 11. THERMAL REACTION OF MCH AT VARIOUS PRESSURES

65230

Table 15. THERMAL REACTION OF MCH AT VARIOUS PRESSURES
GAS PHASE PRODUCT DISTRIBUTION

Run Number: 1.0(8-	119-1	168	123	126-1	169
Pressure, atm	30	68	10	30	68
Block Temperature, °F	<—1112—>		<—1202—>		
ACT, sec	6.7	17.6	1.8	1.3	1.3
LHSV	18	12	16	68	150
MCH Conversion to, %w					
Light Gas and Coke	17.4	21.7	11.5	8.2	7.0
Total	39.8	45.4	48.7	48.6	48.6
Light Gas Composition, %w					
H_2	19.1	29.5	18.0	21.0	24.2
CH_4	41.7	51.0	34.7	47.6	53.2
C_2H_4	10.0	5.7	16.3	10.9	5.8
C_2H_6	13.3	8.2	10.6	10.9	9.8
C_3H_6	8.3	3.0	11.4	5.4	3.5
C_3H_8	4.2	2.0	2.5	2.3	2.2
Butadiene	--	--	1.7	0.3	--
C_4H_8	3.3	1.0	4.0	1.4	1.1
C_4H_{10}	--	--	0.4	0.3	0.4
Cyclopentadiene	--	--	0.4	--	--
C_5H_{10}	--	--	0.8	--	--

Table 16. THERMAL REACTION OF MCH LIQUID
PHASE IN [illegible]

Run Number: 11018-	123	126-1	169
Pressure, atm	10	30	68
ACT, sec	1.8	1.3	1.3
MCH Conversion, %w	48.7	48.6	48.6
First Order Rate Constant, sec^{-1}	0.18	0.25	0.24
Product Analysis, %w			
Benzene	4.2	4.6	3.6
U_1	5.1	10.9	13.6
MCH	51.3	51.4	51.4
U_2	2.6	3.2	5.8
Toluene	3.1	3.0	2.9
U_3	2.7	3.5	3.4
Cracked Liquid	19.6	15.6	12.3
Light Gas and Coke			

Table 17. THERMAL REACTION OF DECALIN AT 10 AND 30 ATM PRESSURE

Reactor filled with quartz chips
Reactor: 1/4" OD stainless steel; Bishop and Co.
Reaction Time: 15 minutes
Feed: F-113 DHN
Feed Composition: 25.0% trans-DHN
74.6% cis-DHN
0.4% THN

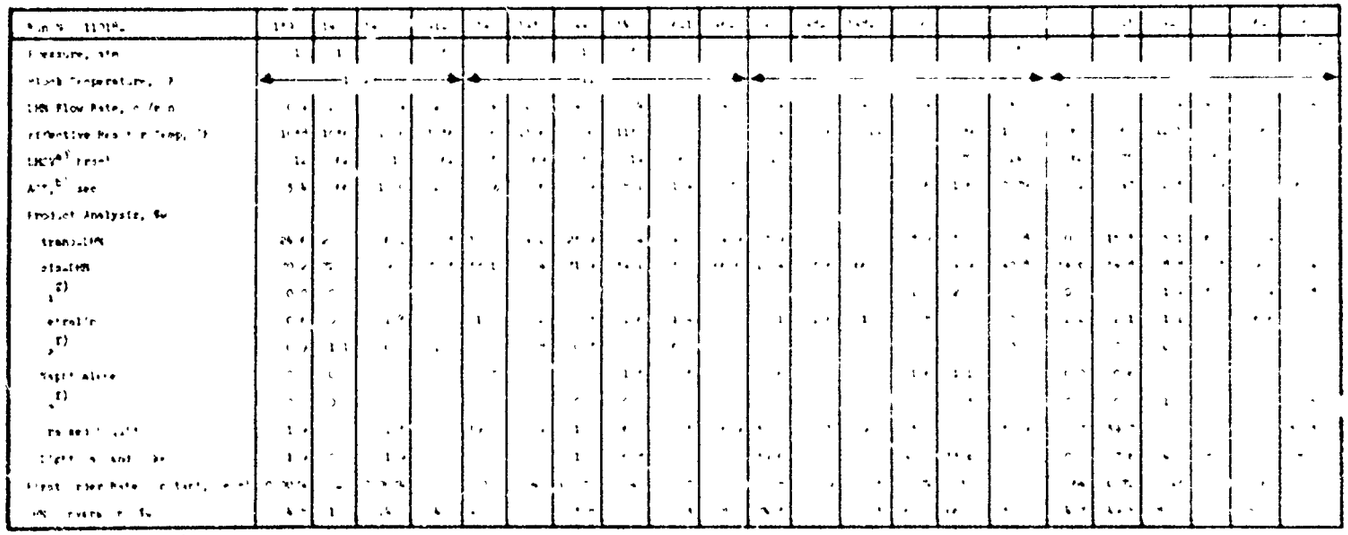

a) [illegible]
b) [illegible]
c) [illegible]
d) [illegible]
e) [illegible]
f) Unidentified.

Table 18. THERMAL REACTION OF DECALIN AT 68 ATMOSPHERES

Reactor filled with quartz chips
Reactor: 1/4-in. OD stainless steel tube, Bishop and Co.
Reaction Time: 15 minutes

Feed: F-113 DHN
Feed Composition: 25.0% trans-DHN
74.6% cis-DHN
0.4% THN

Run No. 11181-	104	105	106	107-1	107-3	108	109
Block Temperature, °F	← 1022 →			← 1112 →			1202
DHN Flow Rate, cc/min	4.0	2.0	0.4	4.0	2.0	0.4	4.0
Effective Reactor Temp, °F	1026	1031	1035	1112	1117	1126	1198
LHSV,[a] hr^{-1}	124	59	12	133	62	13	143
ACT,[b] sec	2.24	4.71	23.1	1.98	4.24	20.1	1.75
Product Analysis, %w							
trans-DHN	26.7	27.4	28.5	26.3	24.2	17.3	10.4
cis-DHN	66.8	60.1	42.9	48.2	34.0	29.0	22.9
U_1[c]	1.4	2.3	3.1	3.5	3.9	3.9	3.8
Tetralin	0.3	0.4	1.1	0.7	1.6	1.1	2.1
U_2[d]	0.1	0.2	0.0	0.0	0.0	0.0	0.0
Naphthalene	0.0	0.0	0.5	0.1	0.5	3.5	1.5
U_3[d]	0.0	0.0	0.3	0.2	0.2	2.3	1.5
Cracked, liquid	4.7	9.6	23.6	21.2	35.6	42.9	49.9
Light gas and coke	0.0	0.0	0.0	0.0	0.0	1.5	19.9
DHN Conversion, %w							
Total	6.5	12.5	28.6	25.5	41.8	53.7	58.7
Light gas and coke	0.0	0.0	0.0	0.0	0.0	1.5	19.9

a) Based on volume of empty tube.
b) Based on void volume (i.e., 1/2 volume of empty tube).
c) Emerged after trans-DHN and cis-DHN.
d) Unidentified.

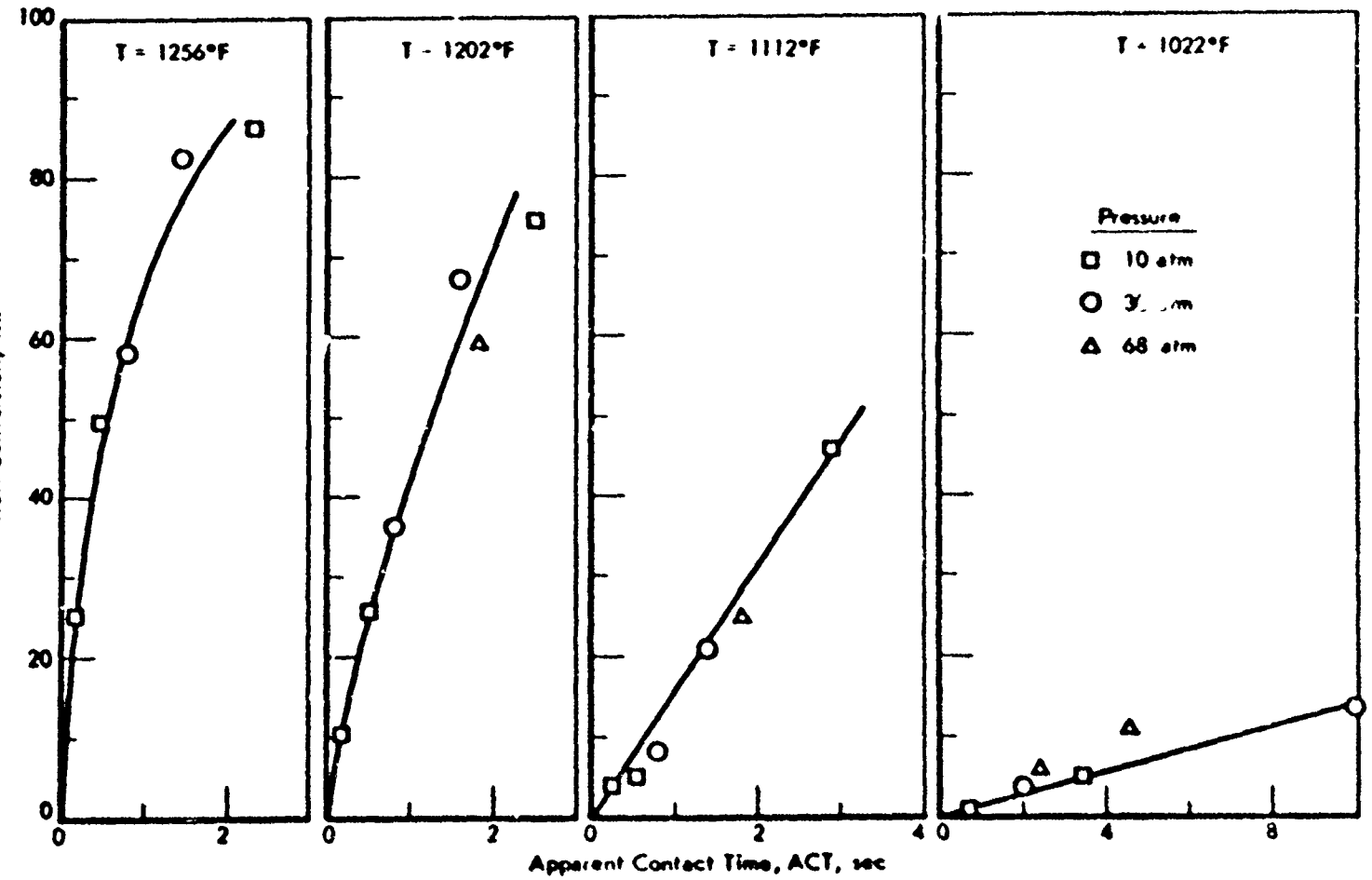

Figure 12. THERMAL REACTION OF DECALIN AT VARIOUS PRESSURES

Table 19. THERMAL REACTION OF DECALIN AT VARIOUS PRESSURES
GAS PHASE PRODUCT DISTRIBUTION

Run Number: 11013-	147	149	154-1	155	154-3	156-1
Pressure, atm	10	30	10	30	10	30
Block Temperature, °F	←1202→		←1252→			
ACT, sec	2.5	7.6	0.47	0.79	2.3	1.5
DHN Conversion to %						
Light Gas and Coke	39.6	41.5	7.6	8.1	24.5	21.8
Total	74.3	68.5	49.5	58.1	85.5	82.7
Light Gas Composition, %						
H_2	19.7	19.1	24.1	30.0	20.0	23.2
CH_4	33.6	40.4	29.0	34.4	35.1	38.7
C_2H_4	16.4	12.4	22.7	14.4	16.1	12.2
C_2H_6	14.9	16.1	11.9	12.3	14.8	15.4
C_3H_6	8.1	5.6	7.6	4.5	7.5	4.9
C_3H_8	4.6	5.2	2.9	3.8	3.5	4.4
Butadiene	0.3	--	0.5	--	0.2	0.8
C_4H_8	1.7	0.1	1.1	0.6	1.6	0.3
C_4H_{10}	0.2	--	0.1	0.2	0.2	--
Pentadiene	0.1	--	--	--	0.2	--
C_5H_{10}	0.0	--	0.1	--	0.1	--
Others	0.0	--	0.1[a]	--	0.2[b]	--

a) Acetylene.
b) 0.1% benzene; 0.1% cyclopentadiene.

was not as pronounced as with MCH. Considerable coke formation was observed at high pressure with Decalin (68 atm) and in one run at 1252°F and 68 atm the reactor plugged after about four minutes reaction (at 6 sec contact time).

Based on conversions and first order rate constants Decalin was at least twice as reactive as MCH in these tests.

Summary

With both monocyclic (MCH) and dicyclic (DCH) naphthenes the overall thermal reaction appeared to be first order in naphthene concentration. Pressure did appear to effect the reaction path and generally, more H_2, CH_4 saturated hydrocarbons (C_2-C_4) and coke were observed at the higher pressures. Further, with the monocyclic naphthene there was less cracked liquids (i.e., lighter than benzene) and more material heavier than benzene at the higher pressures. This pressure effect on liquid products was not observed with the dicyclic. Pressure appeared to enhance coke formation, more so with the dicyclic. However, on the basis of these data it is difficult to separate the effects of pressure and contact time. In these tests the dicyclic was at least two times more reactive than the monocyclic. These results are preliminary and the work is continuing.

RJ-4 (Tetrahydromethylcyclopentadiene Dimer)

RJ-4 is a bridged-ring hydrocarbon, tetrahydromethylcyclopentadiene dimer, obtained from Esso Research and Engineering Co. as TH Dimer Ramjet. There is some interest in this material as a fuel for air breathing and rocket engines and we have evaluated it in our bench-scale reactor.

RJ-4 consisted of a mixture of numerous compounds, possibly isomers, of which three made up 84% of the material. These were present in the ratio I:II:III = 10:51:22. Figure 13 shows a GLC chromatogram of RJ-4. The liquid density is 0.918.

RJ-4 was tested under conditions of vapor phase thermal reaction at furnace block temperatures of 842-1202°F and 1 to 10 atm pressure. The reactor was a 1/4-in. OD stainless steel tube with no packing in the tube.

In the 1/4-in. OD tube the wall temperature was measured at seven points along the tube. The points were 1-1/2 inches apart and the top point was one inch below the top of the secondary liner. The portion of the tube above the secondary furnace liner served as a preheat section and was kept at 770°F. The temperature of the reactor wall varied down the tube.

The maximum reaction rate will occur in the region of maximum temperature. Presumably the rate in that portion of the tube whose temperature was 18°F (10°C) or more below the maximum temperature, did not contribute appreciably to the overall rate. Thus the "effective" volume of the tube was that portion of the tube whose temperature was within 18°F of the maximum wall temperature, and whose volume was determined from a plot such as Figure 14. The "effective" reactor temperature was taken as 9°F below the maximum temperature and space velocities and Apparent Contact Times (ACT) were calculated based on the effective volume and effective reactor temperature.

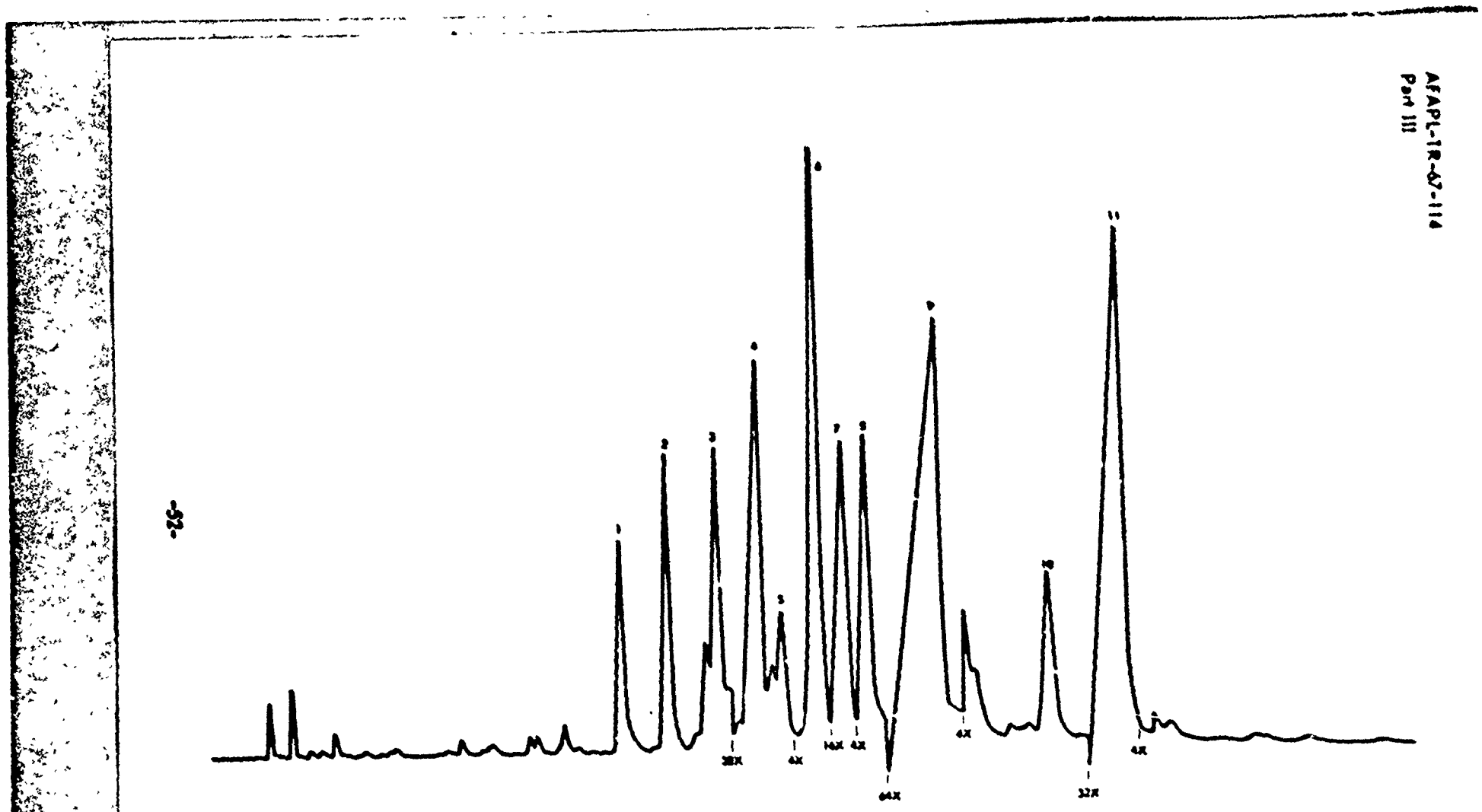

Figure 13. GLC CHROMATOGRAM OF RJ-4

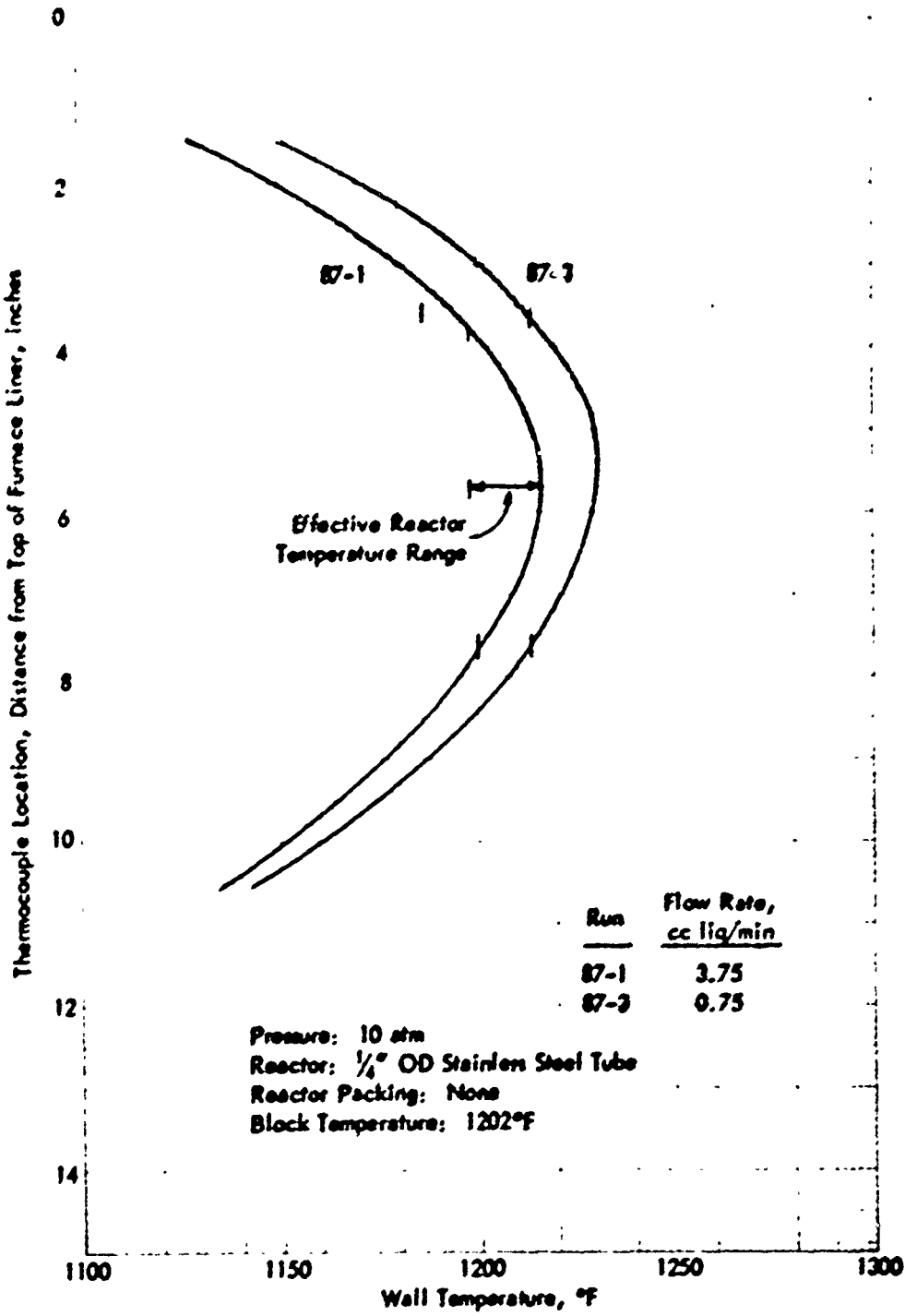

Figure 14. THERMAL REACTION OF RJ-4: REACTOR TEMPERATURE PROFILE

Liquid product material was analyzed by GLC using a 165-ft capillary column (0.018-in. diameter) coated with 20% polyphenyl ethers in DC-710 silicone. Gas products were analyzed by mass spectrometry. Conversions were calculated from product analyses and neglect coke or polymer formed during reaction.

At the lower temperatures and shorter contact times (ACT), RJ-4 was reasonably stable and less than 2% conversion was observed (842-1022°F; 0.6 sec ACT; Table 20). With increased temperature or contact time, conversion increased. For example, at 1202°F 67% conversion was observed at 3 seconds ACT compared to 22-27% at about 0.6 ACT (cf Runs 87-3 with 87-1 and 74-1); while at 1022°F only 5-11% conversion was observed at 4.5-4.7 sec ACT (Runs 73-3 and 86). The complete data are shown in Table 20 which includes data for SHELLDYNE-H obtained under comparable reaction conditions and reported last year[15] (shown in parentheses).

Product analyses are shown in Table 21. Based on the disappearance of the various components it appeared that Component I was the least reactive and Component III was the most reactive. Some coke was formed and in one run the coke formed plugged the reactor tube (Run 74-1). No quantitative measurement was made of the coke formed, however.

Based on overall conversion and on first order rate constants, RJ-4 was somewhat more reactive (i.e., less thermally stable) than SHELLDYNE-H.

Pulse Reactor Studies

Dehydrogenation of Methylcyclohexane With Dispersed Catalyst

The concept of dissolving an additive in a fuel, which would catalyze a chemical reaction when the mixture is passed through a hot tube, is attractive one. For example in such a system there would be no excessive pressure drop at high linear velocities (for a reasonable tube diameter). The feasibility of using such a system with about 1% of a fuel additive as a homogeneous catalyst for methylcyclohexane dehydrogenation was shown by some calculations presented in a previous report.[16] Thus for modest collision efficiencies (10^{-6} to 10^{-10}) high reactivities were indicated in the temperature region of 500-1200°F. In an application to a high speed air vehicle the finely divided catalyst would go into the engine along with the fuel and be exhausted into the atmosphere. Some exploratory experiments, done in a static system, were reported previously.[16] Further exploratory work now has been done in a pulse reactor system, with MCH containing various additives.

In a pulse reactor system a small amount of feed (1 µl) is injected via a syringe into a stream of carrier gas (H_2), which is then passed through a heated reactor tube and into a GLC for product analysis. Our system was described in detail in a previous report.[16] The reactor was a 1/4-in. OD stainless steel tube and contained no quartz chips.

The experiments were carried out at 10 atm pressure, 842-1202°F with H_2 carrier gas at an apparent contact time of about 10 seconds. One microliter of MCH solution was injected as a pulse. Analyses of reaction products were carried out by GLC. Most of the additives were only sparingly

Table 21. THERMAL REACTION OF RJ-4

Product Analyses

Reactor: 1/4-in. OD stainless steel tube
Reactor Packing: None
U_1 = emerged before I, includes cracked liquid
U_2 = emerged after I and before II
U_3 = emerged after II and before III
U_4 = emerged after III

Run No.	Feed	65-1	65-3	66-1	67	68-1	68-3	70	71	72	73-1	73-3	74	85	86	87-1	87-3
Pressure, atm		1	5	10	1	5	10	1	5	10	10	10	10	10	10	10	10
Temperature, °F																	
Block		← 842 →			← 1022 →			← 1202 →			← 1022 →		1202	← 1022 →		← 1202 →	
Effective Wall		848	844	844	1042	1031	1024	1225	1234	1224	1033	1033	1213	1024	1031	1209	1222
Product Analyses, %																	
U_1	2.9	4.9	3.7	1.7	3.0	2.9	2.9	15.2	11.4	8.7	3.7	6.6	29.1	3.4	9.2	77.6	64.8
I	9.9	10.6	10.0	9.8	9.9	9.8	10.8	9.6	9.7	9.5	10.7	10.4	8.2	10.0	11.8	9.4	4.9
U_2	12.6	13.3	12.9	12.8	12.7	14.4	11.8	16.5	13.1	13.4	11.9	13.7	12.2	12.6	12.8	12.5	8.4
II	51.3	50.2	50.3	51.3	51.2	51.5	51.4	45.4	46.9	48.3	50.6	49.3	37.5	48.9	45.4	38.7	13.6
U_3	0.8	0.9	1.0	0.9	0.9	0.6	0.6	0.5	0.5	0.9	1.0	0.9	0.4	2.9	2.6	2.2	2.5
III	22.4	21.7	22.0	22.4	22.2	22.5	22.5	14.8	17.9	19.2	22.2	19.2	12.4	22.0	13.8	13.8	3.5
U_4	0.1	0.1	0.1	0.0	0.1	0.0	0.0	0.0	0.0	0.0	0.7	0.0	0.2	0.1	0.2	0.2	2.3
RJ-4 Conversion, %	-	1.7	1.4	0.2	0.4	0.6	1.3	14.1	9.6	6.7	1.9	5.3	26.8	4.0	10.6	22.4	67.0

soluble in MCH. Thus most of these tests were qualitative as the additive concentrations were not known exactly.

The results for a series of tests at 1022°F (Series I) using twenty-two different additives are summarized in a bar graph (Figure 15); which shows MCH conversions and selectivities for toluene and benzene. DC-11 was the most active additive but selectivity was poor for toluene (12%) and benzene (3%). DC-21 and DC-20 were less active but had greater selectivity for aromatics (20-30%). DC-8 and DC-9 were moderately selective for benzene (4-10%) but gave only 5% MCH conversion. Eight additives were inactive which may have been due to lack of solubility. The data are presented in Table 22. In order to differentiate between conversion due to additives and that due to pure thermal reaction, the series of tests included runs with pure MCH. The conversion due to the additives then was the observed conversion (MCH plus additive) minus the conversion due to thermal reaction (determined in the run with pure MCH). The corrected values were plotted in Figure 15.

A few runs were made with the more active additives to see the effect of temperature and space velocity on conversion. In a series of runs with DC-8 (2%), DC-9 (4.5%) and pure MCH (1112 to 1202°F, LHSV of 6.7-13), increased conversion was observed with increased temperature and decreased space velocity (Figure 16). With DC-8, conversions were about those observed with pure MCH, but product distributions were different. Thus more benzene and less cracked products were obtained (Table 23), which suggests that both catalytic and thermal reactions occurred concurrently with the DC-8 additive. Similar results were observed with DC-9, although conversions were higher than were obtained with DC-8 (Table 23), presumably because of the higher additive concentration.

The effect of temperature on conversion for DC-21 additive (9.5%) is shown in Figure 17. In these tests with increasing temperature (752 to 1202°F, LHSV = 6.7) conversion increased in the region 752 to 932°F, was relatively constant at 932 to 1022°F and then increased markedly in the region 1022 to 1202°F. Further, at the higher temperatures (1112 to 1202°F) conversions were the same as for pure MCH (Table 24). This suggests that the catalyst was poisoned after a certain amount of MCH was converted (i.e., the amount converted at 932°F) and that any further conversion was due to thermal reaction. As there was little or no thermal reaction at 1022°F (Table 24), MCH conversion at this temperature was about that at 932°F.

In another series of tests (Series II), twenty-seven compounds, each containing one of seventeen different elements were tested. The concentration of additive in MCH was 6% or less and in some cases was limited by solubility.

The results at 1022°F are summarized in a bar graph (Figure 18) which shows MCH conversion, selectivity for toluene plus benzene, and the concentration of additive in MCH. The detailed data are shown in Table 25 and summarized in Table 26. In this series of tests 199-27 was the most active with about 22% conversion and 200-3 was the most selective with 31% selectivity for aromatics. However in general conversions were less than 10% and selectivities were 15 to 30%. As there were only seventeen elements represented in the twenty-seven compounds tested, it is obvious that the nature of the additive molecule influenced the activity and selectivity for aromatics in these tests.

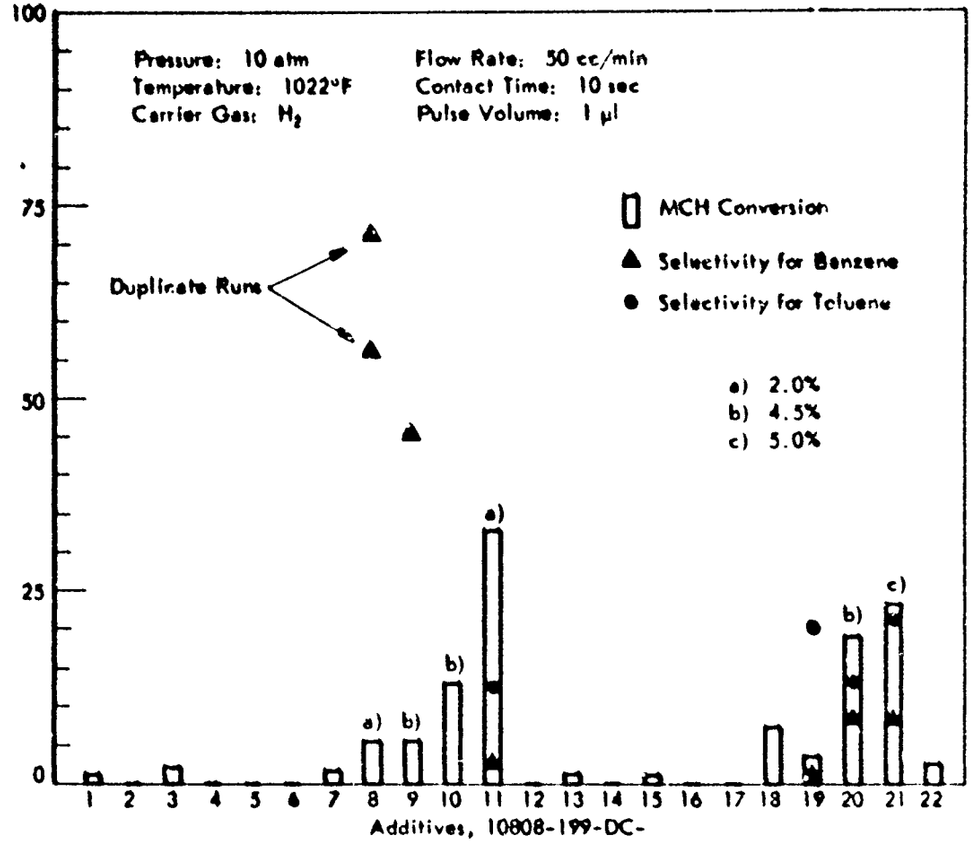

Figure 15. REACTION OF MCH WITH VARIOUS ADDITIVES. PULSE REACTOR

64677

Table 22. EFFECT OF VARIOUS ADDITIVES ON REACTIVITY OF MCH AT 2 WHSV, FIXED BED

Pressure: 10 atm
Carrier Gas: H_2
Flow Rate: 50 cc/min
Feed: MCH plus additive
Pulse Volume: 1 ml
LHSV: 6.7

Run 10808-	Catalyst 10808-199-DC-	Product Analysis, %w					MCH Conversion, %w		Additive in Feed, %w
		Cracked	MCH	Benzene	Toluene	Others	Obs	Corrected	
99-1	none	1.5	97.6	-	-	0.9	2.4	-	-
99-2	1	2.9	96.3	-	-	0.8	3.7	1.2	sat.
99-3	none	2.7	97.0	-	-	0.3	3.0	-	-
100-1	2	2.9	96.4	-	-	0.7	3.6	0.6	sat.
100-2	3	4.9	94.6	-	-	1.1	5.2	2.2	sat.
100-3	none	3.5	95.2	-	-	1.3	4.8	-	-
100-4	4	3.9	95.1	-	-	1.0	4.9	0.1	sat.
101-1	5	3.5	95.4	-	-	1.1	4.6	-0.2	sat.
101-2	6	3.2	95.8	-	0.1	0.9	4.2	-0.6	sat.
101-3	22	5.8	93.4	-	0.1	0.7	6.6	2.2	sat.
102-1	13	3.9	93.9	-	0.1	2.1	6.1	1.3	sat.
102-2	none	2.8	96.9	-	-	0.3	3.1	-	-
102-3	11	30.7	64.6	0.6	3.9	0.0	35.4	32.3	sat.
102-4	none	2.8	96.8	-	-	0.4	3.2	-	-
107-1	none	1.8	98.0	-	-	0.2	2.0	-	-
107-2	7	2.9	96.3	-	-	0.8	3.7	1.7	sat.
107-3	none	2.8	96.3	-	-	0.9	3.7	-	-
107-4	8	3.4	90.8	3.1	-	2.7	9.2	5.5	sat.
108-2	8	2.8	91.9	3.1	-	2.2	8.1	4.4	sat.
108-4	9	5.4	90.7	2.5	-	1.4	9.3	5.6	5.8
109-1	none	2.7	96.6	-	-	0.7	3.4	-	-
109-2	10	13.9	83.6	-	-	2.5	16.4	13.0	5.3
59-1	none	0.3	99.3	0.1	0.1	0.2	0.7	-	-
59-2	21	7.9	87.5	0.4	3.7	0.5	12.5	11.8	9.5
51-1	none	0.4	99.1	-	0.1	0.4	0.9	-	-
51-2	14	0.3	99.3	-	0.1	0.3	0.7	-0.2	sat.
51-3	17	0.3	99.3	-	0.1	0.3	0.7	-0.2	sat.
52-1	12	0.4	99.2	-	0.1	0.3	0.8	-0.1	sat.
52-3	18	4.4	92.6	0.5	1.6	0.9	7.4	6.6	sat.
84-1	none	1.2	97.8	-	0.1	0.8	2.2	-	-
84-2	19	2.6	94.4	0.1	0.8	2.1	5.6	3.4	sat.
74-4	none	0.5	99.1	0.1	0.1	0.2	0.9	-	-
74-5	20	14.3	81.2	1.6	2.4	0.5	18.8	17.9	4.8
46-1	none	0.3	99.1	0.2	0.1	0.3	0.9	-	-
46-4	15	0.4	98.6	-	0.1	0.9	1.4	0.5	sat.
47-1	16	0.4	98.9	0.3	0.1	0.3	1.1	0.2	sat.

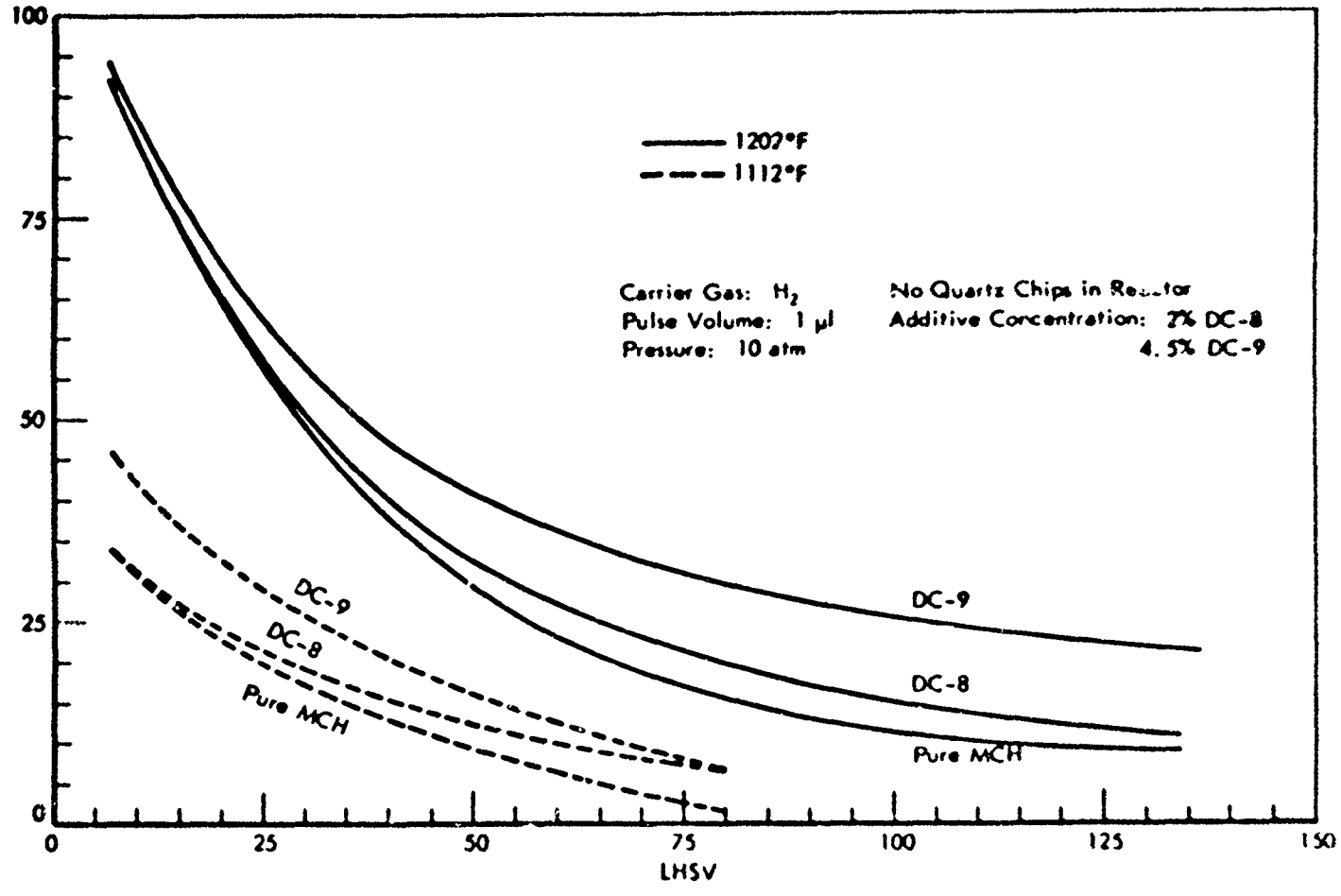

Figure 16. DEHYDROGENATION OF MCH WITH ADDITIVES DC-8 AND DC-9 PULSE REACTOR

Table 23. EFFECT OF ADDITIVES DC-8 AND DC-9 ON REACTIVITY OF MCH AT 1112 AND 1202°F; PULSE REACTOR

Pressure: 10 atm
Carrier Gas: H_2
Additive Concentration: 2% and 4.5%
Feed: MCH Plus Additive
Pulse Volume: 1 µl

Run No 10808-	Additive 10808-199-DC-	Temp, °F	LHSV	Product Analysis, %w					MCH Conversion, %w	
				Cracked	MCH	Benzene	Toluene	Others[a]	Observed	Corrected[c]
111-2	None	1112	6.7	30.3	66.0	0.5	1.8	1.5	34.0	-
111-3	8	1112	6.7	25.5	67.0	4.2	0.2	3.1	33.0	-1
111-4	9	1112	6.7	34.6	54.2	7.1	1.1	3.0	45.8	11.8
110-1	None	1112	80	0.6	98.7	-	-	0.7	1.3	-
110-2	None	1112	80	1.3	98.4	-	-	0.3	1.6	-
110-3	8	1112	80	2.3	93.8	2.6	-	1.3	6.2	4.7
111-1	9	1112	80	2.8	93.5	1.4	-	1.3	6.3	5.0
113-3	None	1202	6.7	85.7	6.3	-	2.6	5.3	93.7	-
113-4	8	1202	6.7	79.3	7.6	8.7[b]	2.0	2.4	92.2	-1.5
113-5	9	1202	6.7	78.3	6.0	12.2	3.5	-	94.0	+0.3
112-4	None	1202	80	13.4	84.5	-	-	2.5	15.5	-
113-1	8	1202	80	12.5	80.6	4.7	-	2.2	19.4	3.9
113-2	9	1202	80	21.6	70.6	4.7	0.4	2.9	29.5	14.0
112-1	None	1202	134	7.7	90.7	-	-	1.6	9.3	-
112-2	8	1202	134	5.4	89.1	2.6	-	1.9	10.9	1.6
112-3	9	1202	134	15.6	78.4	3.3	-	2.8	21.6	12.5

a) Emerged after benzene.
b) Fresh catalyst.
c) Corrected by subtracting amount of thermal reaction.

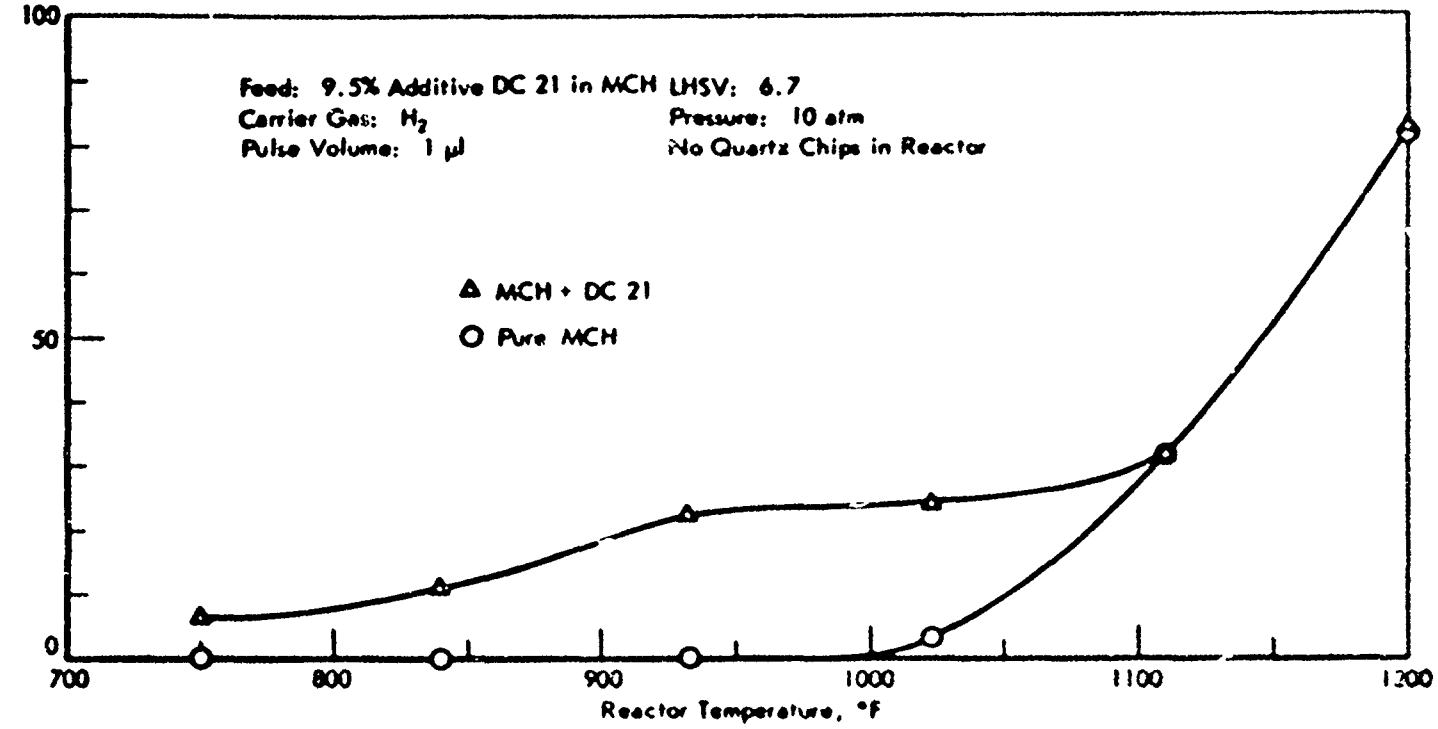

Figure 17. REACTION OF MCH WITH ADDITIVE DC-21 AT VARIOUS TEMPERATURES PULSE REACTOR

Table 24. EFFECT OF ADDITIVE DC-21 ON REACTIVITY OF MCH AT VARIOUS TEMPERATURES: PULSE REACTOR

Pressure: 10 atm Feed: MCH + 9.5% Additive 21
Carrier Gas: N_2 Pulse Volume: 1 µl
Flow Rate 50 cc/min LHSV: 6.7

Run No 10808-	Additive 10808-199-DC-	Temp, °F	Product Analysis, %w				MCH Conversion, %w
			Cracked	MCH	Toluene	Others[a]	
34-1	none	752	-	99.9	0.1	-	0.1
34-3	21	752	5.6	93.3	1.1	-	6.7
35-1	none	842	-	99.9	0.1	-	0.1
35-2	21	842	7.6	89.0	3.3	0.1	11.0
35-3	none	932	0.2	99.7	0.1	-	0.3
36-1	21	932	16.1	77.8	5.9	0.2	22.2
36-3	none	1022	2.8	96.2	0.9	0.1	3.8
37-1	21	1022	19.2	76.2	4.1	0.5	23.8
37-3	none	1112	28.7	68.5	0.5	2.3	31.5
38-1	21	1112	27.7	69.0	1.3	2.0	31.0
38-3	none	1202	76.8	19.0	2.7	1.5	81.0
39-1	21	1202	78.6	17.0	2.8	1.6	83.0

a) Emerged after benzene.

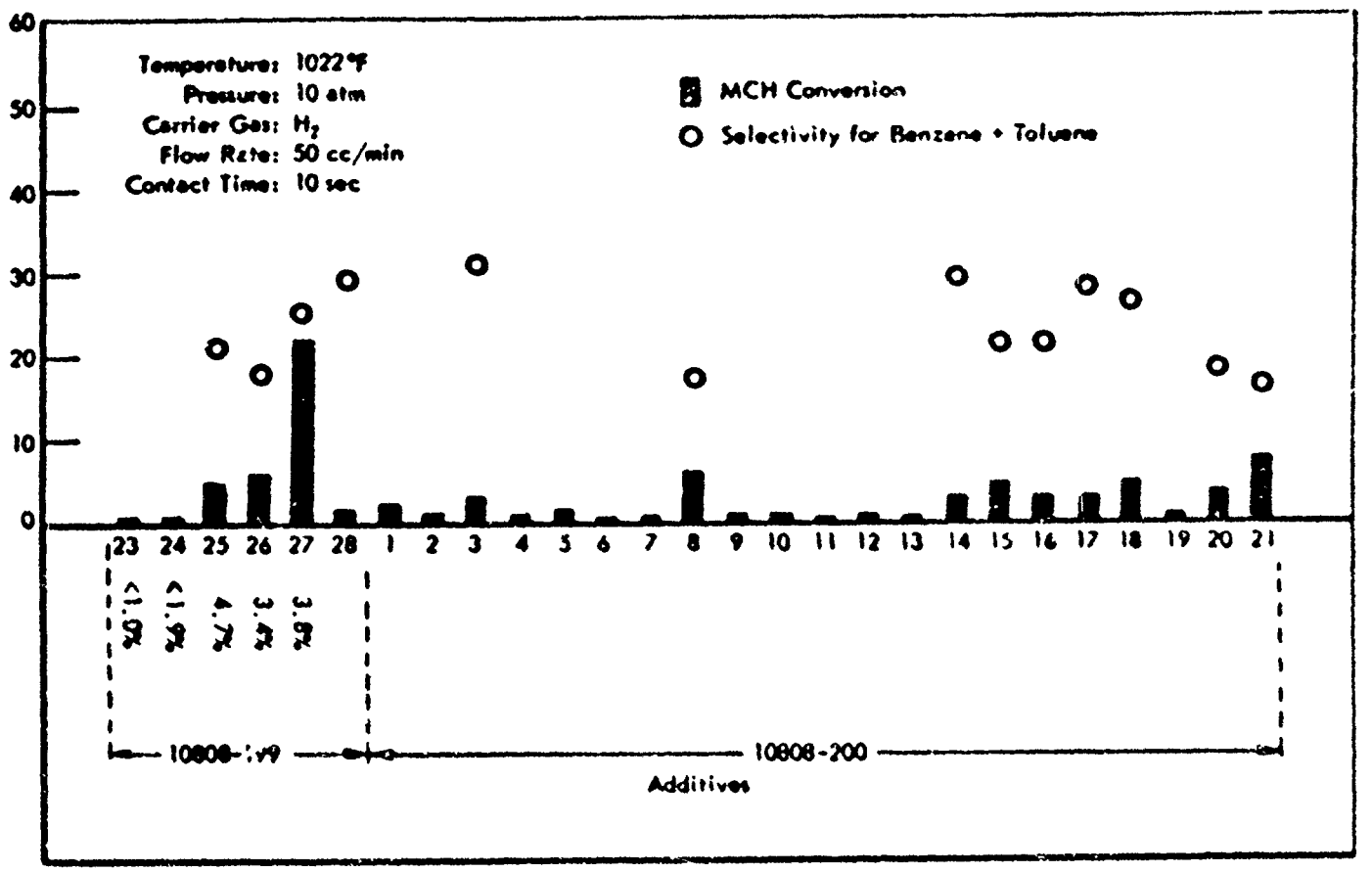

Figure 18 REACTION OF MCH WITH VARIOUS ADDITIVES: PULSE REACTOR

Table 25. EFFECT OF VARIOUS ADDITIVES ON REACTIVITY OF MEH AT 1022°F

Pulse Volume 1 ml
Pressure 15 atm
Carrier Gas N2
Flow Rate 5 cc/min
LHSV 4
Contact Time 0.5 to 0.5 sec
Reactor Temperature 1022°F

Run 11018-	Catalyst: ASA-3-Pellets	Catalyst in Feed, %	Product Analysis					MEH Conversion, %	
			Methane	MEH	Benzene	Toluene	Others	Uncorrected	Corrected
24-1	None		1.7	96.6	0.2	0.2	1.4	3.4	-
24-2	None	5.0	1.7	78.5	6.5	5.1	8.0	21.5	29.1
24-3	None		2.6	97.4	0.1	0.2	0.3	2.1	-
25-1	None		1.6	97.7	0.1	0.2	0.3	1.9	-
25-2	None	Sat. (<1.0)	1.0	98.4	0.2	0.2	0.2	1.6	0.3
25-3	None		1.4	98.6	0.2	0.2	0.6	1.0	-
25-4	None	Sat. <1.0	1.5	97.6	0.6	0.1	0.4	2.4	1.0
25-5	None		1.4	98.6	0.2	0.1	0.4	1.4	-
26-1	None	4.7	6.1	93.9	0.2	0.1	0.8	6.2	6.8
26-2	None		2.1	97.9	0.2	0.2	0.7	2.1	-
26-3	None	4.6	6.1	93.9	0.2	0.1	1.1	7.1	6.2
26-4	None		4.4	97.1	0.6	0.5	1.2	2.9	-
26-5	None	4.7	5.1	96.4	0.2	0.1	0.6	3.1	1.9
26-6	None		2.4	98.4	0.2	0.1	1.6	1.6	-
38-6	17A-A-200-DC 1	1.6	1.4	96.5	0.5	0.2	0.7	3.5	1.9
39-1	None		2.4	98.5	0.2	0.1	0.6	1.9	-
39-2	None	2	1.8	97.7	0.6	0.1	0.6	2.3	0.8
39-3	None		2.7	97.7	0.2	0.1	0.9	1.3	-
39-4	None	3	2.1	95.8	1.4	0.1	0.6	4.2	2.9
40-1	None		1.7	98.6	0.2	0.1	0.4	1.4	-
40-2	None	3.6	1.4	97.6	0.6	0.4	0.5	2.4	1.0
40-3	None		1.4	97.5	0.1	0.1	0.2	0.7	-
40-4	None	2.2	1.7	97.8	0.1	0.1	0.2	2.2	1.6
40-5	None		2.2	98.8	0.2	0.1	0.5	1.2	-
41-1	None	Sat.(<6)	1.1	98.4	0.2	0.1	0.2	1.6	0.2
41-2	None		1.1	98.9	0.2	0.1	0.2	1.1	-
41-3	None	Sat. <1.2	1.4	98.2	0.3	0.1	0.4	1.8	0.7
41-4	None		0.9	98.4	0.3	0.1	0.4	1.6	-
41-5	17A-7	Sat.(<1)	1.0	98.2	0.3	0.1	0.4	1.8	0.2
41-6	17A-21	5	30.4	75.6	0.6	1.6	0.0	24.4	28.6
42-1	None		0.9	98.5	0.2	0.1	0.4	1.5	-
42-2	17A-8	2	2.0	96.0	0.4	0.1	0.6	4.0	2.5
42-3	None		1.0	98.2	0.3	0.1	0.4	1.8	-
60-1	17A-7	Sat. (<1,	1.2	97.8	0.4	0.1	0.5	2.2	0.4
60-2	200-5	2.2	2.2	97.0	0.5	0.1	0.4	3.0	1.9
60-3	None		1.1	98.1	0.3	0.1	0.5	1.9	-
60-4	17A-9	4.5	4.6	92.8	1.0	0.2	1.4	7.2	5.3
61-1	None		0.1	99.6	0.1	0.1	0.1	0.4	-
61-2	200-6	Sat.(<2.7)	4.3	95.7	0.4	0.2	1.0	4.3	5.9
61-3	None		0.1	99.4	0.1	0.1	0.1	0.6	-
62-1	7	2.7	0.6	98.8	0.2	0.2	0.2	1.2	0.8
63-1	None		0.1	99.3	0.0	0.5	0.1	0.7	-
63-2	10	1.5	1.0	98.5	0.1	0.3	0.1	1.5	0.8
63-3	None		0.1	99.1	0.0	0.6	0.2	0.9	-
64-1	11	Sat.(<1.6)	0.6	98.6	0.1	0.5	0.2	1.4	0.5
64-2	None		0.1	99.1	0.0	0.6	0.2	0.9	-
64-3	12	Sat.(<2.4)	0.8	97.2	0.0	0.7	0.3	1.8	0.9
64-4	None		0.4	98.5	0.1	0.4	0.3	1.5	-
65-1	13	1	1.2	97.6	0.4	0.5	0.7	2.4	0.9
65-2	None		0.1	99.2	0.3	0.1	0.3	0.8	-
65-3	14	1	2.7	96.1	0.6	0.3	0.8	3.9	3.1
65-4	None		0.2	99.3	0.1	0.2	0.2	0.7	-
66-1	15	1	3.5	94.6	0.7	0.3	0.9	5.4	4.7
66-2	None		0.1	99.6	0.1	0.1	0.1	0.4	-
66-3	16	Sat.(<1)	1.6	96.3	0.4	0.2	0.5	3.5	2.9
66-4	None		0.1	99.4	0.1	0.2	0.2	0.6	-
67-1	17	1	1.9	96.5	0.5	0.3	0.8	3.5	2.9
67-2	None		0.2	99.3	0.1	0.2	0.2	0.7	-
67-3	18	1	2.8	95.0	0.8	0.3	1.1	5.0	4.3
68-1	None		0.1	99.6	0.1	0.1	0.1	0.4	-
68-2	19	1.6	1.0	98.6	0.2	0.1	0.1	1.4	1.0
68-3	None		0.3	99.2	0.1	0.2	0.2	0.8	-
69-1	20	4.5	3.1	95.4	0.5	0.2	0.8	4.6	3.8
69-2	None		0.6	98.8	0.1	0.3	0.2	1.2	-
69-3	21	6.4	6.1	91.5	0.9	0.3	1.2	8.5	7.1

a) Injected 20 ml before this run.

Table 26. REACTION OF MCH WITH VARIOUS ADDITIVES

Summary

Pulse Volume: 1 μl
Pressure: 10 atm
Carrier Gas: H_2
LHSV: 6.7

Additive	% C-H in Feed	MCH Conversion, %w		Selectivity for Benzene + Toluene, %w	
		450°C	550°C	450°C	550°C
10808-199-DC-23	Sat. <1.0	0.5	0.4	-	-
24	Sat. <1.9	0.2	0.6	-	-
25	4.7	1.0	4.8	-	21
26	3.4	1.5	6.1	-	18
27	3.8	9.7	22.1	41	25
28	1.8	0.2	1.7	-	29
10808-200-DC- 1	1.4	0.2	2.2	-	-
2	1.1	0.0	0.9	-	-
3	1.7	0.1	2.9	-	31
4	3.6	-	0.9		-
5	2.2	-	1.4	-	0
6	Sat. <3.4	-	0.3		-
7	Sat. <1.2	-	0.5		-
8	Sat. <2.7	-	5.9		17
9	2.7	-	0.8		-
10	1.5	-	0.8		-
11	Sat. <1.6	-	0.5		-
12	Sat. <2.4	-	0.9		-
13	1.0	-	0.9		-
14	1.0	-	3.1		29
15	1.0	-	4.7		21
16	Sat. <1.0	-	2.9		21
17	1.0	-	2.9		28
18	1.0	-	4.3		26
19	1.6	-	1.0		-
20	4.5	-	3.8		18
21	6.4	-	7.3		16

In a third series of tests (Series III) 46 compounds, eighteen of which were binary metallics were tested.

The results are shown in Table XI. Conversions were low; less than 15% (1022°F). Cracking appeared to be the main reaction and selectivities for benzene plus toluene were less than 30% except for two additives which gave 69% and 79% selectivity for conversion of 5 and 4%. Some synergism was observed with the bimetallic mixtures.

Summary and Conclusions

The results obtained thus far have demonstrated that fuel additives will catalyze both cracking and dehydrogenation reactions. For dehydrogenation, reaction rates were low with additives compared to those obtained in a fixed bed system with supported platinum catalysts. As an example, the best result obtained with additives was 32% conversion at about 10 seconds contact time, compared to 90% conversion at about 0.1 seconds contact time with the fixed bed (1022°F). Thus to be comparable to fixed bed operation an increase in activity of at least two orders of magnitude over rates now obtained with fuel additives is needed.

Cracking was the principal reaction observed with fuel additives and best yields of aromatics were only about 4% (% yield = % conversion times % selectivity divided by 100).

In these tests some evidence of decomposition products and some residual activity was observed. This suggests that the additive decomposed to form the catalyst, although the possibility that undecomposed additives can act as catalysts has not been abandoned. In all 95 additives were tested. Some of these contained more than one metal and some synergism was observed. Due to poor solubilities of the additives in the feed, quantitative results were obtained for only a few compounds. Other methods for dispensing additives (i.e., catalysts) in MCH are being considered.

Dehydrogenation of Methylcyclohexane Over Various Catalysts

In a previous report it was shown that the rate of dehydrogenation of methylcyclohexane (MCH) with the standard platinum catalyst was about 300 times greater in a pulse reactor than in the standard continuous flow bench-scale reactor.[16] It was presumed that this enhanced activity in the pulse reactor was due to higher catalyst particle temperatures (at a given furnace temperature) and to less diffusion effects in the pulse reactor. Consequently, it was of interest to evaluate a few of these catalysts in the pulse reactor and to compare relative activities under conditions of a very small endothermic heats of reaction and with a minimum of diffusion effect. These catalysts had been evaluated previously in continuous flow bench-scale tests.[20]

Four laboratory-prepared and two commercial catalysts were tested at 10 atm pressure, and 662 and 752°F. These were:

Table XI. REACTION OF MCH WITH VARIOUS ADDITIVES

Pulse Volume: 1 ml
Pressure: 10 atm
Carrier Gas: He
LHSV: 6.7

Additive	Additive in Feed, %	MCH Conversion,[a] %w		Selectivity for Benzene + Toluene, %w	
		842°F	1022°F	842°F	1022°F
10308-200-DC-22	2	3.8	2.9	79.0	76.0
23	2	1.0	0.0	12.5	-
24	2	3.2	1.4	69.0	0.0
25	2	2.7	3.3	6.9	0.0
11018-199-DC- 1	4	-	8.7	-	5.7
2	2	-	4.3	-	11.6
3	4	-	4.4	-	9.1
4	4	-	12.7	-	5.5
5	4	-	14.6	-	4.8
6	4	-	5.4	-	7.4
7	4	-	11.0	-	6.4
8	4	-	6.5	-	9.1
9	2	-	5.7	-	10.5
10	2	-	1.7	-	29.4
11	4	-	11.7	-	5.1
12	4	-	7.7	-	7.8
13	2	-	3.2	-	3.1
14	4	-	4.2	-	2.4
15	4	-	6.0	-	18.3
16	4	-	3.3	-	27.3
17	4	-	12.1	-	8.3
18	4	-	6.8	-	14.7
19	4	-	6.9	-	2.9
20	4	-	10.4	-	8.7
21	4	-	2.1	-	3.2
22	4	-	4.0	-	2.0
23	2	-	4.0	-	2.0
24	2	-	3.0	-	5.0
25	2	-	2.2	-	3.0
26	2	-	2.7	-	3.0
-200-DC- 1	4	1.8	3.1	16.6	25.8
2	4	2.4	2.9	8.2	6.9
3	4	2.4	2.4	8.2	29.2
4	4	2.5	1.3	8.0	46.2
10808-199-DC-21	4.5	5.5	30.2	29.1	3.0

a) Corrected for conversion obtained with pure MCH.

(Continued)

Table 27 (Contd). REACTION OF MCH WITH VARIOUS ADDITIVES

Additive	Additive in Feed, %	MCH Conversion, %w		Selectivity for Benzene + Toluene, %w	
		842°F	1022°F	842°F	1022°F
11018-200-DC- 1	4	3.0	-	13.3	-
2	4	3.9	-	20.5	-
3	4	3.6	-	19.4	-
4	4	3.0	-	13.3	-
10808-199-DC-21	4.5	6.9	-	35.3	-
11018-200-DC- 5[a]	10	0.5	-	0.0	-
6	4	4.5	5.3	15.6	22.9
7	4	3.6	3.4	2.8	4.3
7[a]	4	2.0	-	5.0	-
8	4	2.2	7.0	45.5	8.6
9	4	3.2	6.5	6.1	4.7
10	4	3.4	12.2	2.9	2.1
11	4	-	9.6	-	4.2
12	4	-	8.7	-	4.6
13	4	-	8.9	-	4.5
14	4	-	9.4	-	5.3
15	1	-	0.4	-	
16	4[b]	-	10.2[b]	-	1[c]

a) Helium carrier gas.
b) Feed was I-113 Decalin.
c) Selectivity for naphthalene.

Laboratory Standard 1% Pt on Al_2O_3
10080-46 (Shell 46)
10080-45 (Shell 45)
10080-113 (Shell 113)
Sinclair-Baker RD-150 (RD-150)
UOP-R8

The pulse reactor system was described in detail in a previous report.[16] In this system a carrier gas such as helium or hydrogen flowed through the reactor. A small amount of liquid feed was injected into the gas stream and was carried through the reactor as a "pulse". The exit gas was led directly into a GLC for analysis.

Each catalyst was tested in a series of runs at 2150, 3000, and 4265 LHSV[a] at 662 and 752°F. One microliter of MCH was injected via a syringe as a pulse. Both helium and hydrogen were used as carrier gas. The data are presented in Tables 28 to 33 inclusive.

At 662°F and with He carrier some catalyst deactivation was observed with RD-150 (Table 30) and Shell 45 (Table 29), but not with the other catalysts. This was shown by the loss in conversion between the initial and final runs in the series. No deactivation was observed with any of the catalysts at 752°F using H_2 carrier. This catalyst deactivation with He was observed in earlier work in the pulse reactor[16] and presumably occurred because the partial pressure of hydrogen generated by the dehydrogenation reaction was not great enough to remove the coke precursors from the catalyst surface. This greater sensitivity of the RD-150 catalyst to deactivation correlates with its inferior intrinsic activity.

Hydrogen treatment at the higher temperature (752°F) appeared to regenerate Shell 45 but not RD-150. Thus with Shell 45 at 752°F the conversions observed with fresh catalyst were about those observed with a hydrogen-treated partially deactivated catalyst, (cf Runs 126-2, -3, -4; with Runs 163-2, -3, -4; Table 29). With RD-150, however, conversions were higher with fresh catalyst than with hydrogen-treated used catalyst, (cf Runs 132-1, -2, -3 and Runs 160-2, -3, -4; Table 30).

At both temperatures conversion decreased with increased space velocity. This is shown by Figure 19 which is a plot of conversion as a deactivation by assuming that the deactivation was a linear function of the number of pulses. Hydrogen was used at the higher temperature as previous work with the standard platinum catalyst had shown extensive catalyst deactivation at 752°F with He carrier gas.[16] Using hydrogen at the lower temperature (662°F) gave conversions that were considerably lower than with He, presumably because of an equilibrium effect (Tables 28 to 33).

Product material was principally toluene with lesser amounts of benzene and cracked products (liquids). Product distribution was different at the two temperatures and for the different catalysts. At 662°F with helium, selectivities for toluene were 90% and higher. Also, of the two minor products with hydrogen the reverse was true, and selectivity for cracked

a) Liquid Hourly Space Velocity; volumes of liquid feed per volume of catalyst per hour. In these experiments the LHSV was calculated from the carrier gas flow rate and the bulk volume of the catalyst (i.e., 0.25 ml).

Table 26. DEHYDROGENATION OF MCH OVER STANDARD LABORATORY CATALYST: PULSE REACTOR

Catalyst: 1% Pt on Al_2O_3 Pressure: 10 atm
Catalyst Volume: 0.25 ml Catalyst Diluted With 1.25 ml Quartz Chips.
Catalyst wt: 0.25 g Pulse Volume: 1 µl

Runs 10543-	195-2	195-3	195-4	196-1	196-2	196-3	196-4	10800-10-1	10-2	10-3	10-4	11-1
Carrier Gas	← He →							← H_2 →				
Carrier Gas Flow Rate, cc/min	400	1500	400	2400	400	3200	400	3200	2400	3200	1600	3200
LHSV	534	2150	534	3200	534	4265	534	4265	3200	4265	2150	4265
Temperature, °F	← 932 →							← 752 →				
Furnace												
Reactor Wall	931-58	940-58	949-58	949-58	951-55	951-55	951-53	743-47	743-47	743-47	743-47	741-47
Product Analysis, %												
Cracked	0.3	0.6	0.5	0.3	0.5	0.3	0.4	0.3	5.4	5.0	5.5	8.9
MCH	2.7	10.4	2.7	18.7	2.4	31.9	3.2	15.4	13.2	15.0	11.9	17.2
Toluene	96.7	88.3	96.8	81.0	95.7	67.8	96.4	77.9	80.9	79.0	81.5	70.9
MCH Conversion, %	97.3	89.2	97.3	81.3	97.2	68.1	96.8	84.5	80.3	84.0	68.1	32.8
Selectivity for Toluene, %	99.4	99.4	99.5	99.6	98.5	99.0	99.6	92.2	93.2	94.0	92.5	95.3

Table 29. DEHYDROGENATION OF MCH OVER SHELL 45 (10829-45): PULSE REACTOR

Pressure: 10 atm
Catalyst Volume: 0.25 ml
Catalyst wt: 0.180 g
Catalyst Diluted With 1.25 ml Quartz Chips
Pulse Volume: 1 µl

Run 10,000-	124-1	124-2	125-1	125-2	125-3	123-1	123-2	125-3	126-4	153-1	153-2[b]	153-3	153-4
Carrier Gas	← N_2					← N_2				← N_2			
Carrier Gas Flow Rate, cc/min	1600	2400	3200	1600	1600	1600	2400	3200	1600	1600	2400	3200	1600
LHSV	2150	3200	4255	2150	2150	2150	3200	4255	2150	2150	3200	4255	2150
Temperature, °F													
Furnace	← 902					← 752				← 752			
Reactor Wall	555-56	555-56	54-57	554-56	654-56	740-47	733-45	734-45	741-47	740-47	736-47	734-45	740-45
Product Analysis, %													
Cracked	3.1	2.3	1.6	1.8	0.3	9.0	7.7	6.5	9.8	13.5	11.7[c]	9.0[c]	12.2[c]
Benzene	1.2	2.2	1.7	1.9	0.5	0.5	0.4	0.4	0.5	-	-	-	-
MCH	17.5	29.5	38.2	25.3	58.1	14.2	14.3	22.5	13.4	13.2	17.7[d]	23.0[d]	13.5[d]
Toluene	78.2	65.6	58.2	70.5	28.6	72.3	70.0	64.5	72.7	73.2	70.5	68.0	74.2
Others[a]	0.0	0.0	0.0	0.0	0.0	3.4	2.5	2.1	3.4	-	-	-	-
MCH Conversion, %	82.5	70.4	61.8	74.4	31.9	85.8	80.7	77.5	85.7	86.8	82.3	77.0	86.4
Corrected for Catalyst Deactivation	82.5	70.4	73.8	82.5	40.8	-	-	-	-	-	-	-	-
Selectivity for Toluene, %	94.6	93.5	94.2	91.7	90.2	85.0	85.7	83.4	87.4	84.3	85.8	88.3	85.8

a) Benzene after benzene.
b) Fresh catalyst.
c) Contains "Cracked" and "Others" components.
d) Contains about 0.5% benzene.

Table 30. DEHYDROGENATION OF MCH OVER RD-150: PULSE REACTOR

Pressure: 10 atm
Catalyst Volume: 0.25 ml
Catalyst wt: 0.231 g
Catalyst Diluted With 1.25 ml Quartz Chips
Pulse Volume: 1 µl

Run 10808-	130-1	130-2	131-1	131-2	131-3	132-1	132-2	132-3	132-4	160-2[b]	160-3	160-4	160-5
Carrier Gas	← He →				← H_2 →					← H_2 →			
Carrier Gas Flow Rate, cc/min	1600	2400	3750	1600	1600	1600	2400	3200	1600	1600	2400	3200	1600
LHSV	2150	3200	4285	2150	2150	2150	3200	4285	2150	2150	3200	4285	2150
Temperature, °F													
Furnace	← 882 →				← 752 →					← 752 →			
Reactor Cell	648-58	651-57	650-57	654-57	654-58	740-47	736-47	736-47	741-47	740-47	738-47	736-47	740-47
Product Analysis, %													
Cracked	0.3	0.1	0.0	0.0	0.0	0.1	0.1	0.1	0.5	0.8	0.3	0.7	1.3
Benzene	1.0	0.6	0.4	0.3	0.0	0.2	0.2	0.2	0.3	0.2	0.2	0.1	0.2
MCH	37.0	50.8	67.9	54.5	78.5	31.4	38.2	44.8	29.5	24.5	33.4	40.4	23.7
Toluene	61.8	47.5	31.7	45.2	21.5	67.9	60.2	54.8	68.4	73.6	65.0	58.3	72.9
Others[a]	0.0	0.0	0.0	0.0	0.0	0.4	0.3	0.3	1.2	1.3	1.1	0.5	1.9
MCH Conversion, %	63.0	49.2	32.1	45.5	21.5	68.6	60.8	55.1	70.5	75.5	66.6	59.6	76.3
Correction for Catalyst Deactivation	63.0	54.8	43.3	63.0	32.7	-	-	-	-	-	-	-	-
Selectivity for Toluene, %	98.1	95.8	98.8	99.3	100	99.0	99.0	98.9	97.0	97.2	97.6	97.9	95.5

a) Except after benzene.
b) Fresh catalyst.

Table 31. DEHYDROGENATION OF MCH OVER SHELL 46 (10290-46); PULSE REACTOR

Pressure: 10 atm
Catalyst Volume: 0.25 ml
Catalyst wt: 0.231 g
Catalyst Diluted With 1.25 ml Quartz Chips
Pulse Volume: 1 µl

Run 10290-	118-1	119-2	120-1	120-2	120-3	121-1	121-2	122-1	1123-2	122-3	122-4
Carrier Gas	← H_2 →					← N_2 →					
Carrier Gas Flow Rate, cc/min	1600	2400	3200	1600	1600	1600	3.00	1600	2400	3200	1600
LHSV	2150	3200	.285	2150	2150	2150	8200	2150	3200	4265	2150
Temperature, °F											
Furnace	← 662°F →					← 753°F →					
Reactor Wall	654-58	65.-58	647-57	654-58	651-58	736-47	731-.5	73.- 7	7.-47	729-.5	736-47
Product Analysis, %											
Cracked	3.9	1.5	1.0	1.3	0.2	13.5	10.6	14.9	11.3	8.8	15.5
Benzene	<.5	5.3	4.1	6.0	0.3	1.4	1.3	1.8	1.7	1.4	1.5
MCH	7.8	12.3	20.5	7.1	68.5	8.1	11.5	7.4	10.5	13.7	7.7
Toluene	83.5	81.0	74.5	85.5	31.8	72.8	72.2	71.0	72.5	72.2	70.5
Others[a]	0.0	0.0	0.0	0.0	0.7	<.0	.	.7	3.5	3.0	5.3
MCH Conversion, %	..2	87.7	79.5	92..	33.5	91.6	88.5	92.2	89.5	86.3	92.3
Selectivity for Toluene %	90.9	92..	93.7	92.1	9..9	79.5	81.6	77.0	73.3	83.8	76.8

a) Emerged after benzene; possibly cyclohexene.

Table 32. DEHYDROGENATION OF MCH OVER PDP-R8: PULSE REACTOR

Pressure: 10 atm
Catalyst Volume: 0.25 ml
Catalyst wt: 0.128 g
Catalyst Diluted With ~1.25 ml Quartz Chips
Pulse Volume: 1 µl

Run 10808-	127-1	127-2	128-1	128-2	128-3	129-1	129-2	129-3	129-4
Carrier gas	← H_2				→ ← H_2				→
Carrier gas Flow Rate, cc/min	1600	2400	3200	1600	1600	1600	2400	3200	1600
LHSV	2150	3200	4265	2150	2150	2150	3200	4265	2150
Temperature, °F									
Furnace	← 662				→ ← 752				→
Reactor Wall	654-58	654-58	650-57	654-58	651-57	741-47	736-47	734-47	741-47
Product Analysis, %w									
Cracked	0.8	0.4	0.4	0.3	0.0	4.4	4.4	2.9	5.0
Benzene	5.2	3.2	2.4	3.0	0.1	1.2	1.2	3.9	1.1
MCH	27.0	35.2	44.0	26.9	74.5	20.4	28.5	32.3	19.3
Toluene	67.0	61.2	53.2	69.8	25.4	73.0	64.9	63.3	73.5
Others a)	0.0	0.0	0.0	0.0	0.0	1.1	1.0	0.5	1.2
MCH Conversion, %w	73.0	64.8	56.0	73.1	25.5	79.6	71.5	67.7	80.7
Selectivity for Toluene, %w	91.8	94.4	95.0	95.5	99.6	91.7	90.8	95.5	91.1

a) Emerged after benzene.

Table 33. DEHYDROGENATION OF MCH OVER SHELL 113 (10280-113): PULSE REACTOR

Pressure: 10 atm
Catalyst Volume: 0.25 ml
Catalyst wt: 0.231 g
Catalyst Diluted With 1.25 ml Quartz Chips
Pulse Volume: 1 µl

Run 10808-	115-1	115-2	116-1	116-2	116-3	117-1	117-2	117-3	117-4	118
Carrier gas	← He →					← H_2 →				
Carrier gas Flow Rate, cc/min	1600	2400	3200	1600	1600	1600	2400	3200	3200	1600
LHSV	2150	3200	4265	2150	2150	2150	3200	4265	4265	2150
Temperature, °F										
Furnace	← 662 →					← 752 →				
Reactor Wall	655-60	654-60	651-60	655-60	655-60	736-45	734-45	729-45	729-45	737-47
Product Analysis, %w										
Cracked	1.8	1.2	0.9	1.4	0.0	6.1	5.0	3.7	3.0	7.4
Benzene	3.2	2.4	2.4	3.5	0.3	0.9	1.2	1.4	1.2	1.1
MCH	27.8	38.0	49.0	31.7	70.0	19.3	21.2	30.0	30.6	18.2
Toluene	66.2	58.4	47.7	63.4	28.7	71.7	70.4	65.4	64.3	71.0
Others[a]	0.0	0.0	0.0	0.0	0.0	2.0	2.2	1.5	0.9	2.3
MCH Conversion, %w	72.2	62.0	51.0	68.3	30.0	80.7	78.8	70.0	68.4	81.8
Selectivity for Toluene, %w	91.7	94.2	93.5	92.8	95.7	88.8	89.3	90.7	94.0	86.8

a) Emerged after benzene.

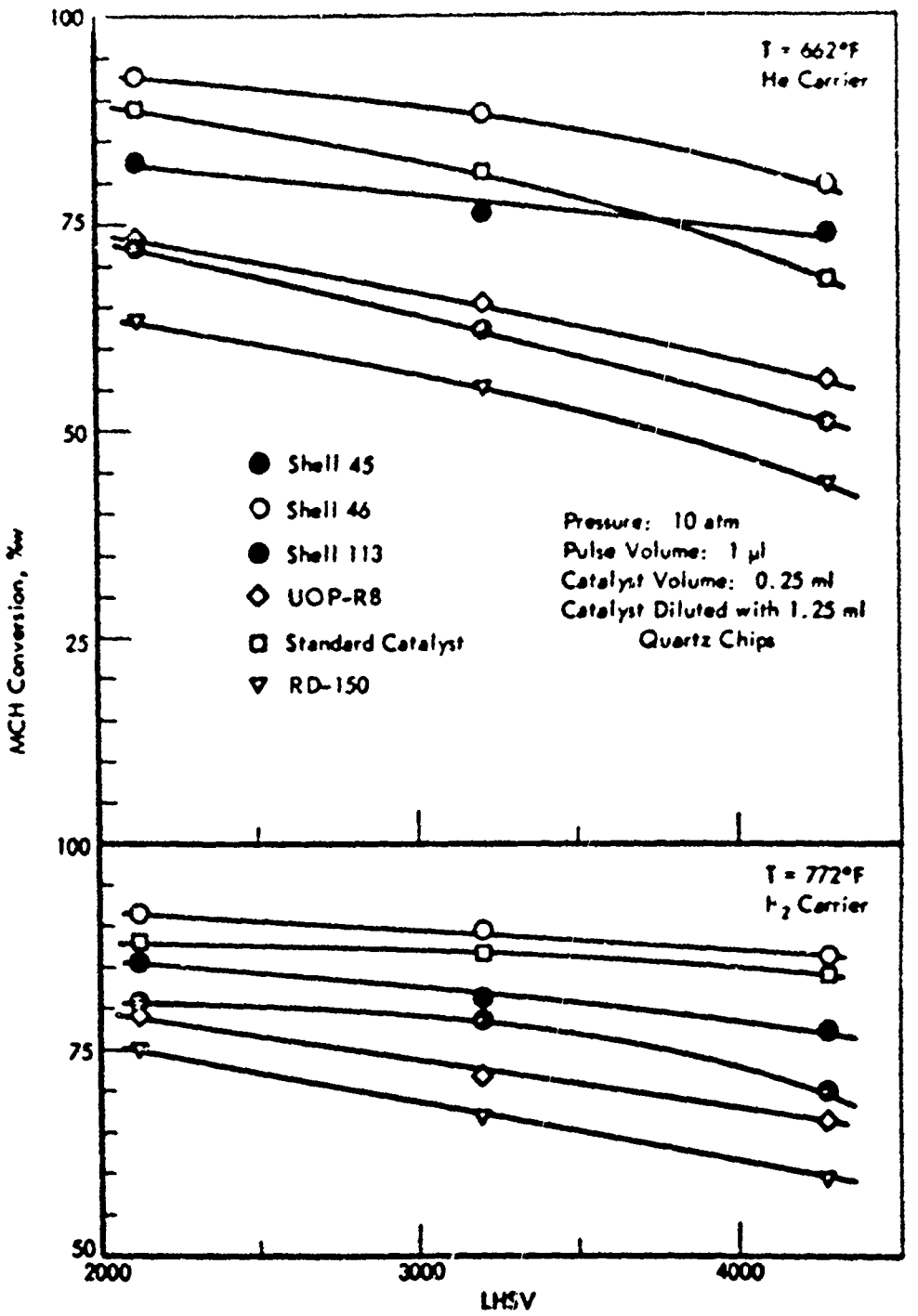

Figure 19. DEHYDROGENATION OF MCH OVER VARIOUS CATALYSTS: PULSE REACTOR

products was higher than that for benzene while that for toluene was generally lower than with He. Table 34 shows selectivities for various products in the runs at highest space velocity. Highest toluene selectivity was obtained with RD-150 where 96-99% was obtained at both temperatures. Poorest selectivity for toluene was obtained with Shell 46 (Table 34). These results suggest that at the higher temperature with hydrogen present, a hydrocracking reaction occurred. Further, the extent of this secondary reaction was different for each catalyst, possibly due to the influence of the different catalyst supports.

Table 34. SELECTIVITIES WITH VARIOUS CATALYSTS

LHSV: 4265

Catalyst	Reaction Temp	Carrier Gas	Selectivity for, %w		
			Toluene	Benzene	Cracked
Standard	662	He	99.6	-	0.4
	752	H_2	94.0	-	6.0
Shell 45	662	He	94.2	3.1	2-7
	752	H_2	88.3	0.5	11.2
Shell 46	662	He	95.7	5.2	1-1
	752	H_2	83.6	1.6	14-8
UOP-R8	662	He	95.0	4.3	0.7
	752	H_2	93.5	1.5	5.0
Shell 113	662	He	93.5	4.7	1-8
	752	H_2	90.7	1.9	7-4
RD-150	662	He	98.8	1.2	0.0
	752	H_2	97.8	0.2	2.0

Relative activities of the various catalysts were different at the two temperatures except for Shell 46 which was the most active and RD-150 which was the least active at both temperatures. Table 35 lists the catalysts in decreasing order of activity based on conversion at LHSV of 4265; the bench-scale results are shown for comparison. The differences in relative activities at different temperatures in the pulse reactor could have been due to differences in activation energies with the various catalysts, or to the use of He at 662°F and H_2 at 752°F. Comparing the results in the two reactor systems, the relative activity of the standard catalyst was considerably less in the bench-scale reactor. This suggests that diffusion effects may have been an important factor and possibly rate controlling of overall activity in the bench-scale test with this catalyst.

Table 35. RELATIVE ACTIVITIES OF VARIOUS CATALYSTS

Catalysts listed in order of decreasing activity (i.e., conversion)

Pressure: 10 atm

Pulse Reactor		Bench-Scale Reactor
LHSV = 4265		LHSV = 100
662°F	752°F	842°F
Shell 46	Shell 46	Shell 46
Shell 45	Standard Catalyst	Shell 45
Standard Catalyst	Shell 45	Shell 113
UOP-R8	Shell 113	UOP-R8
Shell 113	UOP-R8	Standard Catalyst
RD-150	RD-150	RD-150

First order rate constants were calculated from conversions and are tabulated in Table 36. The values for the pulse reactor are probably only qualitative as our system was not designed for quantitative determination of rate coefficients. Thus qualitatively relative reaction rates in the pulse reactor and in the bench-scale reactor were obtained by comparing the first order rate constants obtained in the two systems. Bench-scale rate constants, obtained at reactor temperatures of 842°F were corrected to 752°F using the previously determined activation energies (Table 36). The ratios of the rate constants in the pulse reactor k_P to those in the bench-scale reactor k_B showed that the catalysts appeared to be over two orders of magnitude more active in the pulse reactor system (Table 36). As stated previously, this difference probably was due both to a higher actual catalyst temperature and to less diffusion effects on the rate controlling step in the pulse reactor.

Effect of Reactor Material on Reactivity of Decalin

In preliminary studies on the dehydrogenation of bicycloheptane (BCH), it appeared that the reactor tube was catalyzing both the thermal and the dehydrogenation reactions. This effect was not observed earlier with Decalin; and subsequent investigation showed that for the BCH studies, the reactor tube had been fabricated from material obtained from a different manufacturer. Consequently a few experiments were done to see to what extent the reactor material catalyzed the cracking reaction. In this study the thermal reaction of Decalin was used as a test reaction.

The tests were carried out using reactor tubes fabricated from different types of stainless steel. In order to entirely eliminate the effect of the metal, one reactor tube was fitted with a quartz liner. The various reactor materials were:

Table 36. DEHYDROGENATION OF MCH OVER VARIOUS CATALYSTS. COMPARISON OF RELATIVE ACTIVITIES IN PULSE AND BENCH-SCALE REACTORS

Pressure: 10 atm

Pulse Reactor		Bench-Scale Reactor	
LHSV:	4265	LHSV:	100
Temperature.	752°F	Block Temperature:	842°F
Carrier Gas:	H_2	Catalyst Volume:	7 ml
Catalyst Volume:	0.25 ml		

Catalyst	Pulse Reactor		Bench-Scale Reactor		
	MCH Conv., %w	First Order Rate Constant, sec^{-1}	First Order Rate Constant, sec^{-1}	Eact, kcal/mole	k_p/k_B
1% Pt on Al_2O_3 (Standard)	84.5	94.4	0.652	11.9	267
Shell 46	96.3	100.7	0.873	13.4	230
Shell 45	77.0	74.7	0.854	16.4	205
Shell 113	70.0	58.4	0.788	13.5	149
RD-150	59.6	46.1	0.620	12.0	123
UOP-B3	67.6	57.2	0.692	12.0	153

a) Type 316 Stainless Steel; Patco (No. 316).

b) Type 304 Stainless Steel; Greenville Tubes (No. 304G).

c) Type 304 Stainless Steel, Bishop and Company (No. 304B).

d) Type 304 Stainless Steel; Bishop and Company with a quartz liner.

The reactor tubes were 1/4-in. OD with 0.035-in. wall thickness. The liner was a quartz tube 0.159-in. OD, 0.116-in. ID, that fit snugly inside the steel tube. The lower end of the quartz extended beyond the heated zone; the upper end extended into the injection port, so that feed was injected directly into the quartz tube. At the top end the space between the quartz tube the metal tube was filled with glass wool and sealed with a refractory cement; so that no feed contacted metal in the heated zone. In these tests the reactor tubes were filled with quartz chips (10-20 mesh).

The tests were done at 10 atm pressure, 1022 to 1202°F. One microliter of liquid Decalin (DHN) was injected per pulse. Both helium and hydrogen were used as carrier gas.

The data are summarized in Figure 20 which shows DHN conversion as a function of space velocity at 1112 and 1202°F. Highest reactivity was obtained with the quartz-lined tube. Based on conversions at LHSV of 10-15 relative reactivities in decreasing order at 1112°F were: quartz-lined tube ≅ 304G, >> 316 > 304B ≅ 304; and at 1202°F were: quartz-lined tube > 304B ≅ 304 >> 316. The 304G tube was not tested at the higher temperature.

The complete data obtained with the quartz-lined tube are presented in Table 37 and with the metal tubes in Table 38. The latter table also includes earlier work with a Bishop and Company 304 tube (No. 304B).

Reaction products were principally cracked material except with tube No. 316. With this tube 26.6% Decalin was converted to naphthalene at 1112°F with H_2 carrier (Run 10-2, Table 38). At higher temperature however (1202°F) little or no dehydrogenation was observed under these conditions (Run 11-3; Table 38). While the possibility exists that type 316 stainless steel will catalyze the dehydrogenation of Decalin under carefully controlled conditions, no further investigation in this area is planned at present.

There was some passivation of the metal tube with continued use. Thus with the most active tube (No. 304G) 30% DHN conversion was observed initially at 1112°F. However after contacting the tube with 60 µl of DHN at 1202°F, conversion at 1112°F had declined to 22.6%.

These results showed that the reactor material can affect the reactivity of Decalin for thermal reaction. Under our reaction conditions the effect of the metal was to inhibit the reaction rate. These test results were for small amounts of hydrocarbon in a freshly cleaned tube. Whether the observed affect would persist under continuous flow conditions over several hours reaction time has yet to be determined.

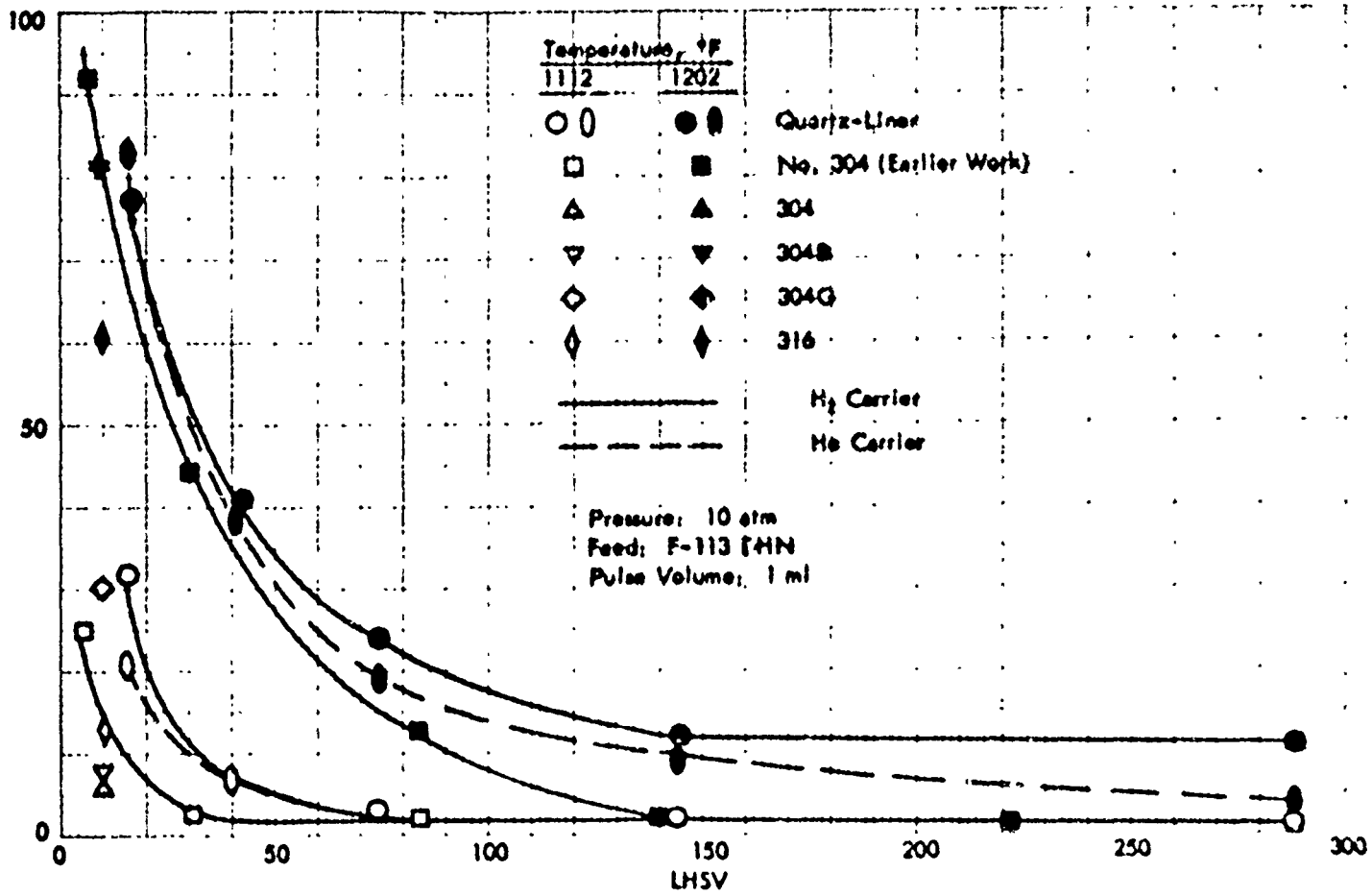

Figure 20. THERMAL REACTION OF DECALIN: PULSE REACTOR
Effect of Reactor Material

Table 25. THERMAL REACTION OF DECALIN: PULSE REACTOR

Quartz-Lined Reactor Tube

Feed: F-113 DHN
Pressure: 10 atm
Pulse Volume: 1 µl (liquid)
Reactor Material: 304 Stainless Steel (Bishop and Co.); reactor filled with quartz chips
Feed Composition: 25.0% trans-DHN
74.6% cis-DHN
0.4% THN

Run	10606-														11181-											
	195-1	195-2	196-1	196-2	197-3	197-4	195-1	195-2	196-1	196-2	196-3	197-1	197-2	197-4	195-1	5	T-4	T-3	T-2	T-1	6	8-1	8-2	7-3	8-4	9-1	9-2
Carrier Gas	← H_2 →		← H_2 →		← H_2 →					← H_2 →					← H_2 →							← N_2 →				
LHSV[a]	59	59	59	59	59	59	75	143	287	59	59	75	143	287	59	59	75	143	287	479	764	59	59	75	143	287	479
ACT, sec[b]	2.9	1.1	2.9	1.1	2.7	1.0	0.53	0.27	0.14	2.7	1.0	0.53	0.27	0.14	2.6	0.95	0.69	0.36	0.13	0.079	0.049	2.6	0.95	0.69	0.36	0.13	0.079
Block Temp, °F	← 1092 →				← 1112 →										← 1202 →											
Product Analysis, %w																											
Cracked	2.7	1.1	2.0	1.2	80.2	5.5	2.7	1.5	0.7	50.8	6.2	3.1	2.5	1.4	18.0	98.4	78.9	11.4	10.1	8.9	2.5	79.7	56.3	19.0	4.3	3.3	1.8
trans- DHN	24.8	24.7	24.6	24.6	21.4	23.8	24.3	24.4	24.2	19.9	23.8	23.8	23.4	24.3	8.3	17.4	20.7	72.6	43.9	23.9	24.3	6.1	17.6	61.0	72.8	23.9	24.0
cis- DHN	71.9	73.5	72.7	73.5	57.0	69.6	72.2	73.5	73.4	47.8	69.4	69.4	71.8	73.6	14.8	62.8	53.0	65.3	45.4	72.3	72.8	10.9	44.4	19.4	67.2	72.0	73.8
THN	0.2	0.3	0.3	0.3	0.8	0.3	0.3	0.3	0.4	0.8	0.3	0.3	0.3	0.4	1.1	0.2	0.1	0.2	0.3	0.3	0.4	1.2	0.2	0.3	0.4	0.3	0.4
H	0.0	0.0	0.0	0.0	0.0	0.0	0.0	0.0	0.0	0.0	0.0	0.0	0.0	0.0	0.0	0.0	0.0	0.0	0.0	0.0	0.0	0.0	0.0	0.0	0.0	0.0	0.0
Chloro[c]	0.4	0.4	0.4	0.4	1.2	1.0	0.5	0.5	0.5	1.9	0.5	0.8	0.8	0.5	1.2	1.8	1.5	0.5	0.3	0.5	0.3	1.5	1.5	0.4	0.5	0.3	0.4
DHN Conversion, %w	3.0	1.4	2.4	1.6	21.3	6.5	3.2	1.7	1.0	52.0	6.4	3.2	2.5	1.8	76.8	40.2	24.0	11.6	10.4	3.3	2.6	20.3	7.8	13.	3.7	3.8	1.4

a) Based on volume of quartz chips = 0.654 ml
b) Based on void volume = 0.45 ml
c) Averaged after cis - DHN and after THN.

Table 38. THERMAL REACTION OF DECALIN: PULSE REACTOR

Effect of Reactor Material

Feed: F-115 DHN — Pulse Volume: 1 ml (as liquid)
LHCV: 10 — Reactor Tube Filled with Quartz Chips
Pressure: 10 atm — Reactor Material: Stainless Steel

Run No. 11018-	Feed	7-1	8-1[b]	8-2[c]	8-3[c]	10-1	10-2	11-1	11-2	11-3	12-1	12-2	14-1	14-2	14-3	14-4	10000-168-1	11-3-4	126-4	130-1
Reactor Tube Material	-	← 304 (Greenville Tubes)[a] →				← No. 316 →					← 304 (Hoke and Co.) →						← 316 (Hoke and Co.) →			
Flash Temperature, °F	-	← 1112 →				1112	1112	1112	1202	1202	1112	1112	1112	1202	1202	1202	1112	1202	1112	1202
Carrier Gas	-	← He →				He	He	He	He	H_2	He	H_2	He	He	H_2	He	He	He	H_2	H_2
Carrier Gas Flow Rate, cc/min	-	50	50	100	50	← 50 →					← 50 →									
Product Analysis, %w																				
Cracked	0.0	27.0	20.1	6.2	10.1	9.9	55.0	5.0	44.7	40.8	7.5	19.4	9.9	70.9	[illegible]	76.0	6.8	69.4	11.9	46.7
trans DHN	24.2	19.2	20.9	25.5	22.4	25.6	12.0	1.7	11.9	6.4	25.5	25.5	22.9	6.6	[illegible]	7.1	23.1	0.8	20.2	5.6
cis DHN	75.2	50.7	56.5	68.5	65.1	64.8	6.8	60.1	37.0	10.0	68.2	61.5	66.0	11.5	8.7	13.0	70.7	18.5	56.*	4.*
THN	0.6	1.4	1.0	0.6	1.5	0.9	1.1	.8	2.4	1.*	0.7	1.7	0.9	1.5	1.*	1.5	0.5	1.5	5.7	1.7
N	0.0	0.4	0.5	0.4	2.6	1.4	.0.6	1.5	5.	*	.1	1.	0.*	1.1	1.1	1.0	0.5	0.6	7.7	1.7
Others	0.0	1.5	0.9	0.*	0.5	0.0	0.5	.1	0.9	0.*	0.*	1.1	.1	.6	1.	1.6	0.*	1.5	0.5	0.2
DHN Conversion, %w		50.1	[illegible]	[illegible]	16	1.*	1	.*	11.1	11.*	4.5	16.*	11.1	91.*	*	9.*	6.*	9.*	*.*	*.1

a) Reactor tube thermally leached with [illegible]
b) Reactor leaked to 1.02 psi and 40 ml of N in three hours, leak sealed before this run.
c) No quartz chips in reactor.

Reactivity of Decalin

In previous work[19] it was shown that the nominal reactivity of methylcyclohexane for dehydrogenation was over two orders of magnitude greater in the pulse reactor than in the continuous flow bench-scale reactor. This enhanced reactivity was attributed to higher catalyst particle temperatures at a given furnace temperature and to less diffusion effects in the pulse reactor. It was of interest now to test a dicyclic naphthene such as Decalin in the pulse reactor system. These results would then provide a basis for a quick evaluation test (in the pulse reactor) for fuels such as dimethano-decalin and substituted fulvenes.

Both thermal and dehydrogenation reactions were studied using F-113 Decalin (DHN) as feed. This material contained 74.6% cis-DHN, 25.0% trans-DHN and 0.4% tetralin (THN). Both helium and hydrogen were used as carrier gas; 1 µl of DHN was injected as a pulse. The reactor tube was 1/4-in. OD stainless steel; Type 304; Bishop and Company. This material was found to be the least reactive with Decalin in special tests (see page 81). Product material was analyzed by GLC using a 150-ft stainless steel column, 0.010-in. ID coated with SF-96.

Thermal Reaction

Thermal reaction studies were done at 10 atm pressure, 1022-1202°F, at LHSV[a] of 7 to 221, which corresponded to apparent contact times (ACT) of 4.8 to 0.13 seconds. Hydrogen was used as carrier gas. The data are presented in Table 39.

Under conditions of thermal reaction conversion increased with increased temperature and increased contact time (Figure 21; ACT ≈1/LHSV). Thus at 1202°F conversions were 3% at 0.2 seconds ACT but increased to 44% and 92% at 1.1 and 4.3 seconds ACT, respectively. Further, at about 4.5 seconds ACT (LHSV = 7) conversion increased from about 3% at 1022°F to about 92% at 1202°F. This corresponded to an activation energy of about 75 kcal/mole. Product material was principally cracked products (liquid) which were not identified further. Run 146-4 (Table 39) appeared anomalous as the yields of THN and naphthalene were high compared to other runs. This experiment will be repeated and the present results must be considered suspect.

In these tests the reactivity of DHN at 1200°F was about that observed in previous work with the continuous-flow bench-scale reactor.[19] In this latter system, 46.6% DHN conversion was observed at 1202°F (LHSV of about 40) compared to 44% conversion in the pulse reactor (LHSV of 28) although at 1112°F the bench-scale reactor induced threefold greater reactivity. The bench-scale data are shown as a dotted line in Figure 21. The apparent activation energies in the two cases are 46 kcal for the bench scale and 75 kcal for the pulse. This compares to 64 kcal found by Monsanto[20] in their work. These differences undoubtedly reflect the difficulty of closely defining the reaction zones in the various types of equipment.

---

a) LHSV calculated from carrier gas flow rate and void volume in reactor tube. Void volume = 1.2 ml = one-half bulk volume of quartz chips.

Table 39. THERMAL REACTION OF DECALIN: PULSE REACTOR

Pressure: 10 atm
Reactor Tube Filled With Quartz Chips
Carrier gas: H_2
Pulse Volume: 1 ml

Feed: F-113 DHN
Feed Composition:
74.6% cis DHN
25.0% trans DHN
0.4% THN

Run No 10^06-	145-1	146-1	146-2	146-4	152-4	147-2	14 -1	14 -2	150-1	150-2	151-3	151-4	152-3
LHSV	7	20	83	7	20	83	138	221	7	20	83	138	221
τ_{CT}, sec	4.8	1.2	0.4	4.5	1.1	0.36	0.23	0.14	4.3	1.1	0.36	0.21	0.13
Temperature, °F													
Furnace	← 1022 →			← 1083 →		1112			← 1202 →				
Wall	997-1013	9:5-1013	1000-13	1075-1103	1083-1103	1075-1103	1025-1103	10 7-1103	1170-93	1170-91	1172-93	1172-93	1173-.1
Product Analysis, %													
Cracked	2.:	3.5	0.0	11.5	4.3	0.5	0.5	0.1	88.5	40.3	6.1	1.8	1.0
t-DHN	25..	25.7	24.7	20.2	23.8	24.0	24.1	24.3	5.6	16.6	22.1	24.2	24.1
c-DHN	66.6	72.6	74.5	54.5	70.6	72.3	73.1	73.7	4.3	35.1	64.5	73.0	73.5
THN	0.6	1.0	0.8	5.7	2.2	1.8	1.3	1.3	1.7	2.2	1.4	1.1	0.3
δ	0.0	0.2	0.0	1.7	1.1	1.0	0.8	0.6	1.7	0.0	0.2	0.0	0.0
Others	0.0	0.0	0.0	0.0	0.2	0.0	0.0	0.0	0.2	1.0	0.0	0.0	0.1
DHN Conversion, %	3.2	1.3	0.4	25.0	5.2	3.4	3.6	2.2	52.1	44.3	13.1	3.0	2.4

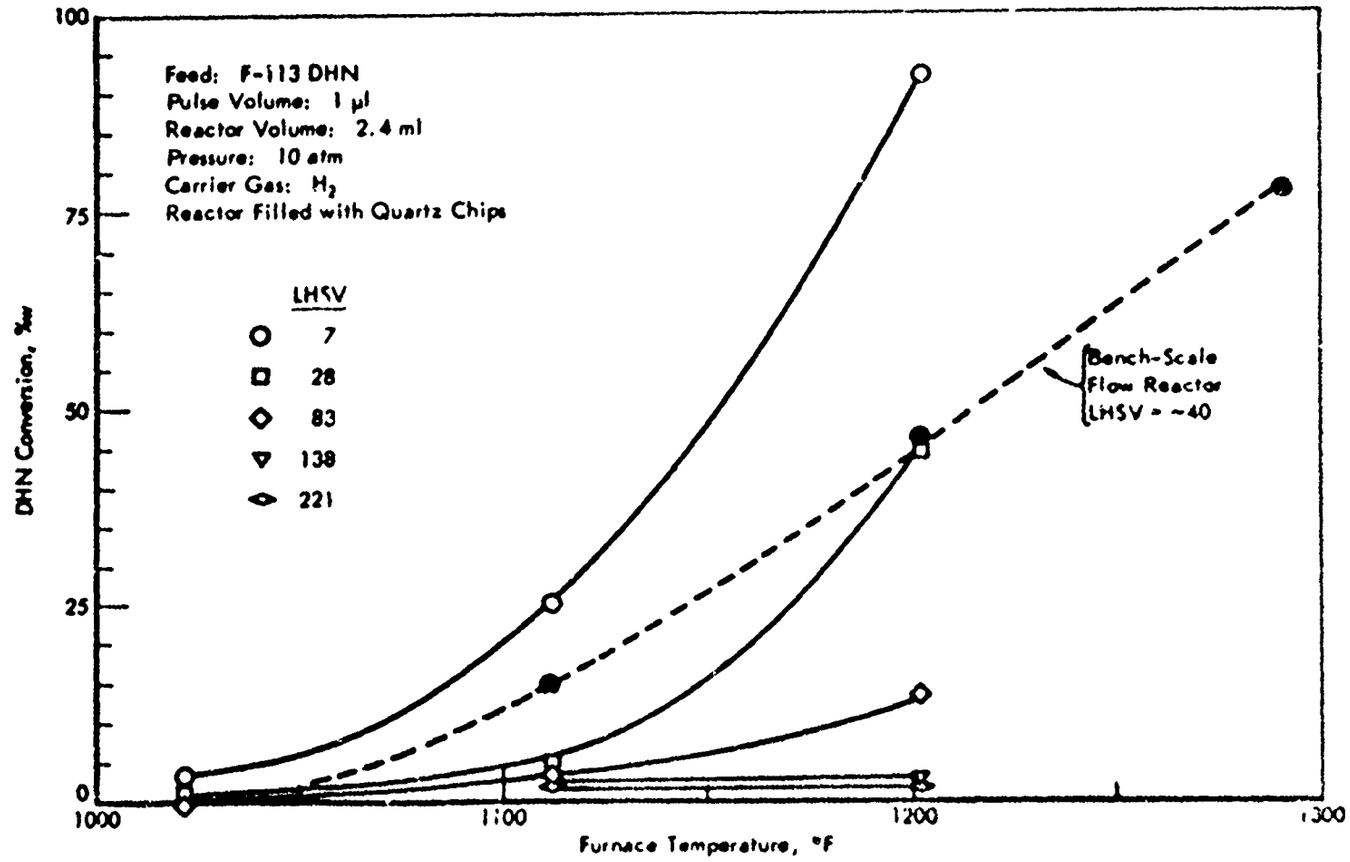

Figure 21. THERMAL REACTION OF DECALIN: PULSE REACTOR

Dehydrogenation

Dehydrogenation was carried out at 10 atm pressure with our standard 1% platinum on alumina catalyst. Only 0.25 ml of catalyst (0.24 g) was used, and the catalyst was diluted with 1.25 ml of quartz chips (10-20 mesh), to give a total catalyst bed of about three inches. Tests were done at 662 and 752°F using both helium and hydrogen as carrier gas. The tests consisted of a series of runs at each temperature at LHSV's of 828 to 4950. The runs were bracketted to detect catalyst deactivation during the tests. The data are presented in Tables 40 and 41.

Catalyst deactivation was observed at 662°F with He carrier, but not at 752°F with H_2 carrier. This was evident as the conversions for conditions of the initial run got progressively lower during the succession of runs (Table 40). This catalyst deactivation with He (also observed with MCH) presumably occurred because the partial pressure of hydrogen generated during dehydrogenation, was not great enough to remove the coke precursors from the catalyst.

The effect of space velocity on conversion is shown in Figure 22 which is a plot of conversion as a function of LHSV. The points at 662°F have been corrected for catalyst deactivation. For this correction it was assumed that the deactivation was linear between the bracketed runs. At both temperatures conversion declined with increased space velocity; more so at the lower temperature. Higher conversions were obtained in the pulse reactor at lower furnace temperatures and much higher space velocities than were used in bench-scale reactor tests. For example in the pulse reactor 85.6% conversion was obtained at an LHSV of 4960 and a furnace temperature of 752°F (Table 41), compared to 40.2% conversion in the bench-scale reactor at an LHSV of 100 and a furnace temperature of 842°F (Table 17).

First order rate constants, calculated from the above conversions were 57.9 sec^{-1} and 0.498 sec^{-1} for the pulse (752°F) and bench-scale reactors (842°F), respectively. Using an activation energy of 7.7 kcal/mole (Table 17)[18] gave a value of 0.352 sec^{-1} at a reactor temperature of 752°F in the bench-scale reactor. Thus as was observed with MCH, the reactivity of DHN was about 200 times or two orders of magnitude greater in the pulse reactor. Presumably this enhanced rate was due to both a higher catalyst particle temperature and less diffusion effects in the pulse reactor system.

Summary

This work substantiates earlier work with MCH namely, that considerably higher reaction rates are possible with our platinum on alumina catalysts than were obtained in the bench-scale reactor. At least part of the observed rate increase was due to the higher catalyst particle temperatures (due to the low heat capacity of the pulse) that prevailed in the pulse reactor system (for a given furnace temperature). Thus high conversions at space velocities higher than those used in the bench-scale work appear feasible if heat can be transferred more rapidly from the furnace block to the catalyst particles.

Table 40. DEHYDROGENATION OF DECALIN AT 662°F: PULSE REACTOR

Pressure: 10 atm
Catalyst Volume: 0.25 ml
Catalyst: 1% Pt on Al_2O_3
Carrier Gas: He

Catalyst Diluted With
1.25 ml Quartz Chips
Pulse Volume: 1 µl
Furnace Temperature: 662°F

Run 10808-	133-1	133-2	134-1	134-2	134-3	134-4	135-1	135-2	135-3
LHSV	828	1655	828	2480	828	3310	828	4960	828
Wall Temperature °F	650-58	650-58	650-58	650-56	651-58	651-58	651-58	650-57	651-58
Product Analysis, %w									
Cracked	0.5	0.4	0.3	0.0	0.3	0.0	0.2	0.0	0.3
t-DHN	1.9	8.2	6.4	11.9	8.2	14.7	11.3	19.0	12.4
c-DHN	1.7	11.7	5.3	22.2	6.3	31.4	9.3	46.6	10.8
THN	0.7	1.9	0.8	4.5	1.4	6.1	1.9	6.4	2.2
N	95.2	77.8	87.2	61.4	83.8	47.8	77.0	28.0	74.4
DHN Conversion, %w	96.4	80.1	88.3	65.9	85.2	53.9	79.1	34.4	76.8
Corrected for Catalyst Deactivation	96.4	84.1	96.4	75.6	96.4	68.2	96.4	52.7	96.4

Table 41. DEHYDROGENATION OF DECALIN AT 752°F: PULSE REACTOR

Pressure: 10 atm
Catalyst: 1% Pt on Al_2O_3
Catalyst Volume: 0.25 ml
Carrier Gas: H_2
Catalyst Diluted With Quartz Chips
Pulse Volume: 1 ml
Furnace Temperature: 752°F

Run 10808-	136-1	136-2	137-1	137-2	137-3	137-4	138-1
LHSV	1655	2480	1655	3310	1655	4960	1655
Wall Temperature, °F	740-48	734-46	734-45	729-43	436-45	725-43	738-45
Product Analysis, %w							
Cracked	1.1	0.9	0.4	0.0	0.8	0.0	0.6
t-DHN	2.2	4.6	3.1	6.1	2.2	7.9	2.5
c-DHN	0.6	2.4	1.0	3.9	0.6	6.5	0.8
THN	17.4	15.7	18.0	17.3	18.8	16.1	18.9
N	78.3	76.1	77.2	72.7	77.2	69.5	76.8
Heavier Than N	0.4	0.3	0.3	0.0	0.4	0.0	0.4
DHN Conversion, %w	97.2	93.0	95.9	90.0	97.2	85.6	96.7

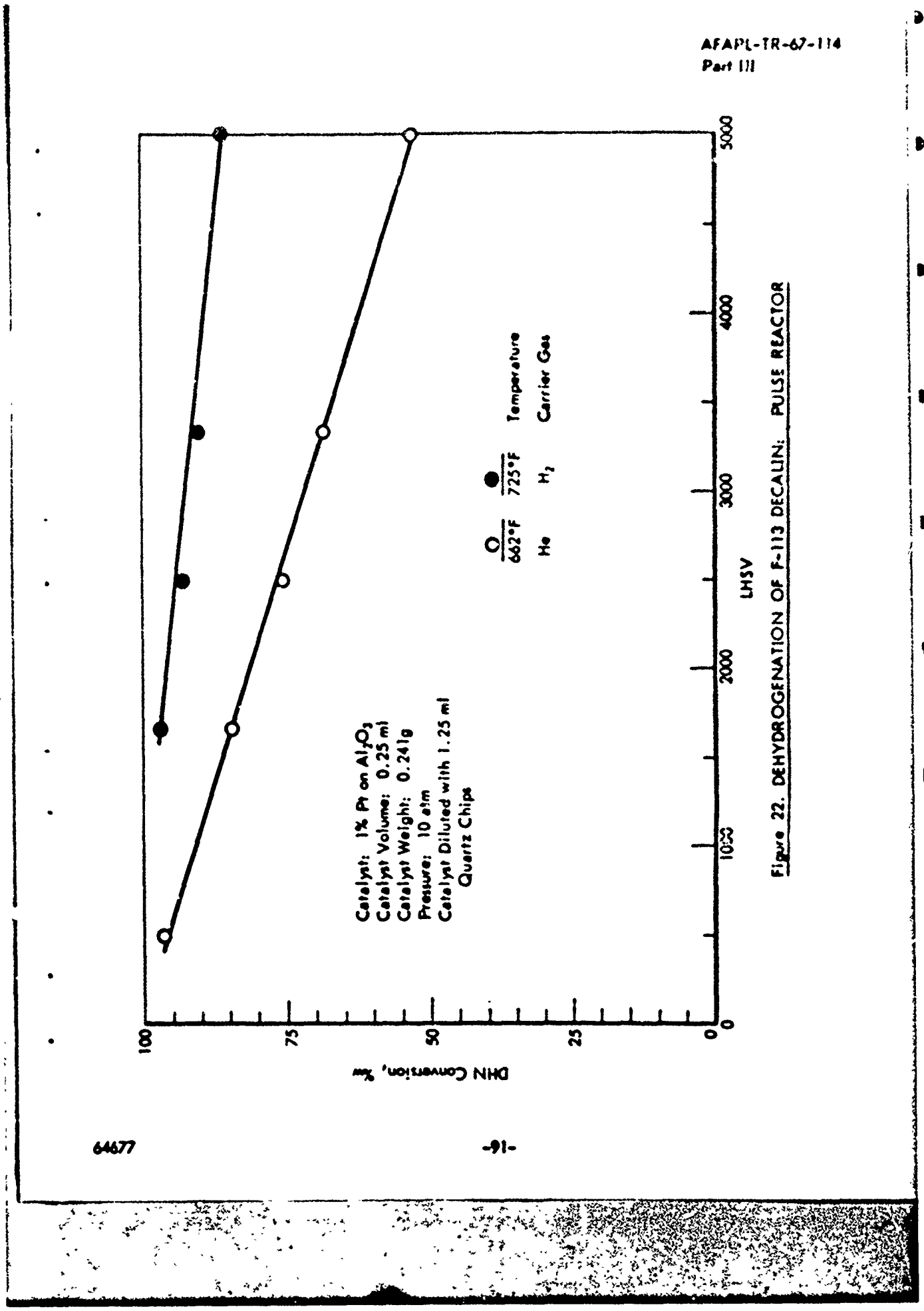

Figure 22. DEHYDROGENATION OF F-113 DECALIN; PULSE REACTOR

Reactivity of Dimethanodecalin

Dimethanodecalin (DMD) $C_{12}H_{18}$, is a dicyclic naphthene containing two fused rings with carbon bridges across the 1,6- and 5,8-positions. It can be dehydrogenated with the removal of two and five molecules of hydrogen according to the following reaction:

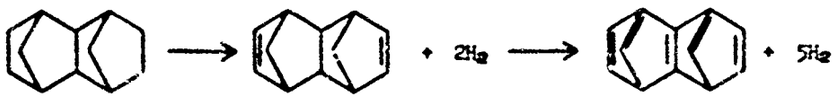

The endothermatic heat of this reaction is about 300 Btu/lb for the first step and could attain about 2000 Btu/lb if all $5H_2$ could be removed. Thus DMD is another attractive candidate fuel even though the removal of more than $2H_2$'s may be difficult to accomplish.

The DMD tested contained a number of components that presumably were various isomers. Two species (69% and 14.7%, respectively) make up about 85% of the feed. Figure 23 is a GLC chromatogram of the feed;[a] Table 42 shows the GLC analysis in which the components are listed in the order of their GLC emergence times.

Table 42. ANALYSIS OF DMD FEED

Component		%w
Before	A	0.6
	A	2.1
After	A	1.2
	B	2.3
	C	5.3
	D	3.5
	E	69.3
After	E	0.8
	F	14.7
After	F	0.2

DMD was tested in the pulse reactor under conditions of both thermal and dehydrogenation reaction conditions. The reactor tube was 1/4-in. OD stainless steel tube; Type 304; Bishop and Company (see page 81). The runs were made at 10 atm pressure; 1 ul of liquid was injected per pulse. Conversions were calculated from the amounts of disappearance of the principal feed components. For computation of conversions only those species present in concentrations of 1% or more were considered principal components (i.e., A through F Figure 23, Table 42). No attempt has been made to identify a particular species nor any of the reaction products as yet. In this reactor system space velocities were calculated from the carrier gas flow rate.

a) GLC analysis were made at 248°F (120°C) using a 150-ft stainless steel column, 0.010-in. ID, coated with SF-96.

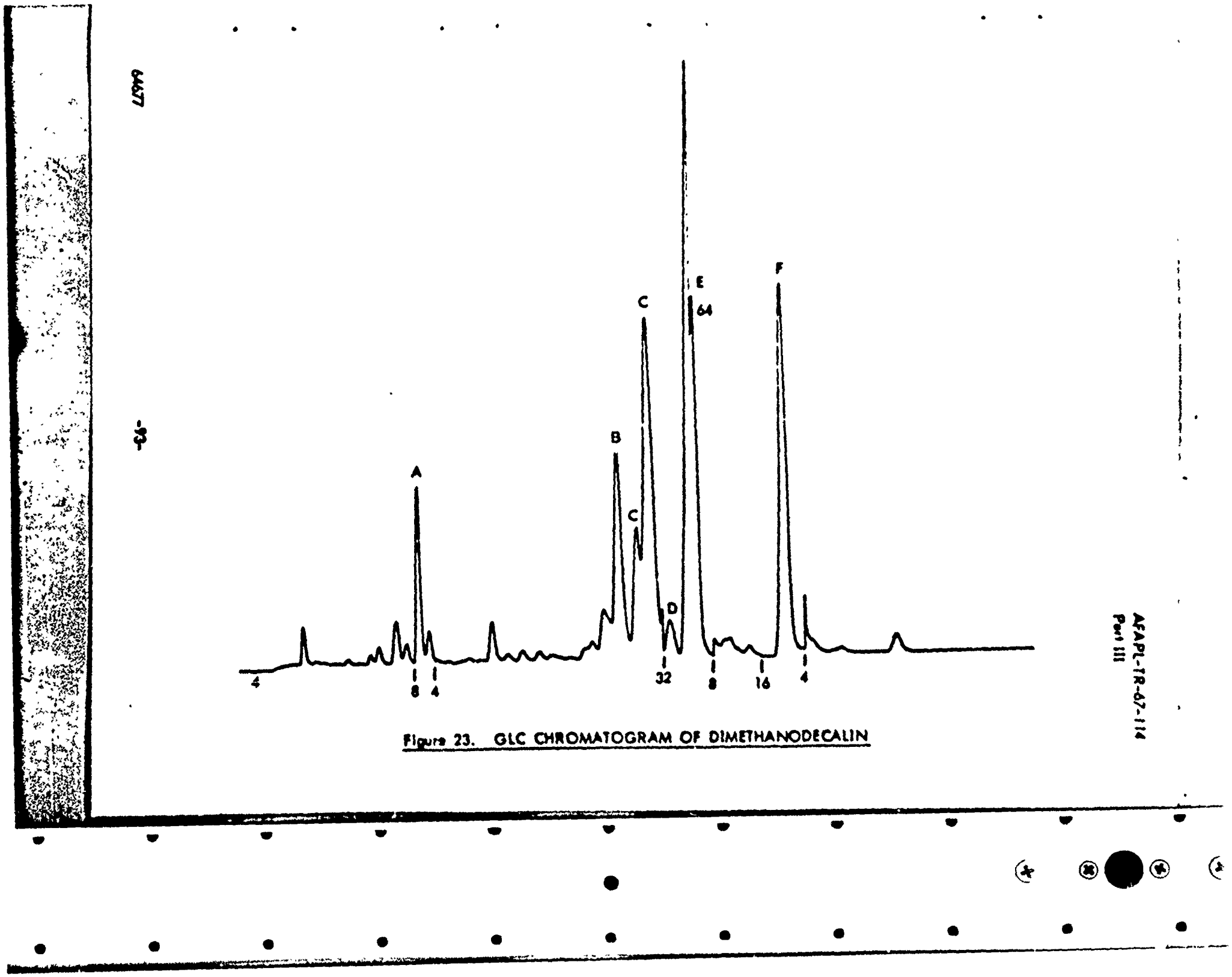

Figure 23. GLC CHROMATOGRAM OF DIMETHANODECALIN

Thermal Reaction

The thermal reaction was studied over the temperature region of 1022-1202°F at LHSV's[a] of 15 to 1590 with both helium and hydrogen carrier gas. This corresponded to apparent contact times (ACT)[b] of 4.2 to 0.32 seconds. Experiments were done in both the stainless steel tube and a tube fitted with a quartz liner.[c] The data obtained with the metal tube are presented in Tables 43 and 44 for hydrogen and helium carrier gas, respectively; and for the quartz-lined tube in Tables 45 and 46 for hydrogen and helium carrier.

In all tests DMD conversion increased with increasing temperature and increasing contact time. This is shown in Figure 23, which is a plot of conversion as a function of temperature for various space velocities (metal reactor tube; H_2 carrier gas); and by Figure 25 which shows DMD conversion as a function of LHSV for various temperatures (LHSV =1/ACT; data for quartz-lined reactor). Reactivity was greater with H_2 than with He; and was greater in the quartz-lined tube than in the metal reactor. For example at 1202°F and LHSV of 100-108, DMD conversions of 14.2% and 4.8% were observed for H_2 (Table 43) and He (Table 44) carrier, respectively, in the metal tube compared to 29% and 24% for H_2 and He in the quartz-lined tube (Figure 25). In all tests product material appeared to be primarily material lighter than DMD (i.e., emerged before compound A) and was assumed to be cracked products. Based on GLC emergence times there was some indication that small amounts (1% or less) of cis-DHN and tetralin were formed. Figure 26 is a chromatogram of the product material for Run 151-1 (Table 41). DMD appeared less reactive than DHN, as at the same temperature and contact time, DMD conversions were lower than those of DHN (cf Run 149-4, Table 43 and Run 150-1, Table 39). Heats of reaction were not calculated pending product identification.

Dehydrogenation

Dehydrogenation of DMD was carried out at 662-752°F with our standard 1% Pt on Al_2O_3 catalyst. In these experiments 0.25 ml of catalyst (0.24 g) was diluted with 1.25 ml quartz chips (10-20 mesh), to give a catalyst bed length of about three inches. Tests were done at 572, 662 and 752°F using helium and hydrogen as carrier gas. The tests consisted of a series of runs at each temperature of LHSV's[d] of 86 to 5178. The runs were bracketed to detect catalyst deactivation during the test. The data are presented in Table 47.

Catalyst deactivation was observed at all three temperatures both with helium and hydrogen carrier gas. This was concluded as the conversions for the conditions of the initial runs got progressively lower during the series of runs. This result was different than was observed with MCH[16] and

a) LHSV was calculated from the carrier gas flow rate and the bulk volume of the quartz chips. The bulk volume = 2.40 ml for the steel tube and 0.87 ml for the quartz-lined tube = volume of the empty reactor.
b) ACT was calculated from the void volume in the tube and which was taken as one-half the volume of the empty reactor.
c) The quartz-lined tube was described in a previous section (page 81).
d) LHSV were calculated from the carrier gas flow rate and the bulk volume (i.e., 0.25 ml) of catalyst.

Table 43. THERMAL REACTION OF DIMETHANODECALIN: PULSE REACTOR

He Carrier Gas

Pressure: 10 atm Pulse Volume: 1 ml
Reactor tube filled with quarts chips.

Run No 19508	145-2	146-2	146-3	147-1	147-2	148-3	148-4	149-3	149-4	151-1	151-2	152-1	152-2
LHSV	9	36	108	9	36	108	180	288	9	36	108	180	288
ACT, sec	4.8	1.1	0.38	4.0	1.0	0.33	0.20	0.12	3.7	0.94	0.31	0.19	0.12
Temperature, °F	←1022→			←1112→					←1202→				
Furnace Wall	997-1013	995-1013	1000-13	1083-1101	1085-1105	1088-1108	1087-1106	1087-1103	1168-91	1170-93	1173-91	1172-91	1173-91
Product Analysis, %													
Before A	10.8	2.8	3.0	22.8	10.1	3.4	4.4	3.4	} 17.6[b]	35.2	10.[illegible]	3.9	1.1
A	3.0	3.0	2.1	1.6	1.8	2.0	2.0	1.9		1.6	1.6	1.7	1.6
After A	6.8	1.9	1.8	2.0	1.9	1.3	1.3	1.3		3.0	2.4	1.3	1.0
B	1.8	2.8	2.1	2.3	2.1	2.0	2.1	2.0	0.6	0.9	2.1	2.0	2.0
C	6.7[a]	6.3	6.2	4.1	5.0	5.2	5.1	5.6	1.2	3.9	4.9	5.1	5.3
D		3.9	3.4	2.8	3.2	3.5	3.5	3.7	1.1	2.5	3.4	3.4	3.3
E	67.8	68.6	67.8	58.6	65.0	68.3	67.1	69.1	28.8	44.7	63.1	66.1	72.4
After E	0.0	0.0	0.2	0.0	0.5	0.5	0.6	0.6	0.6	0.0	0.0	0.0	0.0
F	8.7	11.2	13.8	8.8	10.2	13.2	12.5	13.4	0.0	2.1	7.0	10.4	12.7
After F	0.7	0.0	0.2	0.1	0.1	0.2	0.2	0.0	0.0	0.0	0.0	0.1	0.0
DMD Conversion, %	10.4	4.6	1.7	22.8	9.0	5.9	5.9	3.9	78.4	35.1	14.2	5.5	3.8
First Order Rate Constants, sec⁻¹	0.023	0.040		0.057	0.092	0.168	0.173		0.332	0.<84	0.422	0.410	

a) C + D.
b) No A present.

Table 44. THERMAL REACTION OF DIMETHANODECALIN: PULSE REACTOR

He Carrier Gas

Pressure: 10 atm
Pulse Volume: 1 ml
Reactor tube filled with quarts chips.

Run No. 10808-	165-3	166-1	166-4	167-1	168-3	169-1	169-4	170-1	170-6	172-2	172-3	172-2	170-4
LHSV	9	36	108	9	36	108	180	288	9	36	108	180	288
ACT. sec	4.2	1.1	0.35	4.0	1.0	0.33	0.26	0.12	3.7	0.94	0.31	0.19	0.12
Temperature, °F													
Furnace	← 1022 →			← 1112 →					← 1202 →				
Wall	997-1011	999-1013	999-1011	1085-1101	1085-1101	1085-1101	1083-1103	1090-1103	1166-1190	1166-1190	1166-1190	1166-1190	1166-1188
Product Analysis, %w													
Before A	2.2	0.7	0.4	19.2	3.1	1.0	0.9	0.7	52.1	17.4	6.4	2.2	0.7
A	2.0	2.0	2.0	2.0	1.8	1.8	1.9	1.6	9.6	1.7	1.8	1.7	1.6
After A	1.4	3.6	0.9	3.2	1.0	1.3	0.8	0.4	8.7	3.5	2.0	1.2	0.0
B	2.3	2.3	2.0	2.5	2.5	2.0	1.8	1.8	1.4	2.5	2.6	2.3	1.8
C	4.1	4.9	4.6	4.1	4.9	4.7	4.6	4.6	2.4	3.9	4.3	4.5	4.9
D	3.4	3.7	3.5	3.2	3.6	3.4	3.2	3.6	2.3	3.5	3.6	3.4	3.3
E	70.3	69.1	72.1	57.8	69.9	72.1	72.8	72.7	35.0	60.4	69.8	70.3	74.3
After E	0.4	0.0	0.0	0.0	0.0	0.0	0.0	0.0	0.0	0.5	0.5	0.0	0.0
F	13.7	13.6	14.6	7.9	13.1	13.6	14.0	14.6	0.2	5.6	11.3	14.4	12.9
After F	0.2	0.1	0.0	0.1	0.1	0.0	0.0	0.0	0.3	0.1	0.0	0.0	0.0
Others										0.3[a]	0.7[a]		
DMD Conversion, %w	2.1	2.1	1.8	19.6	1.9	1.7	1.8	1.3	84.7	19.3	4.8	1.3	2.8

a) After B.

Table 45. THERMAL REACTION OF DIMETHANODECALIN IN A QUARTZ-LINED TUBE: PULSE REACTOR

He Carrier Gas

Pressure: 10 atm
Pulse Volume: 1 μl
Reactor tube filled with quartz chips.

Run No. 11181-	10-1	10-2	10-3	11-1	13-1	13-2	13-3	14-1	14-2	14-3	19-3	20-1	20-2	20-3	20-4	21-1	21-2	21-3	21-4
LHSV	15	40	75	149	15	40	75	149	298	497	15	40	75	149	298	497	745	1192	1590
ACT, sec	2.2	0.81	0.43	0.22	2.1	0.77	0.41	0.21	0.10	0.062	1.9	0.73	0.39	0.19	0.10	0.058	0.038	0.024	0.018
Temperature, °F	1022				1112						1200								
Furnace	1000-1013	1004-1015	998-1011	1000-1113	1089-1105	1085-1103	1085-1101	1087-1105	1087-1105	1089-1105	1170-90	1173-91	1171-91	1173-91	1173-91	1173-91	1173-90	1173-91	1173-60
Wall																			
Product Analysis, %																			
Before A	7.2	3.6	2.1	2.1	23.3	9.9	10.0	6.7	3.0	1.4	65.9	47.1	33.1	20.8	13.4	8.7	5.3	4.2	3.8
A	3.5	2.8	2.0	2.2	2.0	1.7	2.2	2.3	2.1	1.7	0.7	1.0	1.3	1.7	1.9	1.7	1.7	1.3	1.6
After A	2.5	1.7	1.8	1.8	4.8	1.9	2.5	2.5	1.8	1.9	5.3	4.8	4.0	3.7	3.6	1.8	2.1	1.3	1.1
B	3.2	3.6	2.2	2.1	3.3	2.6	4.5	2.2	2.1	1.9	1.1	1.9	2.0	2.2	2.2	2.1	2.2	1.9	1.9
C	6.1	6.3	5.0	5.1	4.7	4.8	5.5	5.3	5.3	5.0	1.8	3.0	3.8	4.5	5.0	4.8	5.2	4.9	4.9
D	4.6	4.6	3.5	3.6	3.6	3.6	3.6	3.6	3.6	3.6	2.1	2.5	2.9	3.3	3.5	3.5	3.7	3.6	3.5
E	55.6	64.9	68.4	68.6	49.8	64.3	61.5	64.8	68.5	71.6	24.7	38.3	47.4	56.5	60.4	66.3	66.6	69.8	69.1
After A	-	-	0.8	0.7	0.7	-	-	-	0.7	-	0.2	-	-	-	0.7	-	-	-	-
F	16.6	12.3	14.0	13.6	6.2	11.0	10.0	11.	13.4	13.8	0.1	1.2	3.3	6.7	8.8	10.5	12.7	12.5	13.6
After F	0.4	0.2	0.2	0.1	0.1	0.2	0.1	0.1	0.2	-	0.3	0.1	0.1	0.2	0.1	0.2	0.3	0.2	0.0
DMD Conversion, %	14.2	7.6 (8.6)	2.9	3.3	89.1	10.1 (9.8)	13.4	6.9	3.9 (2...)	2.0	67.6	49.1 (38.)	37.2	23.1	16.3 (9.8)	8.9	6.2	3.9	3.7

Table 46. THERMAL REACTIONS OF DIMETHANODECALIN IN A QUARTZ-LINED TUBE: PULSE REACTOR

He Carrier Gas

Pressure: 10 atm
Pulse Volume: 1 µl
Reactor filled with quartz chips

Run No. 11181-	11-2	11-3	11-4	12-1	14-4	15-1	16-1	16-2	16-3	17-1	17-2	17-3	17-4	18-1	18-2	18-3	18-4	19-1	19-2
LHSV	15	40	75	149	15	40	75	149	298	497	15	40	75	149	298	497	795	1190	1590
ACT, sec	2.2	0.81	0.43	0.22	2.1	0.77	0.41	0.21	0.10	0.062	1.9	0.73	0.39	0.19	0.10	0.058	0.036	0.024	0.018
Temperature, °F	1022				1112						1202								
Furnace Wall	1002-	1002-	998-	998-	1087-	1087-	1097-	1085-	1087-	1087-	1170-	1170-	1170-	1172-	1172-	1173-	1173-	1173-	1175-
Product Analysis, %																			
Before A	4.9	2.5	1.8	1.6	27.8	9.1	5.5	3.4	1.7	1.5	65.6	40.1	27.0	15.8	6.6	4.0	2.5	1.5	1.1
A	2.5	2.0	2.0	1.9	1.5	1.8	1.9	2.2	2.1	1.9	1.2	1.1	1.5	1.8	1.8	1.8	1.7	1.4	1.6
After A	0.6	2.2	1.7	1.7	5.7	2.6	2.1	2.4	2.3	1.9	8.0	4.6	4.1	3.7	2.6	2.7	1.6	1.1	1.2
B	3.1	2.6	2.0	2.0	2.6	2.7	2.2	2.3	2.3	2.2	1.4	2.1	2.5	2.5	2.3	2.2	2.1	2.1	2.0
C	4.5	5.0	5.1	5.1	3.8	4.9	5.1	5.8	5.7	5.6	1.3	3.4	4.3	5.4	5.1	5.3	5.2	5.1	4.9
D	(a)	3.5	3.6	3.6	2.7	3.5	4.4	4.1	4.1	3.9	2.0	2.7	3.1	3.8	3.6	3.7	3.7	3.6	3.6
E	71.9	68.6	68.6	68.1	55.0	64.4	66.0	66.0	67.6	68.2	20.3	43.6	32.7	58.3	66.4	67.1	68.9	70.9	71.3
After E	-	-	0.7	0.7	-	-	0.4	0.7	0.6	-	-	-	-	0.7	-	0.7	-	-	-
F	12.3	13.8	14.1	14.6	4.7	10.5	12.1	12.0	13.2	14.6	0.1	2.1	4.3	7.3	10.9	12.7	13.9	13.7	14.1
After F	0.2	0.6	0.2	0.4	-	0.1	0.1	0.2	0.2	0.2	-	0.1	0.2	0.1	0.1	0.1	0.2	0.1	0.2
DMD Conversion, %	5.2	2.4 (2.1)	2.1	2.1	29.6	10.3 (1.9)	8.3	6.4	4.4	2.6	69.9	43.1 (1.3)	29.4	19.3	8.2	5.3	2.9	2.5	2.1

a) D plus E.

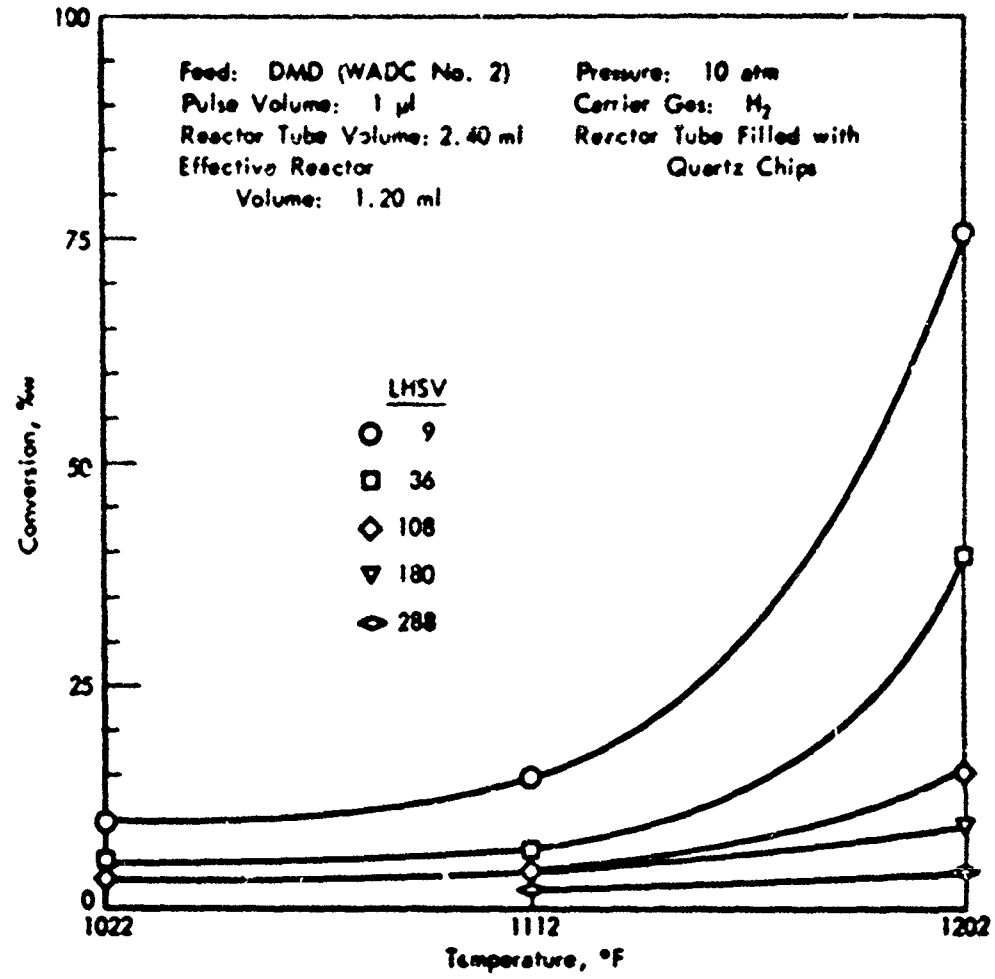

Figure 24. THERMAL REACTION OF DMD: PULSE REACTOR

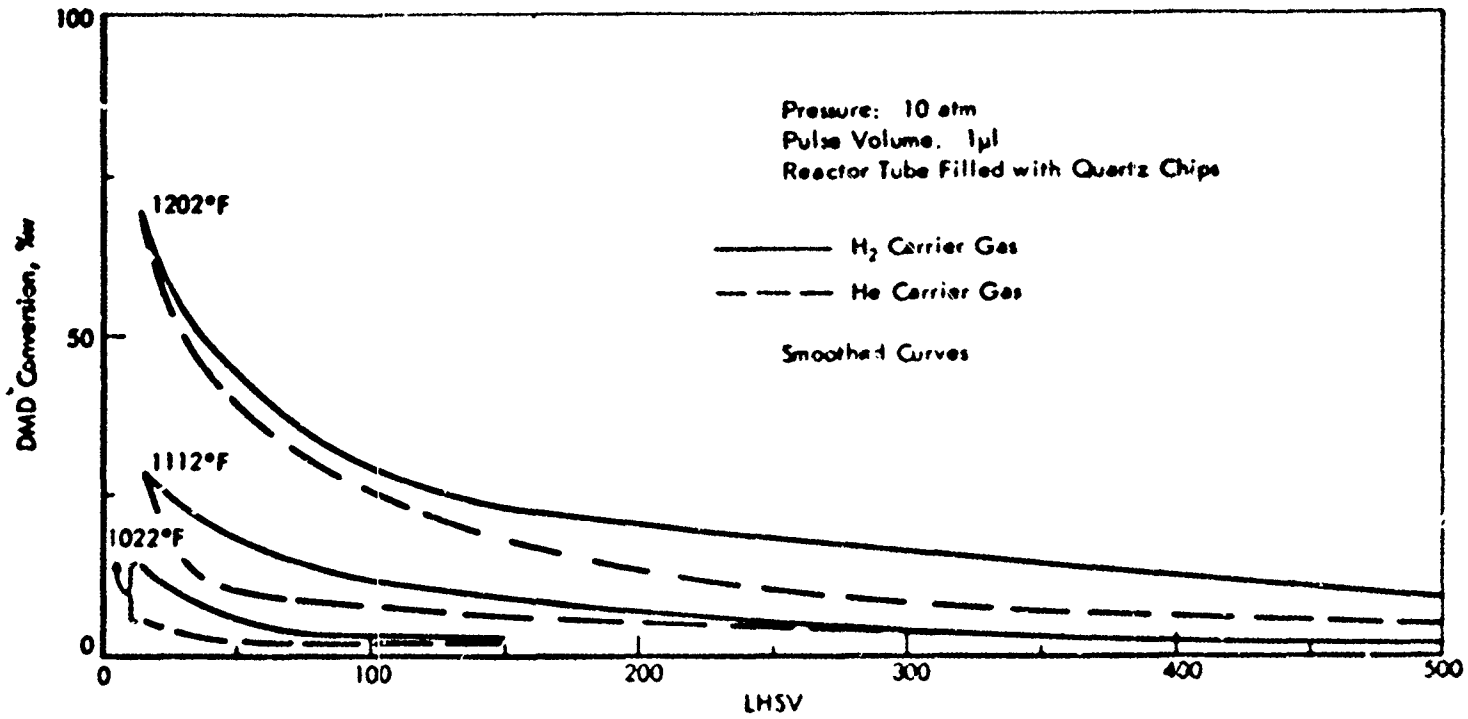

Figure 25. THERMAL REACTION OF DMD IN A QUARTZ-LINED TUBE PULSE REACTOR

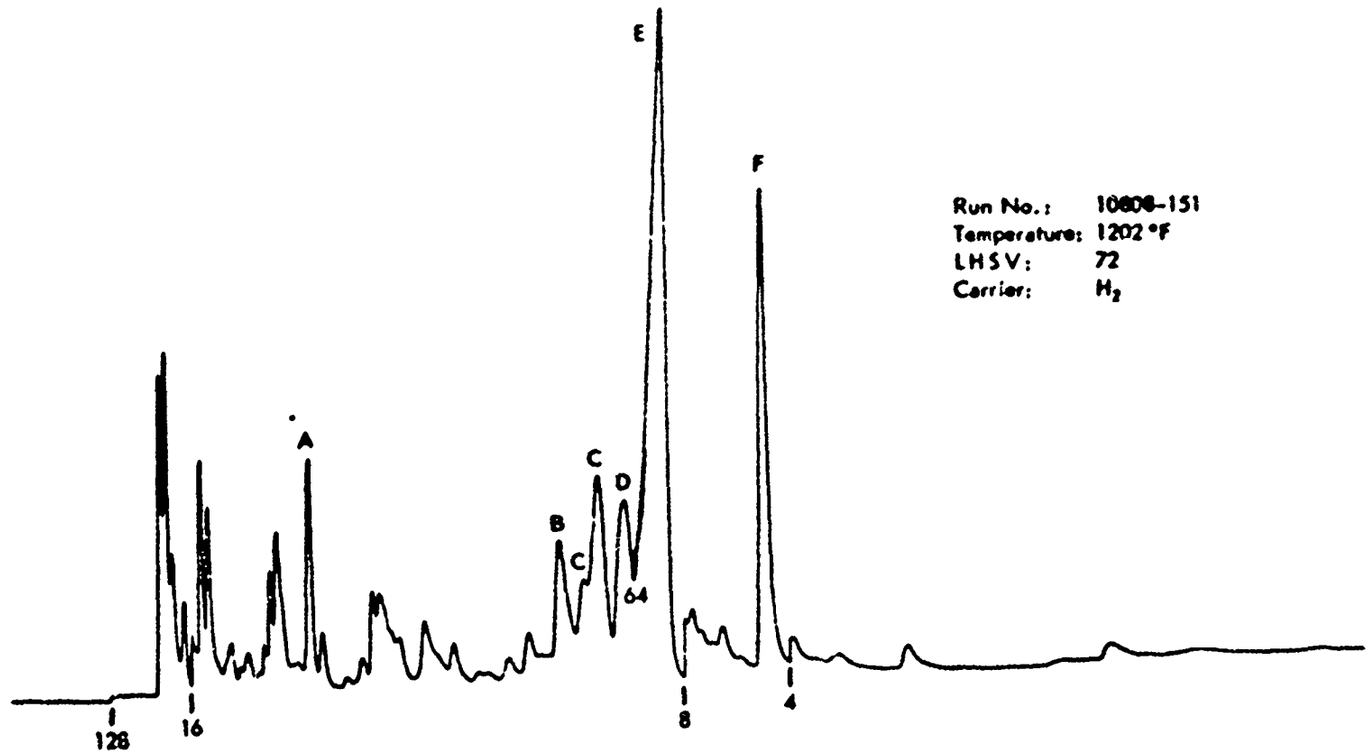

Figure 26. GLC CHROMATOGRAM REACTION PRODUCTS: THERMAL REACTION OF DMD

Table 47. DEHYDROGENATION OF DIMETHANODECALIN: PULSE REACTOR

Pressure: 10 atm
Catalyst: 1% Pt on Al_2O_3
Catalyst Volume: 0.25 ml
Catalyst wt: 0.241 g

Pulse Volume: 1 µl
Catalyst Diluted With
1.25 ml Quartz Chips.

Run No 10808-	142-1	142-2	143-1	143-2	143-3	143-4	144-1	144-2	159-2	160-1	160-2	160-3	160-4	161-1	161-2
Carrier gas	H_2								N_2						
LHSV	86	346	692	1384	86	86	346	692	1726	2590	1726	3452	1726	5178	1726
Temperature, °F			572				662				752				
Furnace															
Wall	565-70	565-70	565-70	565-70	565-70	651-58	651-60	653-60	732-45	740-45	740-47	740-47	740-47	740-47	740-47
Product Analysis, %w															
Before A	14.8[b]	2.0	0.7	0.5	0.4	2.1	1.0	1.3	20.7	14.8	12.7	14.7	17.8	6.3	11.7
A		0.5	0.7	1.2	0.8	0.4	0.6	1.0	3.0	0.7	1.4	1.3	0.4	0.4	1.7
After A		3.1	1.4	1.2	1.3	3.4	2.2	1.6	33.3	27.3	30.6	10.7	29.6	9.4	30.1
B		0.4	0.9	1.3	0.2	0.7	0.6	1.4	1.2	0.7	1.3	0.8	1.3	0.4	1.1
C	7.0	5.7	5.1	4.6	6.0[c]	7.3	4.7	4.3	4.8	3.4	6.1	3.8	6.1	4.7	5.8
D	0.0	4.1	3.9	3.6		0.0	4.0	4.3	2.3	1.7	4.2	3.3	2.0	2.9	1.7
E	69.4	71.7	73.2	73.8	78.7	73.2	73.0	73.6	24.0	38.3	34.6	51.6	34.2	50.8	38.2
After E	1.2	3.9	1.7	0.4	1.3	4.2	1.1	0.7	0	2.7	3.1	3.3	3.1	3.7	3.1
F	6.1	8.6	11.9	13.6	10.7	4.1	10.2	12.2	4.6	2.4	2.2	6.3	1.8	3.7	2.1
After F	1.5	3.3	0.5	0.0	0.0	0.4	0.4	1.2	1.4	1.0	1.3	0.2	0.1	0.0	0.1
Others[a]	0.0	0.0	0.0	0.0	0.0	0.0	0.0	0.0	4.7	3.1	4.3	3.6	3.0	3.4	0.6
DMD Conversion, %w	14.2	9.9	5.6	3.7	9.4	15.9	8.1	6.3	61.4	47.3	50.0	30.6	38.2	29.7	50.7
DMD Conversion Corrected for Catalyst Deactivation, %w	14.2	11.1	8.0	7.3	14.2	18.7	-		61.4	53.2	61.4	41.8	61.4	39.2	61.4

a) After C.
b) No A or B.
c) C + D.

DHN where catalyst deactivation was observed only with helium and not with H_2. This suggests that with DMD: a) the feed may contain a catalyst poison that is not removed by hydrogen; b) the coke precursors formed from DMD are different from those formed from DHN or MCH, and are not as readily removed by hydrogen. Further experiments are contemplated in which the feed will be passed over silica gel prior to use; and the tests will be done at higher partial pressure of hydrogen (i.e., 20 or 30 atm pressure).

The effect of space velocity on conversion is shown in Figure 27 which is a plot of DMD conversion as a function of LHSV. These points have been corrected for catalyst deactivation as was described in the section on dehydrogenation of Decalin. At both temperatures conversion declined with increased space velocity. Reactivity of DMD was considerably less than that of Decalin, possible because of catalyst deactivation. (The amount of deactivation during the initial pulse cannot be determined from our data.) As an example, at about 5000 LHSV at 752°F, 33% DMD conversion was observed (corrected for deactivation) compared to 85.6% DHN conversion (cf Run 141-1, Table 47 and Run 137-4, Table 41). Further, product material appeared to be principally cracked products, particularly at the highest temperature. This conclusion was based on the observation that the lighter components (i.e., before and after A) were greater and component E was less than were present in the starting material. This suggests that hydrogen promoted a catalytic hydrocracking-type reaction some of whose products could have strongly poisoned the catalyst. Figure 28 is a GLC chromatogram of the product of Run 139-2. It is fairly evident from the multiplicity of peaks that a reaction other than simple dehydrogenation occurred. One of the possible reactions is a reverse Diels-Alder reaction following dehydrogenation thus;

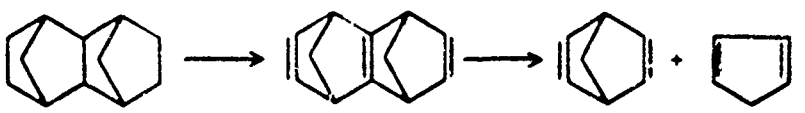

Either the cyclic acetylene or cyclopentadiene could act as catalyst poisons.

First order rate constants were calculated from the rate of disappearance of starting material. At the highest temperature and space velocity (752°F; LHSV = 5178), a value of 19.9 sec^{-1} was computed based on the corrected value of the conversion (Table 47 Run 141-1). This was considerably lower than was obtained with MCH (94.4 sec^{-1}) or DHN (57.9 sec^{-1}) and again suggests that reactions other than dehydrogenation are taking place. Further exploratory work will be done with this naphthene.

Reactivity of Bicycloheptane

Bicycloheptane (BCH) is a monocyclic naphthene with a carbon bridge across the 1,4-position. It can be in principle, dehydrogenated to yield three molecules of hydrogen according to the reaction.

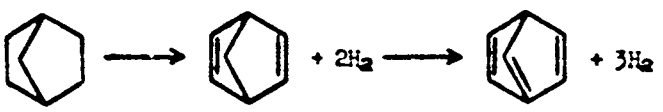

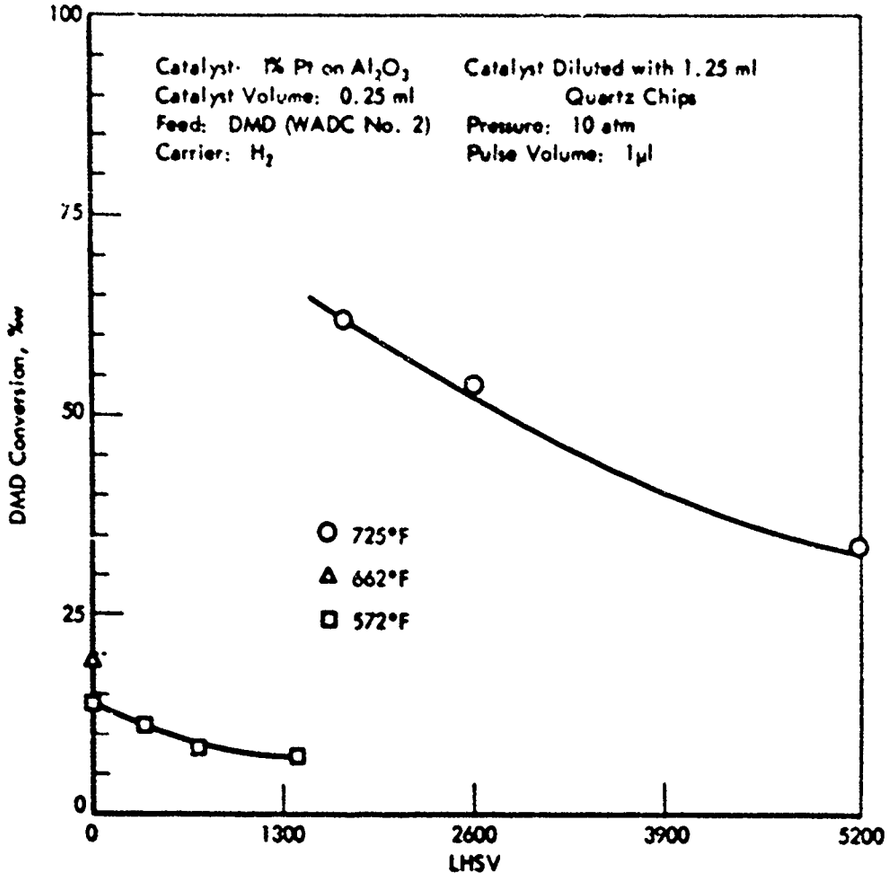

Figure 27. DEHYDROGENATION OF DMD: PULSE REACTOR

64677

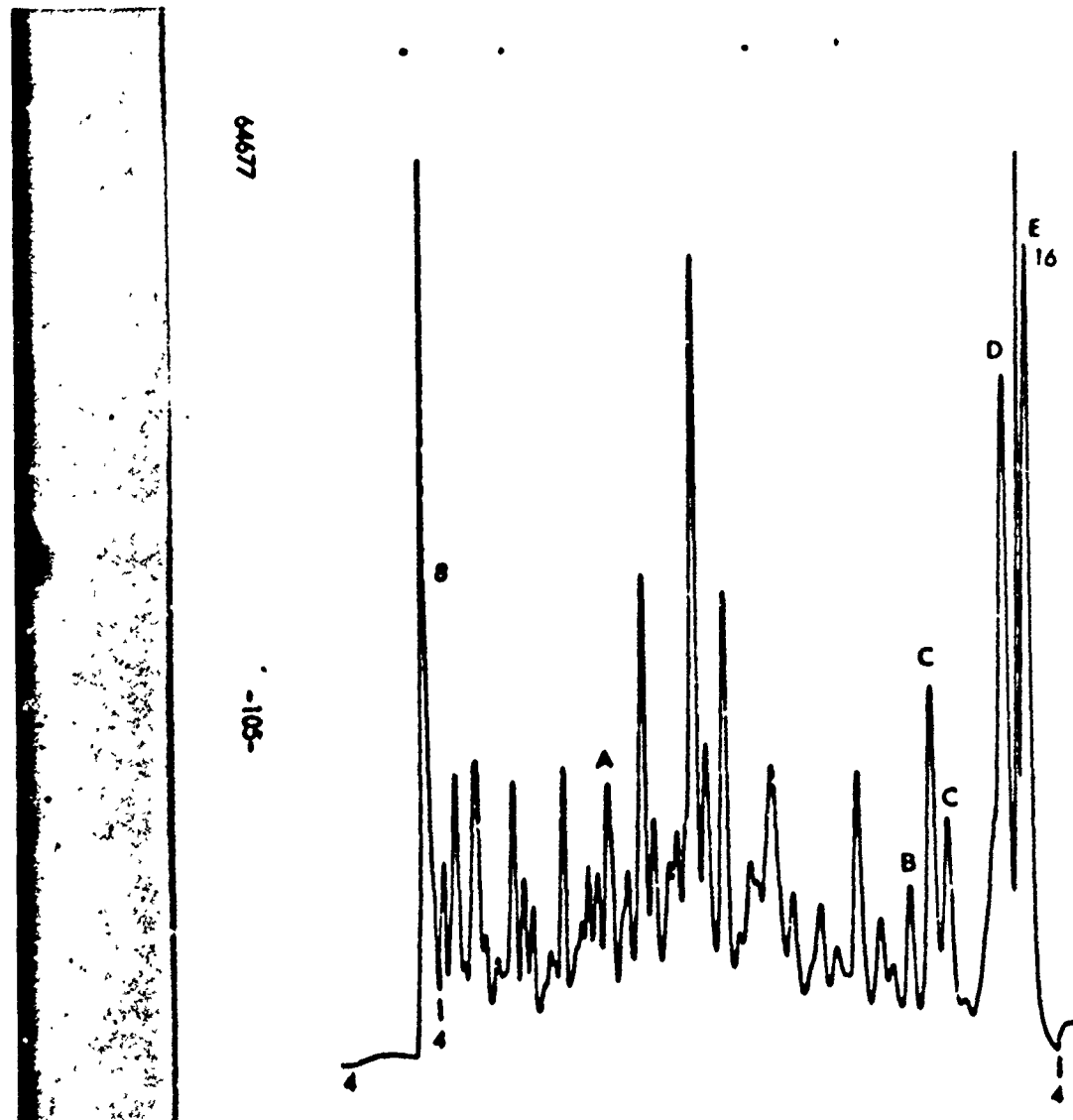

Run No.: 10808-139-2
Pressure: 10 atmospheres
LHSV: 1726
Temperature: 752 °F

Figure 28. GLC CHROMATOGRAM: REACTION PRODUCTS DEHYDROGENATION OF DMD

The endothermic heat of this reaction is 1280 Btu/lb for the first step and possibly 1600 Btu/lb for both steps. Another possible reaction of BCH is the formation of tetracycloheptadiene via the reactions:

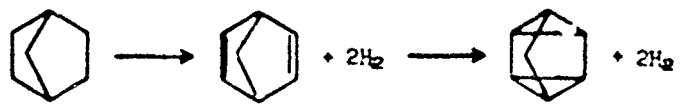

The total endothermic heat for this reaction is estimated to be about 2300 Btu/lb. Thus BCH is a very attractive candidate endothermic fuel, even though it may be difficult to carry the reactions beyond the first step.

BCH was tested in the pulse reactor under conditions of both thermal and catalytic reaction. The runs were made at 10 atm pressure; 1 ul of liquid was injected per pulse. BCH is a solid at room temperature and melts at about 177°F (80°C). Thus it was necessary to heat the syringe in order to inject the feed as a liquid. The reactor was a 1/4-in. OD stainless steel tube, Type 304 (Bishop and Co.) with 0.035-ft wall thickness and was heated by an electric furnace over a five-inch length.

GLC analysis of the BCH feed showed that 98.9% of the material came out as a single peak, followed by several smaller peaks which amounted to 1.1% and which were considered impurities.[a] Conversions were calculated from the disappearance of the principal component of the starting material. No attempt was made to identify the impurities, nor any of the reaction products as yet. In this reactor system space velocities were calculated from the carrier gas flow rate.

Thermal Reaction

Thermal reaction was studied over the temperature region of 1022 to 1202°F at LHSV[b] of 14-271 with both H_2 and He carrier gas. This range of space velocities corresponded to Apparent Contact Times (ACT) of 4.2 to 0.19 seconds. In these experiments the reactor tube was filled with quartz chips (10-20 mesh). The reactor tube was 1/4-in. OD stainless steel tube; Type 304; Bishop and Co. (See page 81.)

In a previous section of this report it was shown that the reactor tube could catalyze a cracking reaction. Thus in order to have a direct comparison between BCH and another naphthene, the thermal reaction of both BCH and Decalin (DHN) were carried out consecutively in this series of tests. The data are presented in Table 48.

With H_2 carrier BCH conversions increased with increased temperature and increased contact time (Figure 29). For example at 1202°F, DCH conversion was about 1.7% at an ACT of 0.19 seconds and increased to 7.8% and 23.8% at ACT's of 0.94 and 3.7 seconds, respectively. Further, at about 4 seconds

a) GLC analyses were made at 70°C using a 165-ft stainless steel capillary column, 0.01-in. OD, coated with SF-96 50 silicone.
b) LHSV was calculated from the carrier gas flow rate and the void volume of the tube (1.0 ml).

Table 48. THERMAL REACTION OF BICYCLOHEPTANE AND DECALIN

Flow System

Reactor Tube Material: 304 S. Stainless Steel
Reactor Filled with Quartz Chips
Pressure: 10 atm
Flow Volume: 1 ml

Run No. 11018-	15-1	15-2	15-3	16-1	16-2	16-3	16-4	17-1	18-1	18-2	18-3	18-4	19-2	19-4	19-5	20-1	20-2	20-3	20-4	21-1	21-2
Feed	DHB	BCH	DHB	BCH	DHB	BCH	←		DHB	←		BCH	→		DHB	←		BCH	→		
Carrier Gas	←	He	→	←	H_2	→	←		H_2	→	←			He	→	←			H_2	→	
Carrier Gas, Flow Rate, cc/min	←	50	→	←	50	→	50	50	200	600	50	50	200	600	50	50	200	600	50	50	200	400	1200
LHSV	10	14	10	7	10	7	27	165	14	7	27	82	10	7	27	82	10	7	27	82	246
ACT, mm	←			4.2	→		4.0	0.99	0.33	4.0	4.0	0.99	0.33	3.7	3.7	0.99	0.33	3.7	3.7	0.99	0.33	0.19
Temperature, °F																					
Block	←			1022	→		←					1112			→	←			1202	→	
Reactor Wall	995-1011	991-1011	995-1015	995-1015	1095-1105	1081-1115	1081-1103	1095-1101	1085-1103	1081-1107	1087-1105	1085-1105	1170-91	1166-89	1166-89	1166-89	1168-93	1170-93	1170-91	1170-91	1170-89
Product Analysis, %w																					
Emerged before BCH[a]		0.2		1.5		6.5	1.6	0.6		3.7	0.4	0.3		14.0	5.0	1.6		25.8	7.0	2.8	1.7
BCH Isomers		98.8		97.5		90.9	97.2	98.2		95.2	97.3	97.5		84.7	95.0	97.6		73.6	91.9	96.1	97.2
Emerged After BCH		1.0		1.2		0.6	1.2	1.2		1.1	1.2	1.6		0.7	1.1	1.0		0.6	0.9	1.1	1.1
Conversion, %w	1.2	0.2	2	1.5	20.8	6.5	1.6	0.6	19.1	3.7	0.9	0.3	98.8	16.0	5.0	1.6	98.5	25.5	7.0	2.8	1.7
First Order Rate Constant, sec^{-1}	-	-	0.0085	0.0080	0.049	0.005	0.008	-	0.018	0.0048	0.0046	-	0.298	0.382	0.086	0.083	1.379	1.097	0.063	0.047	0.043

a) Assumed to be cracked products

Table 49. DEHYDROGENATION OF BICYCLOHEPTANE AT 752°F: PULSE REACTOR

Reactor:
Catalyst: 1% Pt on Al_2O_3
Catalyst Volume: 0.25 cc
Pressure: 10 atm
Pulse Volume: 1 µl
Catalyst Diluted With 1 cc Quartz Chips

Run No. 11018-	52-1	52-2	53-1	53-2	53-3	53-4	54-1	54-2	54-3	54-4	55-1	55-2	55-3
Carrier Gas	← H_2 →									N_2	H_2	N_2	H_2
Carrier Flow Rate, cc/min	3000	1000	3000	800	3000	200	3000	50	3000	50	3000	200	3000
LHSV	3430	1143	3430	686	3430	228	3430	57	3430	57	3430	228	3430
Reactor Cell Temperature, °F	741-47	743-47	739-47	743-47	739-47	743-47	738-45	741-47	739-45	741-47	739-47	743-47	739-45
Product Analysis, %													
Lighter than BCH	36.7	51.4	35.1	82.2	35.6	86.3	36.8		34.2	36.5	23.4	12.3	14.0
BCH	62.7	39.4	64.8	13.4	63.7	6.8	62.6		65.2	65.2	76.1	86.8	84.8
After BCH	0.6	3.2	0.3	4.4[a]	0.7	7.1[a]	0.6		0.6	0.6	0.3	0.9	1.2
NB Conversion, %													
Observed	37.7	61.1	36.2	88.7	36.7	93.4	38.1		36.0	37.1	25.2	13.5	15.0
Corrected for Catalyst Deactivation	-	-	-	-	-	-	-		36.0		36.0	34.5	36.0
First Order Rate Constant, sec^{-1}	23.2	15.4	22.0	10.8	22.5	0.18	24.3		22.2	0.398	22.2[a]	1.85[a]	22.2[a]

a) Corrected for catalyst deactivation.

Table 50. DEHYDROGENATION OF BICYCLOHEPTANE AT 752°F

Reactor:
Catalyst: 1% Pt on Al_2O_3
Catalyst Volume. 0.25 ml

Pressure: 10 atm
Pulse Volume: 1 µl
Catalyst Diluted With 1 ml Quartz Chips

Run No. 11018-	48-1	48-2	49-1	49-2	49-3	50-1	50-2	50-3	50-4	51-1	51-2	51-3
Carrier Gas	← H_2 →						← He →					
Carrier Flow Rate, cc/min	3000	2000	3000	1500	3000	1000	3000	2000	3000	1500	3000	1000
LHSV	3430	2290	3430	1715	3430	1143	3430	2290	3430	1715	3430	1143
Reactor Wall Temperature, °F	740-47	740-47	738-45	740-45	736-45	740-47	738-45	740-45	738-45	741-45	740-45	741-47
Product Analysis, %w												
Lighter than BCH	33.0	44.0	35.9	47.0	32.0	52.8	3.1	1.8	1.5	1.6	1.8	1.8
BCH	66.5	55.6	63.7	52.2	67.1	46.9	95.7	97.1	97.3	97.1	97.0	96.9
After BCH	0.5	0.4	0.4	0.8	0.9	0.3	1.2	1.1	1.2	1.3	1.2	1.3
NB Conversion, %w	33.5	44.4	36.2	47.8	32.9	53.1	4.3	2.9	2.7	2.9	3.0	3.1
First Order Rate Constant, sec^{-1}	20.0	19.2	22.0	15.9	19.5	12.4	2.14	0.978	1.35	0.735	1.47	0.526

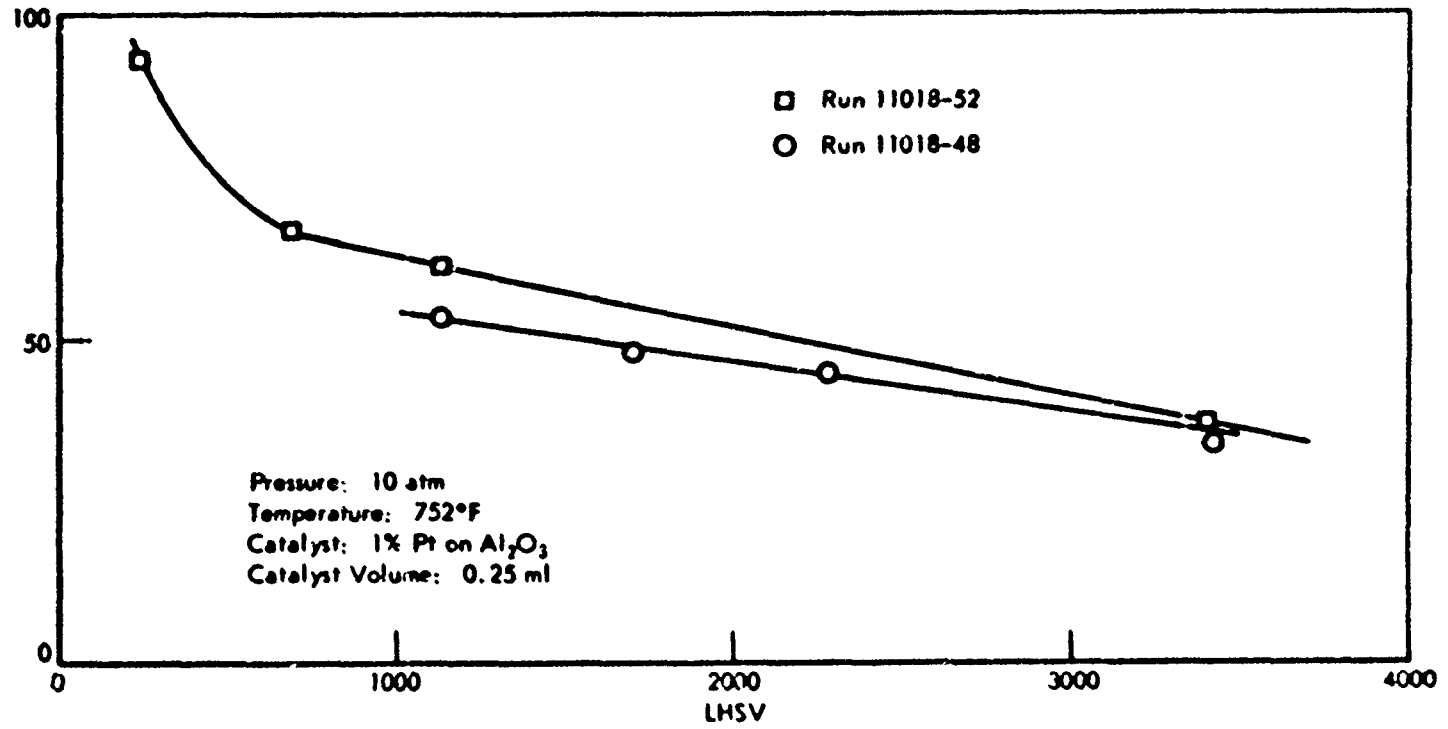

Figure 30. DEHYDROGENATION OF BICYCLOHEPTANE: PULSE REACTOR

Table 51. DEHYDROGENATION OF BICYCLOHEPTANE AT 562°F

Reactor
Catalyst: 1% Pt on Al_2O_3
Catalyst Volume: 0.25 cc
Pressure: 10 atm
Pulse Volume: 1 µl
Catalyst Diluted With 1 cc Quartz Chips

Run No. 11013-	42-2	43-1	43-2	43-3	43-4	44-1	44-3	45-1	45-2	45-3	46-1	46-2	46-4	47-1
Carrier Gas	← N_2 →							← He →						
Carrier Flow Rate, cc/min	1000	600	1000	200	1000	50	1000	1000	600	1000	200	1000	50	1000
LHSV	1143	686	1143	229	1143	57	1143	1143	686	1143	229	1143	57	1143
Reactor Zall Temperature, °F	650-57	655-57	655-57	653-57	655-57	653-57	655-57	653-57	653-57	653-57	653-57	653-57	653-57	653-57
Product Analysis, %														
Lighter than BCH	16.5	19.9	18.5	37.7	19.8	74.2	17.4	3.0	1.3	0.6	1.1	0.7	1.9	0.6
BCH	82.1	78.9	80.2	60.9	79.7	25.2	80.9	96.7	98.0	98.5	97.8	97.9	97.3	98.0
After BCH	1.4	1.2	1.3	1.4	0.5	0.6	1.7	0.3	0.7	0.9	1.1	1.4	0.8	1.4
NB Conversion, %	17.9	21.1	19.8	39.1	20.3	74.8	19.1	3.3	2.0	.15	2.2	2.1	2.7	2.0
First Order Rate Constant, sec^{-1}	3.16	2.17	3.34	1.51	3.41	1.10	3.20	0.521	0.199	0.209	0.070	0.313	0.022	0.313

The results obtained thus far with this catalyst were similar to those obtained with DMD in that under the test conditions, cracking appeared to be the principal reaction. As the reactivity was greater with H_2 this suggests that hydrogen promotes a cracking-type reaction. Possibly less catalyst deactivation and hence improved reactivity might be obtained by operating the reaction at higher pressures.

It proved extremely difficult to inject pure liquid BCH into the pulse reactor. This was because there was only a small temperature difference between the melting point (190°F) and the boiling point (223°F), and hence the syringe could not be maintained at the proper temperature during feed injection. Consequently the other twelve catalysts were tested with a mixture of 68% BCH, 31% benzene and 1% unidentified material. Tests were done at LHSV's of 206 and 21 over the temperature range of 662-1022°F. The complete data are presented in Table 52.

None of the catalysts tested were particularly effective in dehydrogenating BCH to the mono- or diene. In fact the most bicycloheptadiene produced was with the R-8 alumina support (see Runs 154-2 and 154-4), with only about 15% selectivity at about 45-50% BCH conversion. A number of the catalysts did produce benzene plus toluene in about 50% selectivity at 65% BCH conversion or higher (e.g., 10860-92D; 9874-114B; 9874-144). Unfortunately the endothermic heat of this reaction is only about 450 Btu/lb for complete conversion of BCH to toluene, so this is not a very attractive reaction path. Cracked material was one of the principal products and some of the catalysts were more effective for the cracking reaction than others (cf 9874-22B, 9874-39B with 9874-114B and 9874-141B). Of the catalyst supports the silica was the least active and the R-8 alumina was the most active. In fact it appeared that for metals mounted on this latter support a good portion of the catalyst activity was due to the support (cf R-8 Al_2O_3 with 9874-144 and 9874-141B).

From the results obtained in these tests and the tests with our standard catalyst it appears that it will be difficult to dehydrogenate bridged ring naphthenes to the corresponding aromatics with high or even moderate selectivity.

Bench-Scale Evaluation Tests With Methylcyclohexane

Two catalysts were evaluated in the bench-scale reactor. One of these was prepared under our catalyst development program (10860-34) and the other was a commercial platinum on alumina catalyst (Houdry 200-SR; Series A). The test procedure, which has been described in a previous report,[1e] gives a measure of the effect of temperature, pressure, space velocity (i.e., contact time) and catalyst stability over a three-hour test period using a single charge of catalyst. This test involves making a series of runs at 842 and 1022°F, 10 and 30 atm, and LHSV's of 50 and 100. Our standard laboratory platinum on alumina catalyst was also tested for comparison.

The results of the tests, the conditions of each run, and the order in which the runs were made are shown in Table 53. Each catalyst was rated as to "Relative Performance". This rating was designed to show how the catalyst was performing at the end of the test, relative to the standard catalyst and quantitatively was taken as the ratio of the first order rate

Table 52. DEHYDROGENATION OF BICYCLOHEPTANE OVER VARIOUS CATALYSTS: PULSE REACTOR

Pressure: 10 atm
Pulse Volume: 1 µl
Catalyst Volume: 0.25 ml
Catalyst diluted with 1.0 ml quartz chips

Feed
BCH: 68.0%
Benzene: 31.0%
U_1: 0.5%
U_2: 0.7%

Run No. 11181-	Catalyst	Carrier Gas	Reaction Temp, °F	LHSV	Product Analysis, % Cracked Liquid	Benzene	Bicyclo-heptadiene	Bicyclo-heptene	Bicyclo-heptane	U_1 a)	Toluene	U_2 b)	Others c)	Yield Benzene, %	BCH Conversion, %	Selectivity to Benzene from Toluene, %
165-1	Cr_2O_3/Al_2O_3	H_2	662	21	0.1	30.5	0.0	0.5	68.2	0.5	0.0	0.1	0.0	0.0		
165-3	CCI-C-A	H_2	752	21	0.3	30.6	0.0	0.1	67.4	0.0	[illegible]	0.6	0.0	0.0	0.2	
166-2		H_2	1022	21	9.7	37.4	0.0	0.1	48.5	0.1	3.4	0.5	0.0	6.3	45.7	87.7
168-1	10X80-172A	H_2	842	206	49.7	15.8	0.2	0.0	32.1	0.2	2.2	0.1	1.7	47.2	54.8	-
168-2		H_2	842	21	84.1	2.6	0.0	0.0	0.0	0.0	3.3	0.0	0.0	[illegible]	100	
168-3		H_2	842	206	23.2	33.0	0.0	[illegible]	40.8	0.1	1.7	0.1	0.0	[illegible]	[illegible]	17.4
168-4		H_2	842	21	33.5	43.9	0.0	0.0	15.8	0.0	0.4	0.3	0.0	[illegible]	77.6	97.4
169-1		H_2	1022	206	25.6	46.9	0.0	0.0	24.8	0.2	0.6	0.0	0.0	47.4	0.4	97.4
169-2		H_2	1022	21	58.8	28.8	0.2	0.0	27.3	0.3	3.0	3.4	0.6	43.0	54.3	
171-1	10% Pt_2O_3 on Al_2O_3 Harshaw Mo-0502	H_2	662	21	0.2	30.7	0.0	0.0	68.5	0.0	0.0	0.6	0.0	30.5	0.0	
171-3		H_2	752	21	0.7	31.4	0.0	0.0	66.4	0.0	1.0	0.5	0.0	30.4	2.4	97.1
172-2		H_2	842	21	2.1	33.1	0.0	0.0	61.5	0.0	2.3	0.6	0.0	31.1	4.6	94.2
172-4		H_2	1022	21	9.8	42.7	0.0	0.1	31.1	0.1	15.7	0.5	0.0	41.6	54.3	74.1
157-1	BA-1 Al_2O_3	H_2	842	20	0.2	31.2	0.0	0.0	68.0	0.0	0.0	0.6	0.0	31.2	0.0	-
157-3		H_2	842	206	0.2	29.0	0.0	0.1	69.7	0.1	0.7	0.0	0.0	29.0	0.0	
157-4		H_2	842	21	0.7	31.1	0.0	0.0	67.1	0.1	0.0	1.0	0.0	30.1	1.3	-
158-2		H_2	1022	206	0.8	30.7	0.2	0.0	65.5	1.1	1.6	0.0	0.0	30.5	3.7	-
158-3		H_2	1022	21	6.7	31.5	1.7	0.0	45.4	3.8	6.3	2.7	1.9	23.5	33.2	92.7
158-4		H_2	1022	206	0.7	32.5	0.1	0.0	64.6	0.7	0.0	1.1	0.1	31.5	3.0	96.1
159-1		H_2	1022	21	3.8	33.2	0.6	0.0	46.5	2.6	8.9	4.1	0.0	28.2	31.9	91.2
161-1	Davison SiO_2 Cab. Grade 59	H_2	842	206	0.0	30.3	0.0	0.0	68.9	0.0	0.0	0.6	0.0	30.7	0.0	-
161-2		H_2	842	21	0.1	28.8	0.0	0.1	68.3	0.0	0.0	0.6	0.0	28.2	0.0	
161-3		H_2	842	206	0.0	30.1	0.0	0.0	69.0	0.0	0.0	0.7	0.0	30.1	0.0	
161-4		H_2	842	21	0.2	30.4	0.0	0.0	68.3	0.0	0.0	1.1	0.0	30.6	0.0	-
162-2		H_2	1022	206	0.2	30.1	0.0	0.0	68.9	0.2	0.0	0.6	0.0	30.9	0.0	-
162-3		H_2	1022	21	0.5	31.1	0.0	0.0	67.6	0.0	0.0	0.8	0.0	30.1	0.6	-
163-1		H_2	1022	206	0.1	30.5	0.0	0.0	68.3	0.1	0.0	0.6	0.0	30.7	0.0	
163-2		H_2	1022	21	0.6	32.5	0.1	0.0	65.0	0.1	3.0	1.7	0.0	31.5	4.6	90.0
147-1	9874-998	N_2	842	206	55.2	16.1	0.0	0.0	26.4	0.1	2.2	0.0	0.0	[illegible]	61.2	
147-2		N_2	842	21	91.0	5.0	0.0	0.0	2.0	0.0	1.1	0.0	0.0	[illegible]	7.1	-
147-3		N_2	842	206	24.6	24.7	0.0	0.0	41.9	0.0	8.5	0.3	0.0	[illegible]	33.4	-
147-4		N_2	842	21	33.9	39.7	0.0	0.0	11.2	0.0	14.1	1.2	0.0	[illegible]	53.3	92.1
148-2		N_2	662	206	92.1	5.5	0.0	0.0	1.9	0.0	0.0	0.5	0.0	[illegible]	5.5	-
148-3		N_2	662	21	69.5	1.7	0.2	0.0	25.6	0.0	1.8	0.1	0.0	[illegible]	2.3	-
149-1		N_2	662	206	[illegible]	34.4	0.2	0.0	36.7	0.0	3.0	0.8	0.0	[illegible]	12.6	96.6
149-2		N_2	662	21	15.8	32.4	0.0	0.0	46.3	0.0	3.6	0.9	0.0	[illegible]	31.1	96.6

a) U_1 = unidentified; emerged after bicycloheptene.
b) U_2 = unidentified; emerged after toluene.
c) Emerged after benzene.

Table 52 (Contd). DEHYDROGENATION OF BICYCLOHEPTANE OVER VARIOUS CATA. [illegible]; PULSE REACTOR

Run No. 11161-	Catalyst	Carrier Gas	Reaction Temp, °F	LHSV	Product Analysis, %w								Yield Benzene, %w	BCH Conversion, %w	Selectivity for Benzene Formation, %w
					Cracked Liquid	Benzene	Cycloheptadiene	Bicycloheptene	Bicycloheptane	U_1	Toluene	U_2	Others			
151-1	9874-22B	[illegible]	842	206	48.[illegible]	12.0	0.0	0.0	39.5	0.0	0.0	[illegible]	[illegible]	-17.0	41.9	-
151-2		[illegible]	842	21	82.1	6.2	0.0	0.0	[illegible]9.0	1.0	1.6	0.0	0.0	24.8	86.8	-
151-3		[illegible]	842	206	0.8	35.1	0.0	0.1	38.5	0.2	4.4	0.6	0.1	+4.1	14.0	[illegible]
151-4		[illegible]	842	21	4.3	38.1	0.2	1.7	34.6	1.4	[illegible].2	2.7	2.8	+7.1	[illegible].1	[illegible]
154-1	R-8 Al_2O_3	[illegible]	842	206	1.3	32.2	1.8	0.[illegible]	[illegible]9.5	1.5	0.0	1.9	1.6	+1.2	[illegible]5	14.1
154-2		[illegible]	842	21	4.0	31.1	5.5	0.4	[illegible]5.3	3.5	10.6	3.7	3.7	+0.1	[illegible]9.1	[illegible]7
154-3		[illegible]	842	206	0.3	32.2	1.3	0.0	6.6	1.1	5.9	1.4	0.7	+1.2	16.8	[illegible]5
154-4		[illegible]	842	21	1.4	30.0	5.2	0.0	17.6	2.8	8.9	4.0	8.7	-1.0	84.7	-
159-1	9874-14A	[illegible]	842	206	1.9	33.0	0.4	0.0	[illegible]1.2	3.4	4.3	1.1	[illegible].2	[illegible].9	24.7	37.5
159-2		[illegible]	842	21	3.2	27.7	0.4	0.0	1.[illegible]	10.9	11.3	0.6	14.[illegible]	-3.3	58.4	-
159-3		[illegible]	842	206	0.4	34.1	0.3	0.0	[illegible]0.[illegible]	0.5	2.5	1.3	0.3	+3.1	11.3	72.7
160-1		[illegible]	842	21	1.2	27.3	1.8	0.0	[illegible]8.[illegible]	2.5	6.6	3.9	2.6	-3.7	[illegible]1	-
160-3		[illegible]	1022	206	7.2	33.9	2.8	0.0	11.6	3.6	20.2	2.4	6.3	+2.9	[illegible]2	54.[illegible]
162-1		[illegible]	1022	206	2.[illegible]	34.7	1.8	0.0	[illegible]4.2	2.6	16.5	4.7	3.3	+3.7	[illegible].7	57.[illegible]
144-1	9874-141B	[illegible]	842	206	1.0	31.7	0.5	0.0	[illegible]2.2	4.1	5.9	0.7	3.3	+0.7	[illegible]2	[illegible].8
144-2		[illegible]	842	21	3.6	31.9	0.7	0.0	[illegible]6.9	10.4	15.3	0.5	10.7	+0.9	[illegible].4	[illegible]7.4
144-3		[illegible]	842	206	0.4	31.9	0.4	0.0	[illegible]2.4	0.5	2.9	1.3	0.[illegible]	+0.[illegible]	[illegible].	[illegible]7.7
144-4		[illegible]	842	21	1.8	28.3	2.1	0.0	[illegible]0.4	1.9	[illegible].8	2.9	1.7	-2.6	[illegible].1	-
145-2		[illegible]	1022	206	10.5	33.3	2.0	0.0	[illegible]3.7	2.8	[illegible]1.4	1.7	4.4	+2.3	65.1	56.[illegible]
145-3		[illegible]	1022	206	3.2	35.9	1.7	0.7	[illegible]3.8	1.7	14.6	4.8	[illegible].6	+4.9	90.3	57.[illegible]
152-1	10860-92D	[illegible]	842	206	1.6	30.8	0.0	0.0	[illegible]5.6	1.1	5.6	0.3	7.0	-0.2	8.2	-
152-2		[illegible]	842	21	6.6	30.6	1.9	0.0	[illegible]3.0	2.2	10.4	0.1	15.2	-0.4	51.3	-
152-3		[illegible]	842	206	2.6	33.9	0.0	0.0	[illegible]1.4	0.4	1.4	0.0	3.0	+2.9	9.7	69.2
152-4		[illegible]	842	21	8.4	33.3	0.1	0.0	[illegible]2.9	0.4	[illegible].6	0.1	0.1	+2.3	[illegible]2.[illegible]	[illegible].7
153-3		[illegible]	1022	206	17.9	32.9	1.9	0.0	[illegible]2.3	1.2	17.5	0.0	6.3	+1.9	67.2	[illegible].3
153-4		[illegible]	1022	21	35.1	33.1	0.5	0.0	0.7	0.[illegible]	29.0	0.0	1.5	+2.1	9[illegible].0	[illegible].2
154-1		[illegible]	1022	206	18.5	29.8	0.0	0.0	[illegible]9.9	0.6	8.1	13.0	0.1	-1.2	56.0	
128-1	10860-92E	[illegible]	842	206	0.3	31.4	0.0	0.0	[illegible]3.9	1.3	[illegible] 1	0.7	0.3	+0.4	6.[illegible]	61.3
128-2		[illegible]	842	21	0.7	31.3	0.2	0.0	[illegible]0.6	[illegible].9	[illegible].8	0.7	1.[illegible]	+0.3	[illegible].6	[illegible]
128-3		[illegible]	842	206	0.8	31.7	0.0	0.0	[illegible]5.8	0.1	1.0	0.6	[illegible].0	+0.7	[illegible].2	[illegible]
128-4		[illegible]	842	21	1.8	33.3	0.3	0.0	[illegible]5.3	0.8	7.1	1.3	0.1	+2.3	[illegible]7	[illegible]
156-1	10860-92A	[illegible]	842	206	42.0	25.3	1.7	0.0	3.1	0.4	10.7	0.0	16.8	-5.7	[illegible].	-
156-2		[illegible]	842	21	71.4	21.8	0.1	0.0	0.[illegible]	0.0	6.1	0.0	[illegible].6	-9.2	100	-
156-3		[illegible]	842	206	18.5	42.7	0.4	0.0	[illegible]5.[illegible]	0.2	10.5	0.0	[illegible].4	+11.7	61.9	54.[illegible]
156-4		[illegible]	842	21	51.2	30.4	0.0	0.0	0.5	0.0	17.8	0.0	0.1	+[illegible].4	[illegible].3	[illegible]

Table 53. DEHYDROGENATION OF METHYLCYCLOHEXANE

Evaluation of Various Catalysts

Feed: Pure MCH
Reaction Time: 20 minutes

Run No.	1	2	3	4	5	6	7	E_{ACT}, kcal/mole	E_c/E_s	Relative Performance, k_c/k_s
Block Temperature, °F	842	←			1022		→			
Pressure, atm	10	10	30	10	10	10	10			
LHSV	100	100	100	100	50	100	100			
MCH Conversion, % for Catalyst No.										
9874-7[a]	40.0	57.7	59.7	68.2	92.1	65.9	64.4	10.9	-	-
10860-34	42.1	54.9[a]	61.8	44.9	52.3	15.3[b]	-	-	-	-
Houdry 200	57.1	63.1	55.8	63.9	85.5	60.3	58.7	11.9	1.09	0.85

a) Standard Catalyst.
b) Catalyst deactivated badly during runs 2, 4 and 5 as bed temperature increased by 75 to 113°F during each of these runs

constant with the catalyst (k_c) to that with the standard catalyst (k_s) calculated from the MCH conversion of Run No. 7.

Based on these tests the lab prepared catalyst was more active than the standard catalyst initially, but deactivated badly during the test, and became inactive before the completion of the test. Possibly operating the reactor at higher pressure might stabilize this catalyst.

The Houdry catalyst was less active than the standard catalyst, had slightly higher apparent activation energy for dehydrogenation, and deactivated slightly more than the standard catalyst.

Evaluation of Catalysts for the Dehydrogenation of MCH in MICTR, Bench-Scale and FSSTR Tests

In earlier tests in the MICTR[10] and in the bench-scale apparatus,[10] catalyst number 10280-46 and its prototype 9874-199B were shown to be superior to the standard reference catalysts for the dehydrogenation of MCH. These catalysts consisted of platinum mounted on a granular support. On the basis of the good activity found it was decided to test this catalyst in the FSSTR and a large batch was prepared using a spherical support. The spherical support had the same composition as the granular support. The large batch of spherical catalyst was number 10280-113 (Shell 113) and its prototype was 10280-91A.

Shell 113 was evaluated in our bench-scale reactor using our standard test procedure.[a] The results of the tests are shown in Table 54, which also includes the data obtained with 9874-199B (platinum on granular support; obtained earlier)[10] for comparison. Shell 113 was about 15% more active than the standard catalyst, but was definitely inferior to the granular support catalyst.

Activation energies ranged from 10.3 (standard catalyst) to 13.4 kcal/mole. These values were calculated from the rate constants obtained from the data of Runs 1 and 2. All of the activation energies were greater than that of the standard catalyst; this suggests that the new catalysts would be even more active than the standard catalyst at temperatures above 1022°F.

It was of interest to compare the performance of Shell 113 to that of the reference catalyst in the three test apparatii. In these apparatii the reference catalysts and the test conditions were different and are shown in Table 55.

In tests with 10280-91A (Shell 113 prototype) in the MICTR, 76% MCH conversion was observed at 842°F after 13 minutes reaction time compared to 66% conversion with the reference catalyst. Based on first order rate constants, catalyst 10280-91A was about 32% more active than the reference catalyst.

In tests in the bench-scale reactor Shell 113 was about 15% more active than our standard laboratory catalyst.

---

a) See page 15.

Table 54. DEHYDROGENATION OF METHYLCYCLOHEXANE

Evaluation of 10280-113

Feed: Pure MCH
Reaction Time: 30 minutes

Conditions	Run No. 1	2	3	4	5	6	7	E_{act}, kcal/mole	E_c/E_s	Relative Performance K_c/K_s
Block Temp, °F	842	← 1022 →								
Pressure, atm	10	10	30	10	10	10	10			
LHSV	100	100	100	100	100	100	100			
MCH Conversion, %w for Catalyst No.:										
	Series A									
9874-7[a]	39.2	56.0	59.2	69.3	93.6	68.0	66.3	10.3	1.00	1.00
10280-113	41.2	70.1	60.4	71.1	94.7	70.0	69.8	12.6	1.22	1.15
	Series B									
9874-7[a][c]	43.4	67.4	61.2	69.3	94.8	65.5	65.1	11.8	1.00	1.00
9874-199B[b][c]	48.6	78.7	67.4	78.0	97.6	77.1	77.1	13.4	1.14	1.34

a) Standard laboratory 1% Pt on Al_2O_3 catalyst.
b) Prototype of 10280-46 (Shell 46).
c) Table 6, page 28, reference 10).

Table 55. TEST CONDITIONS IN VARIOUS APPARATUS FOR CATALYST EVALUATION

Apparatus	Reference Catalyst	Test Conditions		
		Pressure, atm	Temperature, °F	LHSV
MICTR	9874-24	10	662- 842	100
Bench-scale	9874-7[a)]	10	842-1022	100
FSSTR	UOP-R8	35-58	900- 938	625-1610

a) Standard laboratory 1% Pt on Al_2O_3 catalyst.

In tests in the FSSTR it appeared that Shell 113 was definitely more active than the reference catalyst UOP-R8. The pertinent data obtained in the FSSTR are shown in Table 56. For a more detailed comparison of the two catalysts all of the FSSTR data will be analyzed using our packed bed computer program in future work. For the present it is apparent that the Shell 113 catalyst was more active than the reference catalysts in all tests. Other catalysts that were more active and more stable than Shell 113 or UOP-R8 under MICTR and bench-scale test conditions (such as 10280-46 and 10860-114C) will be evaluated under FSSTR test conditions in the future.

Table 56. DEHYDROGENATION OF MCH OVER UOP-R8 AND SHELL 113 IN THE FSSTR

Reactor Tube Length: Two feet
Reactor OD: 0.375 inches
Initial Pressure: 900 psig
Inlet Temperature: 900°F

Catalyst	MCH Feed		Heat Input		MCH Conversion, %	Outlet Fluid Temp, °F	Outlet Press., psig
	lb/hr	LHSV	Btu/hr	Btu/lb			
R-8	64.5	1610	40,000	620	61	930	500
R-8	25.1	625	20,000	797	77	938	830
113	62.1	1550	40,000	644	64.5	900	525
113	25.1	625	20,000	797	80.5	910	840

Conventional Granular Catalysts and Catalytic Coatings

The conventional catalyst preparation and small scale MCH dehydrogenation screening test (MICTR) program begun under this contract has been continued during the past year.[1A),1A)] Many additional granular catalysts have been prepared that consisted of one, or two, or three or more metals on various supports. Most of these were combinations not previously studied, or optimizations of combinations previously studied. A number of trials were made with chelated single active metals and unchelated binary mixtures with the object of increasing metal dispersion and thus increase dehydrogenation activity and selectivity. Also with this objective the effect of high temperature muffling in air has been studied with the more promising catalyst systems. Special attention has been paid to finding cheaper and more abundant metal or metals to substitute for expensive supported platinum.

Improvement of catalytic coatings for metal surfaces has been continued for application and mechanical properties, particularly adherence to metal surfaces, and catalytic activity. Many new formulations have been studied by strip test evaluation and by MICTR tests of the candidates in platinized granular form. Some of the best formulations have been tested as wall catalysts on 1/4" OD tubes in the MICTR and the best so far on 1/8" OD tubes in the FSSTR.

Through, August 1969, a total of 827 catalysts have been prepared, or obtained from proprietary, or commercial sources; nearly all of these have been evaluated in the MICTR. Most of the catalysts were tested in 10-20 mesh particle sizes, including many catalytic coating candidate formulations. A number of catalytically coated tubes (1/4" OD) have also been evaluated. Screening has been for dehydrogenation activity with MCH and selectivity to toluene, at 10 atm pressure, without added hydrogen, at LHSV 100, and 662, 752 and 842°F. With the 1/8" coated tubes, the same pump rate (90 ml MCH/hr) was maintained as for the usual granular catalyst charge (0.9 ml diluted to 2.0 ml with granular quartz). The tubes were filled with quartz to create better mixing and heat transfer. All catalysts were compared with reference catalysts 9874-139 (1% Pt/UOP R-8 type Al_2O_3). A duplicate stand-by reference catalyst (10866-70, run 878), made 2 years after the original, gave almost identical test results. The purpose of the screening tests is to obtain a quick comparison with the reference catalyst so as to locate the most promising catalyst compositions and eliminate catalysts with activities too low or selectivities too poor to be of practical importance.

A sketch and photographs of the MICTR are shown in Figures 87, 83 and 89 in the Appendix of Reference 18 along with a description of the operational details. Subsequent modifications appear in the Appendix of Reference 16 and more recently the original GLC trace recorder has been replaced with a Westronics recorder. Detailed test data appear in Appendix Tables 131-133.

Various trials have been made to develop better adhesion of support coatings to sand-blasted and smooth stainless steel (304) surfaces, particularly the latter. This has been carried out mostly on flat metal surfaces for convenience of inspection (1/2" x 2").

Catalyst Preparation

Granular Catalysts

Most of the catalysts have been prepared by impregnation of various supports (10-20 mesh) with one or more metal salt or metal complex solutions, followed by oven drying at a moderate temperature and reduction in situ at different elevated temperatures prior to evaluation in the MICTR. Some Type 1 supported bimetallic catalysts, however, were first impregnated with metals K or J in the desired amount, dried, and muffled in air at 932°F to "coat" the support surface, prior to emplacement of the active metal. Subsequently the desired amounts of second solutions were impregnated and the catalysts dried at 259°F. Reduction in hydrogen was usually done in the MICTR but in some cases in an enclosed separate unit, or the catalysts were first muffled at elevated temperature.

Typically only small quantities of any particular catalyst has been prepared, i.e., a few grams to ~25 grams. The amounts of metals employed were usually within the limits of 1 to 14%.

Various catalytic coating candidates were prepared and screened in plati ized 10-20 mesh particle size for activity and selectivity with MCH. Since the primary object has been the mechanical strength and catalytic properties of these materials as thin films on metal surfaces there results will be discussed in proper context in the appropriate following sections.

The objective's of this study are discussed in the previous section. The effects produced by various preparative and operational procedures are discussed in connection with their MICTR catalyst performance under Catalyst Evaluation.

Catalytic Coatings

Metal Strips

Additional candidate catalytic coating materials have been prepared with the object of improving metal adherence, to find more active practical systems, and to optimize for activity the amount of platinum emplaced. Thin coatings have been made mostly on smooth or sand-blasted rectangular stainless steel strips (304, 1/2 x 2"), followed by drying first at ambient temperature and then at higher temperature, and finally muffling at elevated temperatures, usually in air. Similar sand-blasted mild steel strips were used earlier in this period but these tended to oxidize more readily to form a surface scale at elevated temperature which weakened the coating bond strength. In some cases calcination in hydrogen gas at elevated temperatures was employed to avoid surface oxidation. More exacting recent tests consist of examing the coating physical appearances, thickness, and estimating per nt stripped off when a piece of pressure-sensitive labeling tape is firmly pressed on the coating surface and then removed with a steady pull.

Metal Tubes

In granular catalyst impregnations, the desired amount of metal compound is put into solution and thus is virtually all imbibed on the support as it is dried with stirring, so that the metal percentage on the ultimate catalyst is accurately known. However, the amount of metal similarly laid down on a thin support coating on metal cannot be as easily known without controlled conditions and analysis of the coating. Heretofore, a single concentration of platinum metal in solution has been used (16.8 mg Pt/ml) which with granules would give 2-3% Pt. However, the data given in Table 71 indicate that the expected Pt content would be closer to 7% and probably too high for the most efficient catalyst. Experiments were carried out in which four tubes were entirely coated inside with a formulation I support about 6 mils thick; this was controlled by pulling a 0.182" dia tapered Teflon plunger through the thixotropic coating. Before muffling, the top 7-1/2" of the dried coating were drilled out. The tubes were then muffled at 752°F. Three of the tubes (Nos. 20, 16 and 15) were filled (and let stand for two hours) with solutions containing 4.2, 8.4 and 16.8 mgm Pt/ml, respectively. The excess solutions were drained, blown clear with compressed air, and the tubes dried and muffled at 662°C to convert the metal to Pt-PtO. Tube No. 17 was treated similarly except that it was twice successively filled with the Pt containing solution (16.8 mgm Pt/ml). After each impregnation the usual draining, blowing, drying and muffling was carried out. The bottom 3" of each coating was then drilled out by hand and the drilled coatings analyzed for Pt; bed lengths were 4" long and in the usual emplacement. Thus a Pt range of 4.5 to 12.9% was achieved. (10860 - 7 and 8 series)

Tube 27 was coated with Formulation I in which the fibrous and particulate Type 1 supports had been ball milled together, before the Type 6 binder was added. About 5% platinum was emplaced. (10860-18)

Three 1/4" OD stainless steel tubes (304) were thin-coated inside with formulation I, dried, and muffled in the usual manner. The tubes had been filled at the upper end with the thixotropic formulation and then a tapered end Teflon plunger (0.182" in diameter) was drawn through, so that the thickness of the coating measured ca 5 mils, after muffling. The coating formulation has been designed to avoid surface checking and to give minimal shrinking on muffling. Excess coating was drilled out after the drying step, so that the length of the remaining coating, and its position, corresponded to that of the usual granular charge. Tube 24 was impregnated with ca 5% metal A, based on coating weight. Tubes 26 and 23 were coated with roughly 6 and 10% metal K in the usual manner, dried and muffled in air at 932°F, and then each impregnated with the same amount of metal A, and dried. Reduction was carried out in situ, in the usual manner. The actual metal concentrations were not determined. (10860-35 series)

Two 1/4" OD tubes (304) thin coated with Formulation I support were impregnated with two different amounts of metal B ammine (tubes 22 and 25, approximately 4 and 6% metal based on coating, resp.). The 4-1/4" long coatings were muffled at 932°F before metallizing and reducing in situ in the MICTR. The MICTR evaluations of the catalytically coated 1/4" tubes are summarized in Table 71 in the Evaluation Section and given in more detail in Tables 131-133 of the Appendix.

Two 1/8" OD stainless steel tubes (304) and 25" long were coated in a similar manner for evaluation in the FSSTR with MCH, and the test results are reported in a separate section of this report. The uneven inside of each tube (I.D. 0.071") was scarified by working a 0.0625" dia drill rod back and forth with a twisting motion, using No. 200 carborundum powder-water-soap paste as grinding agent. This was then thoroughly removed by water washing and pushing cotton plugs through the tubes. Two similar Formulation I coating materials were used that were designed to differ in ultimate hardness and density. The same general technique was used as for the 1/4" dia tubes, except that the tapered end plunger was a short piece of 0.0625" dia drill rod. Tube L-1 contained 0.074 g coating (10860-47), and tube L-2 contained 0.141 g of a harder and denser coating and was probably more evenly coated (10860-48-1). After heating to 752°F the coatings were ca 4 mils thick. The tube coatings were platinum ammine impregnated (ca 5% Pt) in the usual manner and dried; reduction to Pt metal was done with nitrogen in situ in the FSSTR. The test results and heat flux measurements are reported in another section of this report.

Catalyst Evaluation

Granular Catalysts

Various means of increasing activity of platinum/type 1 support catalysts have been studied by attempting to increase the dispersion of the metal, e.g., cause more of the platinum to be spread out as a mono layer. The activities of the resulting catalysts for MCH dehydrogenation have been used as the criteria of the effects produced. Table 57 summarizes the results and Tables 131-133 of the Appendix gives complete details for each MICTR run. The approaches tried were those of emplacing Pt by ion exchange on a type 10 support, by chelates or complexes on type 1 support, and by multiple instead of single impregnation of platinum. In nearly all cases, the reaction rates at 752°F were equal to or less than the control catalyst (10860-57C). Ammonium thiocyanate caused a decrease in activity which could be restored to the normal level by heating the catalyst in air (10860-91 and 93, resp.). In one instance where ethylene diamine was used, a small improvement in activity resulted (10860-59D). Impregnation of Pt four successive times on type 1 support, followed by thermal decomposition of the tetraamine impregnate at 752°F after each of the first three impregnations gave about the same activity as catalyst prepared with a single impregnation and with the same total Pt content. (Catalysts 10860-115A and 115B, runs 1059 and 1060, Appendix Table 133)

Earlier study showed that increasing platinum content from 1 to 4% on a type 1 support increased activity but much less than 4 fold.[18] Also for a given support with increasing platinum content a maximum of activity was reached and this then declined with a further Pt increase. One gram of Pt as a monolayer would be expected to cover ~276 m^2 of surface area.[23] Thus a 1% Pt/type 1 support having a gross nitrogen adsorption area of 286 m^2/g would have only 2.76 m^2 of surface covered by Pt at most, and a 4% Pt content 11.0 m^2 of surface covered if dispersal were complete. Theoretically there would be ample room for platinum dispersal but this hasn't been achieved in actual practice and apparently a considerable fraction of the Pt atoms form clumps so that the metal is not used catalytically at the maximum efficiency.

Table 57. ATTEMPTS AT INCREASING ACTIVITY BY DISPERSING VARIOUS METALS ON SUPPORTS

Conditions: LHSV 100 with HCl, 10 atm pressure, no added hydrogen, temperature 752°F

Catalyst No. 10860-	Metal		Dispersing Agent	Support	Run No.	kc/ks[a] (752°F)
	Type	%				
57C	Pt	4	None (control)	Type 1	993	1.14
5	Pt	4	Ion exhcnage	Type 10	728	1.03
5B	Pt	4	Ion exchange	Type 10	736	0.69
57A	Pt	4	α,α' dipyridyl	Type 1	992	1.14
57D	Pt	2	ethylene diamine	Type 1	994	1.33
91	Pt	2	thiocyanate	Type 1	961	0.91
93	Pt	2	thiocyanate, oxidized in air	Type 1	961	1.11
105A	Pt	4	ethylene diamine	Type 1	1031	1.20
105B	Pt	4	ethylene diamine, acetic neutr	Type 1	1032	0.81
109	Pt	1	Pt $[(CH_3)_3$ Pt AcAc$]_2$	Type 1	1040	1.00
115A	Pt	4	Control single impregnation	Type 1	1059	1.28
115B	Pt	4	4 impregnations[b]	Type 1	1060	1.21
53B	A	4	None	Type 1	812	1.30
58A	A	4	α,α' dipyridyl	Type 1	876	1.24
58B	A	4	ethylene diamine	Type 1	877	1.13
105C	A	2	ethylene diamine	Type 1	1033	1.14
105D	A	2	ethylene diamine, acetic neutr	Type 1	1034	1.24
58C	B	4	α,α' dipyridyl	Type 1	879	0.76
58D	B	4	ethylene diamine	Type 1	880	0.68
105E	B	2	ethylene diamine	Type 1	1035	0.73
105F	B	2	ethylene diamine, acetic neutr	Type 1	1036	0.75
10C	I	4	Metal trichloride	Type 1	744	0.33
10B	I	4	ethylene diamine 1.1	Type 1	745	0.29
10280-155C	I	5	α,α' dipyridyl 1:2	Type 1	532	0.58
191D	I	3	ethylene diamine (1:3)	Type 1	583	0.71
192C	I	2	ethylene diamine (1:3)	Type 1	591	0.69
192D	I	4	ethylene diamine (1:3)	Type 1	593	0.50
192E	I	3	ethylene diamine (1:3)	Type 1	594	0.24
10860-16	I	4	nitroso salt	Type 1	755	0.31
59	I	4	α,α' dipyridyl (1:3)	Type 1	895	0.59

a) kc = First order rate constant of experimental catalyst.
ks = First order rate constant of reference catalyst 9874-139.
b) After 1st through 3rd impregnation, and during, muffled in air at 752°F.

A case in point is nitrogen reduced catalyst 10869-113, containing 4.4% total platinum/type 1 support (subsequently evaluated in the FSSTR). This adsorbed 55 u moles H_2/g catalyst between 32 and 932°F which at a H/Pt ratio of 1.0 corresponds to only 51% monodispersed Pt.

Generally, the activity of metal A was not improved by chelation impregnation (cf Table 57). This metal is a close competitor to Pt but has the short coming of poorer selectivity at high MCH conversion. As discussed in another section, this disadvantage can be overcome in granular catalysts by addition of metal K.

No improvement of activity resulted on chelation of metal B. Improvement was noted in a few cases with the polynuclear metal I but as discussed below selectivity to toluene is poor at the higher MCH conversions.

Study has continued of using supported metal A as an alternate or supplement to platinum. Unfortunately, this metal is less abundant, in considerable demand, and more expensive than platinum but might be useful if it demonstrated high specific activity, stability or synergy.

Previously, small percentages of supported metal A on a particular type 1 support were found to have low catalytic activity for MCH dehydrogenation. In general, it has required large amounts (10% or more) on another type 1 support to produce activity equivalent to 1-2% supported platinum (catalysts 9874-121A and 121B, runs 156 and 157, respectively, Table 73, ref. 18).[a] Also a disadvantage of this type of catalyst has been formation of cracked products and benzene in addition to toluene (i.e., poor selectivity) when test conditions were made severe enough to produce 70-80% MCH conversion. In addition, the latter two catalysts were found to have poor toluene selectivity and to lose activity when tested with MCH at 1022°F, at LHSV 100, and at 10-50 atm pressure, in the bench-scale test (c.f. Table 6, p. 29, 18). Poor selectivity was also obtained with catalytically coated 1/4" OD tubes (c.f. Table 68, runs 618 and 620, ref. R-2). Combination of metal A with one or two other metals, on a type 1 support, generally has not improved catalytic activity, or selectivity at high conversion, with the exception of platinum.

Quite active catalysts have been obtained with 2-4% metal A on a type 1 support that exceed the activity of the reference catalyst 9874-139 and equal that of control catalyst 10869-29 on the same support. However, serious loss of selectivity begins at about 80% MCH conversion (c.f. catalysts 10860-33A and 33B, runs 811 and 812, Table 58). It has been found that, if the support is first coated with a difficultly reducible metal (K) oxide and calcined before impregnation with metal A complex, while the activity remains the same the selectivity is much improved up to almost complete MCH conversion (c.f. catalyst 10860-28C, runs 789 and 806, respectively, Table 58). Thus this system appears to be a close competitor to the Pt/Al_2O_3 system in granular catalyst form.

---

a) Active catalysts were reported earlier, however, with 4-10% metal A on type 2 and 5 supports that were highly selective at MCH conversions up to 73%. A type 6 support gave a much less active catalyst.

Table 58. MCH DEHYDROGENATION ACTIVITY OF VARIOUS SUPPORTED MONO- AND BIMETALLICS

Conditions: LHSV 100, 10 atm pressure, no added H_2, 0.9 ml 10-20 mesh catalysts diluted with 1.1 ml quarts, temperature variable

Catalyst No.	Composition		Run No.	% MCH Conversion at, °F		
	Metal (1)	Metal (2)		662°F	752°F	842°F
9874-139	1% Pt	0	808	25, 24, 23	48, 46, 46	69, 68, 68
10860-29	4% Pt	0	807	25, 24, 23	54, 52, 53	81, 80, 80 (20)[b]
10860-33A	2% A	0	811	27, 32, 31	52, 52, 57	82, 70, 71 (21) (17) (17)[b]
10860-33B	4% A	0	812	30, 31, 30	53, 55, 55	81, 92, 96
10860-28G	2% A	3.6% K	789	30, 30, 24	55, 55, 54	83, 83, 82 (7) (6) (6)[b]
10860-28G	2% A	3.6% K	806[a]	32, 35, 35	79, 76, 78	98, 98, 98

a) LHSV = 50.
b) Bracketed number benzene, unbracketed numbers total % conversion to benzene plus toluene.

The effect has been further studied of coating type 1 support with salts of difficultly reducible metals V or K oxides prior to impregnation with various metal complexes other than those of metal A (discussed above). A summary of the results are given in Table 59 in which the relative first order rates at 752°F are compared after reduction at 798°F, and in some instances at 977°F. Detailed data are given in Table 130, of the Appendix. The V and K oxides alone on the support were reduced only slightly at 798°F and were found to be inactive (c.f. catalysts 10860-27 and 28, respectively). The 2% Pt, 4% V supported catalyst had a slightly higher rate than the control catalyst (4% Pt/type 1 support) after 798°F reduction, but the two catalysts had about the same rate after 977°F reduction (catalysts 10869-27A and 29, runs 770 vs 807 and 809 vs 815, respectively). Metal B or D on metal V oxide/type 1 support (reduced at 798°F) had rates only slightly lower than that of the control catalyst (10860-27D and 27E, runs 774 and 775, respectively). Metals I and F gave a catalyst with a much lower rate. The 2% Pt, 3.4% K supported catalyst had about the same rate as the control catalyst (10860-28A and 29, runs 782 and 807, respectively) after 798°F reduction and a slightly lower rate after 977°F reduction. Catalyst 10860-28H containing metal B had only a slightly lower rate than catalyst 28A after reduction at both temperatures (c.f. runs 790 vs 810 and 782 vs 804). Catalyst 10360-28E (2% H, 3.4% K/type 1 support) had an even lower rate than the control catalyst after reduction at the lower temperature. Catalysts 28B and 28D (2% I and 2% F, respectively, on 3.4% K/type 1 support) gave about one-half the rate of the control catalyst after reduction at 798°F (c.f. runs 783 and 785, respectively).

Summarized in Table 60 are data reproduced in different form from Table 59 in which various metals were used to promote activity in the K/type 1 supported form. Other than Pt, only metal A (and possibly metal B) showed sufficient activity to be of interest. Both metals are presently less abundant and more expensive than platinum.

A further drawback of promotion by metal A alone was formation of benzene with some observed exothermic effects on testing at MCH conversions over ca 80%, under the usual screening conditions. Catalysts were prepared over a range of compositions of supported A + K in an attempt to optimize activity and selectivity for toluene at high conversions. Supported A in various amounts and separately K in various amounts were tested and the results are summarized in Table 61, and detailed in Appendix Table 130. The latter were incompletely reduced and catalytically inactive over the range 1.1 to 10% K/support.

Supported metal A itself is active at as low as 1% concentration and increases in activity at 2%; no further activity results at 4% metal A concentration (at LHSV 100). At LHSV 50 only the 2% A catalyst shows a further activity increase. At higher conversions selectivity is poor, particularly with higher metal content. The best activity and selectivity with bimetallic catalysts occurs in the region of 2% A and 3.6-10% K type 1 support. In most cases LHSV 50 was used to force the total conversion to the region of 100%. Higher metal A concentration (i.e., 4%) tended to worsen selectivity without improving activity. In view of less favorable effect of metal K on selectivity in the thin coated tube experiments, described in the

Table 59. RELATIVE MCH DEHYDROGENATION RATES OF VARIOUS SUPPORTED BIMETALLIC CATALYSTS, REDUCED AT 798 OR 977°F

Conditions: Same as for Table 1

Catalyst No. 10860-	Composition		Run No.	kc/ka (752°F)[a] Reduced at 798°F	Run No.	kc/ka (752°F)[a] Reduced at 977°F
	Metal, %	Metal, %[b]				
29	(control) 4 Pt	0	807	1.14	813	1.19
27	0	4 V	769	0.00	-	-
33A	2 A	0	811	1.17	-	-
33B	4 A	0	812	1.30	-	-
27A	2 Pt	4 V	770	1.22	809	1.19
27B	2 F	4 V	771	0.54	-	-
27I	2 B	4 V	774	0.81	-	-
27E	2 D	4 V	775	0.84	-	-
27G	2 A	4 V	777	1.20	801	1.17
27J	2 I	4 V	780	0.35	-	-
28	0	3.6 K	805	0.00	-	-
28A	2 Pt	3.6 K	782	1.12	804	1.03
28B	2 I	3.6 K	783	0.48	-	-
28D	2 F	3.6 K	785	0.52	-	-
28E	2 D	3.6 K	787	0.77	-	-
28G	2 A	3.6 K	789	1.20	805	1.08
28H	2 B	3.6 K	790	1.00	810	1.03

a) See footnote a), Table 57 this report.
b) Computed as metal but oxides were only slightly reduced to metal.

Table 60. DEHYDROGENATION OF MCH OVER VARIOUS SUPPORTED BIMETALLICS

Conditions: LHSV 100, atm pressure, no added H_2, 0.9 ml 10-20 mesh catalysts diluted with 1.1 ml quarts, temperature variable.

Catalyst No. 10860-	% Metal 1	% Metal 2	Run No.	Reduction Temp, °C	% MCH Conversion, %w 662°F Toluene	662°F Benzene	752°F Toluene	752°F Benzene	842°F Toluene
28	0	3.6 K	803	971	0,0	0,0	0,0	0,0	0,0
28 F	2 M	3.6 K	788	797	0,0	0,0	0,0	0,0	3,2
28 J	2 E	3.6 K	792	797	5,5,5	0,0	12,11,10	2,2,1	16,18,15
28 D	2 F	3.6 K	795	797	16,14,17	2,1,2	30,30,29	10,8,5	35,35,37
28 C	2 C	3.6 K	784	797	2,2,1	0,0	6,5,5	0,0	13,16,10
28 B	5 I	3.6 K	783	797	14,13,12	0,0	27,28,27	1,<1	39,36,38
28 H	2 B	3.6 K	790	971	22,25,26	0,0	49,48,48	0,0	71,70,69
28 E	2 D	3.6 K	787	797	17,18,19	0,0	40,39,40	0,0	58,57,57
28 I	4 G	3.6 K	791	797	<1	0,0	5,3,3	0,0	8,6,5
28 G	2 A	3.6 K	789	797	34,30,29	0,0	55,55,54	0,0	83,83,82
28 G	2 A	3.6 K	805	971	24,23,23	0,0	52,50,51	0,0	75,74,76
34	2 A	3.6 K	815	797	25,25,26	0,0	50,47,47	0,0	75,73,72
29 D	4 A	3.6 K	825	971	30,30,30	0,0	60,56,56	2,0,0	80,79,80
28 A	2 Pt	3.6 K	804	971	27,27,25	0,0	50,51,50	0,0	82,78,78
29 C	4 Pt	3.6 K	821	971	27,25,32	0,0	57,55,56	0,0	84,85,83

Table 61. INFLUENCE OF METAL % AND METAL/K RATIOS ON ACTIVITY AND TOLUENE SELECTIVITY DURING MCH DEHYDROGENATION

Conditions: LHSV 100, atm pressure, no added H_2, 0.3 ml 10-20 mesh catalysts diluted with 1.1 ml quartz, temperature variable.

Catalyst No.	% Metal 1	% Metal 2	Run No.	Reduction Temp °C	LHSV	% MCH Conversion, % @ 662°F Toluene	@ 662°F Benzene	@ 752°F Toluene	@ 752°F Benzene	@ 842°F Toluene
10880- 31 A	2 Pt	1.1 K	843	971	100	34,33,35	0,0,0	58,52,54	0,0,0	85,84,82
31 B	2 A	1.1 K	844	971	100	37,31,25	0,0,0	55,54,52	0,0,0	77,75,76
31 B	2 A	1.1 K	950	971	50	50,45,48	2,1,0	81,77,77	18,7,8	82,91,92
31 B	2 B	1.1 K	846	971	100	28,25,25	0,0,0	49,47,46	0,0,0	74,71,72
31 C	2 B	1.1 K	845	971	100	8,3,4	0,0,0	16,15,15	0,0,0	24,30,30
28 A	2 Pt	3.6 K	804	971	100	27,27,25	0,0,0	50,51,50	0,0,0	82,78,78
29 C	4 Pt	3.6 K	821	971	100	27,25,32	0,0,0	57,55,56	0,0,0	84,85,83
10280- 119 E	1 A	0	508	797	100	24,18,20	0,0,0	44,43,40	0,0,0	81,80,56
10880- 33 A	2 A	0	811	797	100	27,32,31	0,0,0	52,52,51	20,0,0	82,70,71
33 [illegible]	2 A	0	816	797	50	34,32,27	0,0,0	75,78,77	35,25,16	60,70,82
33 B	4 A	0	812	797	100	30,31,30	0,0,0	53,55,55	21,17,21	58,75,75
33 B	4 A	0	839	797	50	47,42,43	36,28,2	57,58,52	49,46,47	47,46,47
28	0	3.6 K	803	971	100	0,0	0,0	0,0	0,0	0,0
30 B	1 A	3.6 K	826	797	100	24,23,24	0,0,0	48,46,45	0,0,0	70,70,69
30 B	1 A	3.6 K	838	797	50	33,35,36	0,0,0	71,69,65	3,3,3	92,92,93
28 G	2 A	3.6 K	805	971	100	24,23,23	0,0,0	52,50,51	0,0,0	75,74,76
28 G	2 A	3.6 K	806	971	50	32,35,35	0,0,0	79,78,78	7,6,4	91.92,94
34	2 A	3.6 K	815	797	100	25,25,26	0,0,0	50,47,47	0,0,0	75,73,72
29 B	4 A	3.6 K	825	971	100	32,30,30	0,0,0	60,58,58	2,0,0	80,78,80
29 B	4 A	3.6 K	829	971	50	63,48,44	9,2,3	84,81,81	39,36,32	81,54,68
28 H	2 B	3.6 K	810	971	100	19,20,21	0,0,0	47,48,46	0,0,0	69,68,67
29 E	4 B	3.6 K	828	797	100	24,26,27	0,0,0	49,49,48	2,1,0	82,83,84
29 E	4 B	3.6 K	836	797	50	30,31,32	0,0,0	66,65,65	55,35,10	83,55,70
28 A	4 B	3.6 K	827	971	100	15,20,20	0,0,0	45,43,41	0,0,0	83,83,83
29 A	0	10 K	830	971	100	0	0	5,2,2	0	9,7,7
30 B	2 Pt	10 K	832	971	100	21,22,22	0,0,0	53,48,49	0,0,0	78,77,75
30 E	1 A	10 K	833	971	100	18,14,12	0,0,0	26,14,19	0,0,0	36,34,34
30 F	2 A	10 K	834	971	100	24,22,21	0,0,0	39,36,37	0,0,0	54,52,50
30 F	2 A	10 K	847	971	50	23,18,22	0,0,0	57,56,52	0,0,0	82,80,80
30 G	4 A	10 K	840	971	100	33,30,23	0,0,0	54,43,43	0,0,0	64,65,62
30 G	4 A	10 K	849	971	50	23,24,25	0,0,0	52,53,53	2,2,1	37,35,38
30 I	2 B	10 K	842	971	100	17,21, -	0,0,0	44,38,34	0,0,0	82,80,81
30 H	2 B	10 K	841	971	100	15,12,14	0,0,0	34,31,31	0,0,0	50,45,42

next section, it appears that its main function may be to influence secondary reactions whose rates are governed by diffusion phenomena. Figure 11 portrays the selectivity improvement resulting from the inclusion of 3.6% K into a type 1 supported 2% A catalyst. The data were obtained as a function of time in the MICTR test at 842°F. While the bimetallic catalyst gives high and uniform selectivity over the 15-minute period, the monometallic catalyst gives at first poor selectivity which linearly improves with time.

Promotion with different metals of metal X/type 1 support (itself inactive when reduced) gave about the same relative activities with MCH as their counterparts on metal K/type 1 support, obtained previously (10860-32 series vs 27, 28 and 29 series). The metal X/type 1 support had been muffled at 932°F before being promoted. The highest activities were obtained with the Pt promoted catalyst, with metals A and B giving less activity, all being about as active as the reference catalyst. (10860-32A, G and H vs 98[illegible]-139, Table 132 of the Appendix)

The effect of muffling at 1473°F in air has been to reduce considerably the activity of various K metal promoted/type 1 support catalysts (63E-4, Runs 892-895). Muffling at 1364°F in air deactivated to a small extent Pt promoted metal K/type 1 support (10860-65F, Run 905). Muffling at 1292°F in air, however, had little effect on Pt or metal B promoted metal K/type 1 support (10860-62A and 62C, Runs 897 and 898, resp; Table 132 of the Appendix).

Neither metals V or K alone on type 1 support were activated by muffling at 1364°F in air, before reducing (10860-65B and 65D, Runs 900 and 901, resp.). The controls reported earlier were likewise inactive after reduction.

Further study was made of the possibilities of improving catalytic activity by adding various active metals to K promoted type 1 support (heteropoly acids were used as the source of K). Variations have been introduced by only drying the promoted support before impregnation with each second metal (I), and then muffling part of each catalyst in air at 1148°F (II). A second group consisted of muffling the K promoted support at 1148°F in air before impregnation with each second metal (III), and then muffling part of each catalyst in air at 1148°F (IV). These variations were done to change the binding strength of metal K to the support surface, change the extent of alloying of each pair of metals and their degree of dispersions on the support surfaces. The reaction rates at 752°F with MCH in the MICTR made by these variations are shown in Table 62, and the details in Table 133 of the Appendix. The best results with the Pt, K/type support were obtained with variations I and III; also for the metals A and K/type 1 support. The four variations made the difference with the metals B and K/type 1 support. Variation III was best with the metals D and K/type 1 support. The metals E and K/type 1 support was inactive with all variations, as was the metal K/type 1 support alone with all variation. The better catalysts were comparable in activity to the better Pt/type 1 support.

A number of mono- and bimetallics on type support showed some promise but all these had MCH dehydrogenation rates much lower than the

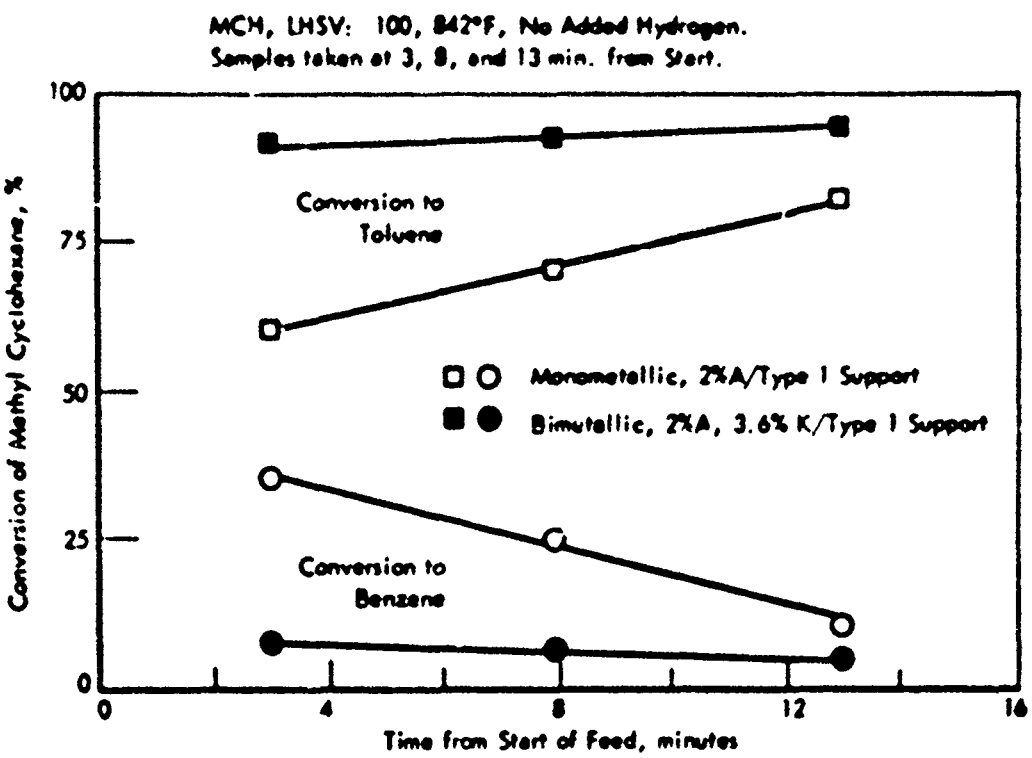

Figure 31. IMPROVEMENT OF TOLUENE SELECTIVITY AT HIGH MCH CONVERSION BY ADDITION OF 3.6%K TO 2% METAL A/TYPE I SUPPORT (MICTR)

64987

Table 62. RELATIVE MCH DEHYDROGENATION RATES AT 752°F WITH VARIOUS TYPE I SUPPORTED BIMETALLICS

Metal K ex heteropolyacid

Conditions: LHSV 100, 10 ata pressure, no added hydrogen
0.8 ml 10-20 mesh catalyst diluted with quartz to 2.0 ml
catalysts reduced in situ

Composition	Support + metal h Dried at 250°F I			Series Muffler at 1148°F in Air II			Support + Metal h Muffler At 1148°F in Air III			Series Muffler At 1148°F in Air IV		
	Run	10860-	kc/ks	Run	10863-	kc/ko[a]	Run	10860-	kc/ko[a]	Run	10880-	kc/ko[a]
3.8% metal h/type I support	908	71	≈0	909	71A	~0	-	-	-	-	-	-
2% Pt, 3.8% metal h/type I support	910	71B	1.26	915	72A	1.17	923	72G	1.26	945	72L	1.11
2% metal A, 3.8% metal h/type I support	911	71C	1.14	916	72B	0.74	924	72H	1.18	946	72M	0.80
2% metal B, 3.8% metal h/type I support	913	71E	1.00	919	72D	1.07	926	72J	1.00	948	72O	1.04
2% metal D, 3.8% metal h/type I support	912	71D	0.70	918	72C	0.53	925	72I	0.91	947	72N	0.54
2% metal E, 3.8% metal h/type I support	914	71F	~0	920	72E	-	931	72K	~0	949	72P	~0

a) ks = first order rate constant of experimental catalyst.
ko = first order rate constant of reference catalyst (9876-139)

reference catalyst. One of these (10660-12A) which appeared to have some promise could not be reproduced by subsequent similar preparations, and was abandoned. The results with these catalysts are summarized in Table 64.

In Table 64 are shown the relative rates of dehydrogenation of MCH at 752°F of platinized catalysts containing various metals attached by cation exchange to a type 10 support. Two temperatures of reduction were employed since the exchanged cations are not easily reduced. Catalyst 10660-5 containing 4% Pt has been used as a control catalyst; the best results being obtained with metals P and R. After 977°F reduction, only metals O,T,R, and S showed higher rates; P gave about the same rate and Q a large decline in rate.

Generally, of the granular catalysts studied, Pt/type 1 support has been the most satisfactory all-around system for MCH dehydrogenation in the MICTR. This type of catalyst has performed best, particularly when life and stability are considered in the bench scale tests, not only with MCH but with other candidate fuels. Several bimetallic systems have competitive activity in the MICTR but are less stable in the bench scale tests. The most competitive single metal (A) tends to form by-products at high conversion, some of which result from exothermic reactions. Although this tendency can be eliminated by addition of metal K, the catalysts are less stable than Pt/type 1 support in the bench scale test. Very few supported bimetallics of the many combinations screened in the MICTR with MCH were sufficiently active to be of interest. Type 1 supports, the variety of which available are legion, have proven to be the most satisfactory of the many diverse types of supports evaluated. Such supports, of suitable physical characteristics and combinations, are the principle ingredients of metal coating formulation I which serve as a support for platinum.

At the very high space velocities (well in excess of 100) required to obtain attractive heat fluxes, many metals and metal combinations on supports are inactive that are known to have reasonable dehydrogenation activity and selectivity at the much lower space velocities (i.e., 1-2), which is generally used in refineries to increase the octane number of gasoline components by dehydrogenation and other types of reactions. In the latter case, acidity is also incorporated into the catalysts to promote acid catalyzed reactions the products of which also increase octane number of the final gasoline.

Coated Metal Strips

Study continued of candidate support coatings for metal surfaces. These were coated onto mild steel strips that had been sandblasted, degreased, coated with a thin (~1 mil) of type 18 binder and muffled at ca 752°F. Coating thicknesses usually were from to 3 to 8 mils, and emplaced as hydrous formulations, dried at 248°F, and muffled at 752°F. Table 65 describes the metal adherence and hardness, and the MCH dehydrogenation rates of the catalysts, using the corresponding formulation as a support. All of these catalysts were more active than the reference catalyst. Among newer formulations good adherence and hardness was achieved with fibrous type 1 support-particulate type 7 support with type 6 binder (10290-195 series), and fibrous type 1 support-particulate type 12 support with type 6 binder (10280-196

Table 63. RELATIVE MCH DEHYDROGENATION RATES WITH MONO- AND BIMETALLICS ON TYPE 1 SUPPORT

Conditions: Same as for Table 62

Catalyst No.	Composition, %		Run No.	k_c/χ_g [a] (752°F) Reduced at 798°F
	Metal (1)	Metal (2)		
9874-139	1 Pt	0	-	1.00
10280-192B	2 Y	6 D	690	0.58
10280-193A	2 Pt	2 W	698	0.79
10280-193B	5 F	2 W	699	0.58
10280-193C	2 D	2 W	700	0.43
10860-8A	5 D	2 I[b]	732	0.79
10860-8B	5 D	0	733	0.65
10860-10A	4 L	0	742	0.43[c]
10860-26A	2 Pt	2 L	764	0.80

a) See footnote b), Table 64, this report.
b) ex ethylene diamine complex.
c) Two additional preparations of this composition were inactive.

Table 64. RELATIVE MCH DEHYDROGENATION RATES WITH Pt ON VARIOUS ION EXCHANGED SUPPORTS, REDUCED AT 752 OR 977°F

Conditions: LHSV 100, 10 atm pressure, no added hydrogen
0.9 ml 10-20 mesh catalysts diluted with quarts to 2.0 ml, temperature 752°F

Catalyst No.	Composition		Run No.	k_c/k_s[b] (752°F) Reduced at 798°F	Run No.	k_c/k_s[b] (752°F) Reduced at 977°F
	% Pt	Exchange Ion[a]				
10860-5	4	(control)	728	1.03	-	-
10280-198A	4	P	711	1.27	721	1.04
10280-199A	4	Q	712	1.04	713	0.68
10280-199B	4	O	714	1.11	715, 722	1.17, 1.09
10280-199C	4	T	716	1.16	717	1.16
10280-199D	4	R	723, 737	1.26, 1.26	724	1.06
10860-5A	4	S	725	1.11	727	1.15

a) Pt exchanged into sieve, displaced alkali metal ions washed out, remaining alkali metal ions exchanged as completely as possible with other ions. Displaced ions then washed out.
b) k_c = First order rate constant of experimental catalyst.
k_s = First order rate constant of reference catalyst (9674-139).

Table 65. METAL ADHERENCE OF VARIOUS FORMULATIONS AND RELATIVE MCH DEHYDROGENATION RATES AT 752°F OF CORRESPONDING CATALYSTS

Test Conditions: Same as Table 64

Formulation	Adherence to Mild Steel Strip	Run No.	Cat. No.	% Pt	k_s/k_o [b] (752°F)
			10126-		
40% type 1 support,[c] 40% type 1 support,[d] 20% type 1 binder	fair, soft	684	196A	1	1.08
40% type 1 support, 40% type 1 support, 20% type 1 binder		685	196B	2	1.03
40% type 1 support, 40% type 1 support, 20% type 1 binder		686	196C	3	1.11
37% type 1 support, 37% type 1 support, 26% type 1 binder	fair, soft	687	191A	1	1.06
37% type 1 support, 37% type 1 support, 26% type 1 binder		688	191B	2	1.06
37% type 1 support, 37% type 1 support, 26% type 1 binder		689	191C	3	1.06
40% type 1 support, 40% type 7 support, 20% type 6 binder	good, hard	701	198C	0.6	1.03
40% type 1 support, 40% type 7 support, 20% type 6 binder		702	198D	1.75	1.15
40% type 1 support, 40% type 7 support, 20% type 6 binder		703	198E	3.6	1.28
84% type 7 support, 16% type 6 binder	poor, cracks	707	195A	0.6	1.07
84% type 7 support, 16% type 6 binder		708	195B	1.8	1.12
38% type 1 support, 36% type 6 support, 32% type 6 binder	poor, soft	709	193D	1	0.97
38% type 1 support, 36% type 6 support, 32% type 6 binder		710	193C	2	1.17
40% type 1 support, 40% type 18 support, 20% type 6 binder	good, hard	713	194A	1	1.01
40% type 1 support, 40% type 18 support, 20% type 6 binder		718	194B	2	1.12
			10066-		
40% type 1 support, 40% type 1 support, 20% type 6 binder	poor	781	12A	2	1.11
40% type 1 support, 40% type 1 support, 20% type 6 binder		782	12B	6	1.17
40%[c] type 1 support, 40% type 1 support, 20% type 6 binder	poor, cracked	786	21A	1	1.31
40%[c] type 1 support, 40% type 1 support, 20% type 6 binder		787	21B	2	1.29
40% type 1 support, 40% type 1 support, 20% type 6 binder	poor, cracked (3 mil)	788	21C	1	1.16
40% type 1 support, 40% type 1 support, 20% type 6 binder		789	21D	2	1.04
38% type 1 support, 38% type 1 support, 24% type 1 binder	fair (3 mil)	781	21E	1	1.18
38% type 1 support, 38% type 1 support, 24% type 1 binder		782	21F	2	1.06

a) The two type 1 supports were ball-milled together.
b) See footnote b), Table 12.
c) In this column type 1 supports all fibrous.
d) In this column particulate supports.

series). Although leading to excellent catalysts (10860-21 series), a modification of the older Formulation I gave poorer metal adhesion. This modification was the ball-milling together of the particulate and fibrous type 1 supports before working them up in a mortar with the hydrous binder, rather than using "as received" fibrous and ball-milled particulate type 1 supports, which led to good metal adherence in the past.

The early Formulation I technique has been re-examined with the object of making thinner coatings than formerly. One such coating was made with good adherence and was fairly hard with a thickness of 3 mils, of which the binder was about 1 mil thick. Other satisfactory coatings were made with thicknesses of 4-5 mils, and 7-8 mils.

Various coating experiments have been carried out on flat mild or stainless strips (c.f. Tables 66 and 67). Much of the study has employed sandblasted stainless (304) surfaces although some of the later tests were obtained on smooth but slightly roughened surfaces. Thinner films have been used generally, than previously and thus there has been less tendency to strip off on thermal flexing of metal surfaces made concave by shearing. Also further experience indicates that there is not much advantage in an undercoat binder such as No. 18 which was used formerly. This undercoat (ca 1 mil thick) could be of concern in a tube catalytically coated with a thin film, since thermal migration of alkali ions to the catalytic coating could gradually cause local mineralization, and possibly phase changes, with consequent loss of activity. The undercoat does not seem to be too necessary in successfully lining tubes, although it has been used up to tube 27 (1/4" tubes only). Generally, better adhesion has been obtained with a sand-blasted rather than a relatively smooth flat surface. Also it makes little difference with stainless surfaces whether the final calcination is made in an air or hydrogen atmosphere since it is less subject to surface oxide formation than mild steel.

Additional Type I formulations have been prepared using various expensive particulate supports (types 1,5,6, and 7) from a different supply source than the corresponding cheaper counterparts studied previously (c.f. last section of Table 67). In this series formulations with types 5 and 7 appeared to give the most satisfactory metal coatings. The support materials of types 1,5,6, and 7, of very small primary particle size, were separately made into pastes by mixing with platinum tetrammine hydroxide solution. Thin films of these pastes were smeared on sandblasted stainless steel strips and dried. All checked and flaked off, except the support 7 preparation. This showed some adhesion but checked. The latter results are not listed in Table 67. All of these latter preparations when dried in thick layers were mechanically strong. After reduction in hydrogen their catalytic performance was determined which is described in the next section.

Generally, after 752-932°F muffling in air (or 752°F reduction in H_2) most type I formulation coating materials adhere fairly well to sand-blasted stainless steel surfaces (304). However, stronger adherence to smooth stainless surfaces is desirable; self-stripping sometimes occurs even on preliminary air drying. Earlier it was shown with a roughened mild steel surface that adherence was improved by first applying and muffling a thin film of type 18 binder, although this was without effect on coating bonding on stainless surfaces. Further efforts were directed mainly towards improving

Table 66. EVALUATION OF PROPERTIES OF VARIOUS CATALYTIC COATINGS ON METAL SURFACES

Symbols: M = Mild Steel; SS = Stainless Steel (304); SB = Sand Blasted; SM = Smooth; L = Lift Off Surface Spontaneously; P = Poor; F = Fair; G = Good

Exp No. 10860-	Metal Strip			Under Coating		Support Coating				
	Metal	Size, in.	Surface	Type	Heated	Type	Muffling		Thickness (mils)	Adhesion
							Atmosphere	Temp, °F		
37A	M	1 x 2	SB	18	752	Form[a] I	Air	752	-	F
37B	M	1 x 2	SB	18	752	Form[a] I	L, on drying	-	5-8	P
37C	M	¼ x 2	SB	None	248	Form[a] I	Air	752	-	G
37D	M	¼ x 2	SB	None	248	Form[a] I	H_2	752	3-4	G
37E	SS	¼ x 2	SB	None	248	Form[a] I	Air	752	-	F-G
37F	SS	¼ x 2	SB	None	248	Form[a] I	H_2	752	5-9	G
37G	SS	¼ x 2	SB	18	752	Form[a] I	Air	752	-	P, L
37H	SS	¼ x 2	SB	18	752	Form[a] I	H_2	752	-	P, L
37I	SS	¼ x 2	SB	18	248	Form[a] I	Air	752	-	P, L
37J	SS	¼ x 2	SB	18	248	Form[a] I	L, on drying	-	-	P, L
39A	M	¼ x 2	SB	None	752	Form[b] I	Air	752	5	F
39B	M	¼ x 2	SB	None	752	Form[b] I	H_2	752	2-3	F
39C	SS	¼ x 2	SB	None	752	Form[b] I	Air	752	6	F
39D	SS	¼ x 2	SB	None	752	Form[b] I	H_2	752	9-10	F
39E	M	¼ x 2	SB	None	752	Form[c] I	Air	752	7-8	G
39F	M	¼ x 2	SB	None	752	Form[c] I	H_2	752	6-7	F
39G	SS	¼ x 2	SB	None	752	Form[c] I	Air	752	6-7	G
39H	SS	¼ x 2	SB	None	752	Form[c] I	H_2	752	6-7	F

a) 40% Fibrous type 1 support - 40% particulate dense type 1 support - 20% type 6 binder.
b) 40% Fibrous type 1 support - 40% particulate less dense type 1 support - 20% type 6 binder (different than for a).
c) 40% Fibrous type 1 support - 40% particulate less dense type 1 support - 20% type 6 binder (different than for a and b).

Table 67. EVALUATION OF PROPERTIES OF VARIOUS CATALYTIC COATINGS ON METAL SURFACES IN AIR OR HYDROGEN

Symbols: M = Mild Steel
SS = Stainless Steel (304)
SB = Sand Blasted
SM = Smooth
L = Lifted Off Surface (Spontaneously)
P = Poor
F = Fair
G = Good

Exp No. 1006a-	Metal Strip			Support Coating				
	Metal	Size, in.	Surface	Type	Baffling Atmosphere	Temp, °F	Thickness (mils)	Adhesion[i]
43-1A	M	½ x 1	SB	Form 1[a]	Air	752	5-7	G
43-1-B	M	½ x 1	SB	Form 1[a]	H_2	932	6-8	G
43-1C	SS	½ x 1	SB	Form 1[a]	Air	752	6-11	G
43-1-D	SS	½ x 1	SB	Form 1[a]	H_2	932	6-10	G
43-1-E	M	½ x 1	SM	Form 1[a]	Air	752	6-14	G
43-1-F	SS	½ x 1	SM	Form 1[a]	H_2	932	18-21	F
43-2-A	M	½ x 1	SB	Form 1[b]	Air	752	7-12	G
43-2-B	M	½ x 1	SB	Form 1[b]	H_2	932	10-12	G
43-2-C	SS	½ x 1	SB	Form 1[b]	Air	752	7-13	G
43-2-D	SS	½ x 1	SB	Form 1[b]	H_2	932	6-13	G
43-2-E	M	½ x 1	SM	Form 1[b]	Air	752	10-15	F-P
43-2-F	SS	½ x 1	SM	Form 1[b]	H_2	932	16-19	F
43-3-A	M	½ x 1	SB	Form 1[c]	Air	752	4-8	G
43-3-B	M	½ x 1	SB	Form 1[c]	H_2	932	8-9	G
43-3-C	SS	½ x 1	SB	Form 1[c]	Air	752	6-13	G
43-3-D	SS	½ x 1	SB	Form 1[c]	H_2	932	6-7	G
43-3-E	SS	½ x 1	SM	Form 1[c]	Air	752	7-10	F-G
43-3-F	SS	½ x 1	SM	Form 1[c]	H_2	932	7-11	G
52 A	SS	½ x 1	SB	Form 1[d]	Air	752	7-8.5	G
52 A	SS	½ x 1	SM	Form 1[d]	Air	752	7-8.5	G
52 B	SS	½ x 1	SB	Form 1[e]	Air	752	5.5	F
52 B	SS	½ x 1	SM	Form 1[e]	Air	752	5.5	F
52 C	SS	½ x 1	SB	Form 1[f]	Air	752	4	F
52 C	SS	½ x 1	SM	Form 1[f]	Air	752	4	F
52 D	SS	½ x 1	SB	Form 1[g]	Air	752	7	F-G
52 D	SS	½ x 1	SM	Form 1[g]	Air	752	7	F-G
52 E	SS	½ x 1	SB	Form 1[h]	Air	752	7	G
52 E	SS	½ x 1	SM	Form 1[h]	Air	752	7	F

a) 40% fibrous type 1 support - 40% particulate type 1 support - 20% type 6 binder (different from a, b, or c of Table 66).
b) 40% fibrous type 1 support - 40% particulate type 1 support - 20% type 6 binder (usual type).
c) 40% fibrous type 1 support - 40% particulate type 2 support (different from a, or b, this Table) - 20% type 6 binder (usual type).
d) 40% fibrous type 1 support - 42% particulate type 7 support - 18% type 6 binder.
e) 40% fibrous type 1 support - 40% particulate type 1 support - 20% type 6 binder.
f) 40% fibrous type 1 support - 40% particulate type 5 support - 20% type 6 binder.
g) 40% fibrous type 1 support - 40% particulate type 5 support - 20% type 6 binder.
h) 40% type 1 support - 40% particulate type 5 support (ball milled) - 20% type 6 binder.
i) Strength of coating adhesion tested by sticking a piece of scotch tape to the coating surface and pulling to test bond strength. (This is a much more severe test than used formerly.)

coating adherence particularly to stainless steel. The results are summarized in Table 68 which also lists the numbers of platinized granular catalysts made from the same coating material.

(1) Type 1, 7 and 5 powders were found to adhere together when mixed with platinum tetramine dihydroxide solution, and on reduction lead to active catalysts (10860-54A, B and C, Table 68). These powders were of a different origin than the corresponding ones reported on earlier. The wet material formulations had excellent metal application properties but self stripped in the cases of 10860-54A and C, although adherence was fair with 54B.

(2) An epoxy binder carbonized (in H_2) as an undercoat led to a soft, poorly adhering coating with no tinning ability for Formulation I coating or type 1 support (10860-56 and 60 series).

(3) A metal salt (21) which was decomposed to type 1 support was found to have poor adhesion itself (10860-66A and 67A) or for type 1 support (10860-66B). This alkaline salt reacted with non-catalytic metal 15 (10860-66C) to give a type 1 support which, after neutralization and drying, adhered fairly well to sand blasted stainless steel. However, this represented no improvement over earlier Formulation I coatings. Use of a compound (23) to aid in alkali removal from muffled end product did not improve metal adherence. Another metal salt (22) which could be decomposed thermally to type 1 support decomposed on 258°F heating on mild steel but not stainless steel surface. The latter on high temperature decomposition cracked and lifted off the metal surface (not shown in Table 68).

(4) Several additional undercoating materials were tried (25, 26, 27) and after muffling in air one of these appeared to improve the binding of Formulation I coating to sand-blasting stainless steel (26, 10860-75B). One of these gave about the same adherence as the control (75C) and the other gave poorer results (75A). On smooth stainless steel, an undercoat with compound 27 gave the best surface for adherence of Formulation I, 26 the next best and 25 by far the poorest; even poorer than the control.

(5) The effect of component ratio of Formulation I on adherence was studied, without use of undercoat. The 45:45:10 ratio gave fair adhesion with both smooth and sand-blasted stainless steel (10860-78A). The 40:40:20 ratio gave fair adhesion with the sand-blasted metal but not with the smooth surface (10860-78B). The 35:35:30 ratio gave poor results with both surfaces (10860-78C). Coating hardness increased in the order 78A<78B<78C

(6) The 35:35:30 ratio Formulation I, pretreatment of sand-blasted and smooth stainless steel surfaces with 1 M HCl at 185°F did not improve adhesion (10860-79-1 and 2). Similar results were obtained earlier with hot nitric acid passivated stainless surfaces. Poor adhesion resulted from a hot HCl treatment of smooth mild steel surface (10860-79-3 and 4, untreated control surface).

(7) Prior pickling in 4 M HCl at 185°F gave poor adherence of the 35:35:30 ratio formulation coating with smooth stainless steel and fair

Table 18. EVALUATION OF PROPERTIES OF VARIOUS SUPPORT COATINGS ON METAL SURFACES

Symbols: M = Mild steel
SS = Stainless steel (304)
SB = Sand blasted
SM = Smooth

L = Lifted off surface spontaneously
P = Poor
F = Fair
G = Good
E = Excellent

Exp. No.	Metal Strip			Undercoating		Support Coating					Corresponding Primer Coating No.
	Metal	Size, in.	Surface	Type	Melting, °F	Material Ratio	Thickness	Melting, °F	Adhesion Rating	Adhesion % Lost	
[illegible]	[illegible]	1/2 x 2	[illegible]	none		Type 1[1]	2	Reduced 952	P		[illegible]
						Type 2[2]	1		P		
						Type 3[3]			P		
									P		
[illegible]	[illegible]	1/2 x 2	[illegible]	Carbonized Epoxy	752 in Mg			Air Dried	P		
						Epoxy bonded Type 1 part 1oo		842 in Mg	P		
[illegible]				Carbonized Epoxy	644 in Mg	Formula 1 (40:40:20)		Air Dried	P		
				As Above		As Above	12	Air Dried	P		
							2		P		
[illegible]	[illegible]	1/2 x 2	[illegible]			No. 21		952 in air	P		
						No. 1 + 21			P		
						No. 15 + 21	4		P		
[illegible]	[illegible]	1/2 1	[illegible]			No. 21[4]		[illegible]	P		
		1/2 x 1				No. 1 + 21 (40:40:20)		[illegible]	P		
						As Above + 2%[5]		[illegible]	P		644, [illegible][6]
[illegible]	[illegible]	1/2 x 1	[illegible]	35		Formulation 1 (40:40:20)	6	952	P	60	
				36		As Above	7	952	F	15	
				37		As Above	8	952	F	30	
				[illegible], control		As Above	7	952	F	25	
[illegible]	[illegible]	1/2 x 1	[illegible]	39		As Above	10		P	75	
				40		As Above	10		F	[illegible]	
				41		As Above	10		F	10	
				[illegible], control		As Above	9		P	55	
[illegible]	[illegible]	1/2 x 2	[illegible]	[illegible]		65:65:10		952	P	20	954, [illegible][7]
				[illegible]		65:65:10		952	F	10	
				[illegible]		60:60:20		952	L, P		842, [illegible][7]
				[illegible]		60:60:20		952	F	20	
				[illegible]		35:35:30		952	L, P		842, [illegible][7]
				[illegible]		35:35:30		952	P		
[illegible]	[illegible]	1/2 x 2	[illegible]	[illegible]		35:35:30	5.6	952			
				[illegible]		35:35:30	8.9	952	L	100	
				[illegible]		35:35:30	11-12	952	L	75	
				[illegible], control		35:35:30	9	952	L	60	
[illegible]	[illegible]	1/2 x 2	[illegible]	[illegible]		35:35:30		952	P	100	
				[illegible]		35:35:30		952	P	[illegible]	
		1 x 2		[illegible]	TBD	35:35:30	5	952	P	[illegible]	
		1/2 x 2		[illegible]		60:60:20	6	952	P	[illegible]	
				[illegible]		60:60:20	9	952	P	[illegible]	
				[illegible]		60:60:20	9-10	952	P	30	

a) Approximate percent stripped off on pressing on and removing a pressure sensitive label tape.
b) Fine powder mixed with $Fe(NH_4)_2(SO_4)_2$ solution and dried.
c) To convert base medium to insoluble form.
d) Sodium exchanged prior to chlorination.
e) Treated with acidic gas to neutralize alkali and then water leached.
f) Test data will be reported in the next Annual Report.
g) Treated with 1 N HCl at 185°F.
h) Treated with 4 N HCl at 185°F.

adherence with smooth mild steel (10860-80-1 and 2, resp.). The 40:40:20 ratio coating gave even poorer adherence.

(8) Unpickled sand-blasted stainless steel gave fair adhesion with the 40:40:20 ratio Formulation I (control, 10860-80-C).

Another technique has been used to improve bonding of coatings to metal. This consists of applying a thin film of type 6 binder to a coating previously bonded by muffling to stainless steel. The coating is then redried and remuffled. Some improvement was obtained with an overall formulation 35% fibrous type 1 support 35% particulate type 5 support - 30% type 6 binder which, however, is mechanically softer than the standard Formulation I (10860-88A and 90, Table 69). Excellent adhesion has been obtained by this technique with the harder Formulation I at overall type 6 binder concentrations of 20 and 30% (10860-94B and 94C vs 94A, Table 69). This technique will probably lead to improvement of adhesion for any coating material which has satisfactory mechanical strength and catalytic activity when suitable promoted. It can easily be applied to the inside walls of metal tubes, or other geometric configurations.

A new type 1 support of fine particulate size substitutes into Formulation I gives about the same general properties as the same Formulation using the standard particulate type 1 support, in general use (10860-107, 107B, Table 69).

Naturally occurring fibrous type 16 materials have been evaluated as substitutes for the synthetic type 1 support which has given good results in Formulation I. Although ample supplies of the latter material are on hand for experimental usage, and a wealth of knowledge about its manufacture, uses, and properties is available in various publications, it is no longer in production. Two of the materials tested appear to give coatings of promising mechanical properties. Further improvements will probably result from type 6 binder overcoating, as just described (10860-109B, 110A, 110B, and 111A, Table 70).

In Tables 65 and 70 are given the relative dehydrogenation rates for MCH at 752°F for 10-20 mesh catalyst counterparts of most of the coating materials studied for mechanical properties. Almost all of them are as active as reference catalyst and most are much more active and compare very favorably with the best granular catalysts made from various conventional solid supports, i.e., catalysts 10280-195E, 10860-55A, 55B, 55C, 81B, 81C, 81D, 81E, 81F, 98B, 98A.

Coated Metal Tubes

A MICTR test was performed in which empty tube No. 13 was packed with steel wool so as to create better mixing and tested at the usual pump rate (90 ml MCH/h4). This corresponds to LHSV 100 when used with the usual quarts diluted granular catalyst packing. The activity at 752°F was intermediate between that of the same tube packed with quarts and that of the same tube without quarts packing (c.f. runs 697 vs 696 and 695, Table 71). The pressure drop for the highly active quarts packed tube No. 16 was only 22 lb sq. in. (c.f. run 730, Table 71).

Table 69. EVALUATION OF PROPERTIES OF VARIOUS SUPPORT COATINGS ON METAL SURFACES

Symbols: M - Mild Steel
SS - Stainless steel (304)
SB - Sand blasted
SM - Smooth

Adhesion: L - Lifted off surface spontaneously
P - Poor
F - Fair
G - Good
E - Excellent

Exp. Number 10860-	Metal Strip			Undercoating		Support Coating					Corresponding Grumman Catalyst
	Metal	Size, in.	Surface	Type	Muffled, °F	Material Ratio	Thickness, mils	Muffled, °F (air)	Adhesion		
									Rating	% Off	
88A	SS	1/2 x 1	SB	(a)	-	35:35:[a][b]30	5	1004	F	20	8x0,8x0
	SS	1/2 x 1	SM	(a)	-	35:35:[a][b]30	8	1004	F	80	
90	SS	1/2 x 1	SB	none	-	35:[b]35:30	-	1112	F	(c)	90A
	SS	1/2 x 1	SM	none	-	35:[b]35:30	-	1112	F	(c)	
	SS	1/2 x 1	SM	27	950	35:[b]35:30	-	1112	F	(c)	
94A	SS	1/2 x 1	SM	none	-	65:65:10	4	914	F	25	
94B	SS	1/2 x 1	SM	none	-	40:40:20[d]	4	1004	E	0	96A
94C	SS	1/2 x 1	SM	none	-	35:35:30[d]	4	1004	E	0	96B,103
107	SS	1/2 x 1	SM	none	-	40:40:[e]20	4	1060	F	30	108A,108B
107	SS	1/2 x 1	SB	none	-	40:40:[e]20	7-10	1060	G	5	
107B	SS	1/2 x 1	SM	none	-	40:40:[f]20	9	1060	F	30	108C,108D
107B	SS	1/2 x 1	SB	none	-	40:40:[f]20	10-11	1060	G	10	
109B	SS	1/2 x 1	SM	none	-	40:40:[g]20	4-6	952	F	20	111B,111C
109B	SS	1/2 x 1	SB	none	-	40:40:[g]20	6-9	952	G	10	
110A	SS	1/2 x 1	SM	none	-	40:[h]40:20	5-9	952	F	80	111D,111E
110A	SS	1/2 x 1	SB	none	-	40:[h]40:20	5	952	F	20	
110B	SS	1/2 x 1	SM	none	-	20:[h]60:20	4-8	952	F	1[illegible]	111F,111G
110B	SS	1/2 x 1	SB	none	-	20:[h]60:20	5-6	952	G	5	
111A	SS	1/2 x 1	SM	none	-	20:[h]60:20	6-10	952	F	60	111H,111I
111A	SS	1/2 x 1	SB	none	-	20:[h]60:20	6-11	952	F	50	

a) 10% additional type 6 binder brushed on over dried coating.
b) 35% particulate type 5 support.
c) Coatings too soft for bond strength to be assessed.
d) Formulation I used, 65:65:10, and after coating 1½° muffled, brushed with type 6 binder solution, dried and muffled.
e) Formulation I, mav, particulate type 1 support (as received).
f) Formulation I, mav, particulate type 1 support muffled at 1220°F.
g) Formulation VI, 40% fibrous type 16 support - 40% particulate type 1 support - 20% type 6 binder
h) Formulation VI, another fibrous type 16 support - 40% particulate type 1 support - 20% type 6 binder.

Table IV. RELATIVE MACH OXIDIZATION RATES AT 752°F OF VARIOUS PLATINUM-WALL COATING CANDIDATES, IN GRAND LAB RUNS

Run No.	Catalyst Number 10860-	% Pt	k_c/k_s a) (752°F)	Corresponding Coating Material		
				10860-	Adhesion Rating	
					SM b)	SB c)
855	55A	2	1.19	52A	G	G
856	55B	2	1.34	52B	P	P
857	55C	2	(1.19)	52C	F	F
858	55D	2	(1.15)	52D	F-G	F-G
859	55E	2	1.03	52E	P	G
854	50A	3	0.62	50A	-	-
852	50B	3	1.01	50B	-	-
860	54A	3	1.05	54A (50C)	P	P
853	50D	3	1.08	50D	-	-
862	54B	3	1.06	54B (50E)	F	P
861	54C	3	0.67	54C (50F)	P	P
906	69A	1	1.03	68C	-	P
907	69B	2	1.09	68C		
962	81A	1	1.05	78A	F	F
963	81B	2	1.22	78A		
964	81C	1	1.20	78B	L,P	P
965	81D	2	1.36	78B		
966	81E	1	1.20	78C	L,P	P
967	81F	2	1.31	78C		
942	89C	2	1.14	88A	F	P
943	89D	3	1.03	88A		
950	90A	2	0.96	90	P	P
1001	98B	2	1.25	94C	E	E
1012	103	3	1.13	94C		
999	98A	2	1.20	94B	E	E
1042	108A	2	1.06	107	F	G
1043	108B	3	1.17	107	F	G
1044	108C	2	1.24	107B	F	G
1045	108D	3	1.12	107B	F	G
1050	111B	1	1.12	109B	F	G
1048	111C	2	1.26	109B	F	G
1051	111D	1	1.02	110A	P	F
1052	111E	2	1.22	110A	P	F
1053	111F	1	1.26	110B	F	G
1055	111G	2	1.26	110B	F	G
1056	112B	1	1.19	111A	P	P
1057	112C	2	1.09	111A	P	P

a) See footnote c, Table ___.
b) SM = smooth surface.
c) SB = sandblasted surface.

The data shown in Table 71 indicate that with the coated 1/4" inch tube series 20, 16, 15 and 17 (quartz packed) maximum dehydrogenation activity for MCH at 752°F is reached at 5.8% Pt loading (based on support coating). Thus the additional Pt present in Tubes 15 and 17 added little or nothing to the activity. Tube 27 in which the fibrous and particulate type I supports were ball-milled together to obtain better adhesion of Formulation I coating had the same Pt content and activity as Tube 16.

After standing idle for sometime coated tube 16 was retested in the MICTR and was slightly less active than formerly in run 73. It was then packed in the normal catalyst zone with the usual quartz diluted reference catalyst, and the remainder of the tube was filled with quartz. The apparent conversion increased only about 5 units at constant MCH flowrate. The coated tube was emptied, heated in air to 852°F to burn out any coke present, repacked with quartz and retested - it gave very nearly the same activity as in the above test (c.f. runs 1047, 1049, and 1054, respectively, in Appendix Table 133). In view of the kinetic considerations advanced in the next section, it seems likely that although the wall catalyst can receive heat rapidly enough to maintain the endothermic reaction and thus operate efficiently close to block temperature, its insulating property probably increases the usual difficulty of transporting heat to the center of the granular catalyst bed which is much less efficient per unit weight of catalyst, because of the much lower operating temperature.

Tube 24, coated with Formulation I and impregnated with metal A alone (Run 819) was very active and formed only a little benzene by-product at virtually complete conversion of MCH to toluene. Tubes 23 and 26 coated with metal A and each with a different amount of metal K were equally active and formed a little less benzene at complete MCH conversion (Runs 817 and 818, respectively, Table 71). Small differences in activity are attributable to differences in the ratios of metals A and K (of K salt). The selectivity advantage of adding metal K is much less than with the corresponding granular catalysts where diffusivity is probably an important factor in controlling rates of side reactions, relative to the principal reaction (MCH dehydrogenation to toluene). The results compare favorably with those obtained with similar tubes with a platinized coating (i.e., Run 754, Appendix Table 130).

Tubes 22 and 25 in which Formulation I coating was impregnated with two different amounts of metal B (ca 5 and 6%) were reasonably active but lost toluene selectivity above 60-70% conversion to toluene at 752°F, and were therefore less attractive than their platinized counterparts. Tube 18 impregnated with metal I was much less active and showed little increase of activity as the temperature was raised from 752 to 842°F (c.f. Table 71).

Wall Catalysts: Analysis of MICTR Operation[a)]

A brief study has been made of the possible nonkinetic effects which may be reflected in the experimental results obtained using the micro-scale test rig, MICTR. The normal use of this reactor is to evaluate catalyst

a) This analysis was done and the report prepared by Dr. R. W. Rolke, as part of a training program assignment.

Table 71. MCH DEHYDROGENATION ACTIVITY OF VARIOUS CATALYTICALLY COATED TYPES

Conditions: 662, 752 and 842°F, 10 atm pressure, 90 ml MCH/hr (no added H_2)

Run No.	Catalyst No.	Tube No.	Formulation and Packing	% Pt	MCH Conversion Mol %		
					662°F	752°F	842°F
695	10860-17Sa	13	Formulation IV, ref to Run 668 rerun without quartz	-	38	65	88
697	10860-17Sa	13	rerun with steel wool		27	67	88
698	10860-17Sa	13	rerun with quartz		29	77	96
705	10860-18F	18	I with quartz	.5[b] metal I	22	57[a]	99[a]
735	10860-8	20	40% type 1 support, 40% I type 1 support, 20% type 6 binder quartz packing	6.9[c]	30	65	89
740	10860-7	16	40% type 1 support, 40% I type 1 support, 20% type 6 binder quartz packing	5.8[d]	59	78	95
729	10860-7	15	40% type 1 support, 40% I type 1 support, 20% type 6 binder quartz packing	7.1[d]	40	76	98
731	10860-7	17	40% type 1 support, 40% I type 1 support, 20% type 6 binder quartz packing	12.9[d]	51	88	96
758	10860-18	27	40% type 1 support (fibrous) and I 40% type 1 support (particulate)[f] 20% type 6 binder	5	30	74	98
817	10860-35	25	40% type 1 support I 40% type 1 support 20% type 6 binder	metals A + E	32	67	92[a]
818	10860-35	26	40% type 1 support I 40% type 1 support 20% type 6 binder	metals A + E	36	79	96[a]
819	10860-35	24	40% type 1 support I 40% type 1 support 20% type 6 binder	A	49	72	95[a]
885	10860-38	28	40% type 1 support I 40% type 1 support 20% type 6 binder	B	18	46	61[a]
886	10860-38	25	40% type 1 support I 40% type 1 support 20% type 6 binder	pt[g]	24	58[a]	(12)[h] 72

a) Includes a small amount of benzene.
b) Metal: Ethylene diamine complex (1.5).
c) By analysis of coating; coating scaled in impregnate containing 4.2 mgm Pt/ml.
d) By analysis of coating.
e) By analysis of coating; coating scaled tube in impregnate; after first impregnation excess solution blown out of tube and dried and muffled at 662°F, then repeated.
f) Ball milled together.
g) Greater concentration of I than in Tube No. 28.
h) Benzene - other number total conversion.

materials by measuring the conversion of methylcyclohexane (MCH) to toluene at three fixed temperature levels, with a fixed flow rate of MCH, and using a catalyst support of fixed porosity and particle size. Under these conditions it is appropriate to compare catalysts on the basis of MCH conversion at the three temperature levels. Diffusion and heat transfer limitations, if they are present, would tend to reduce conversions in all cases and therefore would have no effect on the results of these screening experiments as far as ranking catalysts according to their activities. The effect of these limitations increases with the activity of the catalyst, however, and this will tend to obscure some of the gains offered by a more active catalyst.

It is in evaluating different modes of operation with a given catalyst that one must worry about the nonkinetic effects mentioned above. One would not expect to get the same performance from a catalyst which is coated on the reactor wall as a thin film compared to the same amount of catalyst in the form of spherical packing, unless the rate of reaction is entirely controlled by chemical kinetics. Some recent experimental results indicate that diffusive effects, and possibly also heat transfer effects, are important under normal MICTR operating conditions. Use of the standard platinum catalyst in a coated wall reactor showed a substantial increase in apparent catalyst activity compared to the catalyst in the form of 1/16-in.-1/32-in. particles. Another experiment showed that a screened sample of 10-14 mesh catalyst particles exhibited lower activity than a sample screened for 14-20 mesh particles. This again indicates diffusive effects in the measured reaction rate. That diffusive effects would be predicted for this reaction on 10-20 mesh catalyst will be shown in the following paragraphs. Ways to increase the apparent catalyst activity will also be discussed.

In order to test whether or not a reaction will be diffusion controlled it has been found that the magnitude of the following group (the Thiele Modulus, ϕ) is important:

$$\phi = \left[\frac{dN}{dt}\frac{1}{C_o}\frac{L^2}{D_E}\right]^{1/2}$$

where dN/dt = rate of reaction at concentration Co[=] moles/ft^3hr

C_o = exterior conc of reactant [=]moles/ft^3
L = characteristic length, thickness of a film or radius of spherical particles [=] ft
D_E = effective diffusivity of reactant inside particle [=] ft^2/hr

The size of this group will be a measure of the relative rates of reaction and diffusion of reactant within the catalyst particle. If the group is larger than a critical value, the reaction rate will drop because all of the catalyst surface will not be equally accessible to reactant. This critical value will depend on the order of the reaction since the rate becomes more sensitive to concentration as order increases.

The rate of MCH dehydrogenation is given by[18]

$$\frac{dN}{dt} = \frac{A_1A_2 e^{(B_1 + B_2/R_gT_S)}C_{MCH}}{1 + A_2(e^{B_2/R_gT_S})P_{MCH}} \left[1 - \left(\frac{P_{TOL}\, P_{H_2}^3}{P_{MCH}\, K_{eq}}\right)\right]$$

where $K_{eq} = 4 \times 10^{20}\, e^{-92500/R_gT_S}$

Because of the large value of K_{eq} one finds that

$$1 - \frac{P_{TOL}\, P_{H_2}^3}{P_{MCH}\, K_{eq}} \approx 1 \text{ except for extremely high pressures}$$

or conversions much in excess of 90%. Values of other coefficients in the rate expression are:

$A_1A_2 = 3.38 \times 10^5$
$B_1 + B_2 = -5000$
$A_2 = 4.5 \times 10^{-6}$
$B_2 = 5.4 \times 10^3$

Using these coefficients one calculates the following representative reaction rates at 842°F and 650°F, the high and low temperatures of most MICTR experiments.

Temp, °F	Mole Fract., MCH	Z	C_{MCH}, lb moles/ft^3	Rate dN/dt, lb moles/ hr ft^3 cat.
842	1.0	.95	.01107	343.11
842	0.2	1.0	.002104	92.75
650	1.0	.91	.01356	17.44
650	.2	.99	.002493	14.99

MCH concentration was based on the ideal gas equation of state, i.e.,

$$C_{MCH} = \frac{(\text{mole fraction MCH})P_{total}}{R_g\, T_g\, Z}$$

P_{total} = 10 atmospheres in all runs

$R_g = .73$ ft^{3}atm/(lb mole °F)

Physical properties of the MCH, Toluene, Hydrogen mixtures were obtained from the Appendix of the October, 1967 annual report[18] starting on page 321. These properties include the compressibility, Z.

From the above table we see that the reaction rate is extremely temperature sensitive and that the rate is definitely not zero order. The concentration dependence is much greater at the higher temperature and is roughly 3/4 order at 842°F.

Satterfield and Sherwood[21] (p. 61) present a plot of the effectiveness factor, η, as a function of the Thiele Modulus, $(dX/dt\ 1/C_0\ L^2/D_E)^{1/2}$, taken from the work of Wheeler.[22] From this plot (strictly for diffusion onto a flat plate) one finds that an effectiveness factor greater than .9 (90% of catalyst is accessible) requires a Thiele Modulus, φ, less than the following values.

$\varphi_L \leq \sim .4$ for second order reaction

$\varphi_L \leq \sim .7$ for first order reaction

$\varphi_L \leq \sim 1.6$ for zero order reaction

Satterfield and Sherwood[21] (pp. 16-25) also present an equation for estimating the effective diffusivity, D_E, within catalyst particles.

$$D_E \approx 19{,}400 \frac{\theta^2}{\tau S_g \rho_p} \sqrt{\frac{T}{M}}$$

where for our alumina catalyst and MCH reactant:

θ = void fraction $\approx .55$

τ = tortuosity factor ≈ 8

S_g = total surface area = 250 $\longrightarrow$ 500 m^2/g

ρ_p = particle density $\approx .52/\theta$ g/cm^3

T = temperature = 724°K (842°F)

M = molecular weight = 98

One finds $D_E \simeq 7.5 \times 10^{-4} \longrightarrow 4 \times 10^{-4}$ cm^2 sec for the above parameters.

The authors also present a plot of D_E vs $\theta^2/S_g\rho_p\ T/M$ from the data of Weisz and Schwartz.[35] From this plot we estimate

$D_E \sim 6 \times 10^{-4} \longrightarrow 4 \times 10^{-3}$ cm^2/sec

From these two estimates we shall use $D_E \sim 1 \times 10^{-3}$ cm^2/sec as an order of magnitude value. This bears the expected relation to the estimated $D \sim 1 \times 10^{-2}$ for MCH diffusion through bulk toluene.

The same value of D_E shall be used in calculating φ_L at 650°F since this temperature change causes only an insignificant 8% change in D_E.

Knowing the reaction rate, exterior concentration, and effective diffusivity, it is possible to calculate the maximum catalyst thickness which will result in an effectiveness factor greater than .9, i.e., φ_L less than the above limits. This thickness is calculated to be:

Temp, °F	Mole Fract., MCH	Maximum Catalyst Thickness, mils		
		0 Order	1st Order	2nd Order
842	1.0	6.9	3.1	1.7
842	0.2	5.7	2.6	1.4
650	1.0	33	15	8.3
650	0.2	15	6.9	3.8

The uncertainty in D_E could cause changes in the calculated thickness by a factor of two.

The standard MICTR catalyst pellets have a nominal thickness of 1/32" = 31 mils. Therefore, it is apparent that only a zero order reaction at low temperature and low conversion would exhibit true kinetics. In all other cases reactions are severely diffusion limited. The above table also gives an idea of how thin a tube wall coating must be before diffusion effects are eliminated completely. It must be remembered, however, that the calculation is only an approximate one.

From this it would seem that catalyst activity can be increased by reducing the diffusion path length, i.e., applying the catalyst as a coating on the reactor tube wall. This, however, introduces the possibility that the reaction rate will be limited by mass transfer to and from the bulk gas stream flowing past the coated wall. Turbulent flow is required to avoid this.

Due to the small feed pump in the MICTR apparatus the maximum MCH flow rate is 90 ml/hr. Based on physical properties previously referred to,[18] this corresponds to a maximum Reynolds number of 429 in a .17 inch I.D. reactor tube. This is far below the critical Reynolds number of 2100 where turbulence sets in. In fact it is so low that merely adding wall roughness will have no affect on mixing in the flowing stream. Tube diameter would have to be decreased by a factor of 3 to insure turbulence at this flow rate.

It can be shown from mass transfer rate correlations that at this low Reynolds number one expects a lower rate of mass transfer to the tube walls than the rate of which MCH reacts to form toluene. Also a marked increase in MCH conversion has been observed when the coated reactor tube is packed with 10-20 mesh quartz particles. This increased the linear velocity and the mixing in the bulk phase.

It is still quite possible that the mixing is incomplete even with quartz packing. It was found that decreasing the flow velocity by a factor of two through the standard 10-20 mesh catalyst packing caused a decrease of ~50% in the apparent first order rate constant compared to the maximum flow rate available from the pump.[18] Thus it is conceivable that increasing the flow velocity would increase the apparent rate constant by promoting more rapid mass transfer with the bulk phase. A higher flow rate, smaller tube diameter, or lower void volume packing could be used in an attempt to obtain complete bulk phase mixing. Given such mixing and a thin enough catalyst coating, one will observe the maximum MCH conversion for a given weight of catalyst.

One might also consider packing the coated reactor tube with granular catalyst. In this way additional catalyst can be contacted in a given length of reactor tube. However, in this case heat transfer rate might limit the reaction rate on the packing catalyst. Catalyst coated on the tube wall can rapidly receive heat to maintain the endothermic reaction.

Some isolated (and unchecked) data indicates that this may not be true for particles packed inside the reactor tube. One experiment was done in the MICTR where the standard weight of 10-20 mesh catalyst, was diluted to 4 ml with 10-20 mesh quartz particles rather than to 2 ml as in the standard runs. This higher dilution experiment indicated an apparent first order rate constant ~46% higher than the standard run. Such an increase seems as if it could only be due to heat transfer limitation of the reaction. With the higher dilution the required heat is transferred over larger area. Measured temperature drops for the MICTR may not give an appropriate indication of the seriousness of this heat transfer limitation.

In summary, much care must be taken in interpretating the results of any kinetic experiment in order to account for nonkinetic effects in the measured rates. It would appear that the coated tube MICTR configuration will result in the highest possible specific rates provided that the coating is thin enough and that the flowing gas is well mixed. It would appear that it should be possible to achieve significant test conditions in FSSTR experiments.

*) Reference 18), pages 122-127.

Fuel System Simulation Test Rig

The Fuel System Simulation Test Rig (FSSTR) has been described in detail in the three annual reports associated with the preceding contract on this subject,[10][11][19] therefore no description of the unit will be included here. However, a flow scheme is repeated as Figure 32 for convenience.

During the past year the following studies have been conducted in the FSSTR:

(1) Heat transfer to Decalin, SHELLDYNE H and F-71 in miniature (1/16" OD x 4" and 6" long) heat transfer sections (mini - FSSTR).
(2) Dehydrogenation of MCH in catalyst (Pt on Al_2O_3) lined reactor sections.
(3) Dehydrogenation of MCH and Decalin over Shell 113 Pt on Al_2O_3 catalyst.

Cooling Program, Experimental Study Using Miniature Heat Transfer Sections

The study using miniature heat transfer sections to reach heat flux of 8×10^6 Btu/(hr-ft^2) has been continued. Tests with four fuels (MCH, Decalin, SHELLDYNE H, and F-71) have been completed at temperature levels where coke formation would not be expected to have any effect on heat transfer.

The preceding Annual Report[18] on this subject outlines the procedures and describes the test equipment used for this study. A photograph of the rig with a 1/16" OD x 6" long heat exchange section in place (with insulation removed) is repeated here in Figure 33. Only the feed and product handling and pressure control systems of the FSSTR were used for these tests. The preheaters and reactor sections were bypassed.

Reported here are test results obtained with Decalin, SHELLDYNE H, and F-71. MCH data were presented in the preceding report. Table 72 summarizes the operating conditions at which heat transfer data have been obtained for these three fuels. Sketches of the four heat transfer sections used in these tests are given in Figures 34 through 37. Note that Reactors 10018-110 and 122 were made using 0.0265" ID x 0.0180" wall type 316 S.S. tubes while Reactors 10018-148 and 157 used 0.0344" ID x 0.0144" wall Hastelloy C tubes.

Test Runs With Decalin

Three series of runs were made using Decalin as feed. The first series, using the 4" long Reactor 10018-122, reached the desired maximum heat flux, 8×10^6 Btu/(hr/ft^2), before the closing of a product line valve resulted in tube failure. The other tests using Reactor 10018-110, a 6" long section, were made at lower flow rates to broaden the scope of the heat transfer data. These tests were made with Decalin recycle. Fresh 10 gal charges of N_2 sparged Decalin were made to the system prior to the first (Series 10018-134) and second (Series 10018-138) series of runs.

Data tabulations for these tests which include recorded as well as smoothed and calculated results are presented in Tables 73, 74 and 75.

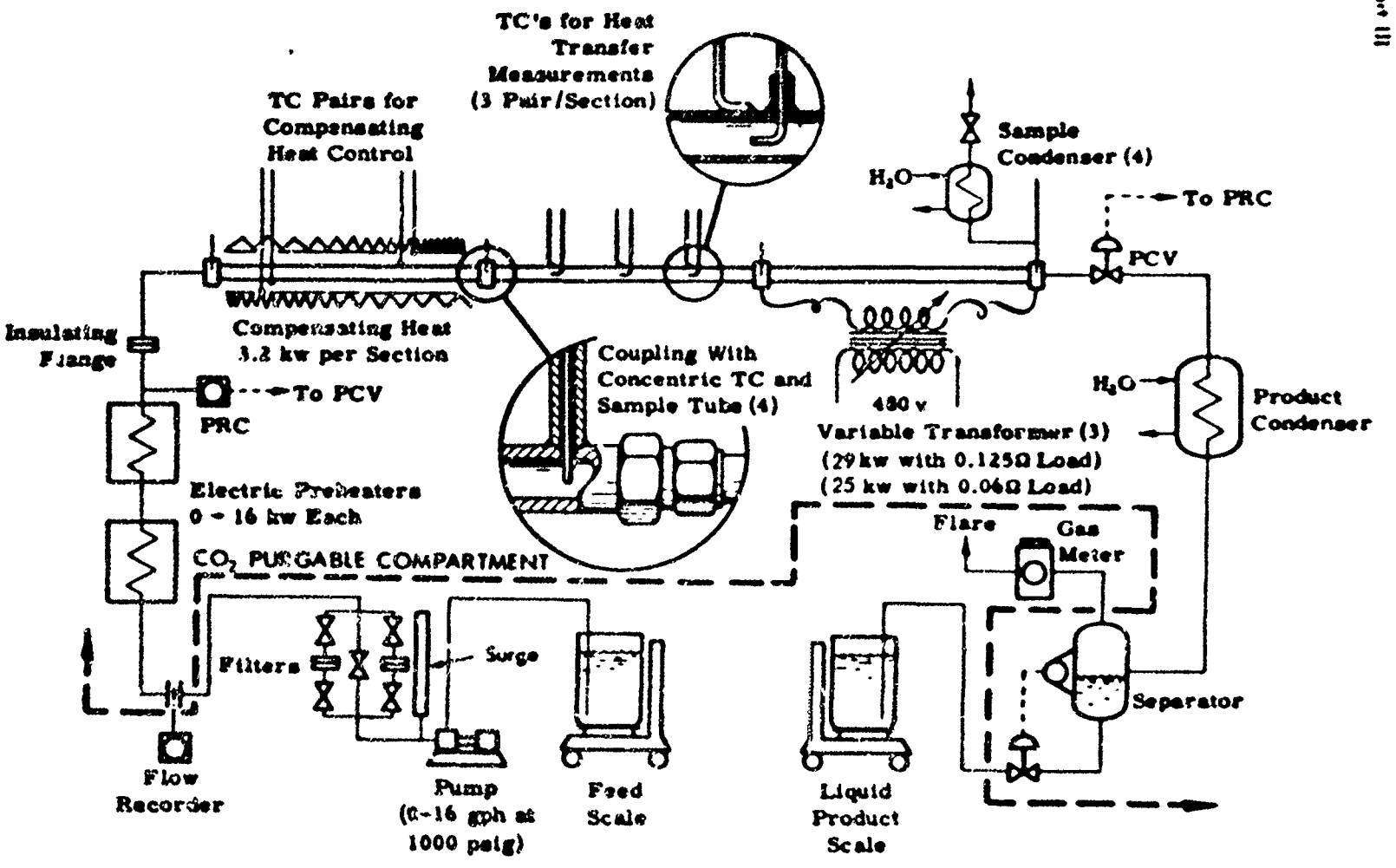

Figure 32. FSSTR - FLOW SKETCH OF FUEL SYSTEM SIMULATION TEST RIG

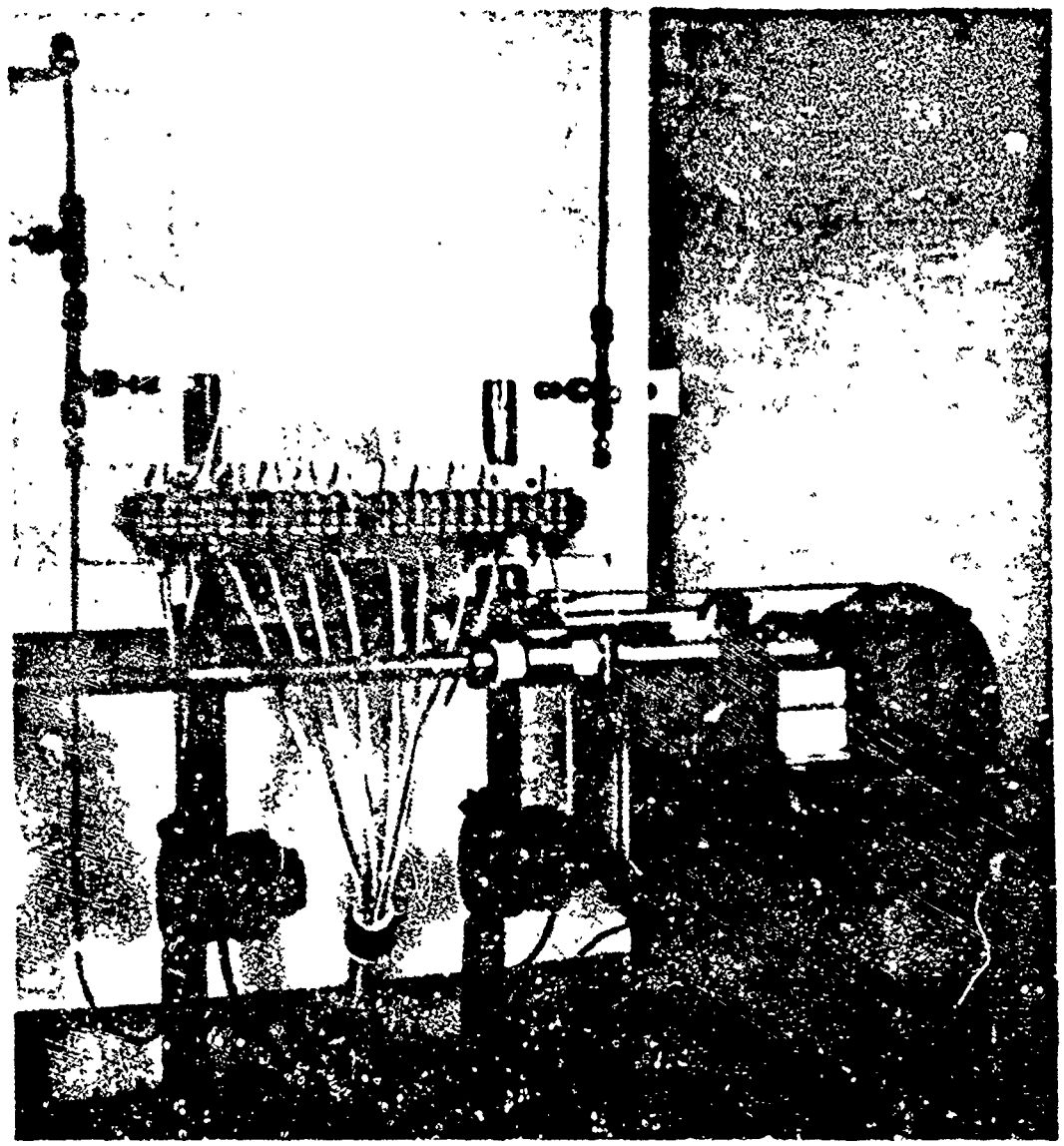

Figure 33. FSSTR - MINIATURE HEAT TRANSFER SECTION TEST STAND

Table IX. POST-SUMMARY OF OPERATING CONDITIONS FOR MINIATURE HEAT TRANSFER SECTIONS

Run No. - Section No.	Coolant	Fuel	Heat Flux			Fluid Temp., °F		Pressure, psig		Avg Heat Flux,	Heat to Fluid,	Max Inside Wall Temp.,	Time at Temp.,
						In	Out	In	Out				
139-14-16	140	Decalin	75.6	19.7	1.979	68	146	338	303	1.088	28.7	333	11
14-17						68	210	333	303	2.720	41.6	357	14
14-18						68	197	333	303	2.720	39.6		13
14-19						68	197	333	303	2.720	39.6		13
14-20						68	197	333	303	2.720	39.6		13
14-21						68	197	333	303	2.720	39.6		13
14-22						68	197	333	303	2.720	39.6		13
14-23						68	197	333	303	2.720	39.6		13
14-24						68	197	333	303	2.720	39.6		13
14-25						68	197	333	303	2.720	39.6		13
14-26						68	197	333	303	2.720	39.6		13
14-27						68	197	333	303	2.720	39.6		13
14-28						68	197	333	303	2.720	39.6		13
14-29						68	197	333	303	2.720	39.6		13
14-30						68	197	333	303	2.720	39.6		13
14-31						68	197	333	303	2.720	39.6		13
14-32						68	197	333	303	2.720	39.6		13
14-33						68	197	333	303	2.720	39.6		13
14-34						68	197	333	303	2.720	39.6		13
14-35						68	197	333	303	2.720	39.6		13
14-36						68	197	333	303	2.720	39.6		13
14-37						68	197	333	303	2.720	39.6		13
14-38						68	197	333	303	2.720	39.6		13

Tube burned out because of operating error

138-9-11	110	Decalin	24.8	7.78	988	68	93	357	288	99	6.9	265	9
9-12						68	93	357	288	100	11.9		14
9-13						68	93	357	288	100	11.9		14
9-14						68	93	357	288	100	11.9		14
9-15						68	93	357	288	100	11.9		14
9-16						68	93	357	288	100	11.9		14
9-17						68	93	357	288	100	11.9		14
9-18						68	93	357	288	100	11.9		14
9-19						68	93	357	288	100	11.9		14
9-20						68	93	357	288	100	11.9		14
9-21						68	93	357	288	100	11.9		14
9-22						68	93	357	288	100	11.9		14
9-23						68	93	357	288	100	11.9		14
9-24						68	93	357	288	100	11.9		14
9-25						68	93	357	288	100	11.9		14
9-26						68	93	357	288	100	11.9		14
9-27						68	93	357	288	100	11.9		14
9-28						68	93	357	288	100	11.9		14
9-29						68	93	357	288	100	11.9		14
9-30						68	93	357	288	100	11.9		14
9-31						68	93	357	288	100	11.9		14
9-32						68	93	357	288	100	11.9		14
9-33						68	93	357	288	100	11.9		14
9-34						68	93	357	288	100	11.9		14
9-35						68	93	357	288	100	11.9		14
9-36						68	93	357	288	100	11.9		14
9-37						68	93	357	288	100	11.9		14
9-38						68	93	357	288	100	11.9		14

Run terminated on inside wall temperature >1000°F

140-13-16	115	Decalin	6.95	1.91	66	68	79	353	7	0.0	0.0	116	0
13-17						68	79	353	7	0.0	0.0	116	0
13-18						68	79	353	7	0.0	0.0	116	0
13-19						68	79	353	7	0.0	0.0	116	0
13-20						68	79	353	7	0.0	0.0	116	0
13-21						68	79	353	7	0.0	0.0	116	0
13-22						68	79	353	7	0.0	0.0	116	0
13-23						68	79	353	7	0.0	0.0	116	0
13-24						68	79	353	7	0.0	0.0	116	0
13-25						68	79	353	7	0.0	0.0	116	0
13-26						68	79	353	7	0.0	0.0	116	0
13-27						68	79	353	7	0.0	0.0	116	0
13-28						68	79	353	7	0.0	0.0	116	0
13-29						68	79	353	7	0.0	0.0	116	0
13-30						68	79	353	7	0.0	0.0	116	0
13-31						68	79	353	7	0.0	0.0	116	0
13-32						68	79	353	7	0.0	0.0	116	0
13-33						68	79	353	7	0.0	0.0	116	0
13-34						68	79	353	7	0.0	0.0	116	0
13-35						68	79	353	7	0.0	0.0	116	0
13-36						68	79	353	7	0.0	0.0	116	0
13-37						68	79	353	7	0.0	0.0	116	0
13-38						68	79	353	7	0.0	0.0	116	0

Run terminated when test power increase caused very high wall temp (>1500°F,

135-15-19	140	PHILLETHE-S	38.9	8.99	357	68	97	338	265	35.8	3.0	328	4
15-20						68	97	338	265	35.8	3.0	328	4
15-21						68	132	338	265	288	23.3	338	13
15-22						68	132	338	265	288	23.3	338	13
15-23						68	132	338	265	288	23.3	338	13
15-24						68	132	338	265	288	23.3	338	13
15-25						68	132	338	265	288	23.3	338	13
15-26						68	132	338	265	288	23.3	338	13
15-27						68	132	338	265	288	23.3	338	13
15-28						68	132	338	265	288	23.3	338	13
15-29						68	132	338	265	288	23.3	338	13
15-30						68	132	338	265	288	23.3	338	13
15-31						68	132	338	265	288	23.3	338	13
15-32						68	132	338	265	288	23.3	338	13
15-33						68	132	338	265	288	23.3	338	13
15-34						68	132	338	265	288	23.3	338	13
15-35						68	132	338	265	288	23.3	338	13
15-36						68	132	338	265	288	23.3	338	13
15-37						68	132	338	265	288	23.3	338	13
15-38						68	132	338	265	288	23.3	338	13

Run terminated on inside wall temperature >1000°F

1456-15:03	130	SHELLETHE-S	53.9	13.8	636	67	150	889	613	305	28.9	733	12
15:36						67	184	888	598	1,246	66.3	893	8

Run terminated on inside wall temperature was approaching 1000°F

146-13:16	130	SHELLETHE-S	9.07	2.57	73	69	78	385	733	11.9	0.6	138	16
14:02						69	108	378	733	61.3	15.8	388	15
14:25						70	151	378	735	96.3	39.9	438	6
14:44						70	233	378	827	198	78.3	388	8
15:06						70	258	378	819	218	85.2	1087	17

Run terminated on inside wall temperature >1000°F

(continued)

(1) Based on inside cross sectional area of tube.
(2) Volume of liquid per volume of heated length of tube per hour.
(3) Fluid temperature and pressure measured across entire length of section. Not just heated length.
(4) Net heat flux to fluid corrected for tube heat loss. Based on inside surface of tube.
(5) Net heat to fluid in entire rocker section.
(6) Maximum measured to be at point 1/8 in. from the bar in steam where one end the hottest portion of rod.

Table 72 (Contd). TEST SUMMARY OF OPERATING CONDITIONS FOR MINIATURE HEAT TRANSFER SECTIONS

Run No.	Section No.	Feed	Feed Rate			Fluid Temp. °F		Pressure psia		Aver. Heat Flux Btu/hr-ft² x 10⁻⁶	Heat to Fluid Btu/lb	Max. Inside Wall Temp. °F	Time at Temp. Hrs.
			lb/hr	lb/hr-in² x 10⁻³	gpm	In	Out	In	Out				
1108	168	[illegible]	[illegible]	7.8	36	[illegible]	[illegible]	851	48	140	[illegible]	958	17
1116						886	1277	860	693	1.14	7.8	976	16
1126						859	1385	851	662	1.91	13.1	848	16
1139						796	916	854	644	1,390	37.2	954	17
1147						843	1 0	868	785	2,210	68.6	889	17
1151						863	998	870	688	2,800	98.1	988	29
1200						888	1158	888	695	4,990	138.9	1,139	30
Series terminated on inside wall temperature >1,025°F													
1154-1610	168	[illegible]	16.9	9.72	981	790	968	888	886	139	7.6	973	12
1625						790	1051	869	882	549	17.1	111	12
1641						791	1121	870	880	1,110	29.8	1,058	13
1648						798	1167	870	887	1,260	55.2	1,298	12
Series terminated on inside wall temperature >1,000°F													
1154-1811	168	F-71	96.8	13.1	950	68	92	998	657	142	5.0	129	25
1834						69	90	895	668	719	14.1	199	18
1841						69	127	896	698	1,14	18.9	779	17
1848						69	165	896	730	1,360	27.3	857	20
1852						70	210	890	710	2,040	71.7	752	23
1900						71	270	898	713	2,389	108.0	848	18
1925						71	329	900	710	3,480	147.0	950	30
1930						72	349	908	708	4,980	176.0	988	30
Series terminated on inside wall temperature approached 1,000°F													
1154-1615	168	F-71	109.5	17.9	1,275	71	90	998	61	100	5.8	178	17
1630						71	125	900	554	160	14.8	253	16
1644						70	190	898	648	1,260	28.6	379	17
1708						71	287	899	698	2,120	58.1	588	26
1729						72	379	898	698	3,990	108.0	887	18
1746						72	395	889	688	5,340	165.0	980	49
1819						76	953	889	577	8,260	281.0	972	25
Series terminated on inside wall temperature approached 1,000°F													
1154-1939	168	F-71	20.1	3.12	198	68	98	900	488	107	16.0	608	22
1946						68	118	901	881	216	32.2	697	19
1953						68	148	899	890	317	47.3	1,063	21
1130						68	188	900	898	398	58.8	1,208	41
Series terminated on inside wall temperature >1,000°F													
1154-1405	154	F-71	55.6	8.78	350	67	98	898	766	141	11.9	196	18
1417						68	138	896	776	288	25.4	396	28
1428						69	196	897	789	586	46.2	778	25
1437						69	251	897	799	1,089	81.8	659	98
1505						70	376	877	798	2,009	170.0	1,088	69
1537						69	450	877	798	2,690	268.8	1,158	28
Series terminated on inside wall temperature >1,000°F													

a) Based on inside cross sectional area of tube.
b) Volume of liquid feed per volume of heated length of tube per hour.
c) Fluid temperature and pressure measured across entire length of section. Not just heated length.
d) Net heat flux to fluid corrected for tube heat loss. Based on inside surface of tube.
e) Net heat to fluid in entire heated section.
f) Maximum assumed to be at point 1/8" from exit end in cases where one end was hottest portion of tube.

64987

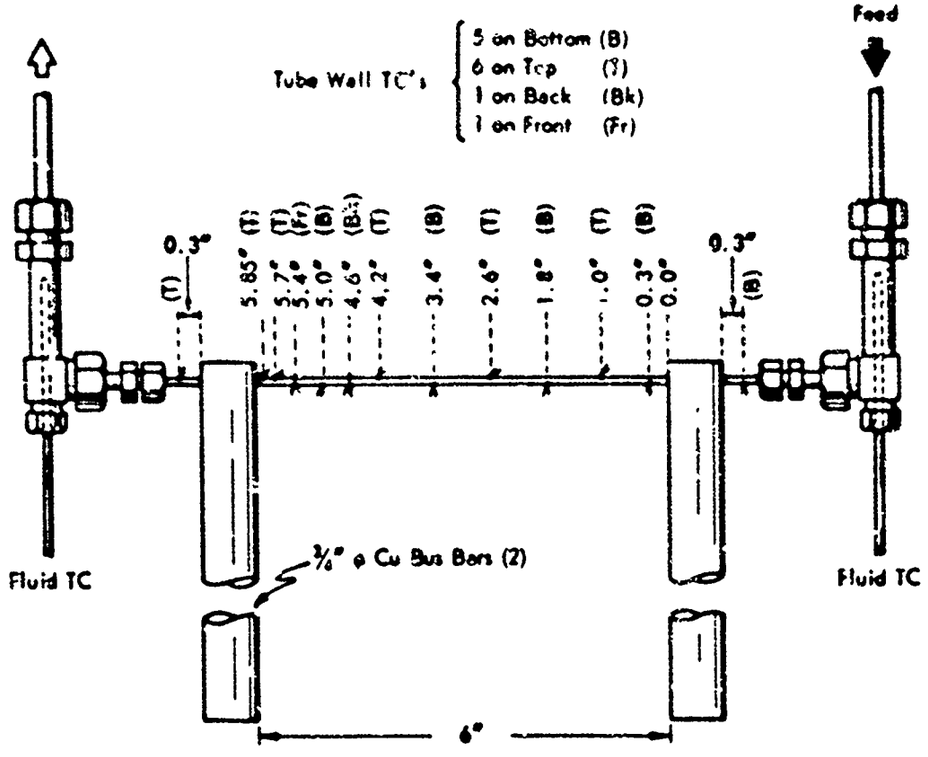

Tube: 1/16" OD x 0.015" Wall Hastelloy C
Thermocouples: Fluid - 1/16" OD Inconel Sheathed Chromel-Alumel
Wall - 0.005" Chromel-Alumel Spot Welded
Scale: None

Figure 34 FSSTR - MINIATURE HEAT TRANSFER SECTION: REACTOR NO. 10018-110

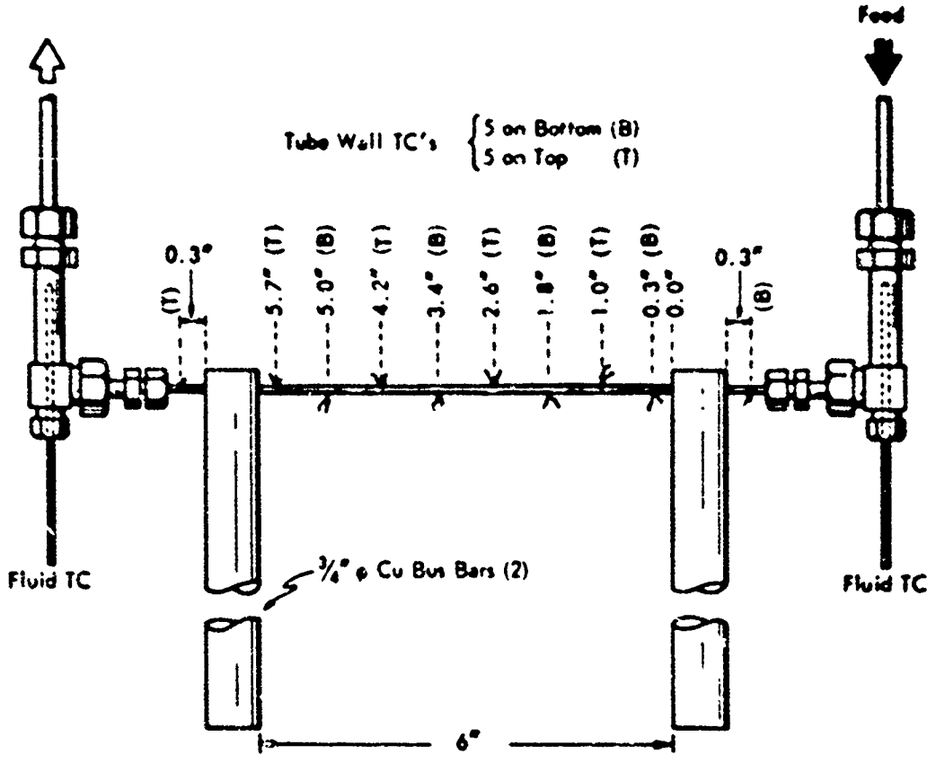

Tube: 1/16" OD x 0.018" Wall Type 316 SS (1/16" Tube 9 1/2" Long Overall)
Thermocouples: Fluid - 1/16" OD Inconel Sheathed Chromel-Alumel
Wall - 0.005" Chromel-Alumel Spot Welded
Scale: None

Figure 35. FSSTR - MINIATURE HEAT TRANSFER SECTION: REACTOR NO. 10013-97

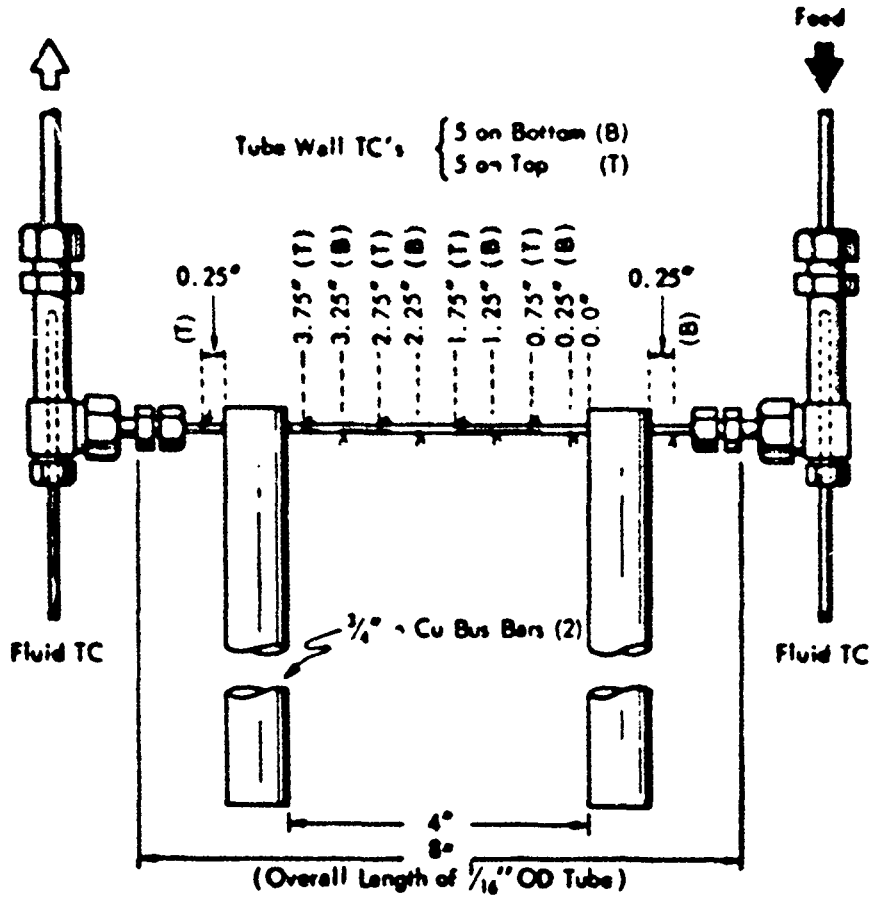

Tube: 1/16" OD x 0.015" Wall Hastelloy C
Thermocouples: Fluid - 1/16" OD Inconel Sheathed Chromel-Alumel
Wall - 0.005" Chromel-Alumel Spot Welded
Scale: None

Figure 36. FSSTR - MINIATURE HEAT TRANSFER SECTION: REACTOR NO. 10018-148

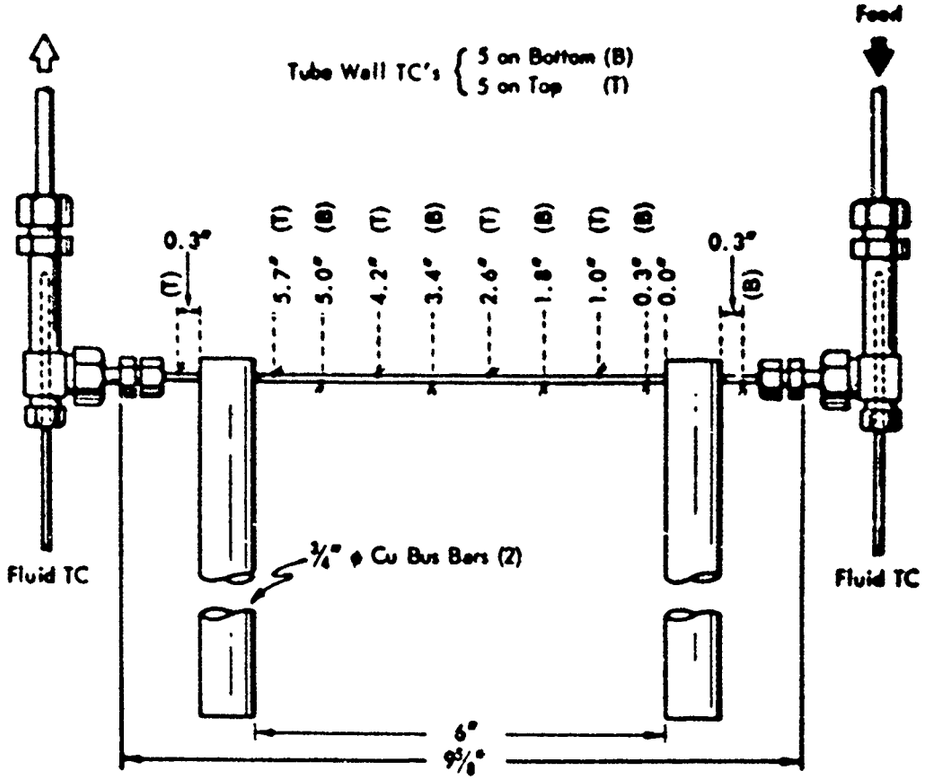

Tube: 1/16" OD x 0.015" Wall Hastelloy C
Thermocouples: Fluid - 1/16" OD Inconel Sheathed Chromel-Alumel
Wall - 0.005" Chromel-Alumel Spot Welded
Scale: None

Figure 37. FSSTR - MINIATURE HEAT TRANSFER SECTION: REACTOR NO. 10018-157

Table 13. FSGTR: DATA SUMMARY SERIES 10019-13
HEAT TRANSFER TO DECALIN IN MINIATURE HEAT TRANSFER SECTION

Reactor No. [illegible] Type 316 S.S.

Feed: Decalin, [illegible]

Run No. 10019-	Measured Power, Btu/lb	Fluid Temp, °F In	Fluid Temp, °F Out	Pressure, psia In	Pressure, psia Out	Tube T.C. Location Inches[a]	Tube T.C. Location Position[b]	Tube T.C. Temp, °F	Length, inches	Wall Temp, °F[c] Outside	Wall Temp, °F[c] Inside	Heat[d] Flux, Btu/hr ft² $\times 10^{-3}$	Cumulative[e] Heat, Btu/lb
13-14:44	2,900	68	146	455	403	0.25	B	540	0	(5[illegible])	(522)		0
						0.75	T	[illegible]	1	6[illegible]7	[illegible]	1.263	600
						1.25	B	623	2	[illegible]	[illegible]	1.095	1,200
						1.75	T	[illegible]	3	[illegible]	[illegible]	1.052	1,800
						2.25	B	[illegible]	4	([illegible])	(535)		2,400
						2.75	T	[illegible]	(0-4)			(1.056)	
						3.25	B	601					
						3.75	T	603					
14:59	4,690	68	210	550	425	0.25	B	640	0	(675)	(5[illegible])		0
						0.75	T	648	1	662	521	2,290	1,170
						1.25	B	[illegible]	2	615	[illegible]	2,305	2,330
						1.75	T	[illegible]	3	[illegible]	[illegible]	1,990	3,500
						2.25	B	[illegible]	4	([illegible])	[illegible]		4,660
						2.75	T	[illegible]	(0-4)			(2,009)	
						3.25	B	5[illegible]0					
						3.75	T	540					
15:10	9,600	68	307	553	480	0.25	B	[illegible]	0	(488)	(771)		0
						0.75	T	[illegible]	1	[illegible]	7[illegible]7	4,110	2,390
						1.25	B	[illegible]	2	[illegible]	666	4,150	4,790
						1.75	T	[illegible]	3	[illegible]	668	4,050	7,180
						2.25	B	773	4	(5[illegible]0)	(670)		9,480
						2.75	T	867	(0-4)			(4,070)	
						3.25	B	[illegible]					
						3.75	T	[illegible]					
15:20	11,860	69	385	555	470	0.25	B	[illegible]	0	([illegible])	(8[illegible])		0
						0.75	T	[illegible]	1	[illegible]	741	5,250	3,060
						1.25	B	1,050	2	[illegible]	781	5,160	6,060
						1.75	T	1,320	3	[illegible]	724	5,140	9,010
						2.25	B	1,701	4	(1,054)	(763)		11,990
						2.75	T	[illegible]	(0-4)			(5,180)	
						3.25	B	1,0[illegible]					
						3.75	T	[illegible]					
15:28	14,260	69	437	558	405	0.25	B	1,1[illegible]7	0	([illegible])	([illegible])		0
						0.75	T	1,153	1	1,1[illegible]	[illegible]	6,210	3,610
						1.25	B	1,15[illegible]	2	1,1[illegible]7	7[illegible]	6,140	7,170
						1.75	T	1,11[illegible]	3	1,1[illegible]	705	6,120	10,710
						2.25	B	1,13[illegible]	4	(1,135)	([illegible])		14,260
						2.75	T	1,0[illegible]	(0-4)			(6,170)	
						3.25	B	[illegible]					
						3.75	T	1,1[illegible]					
15:37	16,290	69	480	553	5[illegible]	0.25	B	1,265	0	(1,170)	(822)		0
						0.75	T	1,246	1	1,1[illegible]	7[illegible]1	7,400	4,180
						1.25	B	1,217	2	1,177	846	7,110	8,300
						1.75	T	1,17[illegible]	3	1,164	[illegible]17	7,100	12,450
						2.25	B	[illegible]	4	(1,177)	(866)		16,540
						2.75	T	1,[illegible]	(0-4)			(7,250)	
						3.25	B	1,17[illegible]					
						3.75	T	1,185					
15:42	18,900	69	532	(553)	(553)	0.25	B	1,356	0	(1,360)	(848)		0
						0.75	T	1,270	1	1,264	867	8,210	4,780
						1.25	B	1,260	2	1,257	861	8,160	9,510
						1.75	T	1,255	3	1,257	862	8,200	14,260
						2.25	B	1,2[illegible]	4	(1,313)	(920)		19,080
						2.75	T	1,261	(0-4)			(8,280)	
						3.25	B	1,2[illegible]					
						3.75	T	1,2[illegible]					

a) T.C.'s spotwelded to outside wall at indicated inches from inlet end bus bar.
b) Location of T.C. junction on horizontal tube B = Bottom, T = Top.
c) Outside wall temperatures by smoothing experimental data. Inside temperatures by calculation.
d) Corrected for losses. Values in () are average over entire heated length.
e) Net heat to fluid up to indicated tube length.

Table 74. FSSTR: DATA SUMMARY SERIES 10018-138 - HEAT TRANSFER TO DECALIN IN MINIATURE HEAT TRANSFER SECTION

Reactor No. 10018-110; 0.0265-in. ID x 0.018-in. Wall x 6-in. Long; Type 316 Stainless Steel
Feed: Decalin, 29.8 lb/hr - 7.78 x 10⁶ lb/(hr-ft²)

Run No. 10018-	Experimental Data: Measured Power, Btu/hr	Fluid Temp. °F: In	Fluid Temp. °F: Out	Pressure, psig: In	Pressure, psig: Out	Tube Wall Thermocouples: Location: Inches(a)	Location: Position(b)	Temp. °F	Smoothed and Calculated Data: Length, Inches	Wall Temp.(c) °F: Outside	Wall Temp.(c) °F: Inside	Heat(d) Flux, Btu/(hr-ft²) x 10⁻³	Cumulative(e) Heat, Btu/hr
138-9:17	211	68	83	987	896	0.3	B	136	0	(125)	(111)	98.4	0
						1.0	T	146	1	146	142	98.9	35
						1.8	B	160	2	164	160	99.2	68
						2.6	T	170	3	172	168	99.4	102
						3.4	B	179	4	167	163	99.5	137
						4.2	T	166	5	161	157	99.2	171
						5.0	B	160	6	(154)	(150)	99.0	205
						5.7	T	157	(0-6)			(99.4)	
9:33	366	67	98	987	884	0.3	B	262	0	(269)	(262)	99.1	0
						1.0	T	300	1	300	193	101.1	38
						1.8	B	287	2	255	286	102.2	117
						2.6	T	264	3	249	262	102.9	156
						3.4	B	254	4	250	243	102.9	233
						4.2	T	249	5	239	238	102.5	295
						5.0	B	237	6	(240)	(213)	101.8	354
						5.7	T	228	(0-6)			(102.2)	
9:42	795	67	123	987	875	0.3	B	362	0	(307)	(195)	198	0
						1.0	T	320	1	312	298	207	117
						1.8	B	367	2	375	361	213	239
						2.6	T	395	3	405	359	215	362
						3.4	B	396	4	388	366	213	488
						4.2	T	378	5	353	359	212	608
						5.0	B	371	6	(388)	(308)	208	738
						5.7	T	354	(0-6)			(212)	
9:54	1,811	67	201	987	875	0.3	B	467	0	(415)	(383)	496	0
						1.0	T	582	1	562	551	520	256
						1.8	B	662	2	646	635	531	510
						2.6	T	635	3	577	566	538	772
						3.4	B	564	4	529	498	512	1,000
						4.2	T	527	5	440	479	517	1,248
						5.0	B	492	6	(480)	(463)	505	1,506
						5.7	T	481	(0-6)			(515)	
10:10	3,460	66	321	987	869	0.3	B	836	0	(836)	(727)	1,270	0
						1.0	T	800	1	802	763	1,269	618
						1.8	B	778	2	765	705	1,255	1,252
						2.6	T	725	3	719	663	1,097	1,856
						3.4	B	685	4	673	613	1,250	2,440
						4.2	T	663	5	672	612	1,288	3,038
						5.0	B	673	6	(680)	(620)	1,051	3,640
						5.7	T	676	(0-6)			(1,249)	
10:25	3,460	66	420	986	868	0.3	B	1,080	0	(995)	(912)	1,629	0
						1.0	T	895	1	951	848	1,608	956
						1.8	B	905	2	876	775	1,579	1,853
						2.6	T	896	3	840	755	1,565	2,780
						3.4	B	852	4	880	735	1,555	3,640
						4.2	T	827	5	825	740	1,557	4,560
						5.0	B	888	6	(848)	(763)	1,566	5,470
						5.7	T	857	(0-6)			(1,576)	
10:32	6,380	66	500	987	865	0.3	B	1,132	0	(1,100)	(998)	2,085	
						1.0	T	977	1	1,087	984	2,044	1,193
						1.8	B	998	2	975	870	2,026	2,366
						2.6	T	950	3	963	838	1,999	3,530
						3.4	B	960	4	956	889	1,996	4,680
						4.2	T	958	5	968	863	2,002	5,840
						5.0	B	996	6	(978)	(873)	2,017	7,080
						5.7	T	965	(0-6)			(2,018)	
11:08	1,811	65	302	987	873	0.3	B	471	0	(425)	(385)	496	0
						1.0	T	598	1	548	562	582	296
						1.8	B	670	2	675	644	555	599
						2.6	T	640	3	594	563	588	905
						3.4	B	577	4	515	484	511	1,208
						4.2	T	504	5	480	449	505	1,497
						5.0	B	481	6	(468)	(457)	505	1,736
						5.7	T	471	(0-6)			(515)	

a) T.C.'s spotwelded to outside wall at indicated inches from inlet end bus bar.
b) Location of T.C. junction on horizontal tube. B = Bottom, T = Top.
c) Outside wall temperatures by smoothing experimental data. Inside temperatures by calculation.
d) Corrected for losses. Values in () are average over entire heated length.
e) Net heat to fluid up to indicated tube length.

6A677

Table 75. FSSTR: DATA SUMMARY SERIES 10018-140
HEAT TRANSFER TO DECALIN IN MINIATURE HEAT TRANSFER SECTION

Section No. 10018-113, 2.000" I.D. x .18" wall x 8.18" heated. Type 316 S.S.

Fluid: Decalin, $k = 75 \times 10^{-6}$ Btu/hr-in-°F, $\mu = .81 \times 10^{-6}$ lb/in-hr, $Pr = 12.3$

Run No. 10018-	Experimental Data								Reduced and Calculated Data				
	Measured Power, Btu/hr	Fluid Temp., °F		Press., psig		Tube Wall Thermocouples			Heated Length, Inches	Wall Temp.[1], °F		Heat[2] Flux, $\frac{Btu}{hr\,(in)^2} \times 10^{-6}$	Calculated[3] Heat, Btu/hr
						Location		Temp., °F					
		In	Out	In	Out	Inches[a]	Position[b]			Outside	Inside		
109-13 09	30	68	75	23	7	0.1	B		0				
						1.0	T						
						1.8	B						
						2.6	T						
						3.4	B						
						4.2	T						
						5.0	B						
						5.7	T		(24)				
13:57	99	68	96	21	5	0.1	B		0				
						1.0	T						
						1.8	B						
						2.6	T						
						3.4	B						
						4.2	T						
						5.0	B						
						5.7	T		(24)				
14 09	239	69	130	17	6	0.1	B		0				
						1.0	T						
						1.8	B						
						2.6	T						
						3.4	B						
						4.2	T						
						5.0	B						
						5.7	T		(24)				
14:15	409	68	180	16	6	0.1	B		0				
						1.0	T						
						1.8	B						
						2.6	T						
						3.4	B						
						4.2	T						
						5.0	B						
						5.7	T		(24)				
14:22	557	68	220	17	6	0.1	B		0				
						1.0	T						
						1.8	B						
						2.6	T						
						3.4	B						
						4.2	T						
						5.0	B						
						5.7	T		(24)				
14:31	720	68	259	17	6	0.1	B		0				
						1.0	T						
						1.8	B						
						2.6	T						
						3.4	B						
						4.2	T						
						5.0	B						
						5.7	T		(24)				
14:38	958	68	317	17	5	0.1	B		0				
						1.0	T						
						1.8	B						
						2.6	T						
						3.4	B						
						4.2	T						
						5.0	B						
						5.7	T		(24)				

a) T.C.'s spotwelded to outside wall at indicated inches from inlet end hub bar.
b) Location of T.C. junction on horizontal tube B = Bottom, T = Top.
c) Outside wall temperatures by smoothing experimental data. Inside temperatures by calculation.
d) Corrected for losses. Values in () are average over entire heated length.
e) Net heat to fluid up to indicated tube length.

Test Runs With SHELLDYNE-H

Prior to starting tests using SHELLDYNE-H the system volume was reduced by installing 1/4" S.S. tubing lines directly from the feed pump to the mini-FSSTR test stand and returning from the product condenser back to a new surge vessel (a 2-ft length of 3" industrial glass pipe, which was mounted directly above the pump suction. An 18" length of 1-1/2" glass pipe, calibrated at 100 ml intervals, was also included in the revised return system, with appropriate valving to divert the product flow, to allow spot checks on the feed rate. At the end of a rate check the product accumulated in this chamber can be drained back into the surge vessel without loss or air contact. With these modifications a charge of ca 1 gal of feed in sufficient to operate the system in a recycle mode.

A single one gallon charge of SHELLDYNE-H, N_2 sparged as usual was used for all tests on this fuel. Reactor 10018-110 was used for the first three test series (10018-145,145A, and 146), for which tests data tabulations are given in Tables T6, T7 and T8. Following these tests new 4" and 6" long heat exchange sections were constructed using 0.0344" ID x 0.0144" wass Hastelloy C tubing. One of these sections (4" long Reactor 10018-148) was used for the remaining two SHELLDYNE H test series. Also at this time a preheat section was incorporated into the system to permit operation at a feed temperature of ca 250°F. This increase in feed temperature reduced the fuel viscosity and this, along with the 2" shorter tube length, permitted operation at higher flow rates and a mixmum heat flux of 4×10^6 Btu/(hr·ft^2) was reached. Tables T9 and 80 present the data tabulations for Series 10018-156 and 153.

Test Runs With F-71

Four tests series were conducted using F-71 with a maximum heat flux of 8×10^6 Btu/(hr·ft^2) being reached. During these tests the inside tube wall temperature was allowed to reach ca 1200°F and was maintained there for about 40 minutes with no apparent effect on heat transfer.

Tables 81 through 84 present data summaries for the F-71 heat transfer tests.

Catalyst Lined Reactor, MCH Dehydrogenation

Two test series using reactor tubes lined with a coating of Pt/alumina catalyst rather than being packed with catulyst particles have been completed. For these tests the FSSTR was adapted as necessary to accommodate the 1/8" OD x 23" long reactor sections which were mounted immediately following the 10 ft lone Sections I and II which served as preheaters for this study. A sketch of the lined reactors is given in Figure 38.

Test Series 10018-164

The first lined reactor tested (Reactor 10018-162) was made using catalyst lined tube 10860-47 (refer to catalyst preparation section). The tube was mounted between end fittings equipped with sheathed thermocouples for fluid temperature measurement and had thermocouples spot welded on the outer wall at 10 locations. No provision was made for supplying power to the

Table 16. [illegible] DATA SUMMARY SERIES 10018-1-5 - HEAT TRANSFER TO "SHELLDYNE-H" IN MINIATURE HEAT TRANSFER TEST RIG

Reactor No. 10018-110; 0.0865-in. ID x 0.018-in. Wall x 6-in. Long; Type 316 Stainless Steel
Feed: SHELLDYNE-H, 33.9 lb/hr - 8.59 x 10^6 lb/hr-ft^2)

Run No. - Hr.	Measured Power, Watts	Wall Temp., °F		Fluid Temp., °F		Thermocouple Location		Temp., °F	Length, Inches	Wall Temp., °F		Heat Flux, $\frac{Btu}{(hr)(ft^2)} \times 10^6$	Calculated Power, Watts
		Bottom	Top	Bottom	Top	Inches[a]	Position[b]			Outside	Inside		
05-33-29	208	66	78	540	581	0.3	B	535	0	(.41)	(.47)	.4	3
		1.0	T	556		1		556	.66	560	3.7	3.0	
		1.8	B	558		2		558	1.38	560	3.5	3.0	
		2.6	T	560		3		560	2.08	565	3.3	3.0	
		3.4	B	562		4		562	2.80	566	3.4	3.0	
		4.2	T	564		5		564	3.52	568	3.2	3.0	
		5.0	B	566		6		566	4.24	570	3.7	3.0	
		5.7	T	567		(0.4)			(4.4)		(2)		
14 46	317	66	85	571	588	0.3	B	574	0	(.72)	(.78)	.5	3
		1.0	T	577		1		577	.66	580	4.6	4.0	
		1.8	B	579		2		579	1.38	582	4.5	4.0	
		2.6	T	582		3		582	2.08	586	4.3	4.0	
		3.4	B	584		4		584	2.80	588	4.4	4.0	
		4.2	T	586		5		586	3.52	590	4.2	4.0	
		5.0	B	588		6		588	4.24	(592)	(4.4)	4.0	
		5.7	T	587		(0.4)							
15 03	739	66	127	591	608	0.3	B	596	0	(.98)	(1.05)	.7	3
		1.0	T	599		1		599	.66	602	5.4	5.3	
		1.8	B	601		2		601	1.38	604	5.3	5.3	
		2.6	T	604		3		604	2.08	608	5.1	5.3	
		3.4	B	606		4		606	2.80	610	5.2	5.3	
		4.2	T	608		5		608	3.52	612	5.0	5.3	
		5.0	B	610		6		610	4.24	(614)	(5.2)	5.3	
		5.7	T	610		(0.4)							
15 20	1,054	67	148	591	619	0.3	B	605	0	(.90)	(1.11)	.9	3
		1.0	T	608		1		608	.66	611	6.1	6.0	
		1.8	B	610		2		610	1.38	613	6.0	6.0	
		2.6	T	613		3		613	2.08	617	5.8	6.0	
		3.4	B	615		4		615	2.80	619	5.9	6.0	
		4.2	T	617		5		617	3.52	621	5.7	6.0	
		5.0	B	619		6		619	4.24	(623)	(5.9)	6.0	
		5.7	T	618		(0.4)							
15 49	1,399	67	208	590	636	0.3	B	613	0	(.90)	(1.05)	.8	3
		1.0	T	626		1		626	.66	629	7.1	7.0	
		1.8	B	628		2		628	1.38	631	7.0	7.0	
		2.6	T	631		3		631	2.08	635	6.8	7.0	
		3.4	B	633		4		633	2.80	637	6.9	7.0	
		4.2	T	635		5		635	3.52	639	6.7	7.0	
		5.0	B	637		6		637	4.24	(641)	(6.9)	7.0	
		5.7	T	636		(0.4)							
16 [illegible]	2,425	67	254	590	656	0.3	B	623	0	(.96)	(1.13)	.9	3
		1.0	T	646		1		646	.66	649	8.1	8.0	
		1.8	B	648		2		648	1.38	651	8.0	8.0	
		2.6	T	651		3		651	2.08	655	7.8	8.0	
		3.4	B	653		4		653	2.80	657	7.9	8.0	
		4.2	T	655		5		655	3.52	659	7.7	8.0	
		5.0	B	657		6		657	4.24	(661)	(7.9)	8.0	
		5.7	T	656		(0.4)							
16 26	2,861	67	282	590	656	0.3	B	623	0	(.98)	(1.15)	.9	3
		1.0	T	646		1		646	.66	649	8.3	8.0	
		1.8	B	648		2		648	1.38	651	8.2	8.0	
		2.6	T	651		3		651	2.08	655	8.0	8.0	
		3.4	B	653		4		653	2.80	657	8.1	8.0	
		4.2	T	655		5		655	3.52	659	7.9	8.0	
		5.0	B	657		6		657	4.24	(661)	(8.1)	8.0	
		5.7	T	656		(0.4)							

a/ T.C.'s spotwelded to outside wall at indicated inches from inlet end bus bar
b/ Location of T.C. junction on horizontal tube. B = Bottom, T = Top.
c/ Outside wall temperatures by smoothing experimental data. Inside temperatures by calculation.
d/ Corrected for losses. Values in ( ) are average over entire heated length.
e/ Not heat to fluid up to indicated tube length.

Table 77. ESSTR: DATA SUMMARY SERIES 10018-145A - HEAT TRANSFER TO "SHELLDYNE-H" IN MINIATURE HEAT TRANSFER SECTION

Reactor No. 10018-110; 0.0265-in. ID x 0.015-in.
Wall x 6-in. Long; Type 316 Stainless Steel
Feed: SHELLDYNE-H, 53.0 lb/hr - 13.84 x 10⁶ lb/(hr·ft²)

Run No. 10018-	Experimental Data								Smoothed and Calculated Data				
	Measured Power, Btu/hr	Fluid Temp, °F		Pressure, psig		Tube Wall Thermocouples			Length, Inches	Wall Temp, °F [c)]		Heat[d)] Flux, Btu/(hr·ft²) x 10⁻³	Cumulative[e)] Heat, Btu/hr
		In	Out	In	Out	Location Inches[a)]	Location Position[b)]	Temp, °F		Outside	Inside		
145A-16:45	1,7X	67	750	885	413	0.[illegible]	B	485	0	(550)	(510)	460	0
						1.0	T	549	1	592	520	482	273
						1.8	B	589	2	602	633	510	543
						2.6	T	658	3	640	617	505	848
						3.4	B	633	4	723	694	515	1,152
						4.2	T	748	5	746	695	515	1,450
						5.0	B	725	6	(600)	(570)	491	1,743
						5.7	T	659	(0-6)			(503)	
16:54	3,570	67	744	886	598	0.3	B	699	0	(550)	(471)	845	0
						1.0	T	887	1	840	833	1,065	575
						1.8	B	950	2	845	840	1,064	1,170
						2.6	T	727	3	700	643	941	1,765
						3.4	B	722	4	775	713	1,011	2,344
						4.2	T	770	5	870	815	1,037	2,975
						5.0	B	870	6	(700)	(643)	941	3,345
						5.7	T	745	(0-6)			(1,016)	

a) T.C.'s spotwelded to outside wall at indicated inches from inlet end bus bar.
b) Location of T.C. junction on horizontal tube. B - Bottom, T - Top.
c) Outside wall temperatures by smoothing experimental data. Inside temperatures by calculation.
d) Corrected for losses. Values in () are average over entire heated length.
e) Net heat to fluid up to indicated tube length.

64677

Table 78. FOSTR: DATA SUMMARY SERIES 10018-186
HEAT TRANSFER TO "SHELLSYNF"-H IN MINIATURE HEAT TRANSFER SECTION

Heater No. 10018-110, 0.0845 in. ID x 0.248 in. Wall x 6 in. Long. Type 304 S.S.

Fuel - SHELLSYNF-H, 1 BTU lb/hr = 2.32 x 10^{4} lb/(hr-(°F))

Run No. 10018-	Experimental Data								Smoothed and Calculated Data				
	Measured Power, Btu/hr	Fluid Temp., °F		Pressure, psia		Tube Wall Thermocouples			Length, inches	Wall Temp.[c], °F		Heat[d] Flux, $\frac{Btu}{hr-(ft^2)} \times 10^{-6}$	Cumulative[e] Heat, Btu/hr
						Location		Temp., °F					
		In	Out	In	Out	Inches[a]	Position[b]			Outside	Inside		
146-13:36	65	69	78	859	713	0.3	B	118	0	129	93	12.2	0
						1.0	T	118	1	128	105	12.2	12.0
						1.8	B	118	2	126	117	11.9	23.7
						2.6	T	118	3	125	125	11.8	35.4
						3.4	B	118	4	124	131	11.8	47.1
						4.2	T	119	5	123	137	11.7	58.6
						5.0	B	128	6	122	142	11.7	81.5
						5.7	T	139	(0.4)			(11.9)	
16:09	134	69	98	870	773	0.3	B	135	0	140	110	25.8	0
						1.0	T	138	1	138	122	25.7	25.7
						1.8	B	140	2	136	134	25.5	51.4
						2.6	T	142	3	134	146	25.4	76.8
						3.4	B	144	4	132	158	25.3	102.1
						4.2	T	146	5	130	170	25.2	127.3
						5.0	B	151	6	128	182	25.1	152.4
						5.7	T	157	(0.4)			(21.52)	
16:25	137	69	131	868	739	0.3	B	154	0	158	128	26.0	0
						1.0	T	157	1	156	142	25.9	26.1
						1.8	B	160	2	154	156	25.8	52.0
						2.6	T	163	3	152	170	25.7	77.8
						3.4	B	166	4	150	184	25.6	103.5
						4.2	T	169	5	148	198	25.5	129.1
						5.0	B	175	6	146	212	25.4	154.6
						5.7	T	188	(0.4)			(24.38)	
16:44	713	70	333	872	847	0.3	B	358	0	363	313	152.1	0
						1.0	T	358	1	362	327	147.6	148.8
						1.8	B	358	2	360	341	143.7	292.5
						2.6	T	358	3	358	355	140.2	433.3
						3.4	B	358	4	356	369	137.0	570.3
						4.2	T	358	5	354	383	134.1	704.4
						5.0	B	358	6	352	397	131.4	835.8
						5.7	T	1,000	(0.4)			(134.2)	
15:01	888	70	358	870	813	0.3	B	513	0	518	388	188.0	0
						1.0	T	510	1	510	405	183.8	119.5
						1.8	B	510	2	504	420	179.9	239.0
						2.6	T	510	3	500	434	176.3	358.1
						3.4	B	510	4	496	448	173.0	477.1
						4.2	T	1,017	5	1,000	1,000	1,000	596.1
						5.0	B	1,000	6	1,000	1,000	1,000	715.2
						5.7	T	1,000	(0.4)			(217.6)	

a) T.C.'s approached to outside wall at indicated inches from inlet end hub.
b) Location of T.C. junction on horizontal tube. B = Bottom, T = Top.
c) Outside wall temperatures by smoothing experimental data. Inside temperatures by calculation.
d) Corrected for losses. Values in () are average over entire heated length.
e) Net heat to fluid up to indicated tube length.

Table 79. [illegible] - DATA SUMMARY SERIES 10018-142

Heat Transfer to SHELLDYNE-H in Miniature Heat Transfer Section

Reactor No. 10018-148; 0.0344" ID x 0.0144" Wall x 4" Long Hastelloy C
Fuel: SHELLDYNE-H, 121.6 lb/hr = 18.8 x 10^6 lb/(hr·ft²)

Run No. 10018-142-	Experimental Data								Smoothed and Calculated Data				
	Measured Power, Btu/hr	Fluid Temp, °F		Pressure, psig		Tube Wall Thermocouples			Length, inches	Wall Temp.[a] °F		Heat Flux,[b] Btu/(hr·ft²) x 10^{-6}	Cumulative Heat,[c] Btu
		In	Out	In	Out	Location (inches)[d]	Position[e]	Temp, °F		Outside	Inside		
1083	675	252	262	735	614	0	B	308	0	(308)	(308)		
						0.333	B	312	1	312	308	140	195
						1.333	B	312	2	312	308	140	330
						1.833	T	312	4	317	309	140	515
						2.333	B	312		(314)	(309)		620
						2.833	T	316	(0-4)			(140)	
						3.333	B	316					
						3.833	T	320					
1096	960	260	277	980	630	0	B	333	0	(347)	(341)		
						0.333	B	333	1	338	338	216	337
						0.833	T	333	2	347	341	216	678
						1.333	B	333	4	358	338	216	1,018
						1.833	T	333		(348)	(338)		
						2.333	B	333	(0-4)			(216)	
						2.833	T	333					
						3.333	B	333					
						3.833	T	333					
1118	1,610	353	389	885	640	0	B	555	0	(630)	(588)		
						0.333	B	555	1	655	618	331	550
						0.833	T	555	2	660	619	331	1,100
						1.333	B	555	4	675	625	331	1,650
						1.833	T	555		(673)	(622)		
						2.333	B	555	(0-4)			(331)	
						2.833	T	555					
						3.333	B	555					
						3.833	T	555					
1129	3,680	356	388	965	657	0	B	558	0	(571)	(699)		
						0.333	B	558	1	558	552	1,888	1,258
						0.833	T	558	2	558	550	1,888	3,388
						1.333	B	558	4	688	555	1,888	5,018
						1.833	T	558		(688)	(558)		
						2.333	B	558	(0-4)			(1,888)	
						2.833	T	558					
						3.333	B	558					
						3.833	T	558					
1147	5,130	361	378	950	655	0	B	588	0	(688)	(715)		
						0.333	B	588	1	588	738	2,888	1,918
						0.833	T	588	2	588	738	2,888	3,838
						1.333	B	588	4	688	738	2,888	6,958
						1.833	T	588		(688)	(742)		
						2.333	B	588	(0-4)			(2,888)	
						2.833	T	588					
						3.333	B	588					
						3.833	T	588					
1160	8,180	363	395	930	682	0	B	1,038	0	(1,088)	(982)		
						0.333	B	1,138	1	1,188	988	2,888	2,888
						0.833	T	1,138	2	1,288	988	2,888	5,778
						1.333	B	1,088	4	1,888	982	2,888	11,558
						1.833	T	1,088		(1,888)	(982)		
						2.333	B	1,088	(0-4)			(2,888)	
						2.833	T	1,088					
						3.333	B	1,088					
						3.833	T	1,088					
1300	12,250	368	438	960	695	0	B	1,388	0	(1,788)	(1,886)		
						0.333	B	1,388	1	1,888	1,113	4,888	3,888
						0.833	T	1,388	2	1,888	1,888	4,888	7,888
						1.333	B	1,388	4	1,888	1,888	4,888	19,558
						1.833	T	1,388		(1,888)	(1,888)		
						2.333	B	1,388	(0-4)			(4,888)	
						2.833	T	1,388					
						3.333	B	1,388					
						3.833	T	1,388					

a) T.C.'s spotwelded to outside wall at indicated inches from inlet end hub rer.
b) Location of T.C. junction on horizontal tube. B = Bottom, T = Top.
c) Outside wall temperatures by smoothing experimental data. Inside temperatures by calculation.
d) Corrected for losses. Values in () are average over entire heated length.
e) Net heat to fluid up to indicated tube length.

Table 80. FSSTR - DATA SUMMARY SERIES 10018-153

Heat Transfer to SHELLDYNE-H in Miniature Heat Transfer Section

Reactor No. 10018-148; 0.0344" ID x 0.0144" Wall x 4" Long Hastelloy C
Feed: SHELLDYNE-H, 56.3 lb/hr = 8.72×10^6 lb/(hr·ft²)

Run No. 10018-153	Experimental Data								Derived and Calculated Data				
	Measured Power, Btu/hr	Fluid Temp, °F		Pressure, psig		Tube Wall Thermocouple			Length, inches	Wall Temp, a) °F		Heat Flux, d) Btu/(hr·ft²) × 10^{-6}	Cumulative Heat, e) Btu/hr
						Location		Temp, °F					
		In	Out	In	Out	Inches b)	Position c)			Outside	Inside		
1430	405	350	365	980	985	0.25	B	365	0	(333)	(321)		0
						0.75	T	369	1	370	359	159	105
						1.25	B	372	2	374	369	159	210
						1.75	T	375	3	379	368	159	315
						2.25	B	375	4	(385)	(372)		417
						2.75	T	378	(0-4)			(159)	
						3.25	B	379					
						3.75	T	382					
1432	980	350	385	980	990	0.25	B	457	0	(429)	(408)		0
						0.75	T	512	1	525	508	388	260
						1.25	B	530	2	530	509	388	680
						1.75	T	535	3	529	506	388	775
						2.25	B	530	4	(536)	(511)		980
						2.75	T	540	(0-4)			(388)	
						3.25	B	540					
						3.75	T	550					
1435	1,720	351	387	970	980	0.25	B	586	0	(550)	(509)		0
						0.75	T	680	1	700	686	958	600
						1.25	B	725	2	730	686	958	979
						1.75	T	737	3	711	674	958	1,350
						2.25	B	727	4	(705)	(668)		1,680
						2.75	T	715	(0-4)			(958)	
						3.25	B	703					
						3.75	T	705					
1440	3,160	350	387	970	987	0.25	B	895	0	(795)	(678)		0
						0.75	T	1,052	1	1,075	1,017	1,480	770
						1.25	B	1,089	2	1,070	1,024	1,450	1,550
						1.75	T	1,088	3	979	950	1,040	2,350
						2.25	B	1,050	4	(970)	(911)		3,120
						2.75	T	1,000	(0-4)			(1,040)	
						3.25	B	958					
						3.75	T	979					

a) T.C.'s cemented to outside wall at indicated inches from inlet end tube bar.
b) Location of T.C. junction on horizontal tube. B = bottom, T = Top.
c) Outside wall temperatures by connecting experimental data inside temperatures by calculation.
d) Corrected for losses. Values in () are average over entire heated length.
e) Heat input to fluid up to indicated tube length.

Table 81. PSSTR - DATA SUMMARY SERIES 10018-154

Heat Transfer to F-71 in Miniature Heat Transfer Section

Reactor No. 10018-148; 0.0344" ID x 0.0144" Wall x 4" Long Hastelloy C
Feed: F-71, 84.8 lb/hr = 13.1 x 10^6 lb/(hr·ft²)

Run No. 10018-154-	Experimental Data								Measured and Calculated Data				
	Measured Power, Btu/hr	Fluid Temp., °F		Pressure, psig		Tube Wall Thermocouples			Length, inches	Wall Temp.,a) °F		Heat Flux,d) Btu/(hr·ft²)×10⁻⁶	Cumulative Heat,e) Btu/hr
						Location		Temp., °F					
		In	Out	In	Out	(In.-from)b)	Pos'tion b)			Outside	Inside		
151	645	68	88	998	997	0.35	B	130	0	(128)	(116)		0
						0.35	T	143	1	135	121	160	160
						1.35	B	136	2	138	126	142	313
						1.35	T	156	3	141	127	140	519
						2.35	B	179	4	(145)	(129)		686
						2.35	T	160	(0-4)			(142)	
						3.35	B	161					
						3.35	T	163					
1005	954	68	90	991	989	0.35	B	200	0	(198)	(168)		0
						0.35	T	214	1	214	185	313	735
						1.35	B	215	2	219	198	315	978
						1.35	T	216	3	223	198	313	1,291
						2.35	B	221	4	(228)	(199)		1,604
						2.35	T	221	(0-4)			(313)	
						3.35	B	224					
						3.35	T	228					
1051	1,980	69	107	991	989	0.35	B	253	0	(272)	(246)		0
						0.35	T	304	1	307	262	518	788
						1.35	B	309	2	311	266	518	1,788
						1.35	T	306	3	314	269	518	2,170
						2.35	B	312	4	(317)	(273)		2,688
						2.35	T	312	(0-4)			(518)	
						3.35	B	315					
						3.35	T	317					
1109	3,130	69	145	991	988	0.35	B	461	0	(458)	(355)		0
						0.35	T	516	1	513	434	1,060	1,060
						1.35	B	512	2	508	439	1,060	2,120
						1.35	T	508	3	498	420	1,060	3,180
						2.35	B	502	4	502)	(429)		3,708
						2.35	T	500	(0-4)			(1,060)	
						3.35	B	498					
						3.35	T	498					
1150	4,110	70	210	990	713	0.35	B	728	0	(745)	(633)		0
						0.35	T	824	1	824	667	2,050	2,050
						1.35	B	823	2	780	668	2,050	4,100
						1.35	T	795	3	750	650	2,050	6,150
						2.35	B	788	4	(779)	(649)		8,200
						2.35	T	780	(0-4)			(2,050)	
						3.35	B	778					
						3.35	T	779					
1170	8,990	71	270	990	715	0.35	B	1,014	0	(1,005)	(840)		0
						0.35	T	1,025	1	1,010	893	2,980	2,980
						1.35	B	1,008	2	988	827	2,980	5,960
						1.35	T	993	3	973	808	2,980	8,940
						2.35	B	988	4	(981)	(811)		11,920
						2.35	T	977	(0-4)			(2,980)	
						3.35	B	978					
						3.35	T	980					
1205	11,750	71	320	990	720	0.35	B	1,160	0	(1,168)	(956)		0
						0.35	T	1,149	1	1,139	949	3,970	3,970
						1.35	B	1,127	2	1,111	999	3,960	7,930
						1.35	T	1,110	3	1,113	904	3,960	11,890
						2.35	B	1,124	4	(1,127)	(987)		15,850
						2.35	T	1,112	(0-4)			(3,960)	
						3.35	B	1,112					
						3.35	T	1,123					
1300	15,060	72	382	988	708	0.35	B	1,230	0	(1,252)	(995)		0
						0.35	T	1,239	1	1,238	979	4,980	4,980
						1.35	B	1,234	2	1,238	970	4,980	9,960
						1.35	T	1,230	3	1,239	972	4,980	14,940
						2.35	B	1,239	4	(1,253)	(996)		19,920
						2.35	T	1,248	(0-4)			(4,980)	
						3.35	B	1,257					
						3.35	T	1,248					

a) T.C.'s embedded in outside wall at indicated inches from inlet end tee bar.
b) Location of T.C. junction on horizontal tube. B = Bottom, T = Top.
c) Outside wall temperatures by matching experimental data. Inside temperatures by calculation.
d) Corrected for losses. Values in () are average over entire heated length.
e) Net heat to fluid up to indicated tube length.

Table 82. PSSTR - DATA SUMMARY SERIES 10018-155

Heat Transfer to F-Ti in Miniature Heat Transfer Section

Reactor No. 10018-148: 0.0344" ID x 0.0144" Wall x 4" Long Hastelloy C
Feed: F-Ti, 109.5 lb/hr = 17.0 x 10^6 lb/(hr·ft²)

Run No. 10018-155-	Experimental Data								Standard and Calculated Data				
	Measured Power, Btu/hr	Fluid Temp, °F		Pressure, psig		Tube Wall Thermocouples			Length, inches	Wall Temp,[c] °F		Heat Flux,[d] Btu/(hr·ft²) x 10^{-6}	Cumulative Heat,[e] Btu/hr
		In	Out	In	Out	Location		Temp, °F		Outside	Inside		
						Inches[a]	Position[b]						
1413	500	71	90	680	561	0 0.333 1.333 1.333 2 2.333 3 3.33	T T T T T T T T	1[illegible] 1[illegible] 1[illegible] 1[illegible] 2[illegible] 2[illegible] 3[illegible] 3[illegible]	0 1 2 3 4 (0-4)	(1[illegible]) 1[illegible] 1[illegible] 1[illegible] (2[illegible]) [illegible]	(1[illegible]) 1[illegible] 1[illegible] 1[illegible] (2[illegible]) [illegible]	[illegible] [illegible] (3[illegible])	[illegible] [illegible]
1408	1,650	71	105	680	556	0 0.333 1.333 1.333 2 2.333 3 3.33	T T T T T T T T	2[illegible] 2[illegible] 2[illegible] 2[illegible] 3[illegible] 3[illegible] 3[illegible] 3[illegible]	0 1 2 3 4 (0-4)	(2[illegible]) 2[illegible] 2[illegible] (2[illegible]) [illegible]	(2[illegible]) 2[illegible] 2[illegible] (2[illegible]) [illegible]	[illegible] [illegible] (3[illegible])	1,[illegible] 1,[illegible]
1445	3,180	70	130	680	558	0 0.333 1.333 1.333 2 2.333 3 3.33	T T T T T T T T	3[illegible] 3[illegible] 3[illegible] 3[illegible] 4[illegible] 4[illegible] 4[illegible] 4[illegible]	0 1 2 3 4 (0-4)	(3[illegible]) 3[illegible] 3[illegible] 3[illegible] (3[illegible]) [illegible]	(3[illegible]) 3[illegible] 3[illegible] 3[illegible] (3[illegible]) [illegible]	1,[illegible] 1,[illegible] (1,[illegible])	[illegible] 1,[illegible] 2,[illegible] 3,[illegible]
1508	6,350	71	157	680	556	0 0.333 1.333 1.333 2 2.333 3 3.33	T T T T T T T T	4[illegible] 4[illegible] 4[illegible] 4[illegible] 5[illegible] 5[illegible] 5[illegible] 5[illegible]	0 1 2 3 4 (0-4)	(4[illegible]) 4[illegible] 4[illegible] 4[illegible] (4[illegible]) [illegible]	(5[illegible]) 5[illegible] 5[illegible] 5[illegible] (5[illegible]) [illegible]	2,[illegible] 2,[illegible] 2,[illegible] (2,[illegible])	1,[illegible] 3,[illegible] 4,[illegible] 6,[illegible]
1536	12,000	72	279	680	558	0.33 0.333 1.333 1.333 2.333 2.333 3.33 3.33	T B T B T B T B	1,[illegible] 1,[illegible] 1,[illegible] 1,[illegible] 1,[illegible] 1,[illegible] 1,[illegible] 1,[illegible]	0 1 2 3 4 (0-4)	(1,[illegible]) 1,[illegible] 1,[illegible] 1,[illegible] (1,[illegible]) [illegible]	(1,[illegible]) 1,[illegible] 1,[illegible] 1,[illegible] (1,[illegible]) [illegible]	3,[illegible] 3,[illegible] 3,[illegible] (3,[illegible])	2,[illegible] 5,[illegible] 8,[illegible] 11,[illegible]
1566	18,000	72	365	680	558	0.33 0.333 1.333 1.333 2.333 2.333 3.33 3.33	T B T B T B T B	1,[illegible] 1,[illegible] 1,[illegible] 1,[illegible] 1,[illegible] 1,[illegible] 1,[illegible] 1,[illegible]	0 1 2 3 4 (0-4)	(1,[illegible]) 1,[illegible] 1,[illegible] 1,[illegible] (1,[illegible]) [illegible]	(1,[illegible]) 1,[illegible] 1,[illegible] 1,[illegible] (1,[illegible]) [illegible]	5,[illegible] 5,[illegible] 5,[illegible] (5,[illegible])	[illegible] 8,[illegible] 13,[illegible] 17,[illegible]
1612	24,100	74	433	680	557	0.33 0.333 1.33 1.333 2.333 2.333 3.33 3.33	T B T B T B T B	1,[illegible] 1,[illegible] 1,[illegible] 1,[illegible] 1,[illegible] 1,[illegible] 1,[illegible] 1,[illegible]	0 1 2 3 4 (0-4)	(1,[illegible]) 1,[illegible] 1,[illegible] 1,[illegible] (1,[illegible]) [illegible]	(1,[illegible]) 1,[illegible] 1,[illegible] 1,[illegible] (1,[illegible]) [illegible]	8,[illegible] 8,[illegible] 8,[illegible] (8,[illegible])	[illegible] 12,[illegible] 18,[illegible] 24,[illegible]

a) T.C.'s spotwelded to outside wall at indicated inches from inlet end tee bar.
b) Location of T.C. junction on horizontal tube. B = Bottom, T = Top.
c) Outside wall temperatures by smoothing experimental data. Inside temperatures by calculation.
d) Corrected for losses. Values in () are average over entire heated length.
e) BTU heat to fluid up to indicated tube length.

Table 83. PSSTR - DATA SUMMARY SERIES 10018-156

Heat Transfer to F-71 in Miniature Heat Transfer Section

Reactor No. 10018-148: 0.0344" ID x 0.0144" Wall x 4" Long Hastelloy C
Feed: F-71, 20.1 lb/hr = 3.12×10^6 lb/(hr·ft²)

Run No. 10018-156-	Experimental Data								Measured and Calculated Data				
	Measured Power, Btu/hr	Fluid Temp, °F		Pressure, psig		Tube Wall Thermocouples			Length, inches	Wall Temp, °F [c]		Heat Flux, [d] Btu/(hr·ft²) x 10^{-6}	Cumulative Heat, [e] Btu/hr
		In	Out	In	Out	Location [a]		Temp, °F		Outside	Inside		
						Inches	Position [b]						
999	307	64	90	988	888	0.25	B	256	0	(190)	(180)		0
						0.75	T	288	1	309	298	168	81
						1.25	B	308	2	326	315	197	162
						1.75	T	334	3	355	337	197	243
						2.25	B	358	4	(459)	(445)		325
						2.75	T	360	(0-4)			(197)	
						3.25	B	388					
						3.75	T	416					
996	690	64	118	988	884	0.25	B	344	0	(388)	(368)		0
						0.75	T	468	1	488	478	317	184
						1.25	B	505	2	578	555	256	388
						1.75	T	568	3	630	636	215	488
						2.25	B	578	4	(729)	(715)		648
						2.75	T	630	(0-4)			(256)	
						3.25	B	660					
						3.75	T	725					
1018	990	64	149	988	884	0.25	B	491	0	(412)	(388)		0
						0.75	T	686	1	738	697	329	256
						1.25	B	766	2	852	893	317	479
						1.75	T	896	3	968	965	314	736
						2.25	B	896	4	(1,089)	(1,051)		953
						2.75	T	988	(0-4)			(317)	
						3.25	B	977					
						3.75	T	1,059					
1188	1,297	64	184	988	884	0.25	B	573	0	(588)	(572)		0
						0.75	T	886	1	862	820	388	388
						1.25	B	998	2	988	987	388	776
						1.75	T	978	3	1,115	1,095	377	888
						2.25	B	988	4	(1,256)	(1,218)		1,360
						2.75	T	1,115	(0-4)			(388)	
						3.25	B	1,158					
						3.75	T	1,207					

a) T.C.'s spotwelded to outside wall at indicated inches from inlet end Run bar.
b) Location of T.C. junction on horizontal tube. B - Bottom, T - Top.
c) Outside wall temperatures by smoothing experimental data. Inside temperatures by calculation.
d) Corrected for losses. Values in () are average over entire heated length.
e) Net heat to fluid up to indicated tube length.

Table 8h. FSSTR - DATA SUMMARY SERIES 10018-158

Heat Transfer to F-71 in Miniature Heat Transfer Section

Reactor No. 10018-157; 0.0344" ID x 0.0144" Wall x 6" Long Hastelloy C
Feed: F-71, 53.6 lb/hr = 8.39 x 10^6 lb/(hr·ft²)

Data Point No.	Experimental Data: Measured Power, Btu/hr	Fluid Temp., °F: In	Fluid Temp., °F: Out	Pressure, psig: In	Pressure, psig: Out	Tube Wall Thermocouples: Location: Inches[1]	Location: Position[2]	Tube Wall Thermocouples: Temp., °F	Calculated and Simulated Data: Length, Inches	Wall Temp.[3], °F: Calculated	Wall Temp.[3], °F: Desired	Heat Flux,[4] Btu/(hr·ft²) x 10^{-6}	Calculated Heat, Btu/hr
1005	605	97	99	970	966	0.5	B	150	0	(160)	(150)		0
						1.0	T	170	1	168	167	361	165
						1.0	B	165	2	162	160	361	332
						2.6	T	160	3	159	156	361	328
						3.6	B	166	4	165	151	361	495
						4.2	T	165	5	167	155	361	329
						5.0	B	168	6	(172)	(158)		659
						5.7	T	170	(0-6)			(361)	
997	1,370	88	130	970	776	0.5	B	231	0	(207)	(198)		0
						1.0	T	270	1	275	266	388	285
						1.0	B	271	2	271	264	388	575
						2.6	T	280	3	280	262	388	680
						3.6	B	270	4	268	261	388	885
						4.2	T	285	5	288	261	388	1,130
						5.0	B	288	6	(278)	(265)		1,360
						5.7	T	270	(0-6)			(388)	
1008	2,340	88	155	977	965	0.5	B	331	0	(300)	(277)		0
						1.0	T	425	1	468	378	516	395
						1.0	B	415	2	416	368	516	790
						2.6	T	395	3	395	351	516	1,160
						3.6	B	395	4	388	361	516	1,580
						4.2	T	388	5	388	357	516	1,970
						5.0	B	385	6	(369)	(362)		2,370
						5.7	T	380	(0-6)			(516)	
1007	3,370	88	225	977	958	0.5	B	577	0	(535)	(539)		0
						1.0	T	685	1	695	657	1,000	825
						1.0	B	680	2	695	588	1,000	1,770
						2.6	T	688	3	695	588	1,000	2,500
						3.6	B	688	4	675	588	1,000	3,290
						4.2	T	687	5	688	588	1,000	4,000
						5.0	B	678	6	(671)	(657)		4,830
						5.7	T	668	(0-6)			(1,000)	
1005	5,850	70	375	977	958	0.5	B	1,117	0	(1,159)	(1,096)		0
						1.0	T	998	1	1,083	988	2,000	1,580
						1.0	B	987	2	990	863	2,000	3,090
						2.6	T	885	3	890	768	2,000	4,990
						3.6	B	895	4	895	773	2,000	6,000
						4.2	T	897	5	905	785	2,000	7,990
						5.0	B	905	6	(895)	(886)		9,130
						5.7	T	918	(0-6)			(2,000)	
1137	11,250	88	650	977	958	0.5	B	1,258	0	(1,298)	(1,178)		0
						1.0	T	1,052	1	1,085	952	2,650	1,880
						1.0	B	1,050	2	1,085	857	2,650	3,860
						2.6	T	985	3	972	851	2,650	5,660
						3.6	B	988	4	95	748	2,650	7,790
						4.2	T	1,002	5	1,060	388	2,650	9,130
						5.0	B	1,056	6	(1,189)	(978)		10,280
						5.7	T	1,070	(0-6)			(2,650)	

1) T.C.'s epotwelded to outside wall at indicated inches from inlet end hub bar.
2) Location of T.C. junction on horizontal tube. B = Bottom, T = Top.
3) Outside wall temperatures by smoothing experimental data. Inside temperatures by calculation.
4) Corrected for losses. Values in ( ) are average over entire heated length.
5) Net heat to fluid up to indicated tube length.

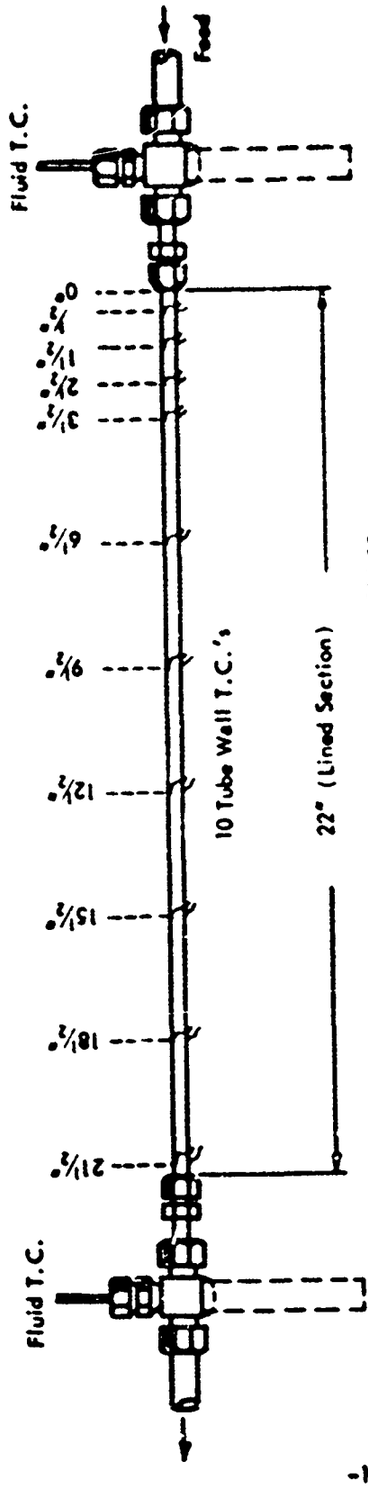

Tube: 1/8" OD x 0.018" Wall Type 304 SS
Lined to 1/8" ID with Catalyst

Thermocouples: Fluid - 1/16" OD Inconel Sheathed Chromel Alumel
Wall - 0.010" Chromel-Alumel, Wires Spotwelded to Tube Wall

Scale: None

Figure 38. FSSTR - CATALYST LINED REACTOR SECTIONS: REACTORS 10018-162 AND 162A

64987

reactor section for this test. Heat of reaction was supplied only by preheating the feed stream. Figure 39 shows total MCH conversion as well as conversion to Toluene and also shows preheater exit, feed and product temperature, through the course of the test. Table 8b lists the analyses of liquid product samples. (No samples were taken of product gas.) The course of the test may be followed by referring to Figure 39. Initial operation at a feed temperature of 950°F resulted in a total MCH conversion of ca 11% with 10% being converted to Toluene. Increasing the feed temperature to 1010°F increased total conversion to 25.5%. However, it is evident that this increased conversion was due to thermal reaction rather than dehydrogenation to Toluene. It appears that, at the long preheater residence time (LHSV = 30 for the 10-ft section), considerable thermal reaction was occurring before the feed reached the catalyst section. Finally, when a preheat temperature of 1085°F was reached, sufficient cracked products were formed to deactivate the catalyst and on returning to a feed temperature of 950°F total conversion had declined to 7.5% (6.5% to Toluene).

Test Series 10018-167

The second lined reactor section tested had the same general configuration as the first, 1/8" OD x 0.028" wall x 25" long overall (22" catalyst lined) Type 304 S.S. lined to ca 1/16" ID with 5% Pt on alumina catalyst. The catalyst support used for lining this tube was about twice as dense as that used for the first section however, which resulted in two times as much platinum being available. Bus bars were brazed to the end fittings making it possible to supply power during this test series. This reactor is designated 10018-162A and was made using catalyst lined tube 10860-8-1.)

For this test the feed rate was 19.7 lb MCH/hr (LHSV = 8590 based on metal tube inside dimensions), and fuel inlet temperature was maintained at ca 950°F. Reactor pressure was ca 860 psig.

Initial operation with no additional power gave a conversion to toluene of 11.5%. Applying power equivalent to 160 Btu/lb increased conversion to toluene to 25% and further power increase to 330 Btu/lb raised conversion to 35.5%. The catalyst started deactivating rapidly at this point and power had to be reduced as wall temperatures were increasing rapidly. On returning to the 330 and 0 Btu/lb power levels previously supplied, conversions were found to have decreased to 21.5 and 10.0% respectively. Selectivity for toluene was excellent, being better than 98% throughout the series.

Figure 40 shows the fluid inlet and outlet temperatures at five minute intervals and MCH conversion to toluene for consecutive ten minute sampling periods through the 200 minute test cycle. Table 8b lists the analyses of the liquid product samples. Outside tube wall temperature profiles are shown in Figure 41 for the five lined out periods. Note the higher temperatures found in the last two periods as compared to the first two (at the same power levels) resulting from partial catalyst deactivation. The 11:50 (330 Btu/lb power level) profile was recorded under transient conditions in that tube wall temperatures were rising as the catalyst deactivated. A maximum of 1300°F was reached at 1-1/2" length at 12:01 when the power was reduced.

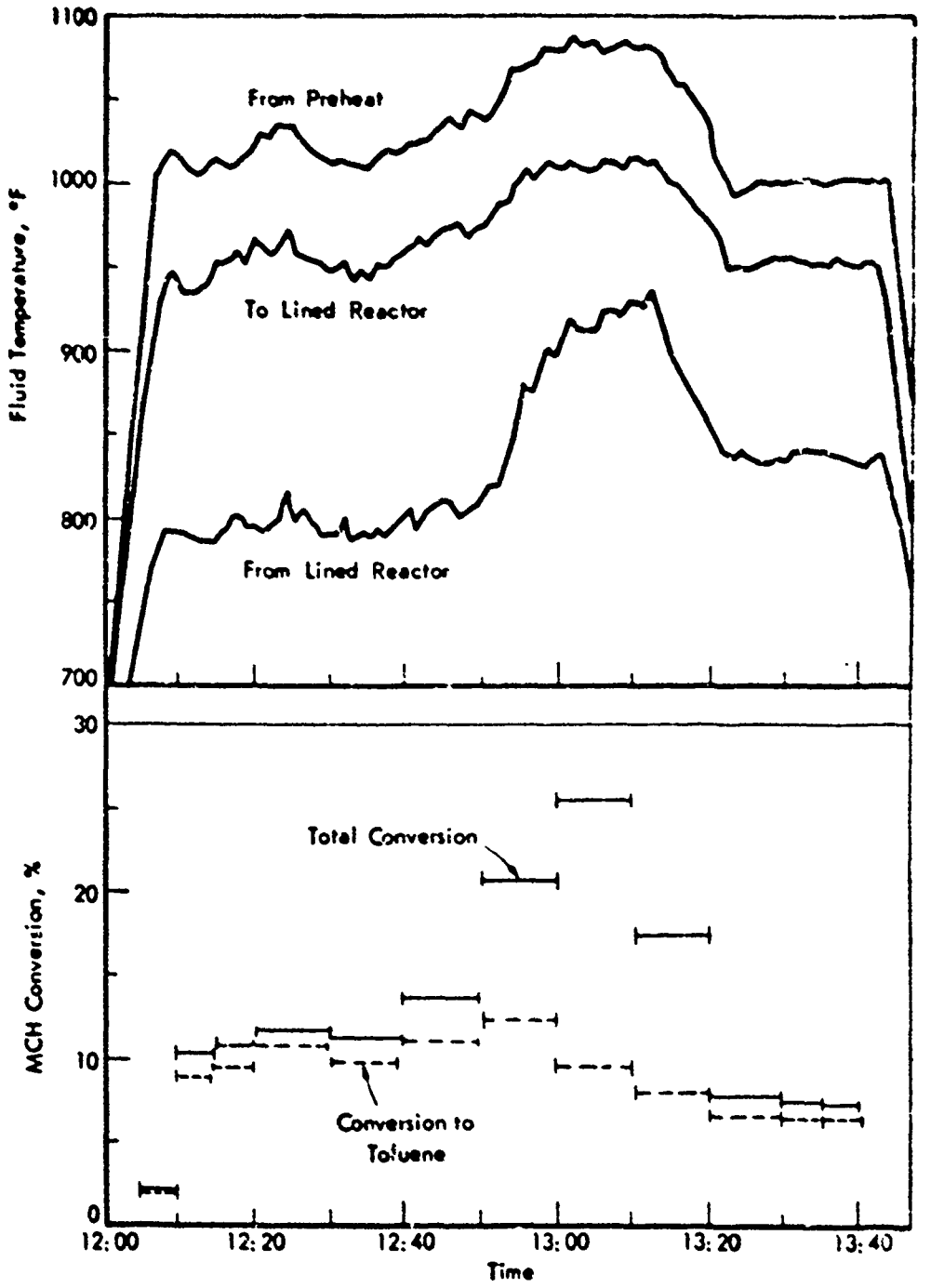

Figure 39. FSSTR: DEHYDROGENATION OF MCH IN LINED REACTOR
Fluid Temperatures and Conversions for Series 10018-164

Table 8[illegible]. FCSTR - DEHYDROGENATION OF MCH IN LINED REACTOR, EFFECT OF [illegible]

Lined Reactor: 10018-162, 1/8" OD x 22" Long
MCH Feed: 6.14 lb/hr
Pressure: 860 psig
Temperature: Refer to accompanying figure.

Sample Interval		Liquid Product Analysis, % w					
Start	End	Cracked[a]	Cyclohexane	MCH	Methyl-cyclohexenes	Benzene	Toluene
1205	1210	0.0	0.2	97.9	0.0	0.0	1.9
1210	1215	0.1	0.9	90.1	0.3	0.1	8.5
1215	1220	0.1	1.0	89.7	0.2	0.1	8.8
1220	1230	0.2	1.4	87.9	0.2	0.1	10.1
1230	1240	0.1	0.9	89.2	0.2	0.2	9.4
1240	1250	0.2	1.7	86.9	0.2	0.2	10.5
1290	1300	1.7	4.5	80.8	0.6	0.8	11.6
1300	1310	3.2	7.9	76.5	1.7	1.5	9.1
1310	1320	1.6	4.7	83.3	1.3	0.9	7.6
1320	1330	0.1	0.7	92.6	0.3	0.1	6.1
1330	1335	0.1	0.7	92.8	0.3	0.0	5.1
1335	1340	0.0	0.7	92.9	0.3	0.1	6.0
Feed			0.1	99.8			0.1

a) Material lighter than cyclohexane.

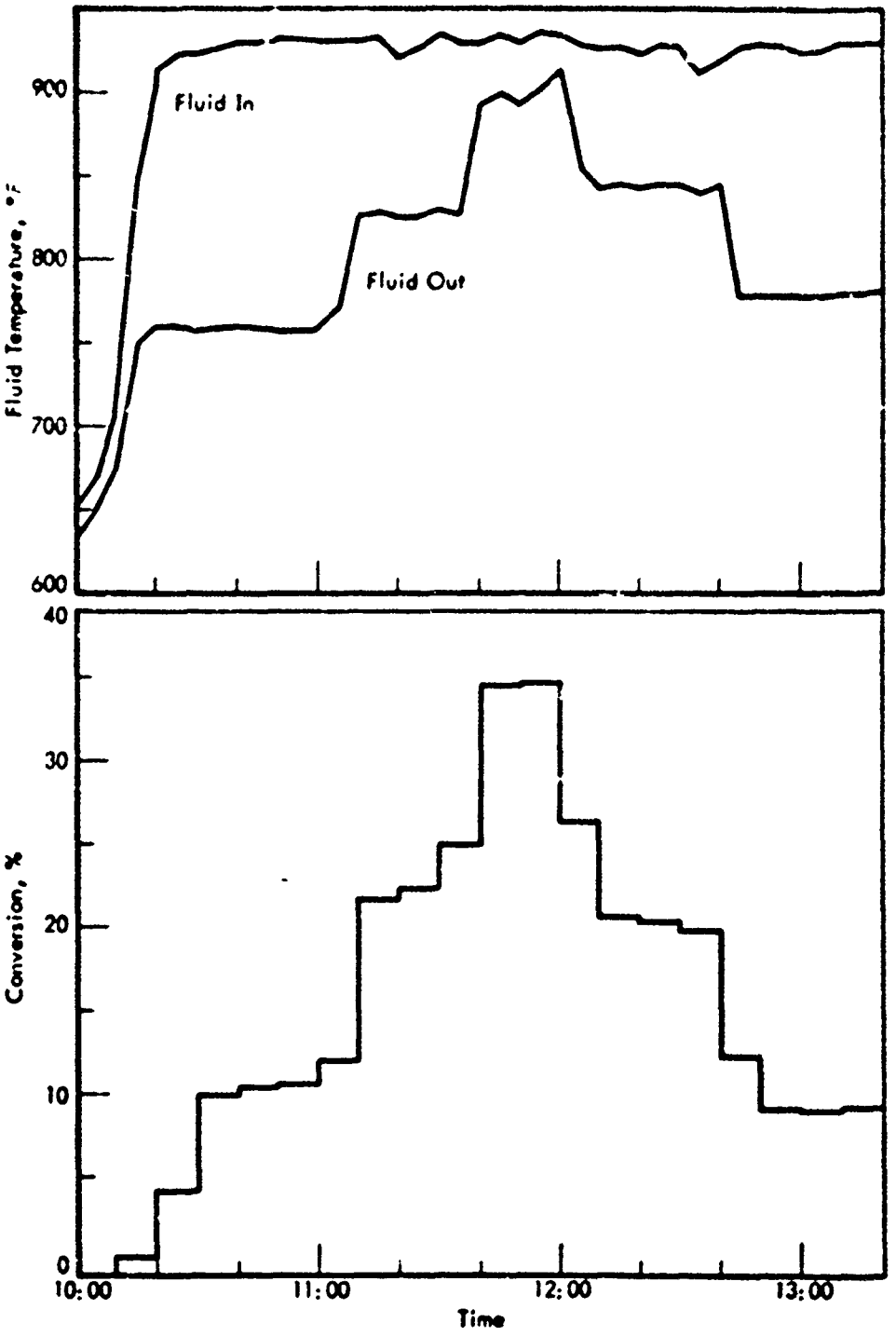

Figure 40. FSSTR: DEHYDROGENATION OF MCH IN LINED REACTOR:
Fluid Temperatures and Conversion for Series 10018-167

Table [illegible]: DEHYDROGENATION OF MCH IN LINED REACTOR
PRODUCT ANALYSES FOR SERIES 10018-107

Lined Reactor: 10018-162A, 1/8" OD x 22" Long
MCH Feed: 19.7 lb/hr
Pressure: 160 psig
Temperature: Refer to accompanying figure

Sample Interval		Liquid Product Analyses, %w				
Start	End	Cyclo-hexane	MCH	Methyl-Cyclo-hexenes	Benzene	Toluene
1010	1020	0.1	98.3	0.0		1.1
1020	1030	0.1	94.9	0.1		4.9
1030	1040	0.1	89.7	0.1		10.2
1040	1050	0.2	88.9	0.1		10.8
1050	1100	0.1	88.9	0.1		10.9
1100	1110	0.2	87.5	0.1		12.3
1110	1120	0.1	78.3	0.1		21.5
1120	1130	0.1	77.6	0.1		22.2
1130	1140	0.1	74.9	0.1	0.04	24.8
1140	1150	0.1	65.6	0.2	0.05	34.1
1150	1200	0.1	65.4	0.2	0.06	34.2
1200	1210	0.1	73.5	0.2		26.1
1210	1220	0.1	79.2	0.1		20.6
1220	1230	0.1	79.5	0.1		20.3
1230	1240	0.1	79.8	0.1		19.9
1240	1250	0.1	87.1	0.1		12.6
1250	1300	0.2	90.2	0.1		9.5
1300	1310	0.2	90.3	0.1		9.4
1310	1320	0.2	90.3	0.1		9.5
Feed		0.1	99.8			0.1

Table 19 summarizes the test conditions and results for the two test series using the catalyst lined reactors. No tests have been made using a packed reactor of these dimensions, however, some typical results obtained using a 0.277" ID x 2' long packed section are included in the table for comparison. Particularly, the high efficiency of the wall catalyst, in terms of conversion per unit of catalytic metal, and the negligible pressure drop compared to the bed catalyst should be noted. These results are very encouraging although it is obvious that a catalyst of greater stability must be developed. However, it was gratifying that neither catalyst showed any evidence of spalling as a result of the experiment. This work will continue.

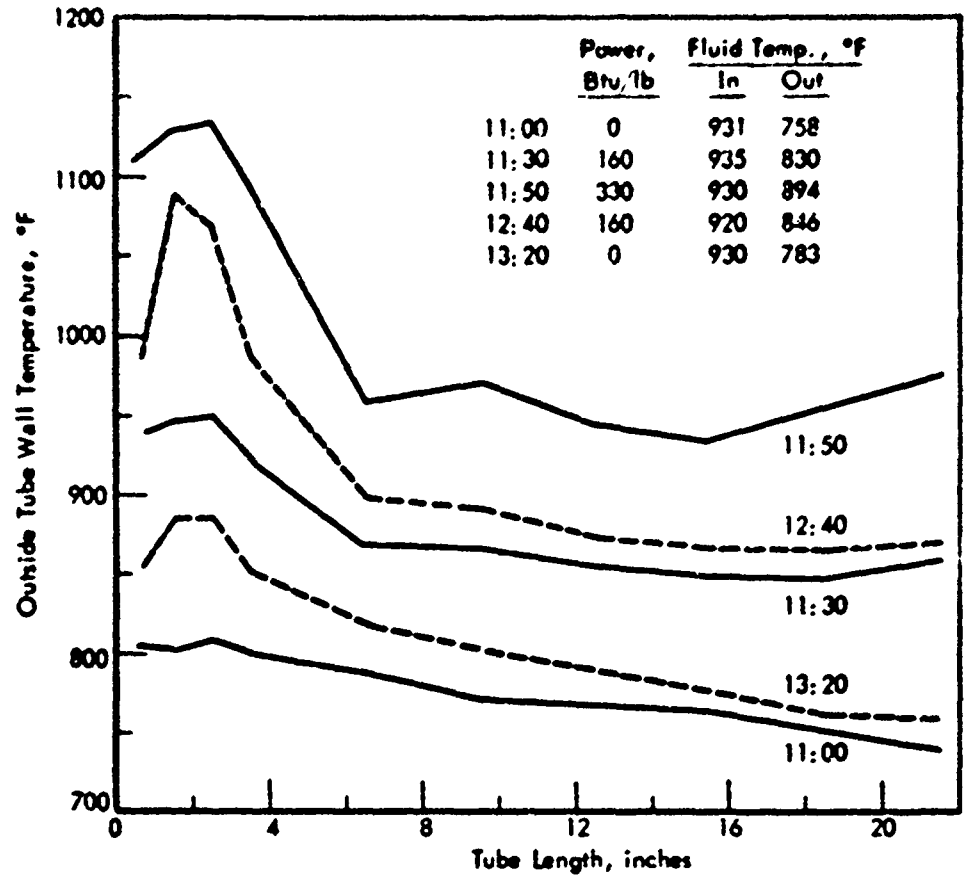

Figure 41. FSSTR: DEHYDROGENATION OF MCH IN LINED REACTOR:
Temperature Profiles for Series 10018-167

Table 87. FSSTR: DEHYDROGENATION OF MCH IN LINED REACTOR; COMPARISON WITH PACKED REACTOR SECTION

Lined Reactor - 10018-162
Tube: 1/8" OD x .028" wall x 23" long Type 304 S.S.
Lining: 1/16" ID x 22" long
0.074 g lining ca. 0.004" thick
ca. 5% Pt (0.0037 g)

Lined Reactor - 10018-162A
Tube: 1/8" OD x .028" wall x 23" long Type 304 S.S.
Lining: 1/16" ID x 22" long
0.141 g lining ca. 0.004" thick
ca. 5% Pt (0.0071 g Pt)

Packed Reactor
Tube 0.277" ID x 2 ft long Hastelloy C
12.9 g of UOP R-8 1/16" dia. spheres
ca. 0.8% Pt (0.103 g Pt)

Test Using Reactor 10018-	MCH Feed Rate			Fluid Temp °F		Press. psig		Conversion		lbs Toluene / (g Pt)(hr)	Power	
	lb/hr	LHSV[a]	lb[a] / hr ft²	In	Out	In	Out	Total %	To Toluene %		Btu / lb Fd.	Btu[a] / hr. ft²
162	6.14	2,680	236,000	950	800	860	860	12	9.5	158	0	0
	6.14	2,680	236,000	1010	915	860	860	13	11.5	191	0	0
162A	19.7	8,590	757,000	931	758	860	860	11.7	11.5	325	0	0
	19.7	8,590	757,000	935	830	860	860	23.2	23.0	638	160	95,000
	19.7	8,590	757,000	930	324	860	860	35.7	35.5	985	330	195,000
Packed Bed	64.5	1,600	154,000	898	698	885	700	-	15	94	0	0
	64.5	1,600	154,000	895	831	885	604	-	39	244	333	148,300
	25.1	625	60,000	902	899	892	865		14	34	0	0
	25.1	625	60,000	901	770	891	855	-	29	71	194	33,600

a) Based on inside dimensions of metal tube.

Table 87 summarizes the test conditions and results for the two test series using the catalyst lined reactors. No tests have been made using a packed reactor of these dimensions, however, some typical results obtained using a 0.277" ID x 2' long packed section are included in the table for comparison. Particularly, the high efficiency of the wall catalyst, in terms of conversion per unit of catalytic metal, and the negligible pressure drop compared to the bed catalyst should be noted. These results are very encouraging although it is obvious that a catalyst of greater stability must be developed. However, it was gratifying that neither catalyst showed any evidence of spalling as a result of the experiment.

Dehydrogenation of MCH Over Shell 113 Catalyst

One of the most promising of the laboratory prepared catalysts (based on bench-scale testing) has been run through a testing program in the FSSTR so that its activity may be compared with that of VOP-88. This catalyst consists of 4% Pt on type 1 spheres and is designated Catalyst 10280-113 (Shell 113).

Tests Using 3/8" x 2ft Reactor

Three series of tests were conducted using two charges of Shell 113 catalyst in the 3/8" OD x .049 wall x 2ft long reactor section. A sketch of the reactor is given in Figure 42. Each charge consisted of 19.8gm (ca 24ml) of catalyst and was activated in place for 1 hr in N_2 at ca 1050°F before starting the test run. All runs were made at nominal inlet conditions of 900°F and 900psig. Selectivity for dehydrogenation to Toluene was better than 99% for this entire group of tests.

The first test series (Series 10018-177) was made at a feed rate of 62.1 lb/hr (LHSV = 1550) at four power levels. Table 88 summarizes the run data and Figures 43 and 44 show fluid inlet and outlet temperatures and MCH conversion through the course of the test. The first run was made at zero heat input, then power was increased in steps until it became evident that the catalyst activity was declining. At the maximum heat input (810 Btu/lb) conversion started at 77% and declined to 73% over a 40 min. period. At the same time outlet fuel temperature was increasing from 970° to 1020°F. On returning to a power level of 290 Btu/lb conversion was found to be 36% at an outlet temperature of 817°F where as prior operation at this condition had resulted in 37% conversion at 791°F outlet temperature.

Before starting the next test the partially deactivated catalyst was H_2 treated at an 1050°F for 45 min.

The data summary table and temperature and conversion plots for Series 10018-181 which was made using the H_2 treated catalyst are given in Table 89 and Figures 45 and 46. Comparison of the conversion and outlet temperatures of this test with those at comparable power levels of Series 10018-177 shows that the H_2 treatment had essentially restored the original catalyst activity. Again, however, operation at the highest heat input resulted in declining catalyst activity.

Following this test the used catalyst was dumped and the reactor was recharged with fresh Shell 113 catalyst.

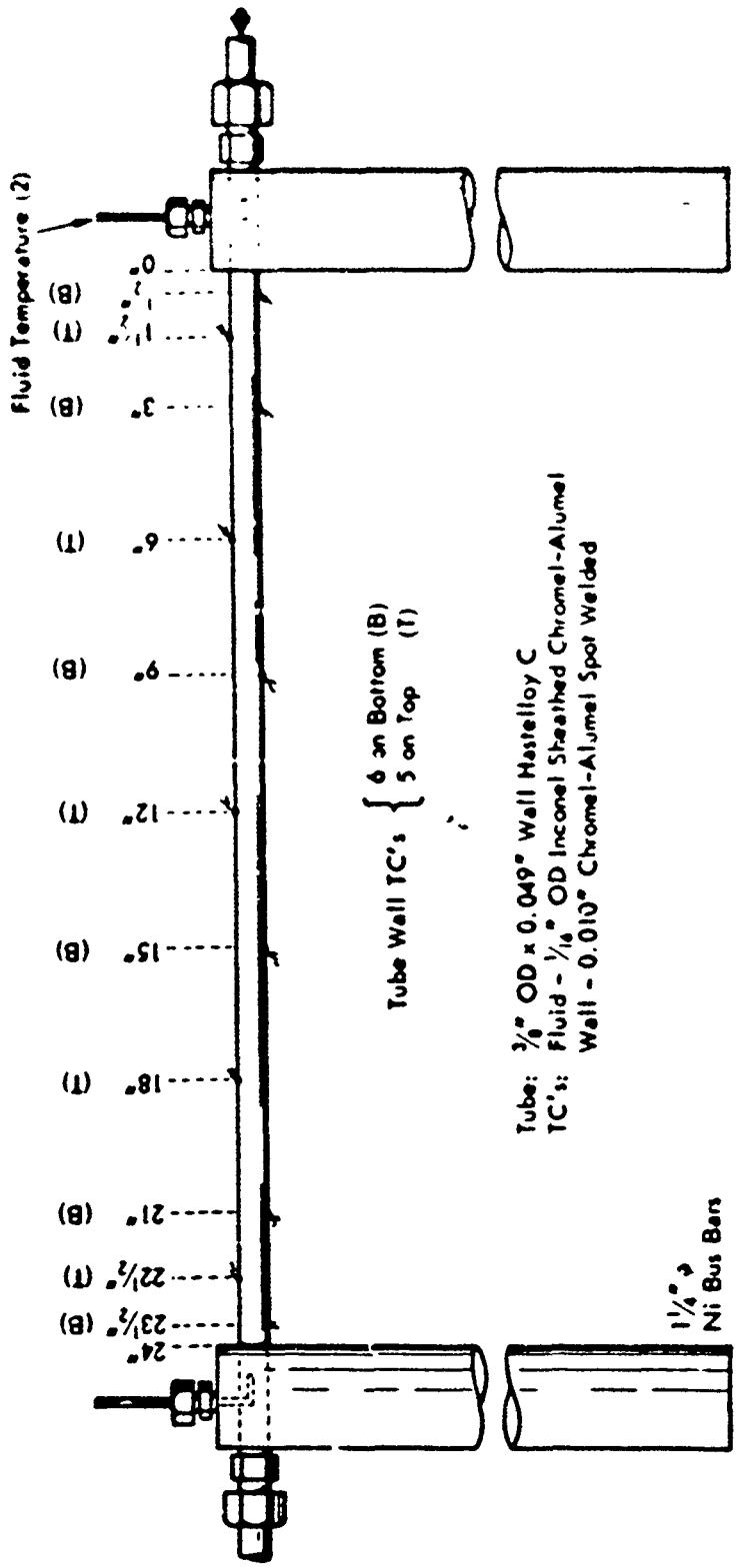

Figure 42. FSSTR - 0.277" ID x 2 FT-LONG REACTOR SECTION

[illegible]

[illegible]

[illegible]

[illegible]	[illegible]	[illegible]	[illegible]	[illegible]	[illegible]	[illegible]	[illegible]	[illegible]	[illegible]	[illegible]	[illegible]	[illegible]	[illegible]	[illegible]
[illegible]	[illegible]	[illegible]	[illegible]	[illegible]	[illegible]	[illegible]	[illegible]	[illegible]	[illegible]	[illegible]	[illegible]	[illegible]	[illegible]	[illegible]
[illegible]	[illegible]	[illegible]	[illegible]	[illegible]	[illegible]	[illegible]	[illegible]	[illegible]	[illegible]	[illegible]	[illegible]	[illegible]	[illegible]	[illegible]
1400	[illegible]	[illegible]	[illegible]	[illegible]	77	0.5	B	1076	0	(1075)	(1004)		[illegible]	0.0
						1.5	T	1062	2	1056	996	546.8	4192	67.5
						3	B	1062	6	1052	992	546.9	12580	202.5
						6	T	1071	10	1072	992	546.9	20966	337.5
						9	B	1055	14	1074	996	546.8	29340	472.5
						12	T	1049	18	1096	1017	546.8	37730	607.5
						15	B	1067	22	1116	1063	546.7	46110	742.5
						18	T	1100	24	(1115)	(1064)		50500	810.0
						21	B	1112	(0.26)			(546.8)		
						22.5	T	1112						
						23.5	B	1119						
[illegible]	900	1016	[illegible]	[illegible]	[illegible]	0.5	B	1070	0	(975)	(1006)		0	0.0
(continuation of Run 1400)						1.5	T	1056	2	1044	995	546.8	4192	67.5
						3	B	1077	6	1050	990	546.9	12590	202.5
						6	T	1049	10	1050	980	546.8	20960	337.5
						9	B	1050	14	1060	980	546.9	29350	472.5
						12	T	1045	18	1087	1018	546.8	37730	607.5
						15	B	1095	22	1139	1065	546.7	46110	742.5
						18	T	1095	24	(1165)	(1097)		50500	809.9
						21	B	1114	(0.26)			(546.8)		
						22.5	T	1140						
						23.5	B	1114						
[illegible]	900	817	797	449	56	0.5	B	946	0	(952)	(926)		0	0.0
						1.5	T	912	2	905	878	125.9	1542	26.5
						3	B	889	6	925	855	126.0	4567	78.5
						6	T	965	10	887	829	126.0	7614	122.6
						9	B	958	14	864	830	126.0	10660	171.7
						12	T	947	18	865	847	126.0	13710	220.7
						15	B	860	22	876	848	126.0	16750	269.8
						18	T	969	26	(902)	(855)		18280	294.5
						21	B	871	0.26)			(126.0)		
						22.5	T	879						
						23.5	B	950						

a) T.C.'s spotwelded to outside wall at indicated inches from inlet end bus bar.
b) Location of T.C. junction on horizontal tube. B= Bottom, T= Top.
c) Outside wall temperature, by smoothing experimental data. Inside temperatures by calculation.
d) Corrected for losses. Values in ( ) are average over entire heated length.
e) Net heat to fluid up to indicated tube length.

65868

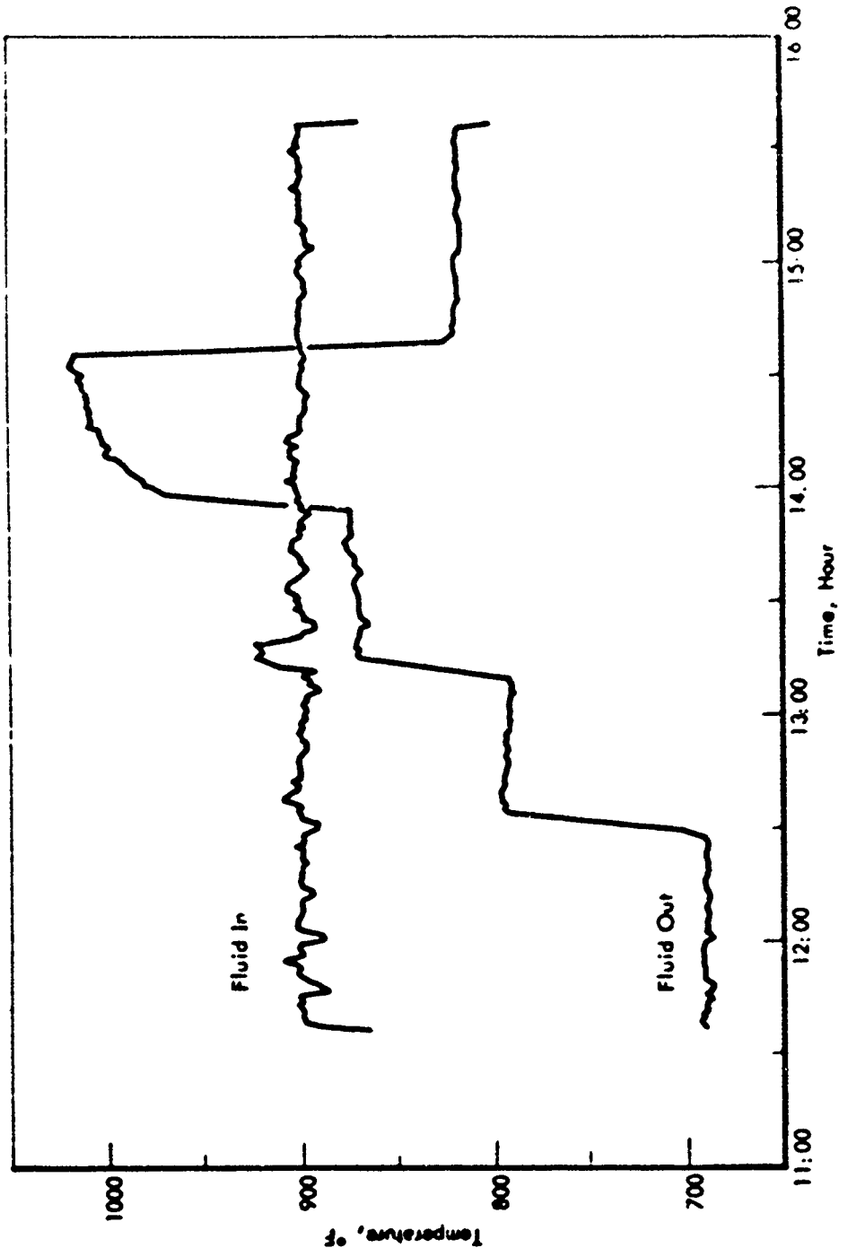

Figure 43. FSSTR: DEHYDROGENATION OF MCH OVER SHELL 113 CATALYST IN 2 FOOT REACTOR
Fluid Temperatures, Series 10018-177

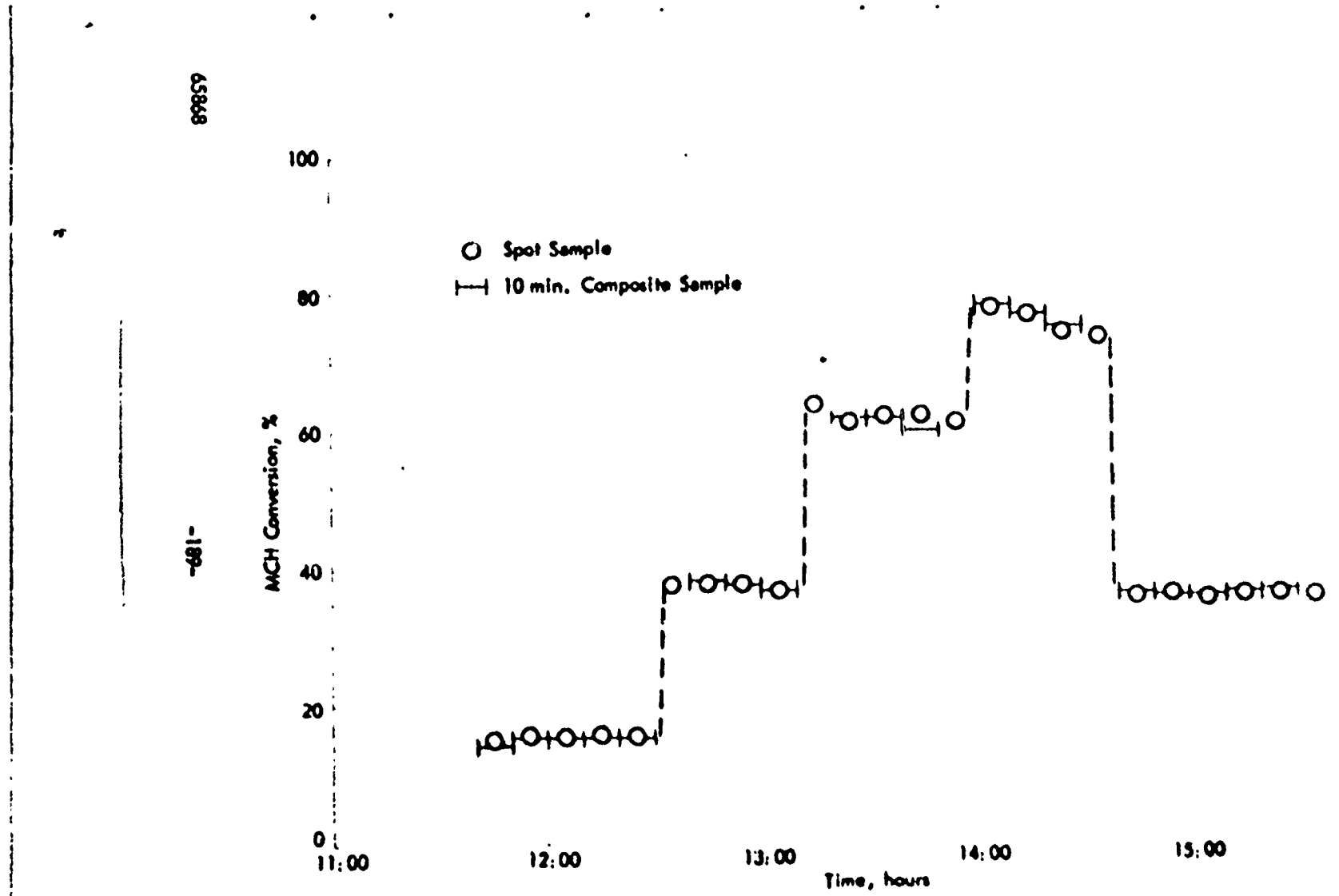

Figure 44. FSSTR: DEHYDROGENATION OF MCH OVER SHELL 113 CATALYST IN 2 FOOT REACTOR
MCH Conversion, Series 10018-177

Table 89. FSSTR: DEHYDROGENATION OF MCH OVER SHELL 115 IN 2-FT LONG HASTELLOY C

Data Summary Series 10018-181

Reactor No. 10018-49; 0.277" ID x 0.049" wall x 2-ft long Hastelloy C
Feed: 99.8% MCH; 62.1 lb/hr, 1550 LHSV, 148,400 lb/(hr·ft²)

Run No. 10018-181-	Experimental Data: Fluid Temp., °F In	Fluid Temp., °F Out	Pressure, psig In	Pressure, psig Out	MCH Conv. %	Tube Wall T.C.'s: Location Inches[a]	Location Position[b]	Temp., °F	Smoothed and Calculated Data: Tube Length, In.	Wall Temp., °F[c] Outside	Wall Temp., °F[c] Inside	Heat[d] rate, Btu/(hr·ft²) x 10⁻³	Cumulative heat[e] Btu/lb	Cumulative heat[e] kcal/kg
1215	900	786	894	656	38	0.5	B	952	0	(946)	(919)			
						1.5	T	911	2	951	874	124.0	17.1	24.1
(Partially deactivated catalyst from Series 177 H_2 treated in place at ca 1050°F for 45 min. prior to Series 181)						3	B	882	6	892	834	127.2	51.4	71.3
						6	T	851	10	846	818	127.2	85.7	118.6
						9	B	847	14	847	819	127.2	120.0	166.2
						12	T	845	18	850	822	127.2	154.3	213.7
						15	B	840	22	856	828	127.2	188.6	261.2
						18	T	853	24	(859)	(831)		205.7	284.9
						21	B	853	(0-24)			(127.1)		
						22.5	T	6.8						
						23.5	B	855						
1250	898	971	894	448	76	0.5	B	1078	0	(1081)	(1011)		0	0.0
						1.5	T	1063	2	1062	991	552.3	68.6	68.6
						3	B	1060	6	1044	872	552.3	205.7	205.7
						6	T	1044	10	1041	969	552.3	342.9	342.9
						9	B	1041	14	1047	975	552.3	480.0	480.0
						12	T	1042	18	1065	994	552.3	617.2	617.2
						15	B	1049	22	1105	1035	552.2	754.3	754.3
						18	T	1077	24	(1135)	(1064)		822.9	822.9
						21	B	1090	(0-24)			(552.2)		
						22.5	T	1110						
						23.5	B	1120						
1550	900	1050	891	455	71	0.5	B	1085	0	(1094)	(1024)		0	0.0
						1.5	T	1072	2	1070	999	552.3	68.6	68.6
(Continuation of Run 1250)						3	B	1069	6	1	980	552.3	205.7	205.7
						6	T	1050	10	1049	977	552.3	342.9	342.9
						9	B	1050	14	1058	987	552.3	480.0	480.0
						12	T	1051	18	1069	1019	552.3	617.1	617.1
						15	B	1063	22	1159	1091	552.3	754.2	754.2
						18	T	1103	24	(1210)	(1144)		822.7	822.7
						21	B	1158	(0-24)			(552.2)		
						22.5	T	1170						
						23.5	B	1188						

a) T.C.'s spotwelded to outside wall at indicated inches from inlet end bus bar.
b) Location of T.C. junction on horizontal tube. B= Bottom, T= Top.
c) Outside wall temperatures by smoothing experimental data. Inside temperatures by calculation.
d) Corrected for losses. Values in ( ) are average over entire heated length.
e) Net heat to fluid up to indicated tube length.

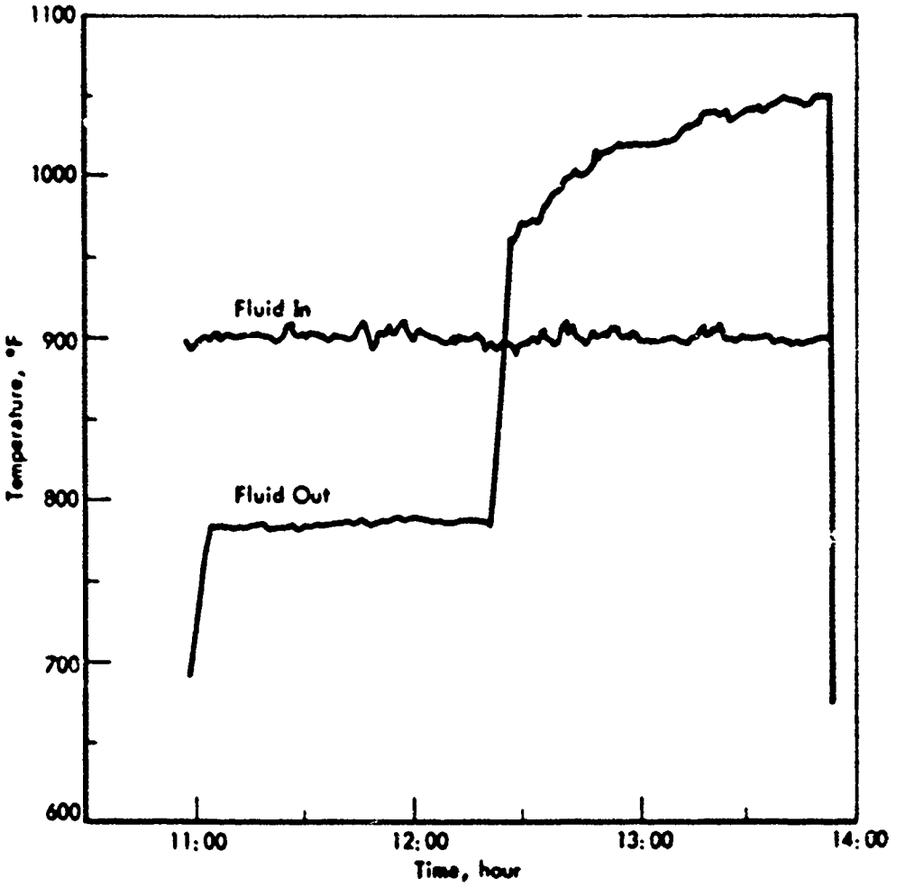

Figure 45. FSSTR: DEHYDROGENATION OF MCH OVER H_2 REGENERATED SHELL 113 CATALYST IN 2-FOOT REACTOR
Fluid Temperatures, Series 10018-181

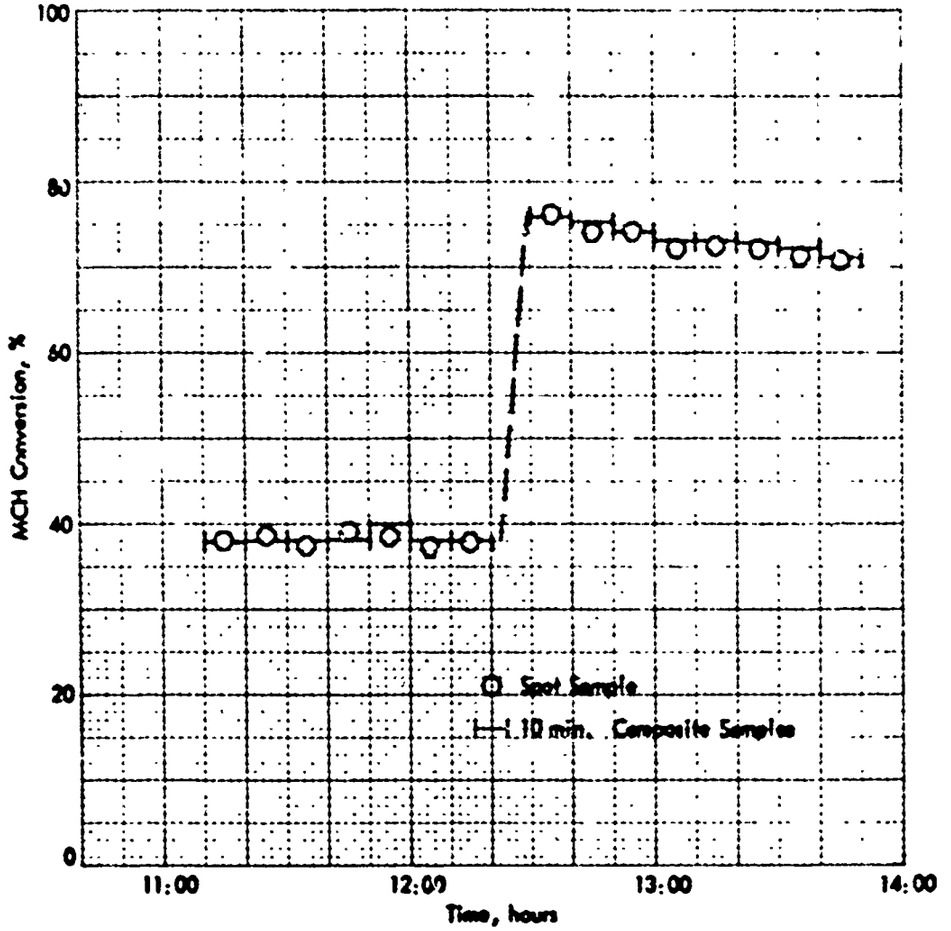

Figure 46. FSSTR: DEHYDROGENATION OF MCH OVER H_2 REGENERATED SHELL 113 CATALYST IN 2 FOOT REACTOR
MCH Conversion, Series 10018-181

Data obtained on some of the catalyst recovered after Series 10018-181 and on fresh 10280-113 catalyst follow:

	Specific Surface Area, m^2/g	H_2 Adsorption 0-500°C, μ mol H_2/g	%	%Pt
Fresh 10280-113 (N_2 Reduced)	229	35	.01	4.4
Recovered		17	2.02	
Recovered (Burned in 1% O_2)	206	25		

The final test series (Series 10018-184) in the 2ft reactor was made at a feed rate of 25.1 lb MCH/hr (LHSV = 625). Table 90 and Figures 47 and 48 present the data for these runs. A maximum conversion of 91% was reached at the start of Run 10018-184-1430. However, after one hour operation conversion had declined to ca 87% while outlet temperature increased from 1006° to 1052°. No attempt was made to reactivate this catalyst charge.

The 2ft reactor developed a leak at one of the welds during this last test and will have to be rebuilt before it can be used again.

The following tabulation of smoothed data indicates the improvement obtained using the 113 catalyst while dehydrogenating MCH in the 3/8" OD x 2ft long reactor. (All tests were run at ca 900 psig and 900°F inlet conditions.)

Catalyst	MCH Feed		Heat Input		MCH Conversion,%	Outlet Fluid Temp. °F
	lb/hr	LHSV	Btu/hr	Btu/lb		
R-8	64.5	1610	40,000	620	61	930
R-8	25.1	625	20,000	797	77	938
113	62.1	1550	40,000	644	64.5	900
113	25.1	625	20,000	797	80.5	910

The true difference in effectiveness is not indicated solely by the increased conversion produced by the Shell 113 catalyst since the exit temperatures were lower in those cases. The true effect (at constant exit T) on conversion will be calculated using the reactor computer program.

Test Using 3/8" x 10ft Reactor

Section II of the FSSTR (3/8" OD x 0.049" wall x 117½" long) was charged with 94.3 g (110.5 cc) of Shell 113 catalyst which was then activated in N_2 at 1100°F for . hr. Series 10018-189 was then run at an MCH feed rate of 25.2 lb/hr (128 LHSV), inlet pressure of 900 psig and inlet temperature of 800° and 900°F. A total of eight lined out run periods at different inlet temperature and power level combinations were run with a maximum conversion of

Table 20. ESSOR: DEHYDROGENATION OF MCH OVER SHELL 113 IN 2-FT REACTOR

Data Summary Series 10018-184

Reactor No. 10018-49; 0.277" ID x 0.049" wall x 2-ft long Hastelloy C
Feed: 99.8% MCH; 25.14 lb/hr, 625 LHSV, 60,000 lb/(hr·ft²)

Run No.	Experimental Data								Theoretical and Calculated Data					
	Fluid Temp., °F		Pressure, psig		MCH Conv. %	Tube wall T.C.'s			Tube Length, in.	Wall Temp., °F[c]		Heat[d] Flux, Btu/(hr·ft²) x 10⁻³	Cumulative Heat[e]	
						Location		Temp., °F						
	In	Out	In	Out		Inches[b]	Position[b]			Outside	Inside		Btu	lb
1200	901	901	895	889	14	0.5	B	795	0	(810)	(811)		0	0.0
						1.5	T		2					
	Fresh catalyst charge activated 1 hr in H₂ at 1050°F)					3	B		6					
						6	T		10					
						9	B		14					
						12	T		18					
						15	B		22					
						18	T		26					
						21	B		(0.2%)			(21.5)		
						22.5	T							
						25.5	B							
1320	907	905	894	848	60	0.5	B	860	0	(879)	(866)		0	0.0
						1.5	T	930	2	879	867	55.1	665	26.6
						3	B	809	6	882	870	55.1	1996	79.8
						6	T	868	10	921	909	55.1	4995	199.8
						9	B	810	14	922	910	55.0	6659	266.3
						12	T	815	18	915	921	55.0	7989	319.2
						15	B	885	22	878	867	55.0	7319	292.1
						18	T	893	26	(900)	898		7988	317.6
						21	B	917	(0.2%)			(55.0)		
						22.5	T	880						
						25.5	B	880						
1420	900	897	898	851	66	0.5	B	920	0	(940)	(917)		0	0.0
						1.5	T	998	2	955	941	109.0	1516	52.4
						3	B	876	6	988	960	109.0	4971	171.1
						6	T	886	10	998	976	108.9	6558	241.9
						9	B	888	14	913	990	108.7	9917	466.6
						12	T	909	18	929	906	108.4	11840	671.5
						15	B	915	22	985	922	108.8	14830	771.9
						18	T	942	26	(953)	(950)		15730	648.5
						21	B	981	(0.2%)			(108.9)		
						22.5	T	948						
						25.5	B	948						
1450	902	1006	898	850	91	0.5	B	980	0	(1016)	(981)		0	0.0
						1.5	T	989	2	983	977	171.0	2067	82.2
						3	B	954	6	988	952	171.0	6602	266.7
						6	T	978	10	984	950	171.0	10940	411.1
						9	B	988	14	1010	975	170.9	14470	575.5
						12	T	1001	18	1047	1013	170.8	18600	779.8
						15	B	1016	22	1101	1068	170.7	22730	904.0
						18	T	1050	26	(1132)	(1099)		26790	986.0
						21	B	1079	(0.2%)			(170.9)		
						22.5	T	1107						
						25.5	B	1134						
1960	898	1052	898	855	87	0.5	B	990	0	(1016)	(981)		0	0.0
						1.5	T	987	2	983	977	171.0	2067	82.2
	(Continuation of Run 1450)					3	B	953	6	988	952	171.0	6602	266.7
						6	T	971	10	984	950	171.0	10940	411.1
						9	B	980	14	1010	975	170.9	14470	575.5
						12	T	999	18	1052	1018	170.8	18600	779.8
						15	B	1015	22	1121	1088	170.6	22730	904.0
						18	T	1056	26	(1167)	(1135)		26790	986.0
						21	B	1100	(0.2%)			(170.9)		
						22.5	T	1124						
						25.5	B	1156						
1690	898	884	890	854	39	0.5	B	865	0	(895)	(879)		0	0.0
						1.5	T	893	2	897	885	55.4	669	26.6
						3	B	807	6	895	795	55.5	2009	79.9
						6	T	805	10	813	801	55.4	3350	133.2
						9	B	810	14	826	812	55.4	4679	186.5
						12	T	820	18	899	827	55.4	6026	239.8
						15	B	827	22	893	881	55.3	7346	294.0
						18	T	840	26	(865)	(851)		8055	319.6
						21	B	850	(0.2%)			(55.4)		
						22.5	T	852						
						25.5	B	852						

a) T.C.'s eyeholeted to outside wall at indicated inches from inlet gas bottom.
b) Location of T.C. junction on horizontal tube. B = Bottom, T = Top.
c) Outside wall temperatures by smoothing experimental data. Inside temperatures by calculation.
d) Corrected for losses. Values in ( ) are average over entire heated length.
e) Net heat to fluid up to indicated tube length.

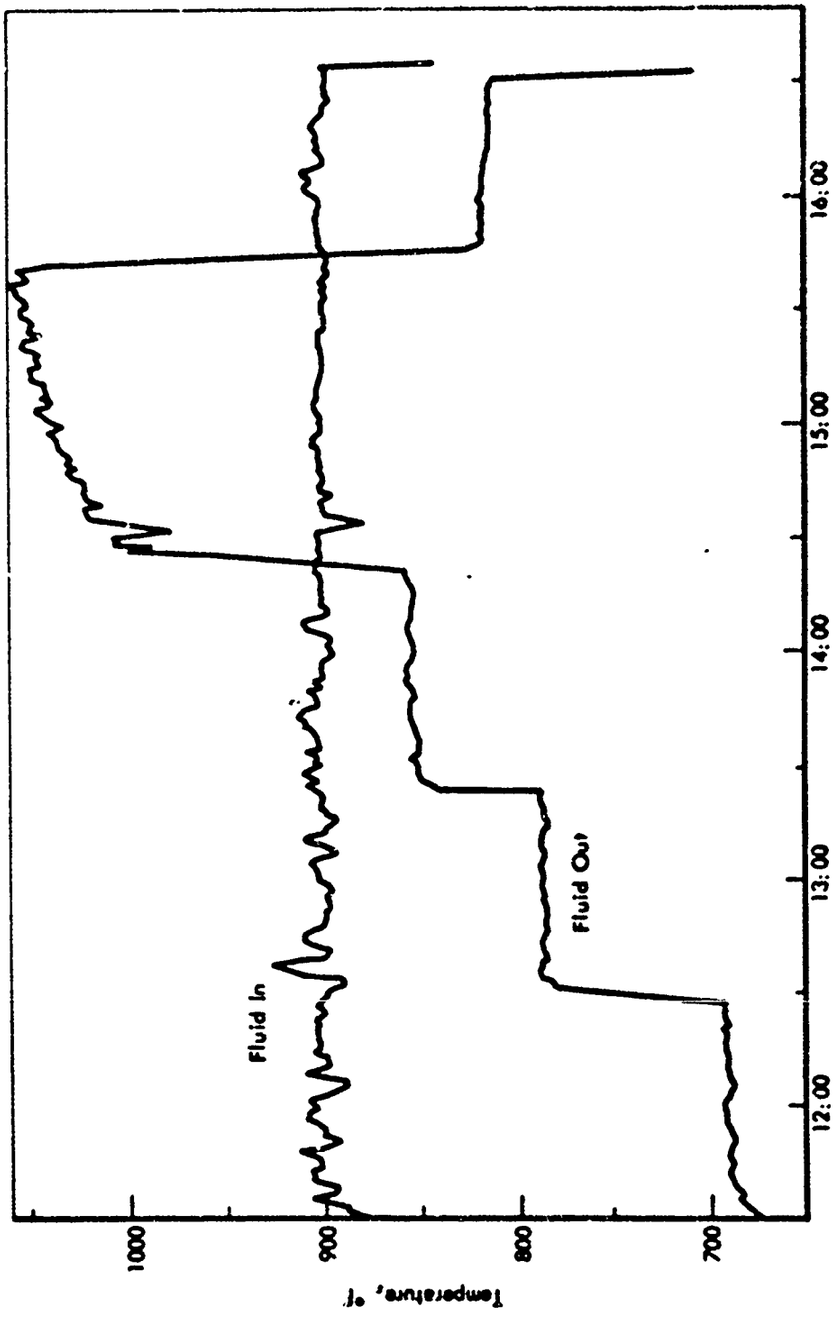

Figure 47. FSSTR: DEHYDROGENATION OF MCH OVER SHELL 113 CATALYST IN 2 FOOT REACTOR
Fluid Temperatures, Series 10018-184

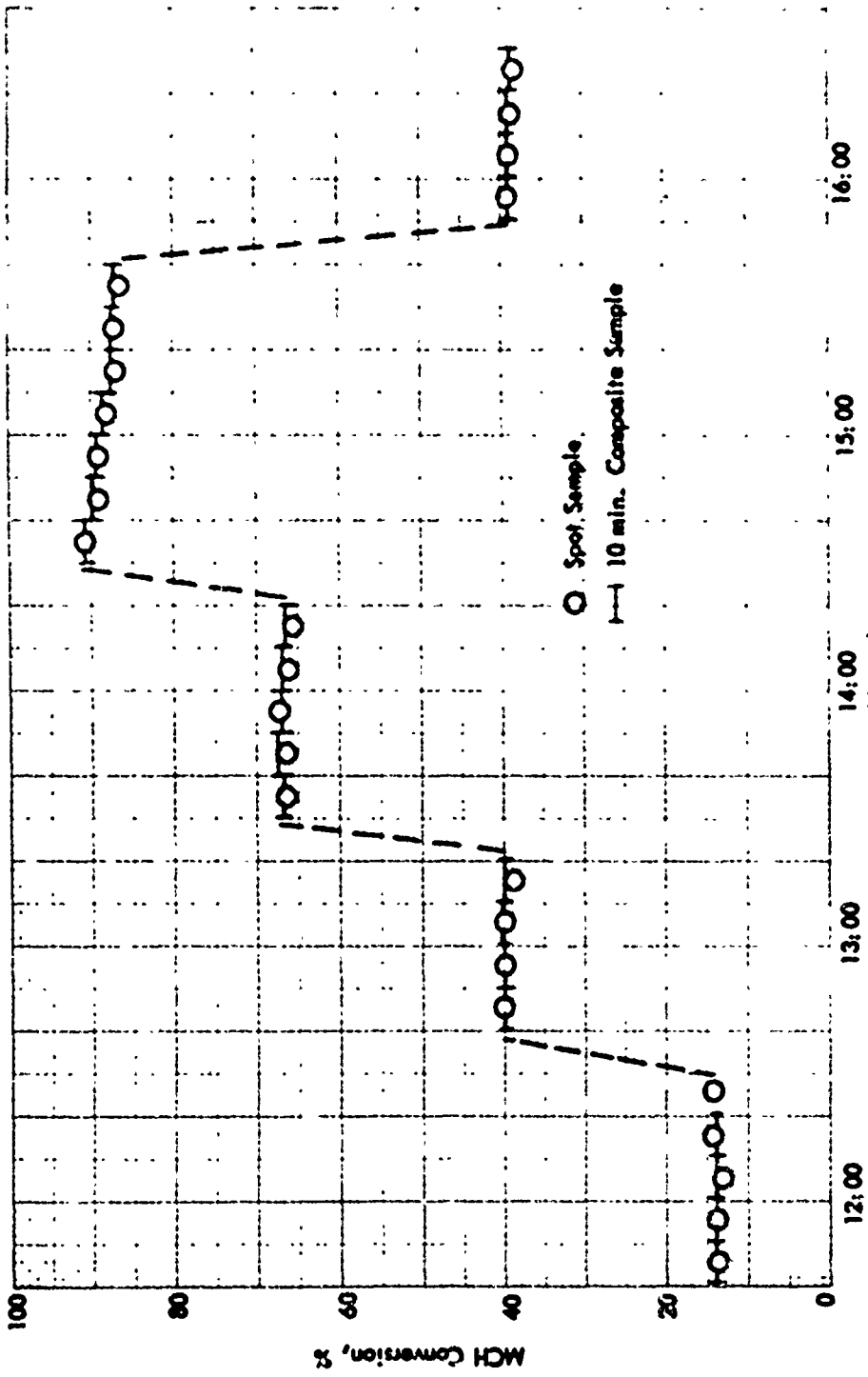

Figure 48. FSSTR: DEHYDROGENATION OF MCH OVER SHELL 113 CATALYST IN 2-FOOT REACTOR
MCH Conversion, Series 10018-184

65868

96% being reached at a heat input of 1,020 Btu/lb. The data summary table and fuel inlet and outlet temperature and conversion plots for this test series are given in Table 91 and Figures 48, 50 and 51. It appears that a very slight reduction in catalyst activity took place during the highest heat input run.

Dehydrogenation of Decalin (DHN) Over Shell 113 Catalyst

Tests Using 3/8" OD x 10ft Reactor

The same catalyst charge which was used for Series 10018-189 with MCH feed was used without further treatment in Series 10018-191 with Decalin (DHN) feed.

Prior to this first use of DHN feed in the FSSTR it was necessary to modify the flow scheme of the unit by adding a toluene diluent stream to the product immediately before the condenser so as to prevent crystallization of naphthalene, one of the reaction products, and consequent plugging of the condenser coil. This expedient, which, of course, would not be required in actual operation where reaction products would not be cooled before being burned, worked well and no problems were encountered during the test period.

The course of Series 10018-191 can be followed by refering to the data summary in Table 92, product analysis in Table 93, fuel inlet and outlet temperatures and DHN conversion in Figures 52, 53 and 54. Of interest is the rapid decline in catalyst activity found in the run at 900°F inlet and outlet (10018-191-14:50). Note, however, that the decline in conversion (82% to 72%) was emphasized in this test since the power level was reduced to maintain a constant 900°F outlet temperature and in previous tests with MCH, where power was held constant during a run, a rise in outlet temperature partially counteracted the decline in catalyst activity. This effect confirms results obtained in bench scale equipment which indicated that DHN had a more adverse effect on the stability of a variety of Pt/Al_2O_3 catalysts than MCH. This appears to be related to a lower rate of hydrogenation of coke precursors in the DHN case. Isomerization of cis to trans DHN and high selectivity for the reaction to Tetralin at lower temperatures are evident from the product analyses.

Table 91. FSSTR: DEHYDROGENATION OF MCH OVER SHELL 113 IN 10-FT REACTOR

Data Summary Series 10018-189

Reactor: 0.277" ID x 0.049" wall x 117½" long Hastelloy C
Feed: 99.8% MCH; 25.2 lb/hr, 128 LHSV, 60,230 lb/(hr·ft²)

Run 10018-189-	Fluid Temp., °F		Pressure, psig		Heat			Intermediate Temperatures, °F[b]				MCH Converted, %	Selectivity Fortoluene, %
	In	Out	In	Out	Btu/hr	Btu/lb	Btu[a]/(hr·ft²)	T.C. Location	Fluid	Outside Wall	Inside Wall		
1145	803	671	885	797	0	0	0	A	683	679	679	8.8	99.1
(Fresh catalyst charge. Activated 1hr in H_2 at 1100°F)								B	678	677	677		
								C	675	675	675		
1245	801	799	881	702	12,000	476	16,900	A	733	747	743	46.3	99.1
								B	759	772	768		
								C	777	792	788		
1345	891	700	883	765	0	0	0	A	714	711	711	65.6	98.8
								B	710	708	708		
								C	706	704	704		
1455	894	901	886	589	22,000	874	31,000	A	783	812	805	89.2	98.6
								B	820	845	838		
								C	849	872	865		
1545	904	1017	886	542	25,700	1,020	36,200	A	795	828	820	96.0	98.7
								B	837	864	856		
								C	878	908	900		
1645	810	809	881	696	12,000	476	16,900	A	735	750	746	48.1	99.2
								B	762	776	772		
								C	781	798	794		

a) Based on inside surface area.
b) Fluid and Outside Wall temperatures are average of recorded values over 10 min. interval. Inside Wall temperatures are calculated. T.C. location A = 20.8, B = 58.9 and C = 89.1 inches from inlet to catalyst section.

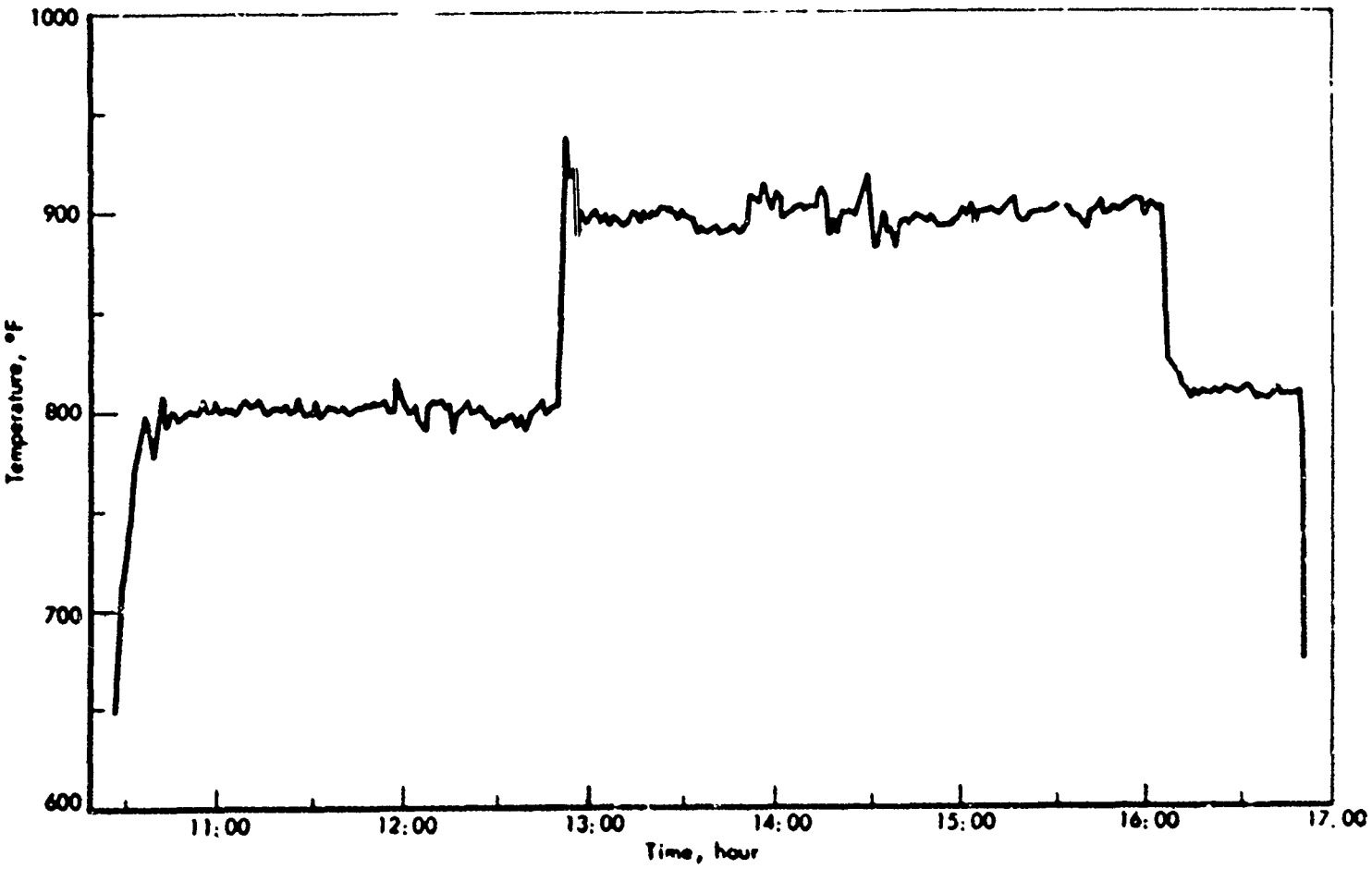

Figure 49. FSSTR: DEHYDROGENATION OF MCH OVER SHELL 113 CATALYST IN 10 FOOT REACTOR
Inlet Fluid Temperature, Series 10018-189

AFAPL-TR-67-114

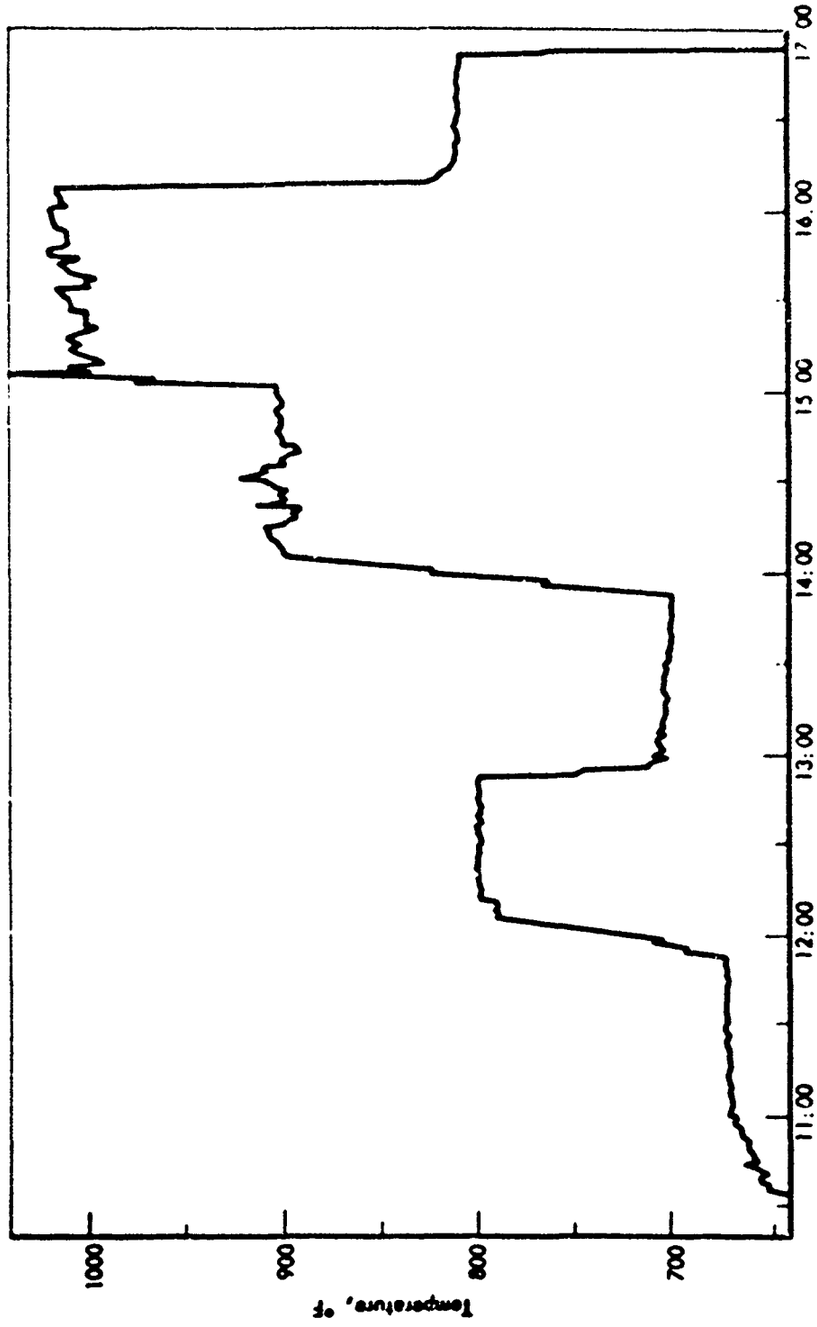

Figure 50. FSSTR: DEHYDROGENATION OF MCH OVER SHELL 113 CATALYST IN 10 FOOT REACTOR
Outlet Fluid Temperature, Series 10018-189

65868

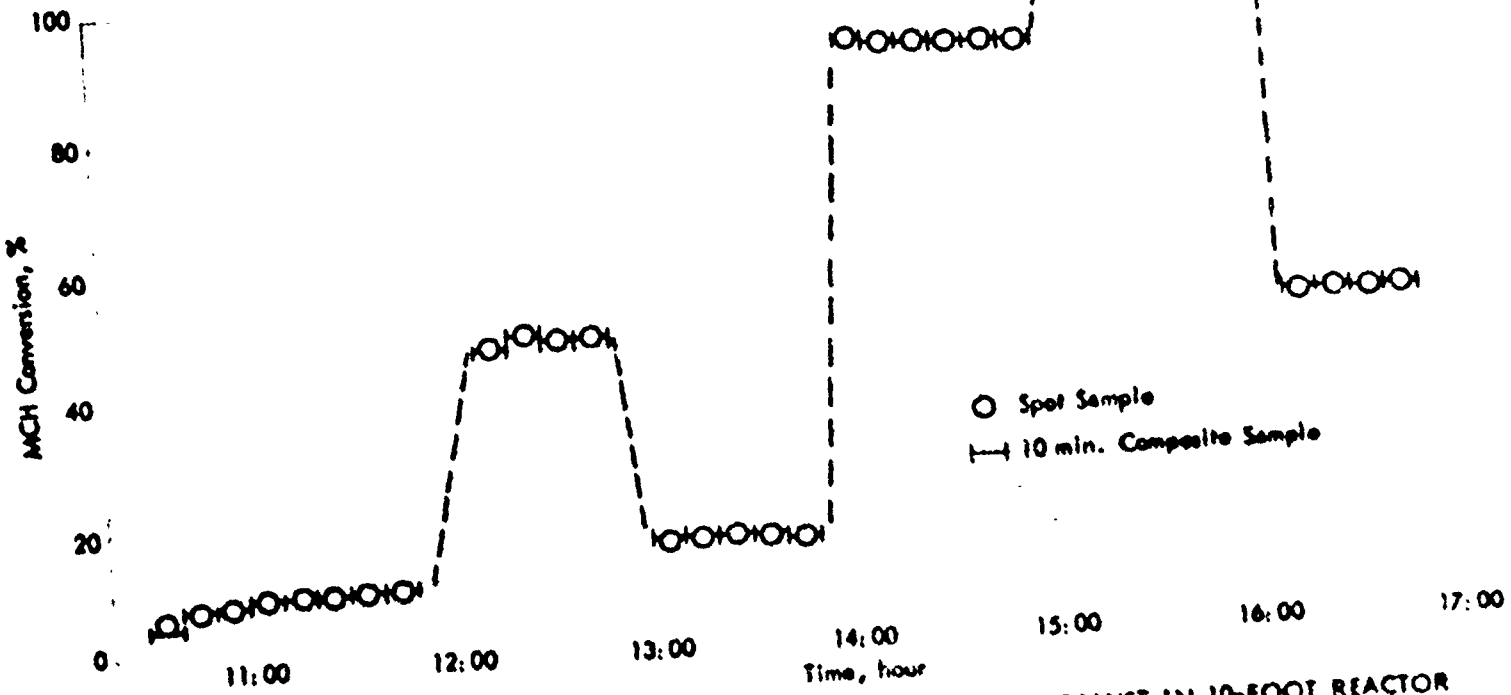

Figure 51. FSSTR: DEHYDROGENATION OF MCH OVER SHELL 113 CATALYST IN 10-FOOT REACTOR
MCH Conversion, Series 10018-189

Table 92. FSSTR: DEHYDROGENATION OF DECALIN OVER SHELL 115 IN 10-FT REACTOR

Data Summary Series 10018-191

Reactor: 0.277" ID x 0.049" wall x 117½" long Hastelloy C
Feed: 99.5% Decalin, 0.5% Tetralin
Rate: 26.5 lb/hr, 118 LHSV, 65,300 lb/(hr·ft²)

Run 10018-191-	Fluid Temp., °F		Pressure, psig		Heat			Intermediate Temperatures, °F[b]				Decalin Converted, %	Selectivity, %	
	In	Out	In	Out	Btu/hr	Btu/lb	Btu/(hr·ft²)[a]	T.C. Location	Fluid	Outside Wall	Inside Wall		To Tetralin	To Decalin
1130	800	704	900	849	0	0	0	A	709	705	705	8.7	95	5
								B	705	705	705			
(Same catalyst charge as used in Series 10018-189)								C	704	704	704			
1230	798	800	893	755	13,400	505	18,800	A	744	757	753	50.3	63	37
								B	758	772	768			
								C	773	792	788			
1330	902	718	893	810	0	0	0	A	723	720	720	16.9	91	10
								B	720	719	719			
								C	719	718	718			
1400	899	908	890	818	23,400	884	33,000	A	780	807	799	82.3	26	74
								B	816	839	831			
								C	847	868	860			
1425[c]	900	905	887	663	21,900	826	30,800	A	775	800	793	76.0	29	71
								B	810	933	326			
								C	844	867	860			
1450[c]	903	907	896	651	21,200	799	29,800	A	774	801	794	72.9	31	69
								B	809	832	825			
								C	844	868	861			
1610	801	802	899	782	10,500	395	14,700	A	738	750	747	37.7	65	35
								B	750	758	755			
								C	770	783	780			

a) Based on inside surface area
b) Fluid and Outside Wall temperatures are average of recorded values over 10 min. interval. Inside Wall temperatures are calculated. T.C. location A= 28.6, B= 58.9 and C= 89.1 inches from inlet to catalyst sections.
c) Continuation of Run 1400. Power input reduced to hold ca 900°F outlet temp.

Table 93. ESSO: DEHYDROGENATION OF DECALIN OVER SHELL 115 IN 10-FT REACTOR

Product Analyses Series 10018-191

Run[1] No.	Product Composition, %w			
	t-Decalin	c-Decalin	Tetralin	Naphthalene
Feed	33.6	65.9	0.5	0
1130	72.1	18.8	8.7	0.4
1230	43.4	7.4	31.6	17.6
1330	66.9	16.5	15.1	1.5
1400	16.6	2.0	22.2	59.2
1425	22.1	3.0	22.7	52.1
1450	24.7	3.6	23.2	47.9
1610	52.6	10.7	24.2	12.5

1) See Data Summary Table for operating conditions.

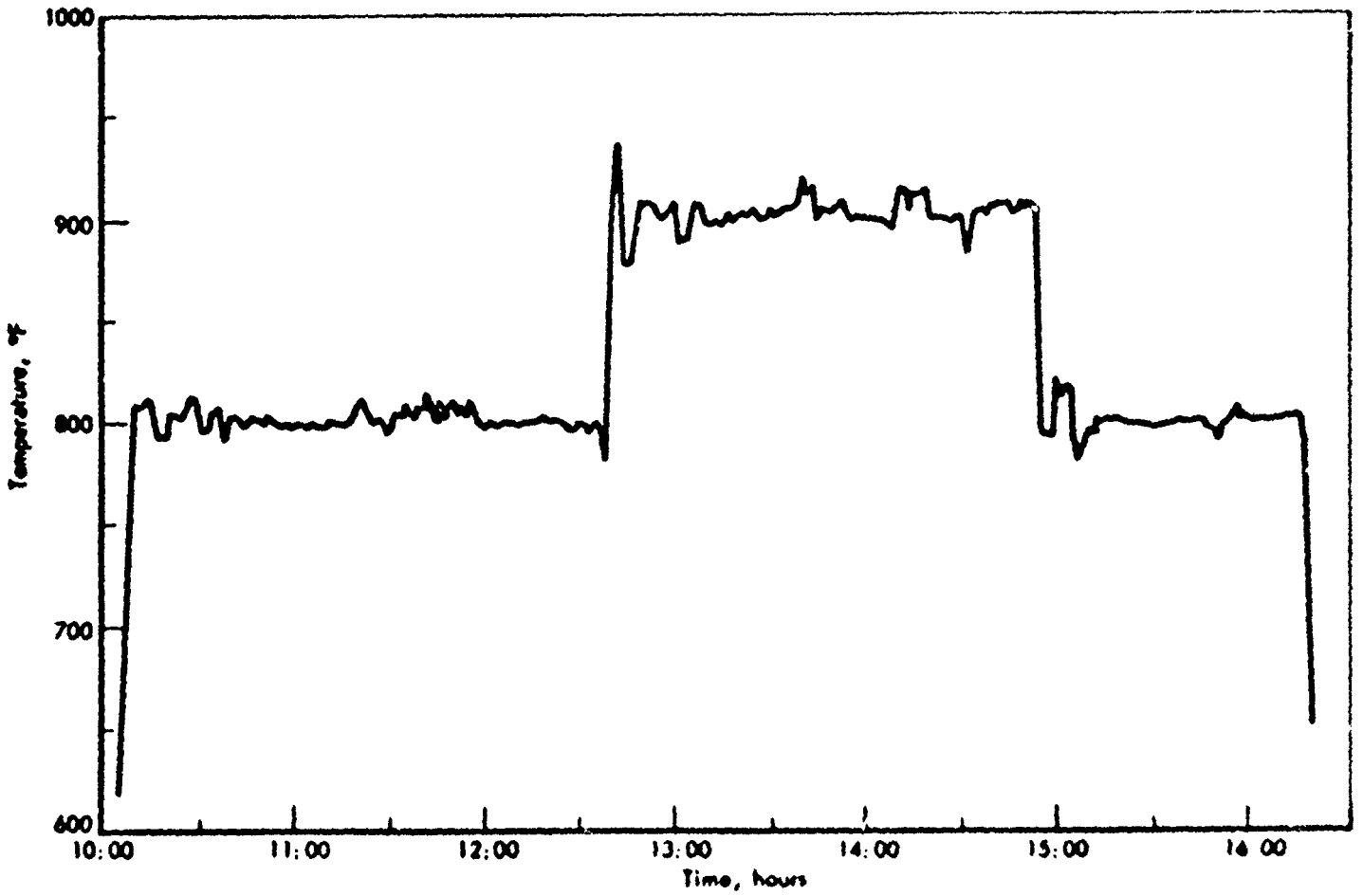

Figure 52. FSSTR: DEHYDROGENATION OF DECALIN OVER SHELL 113 CATALYST IN 10 FOOT REACTOR
Inlet Fluid Temperature, Series 10018-191

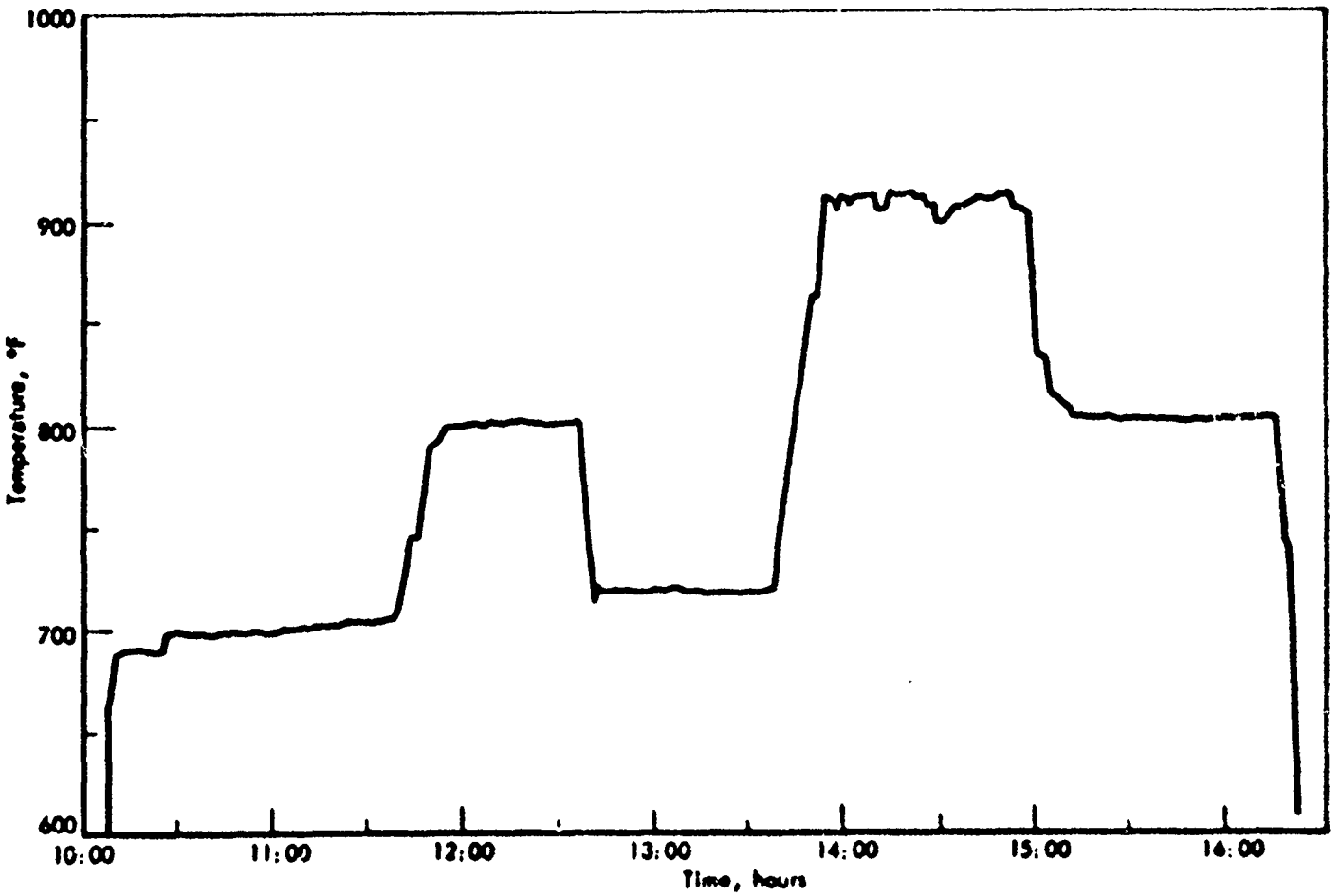

Figure 53. FSSTR: DEHYDROGENATION OF DECALIN OVER SHELL 113 CATALYST IN 10 FOOT REACTOR
Outlet Fluid Temperature, Series 10018-191

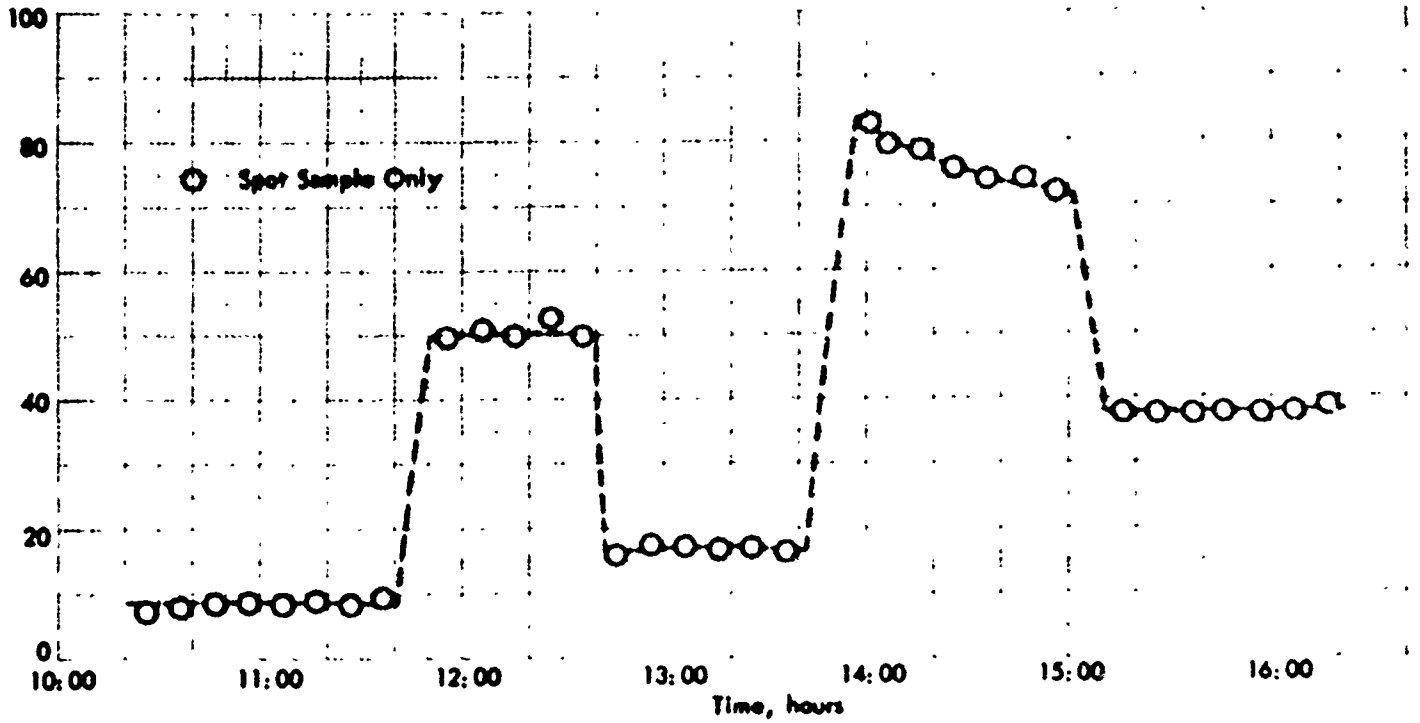

Figure 54. FSSTR: DEHYDROGENATION OF DECALIN OVER SHELL 113 CATALYST IN 10 FOOT REACTOR
Decalin Conversion, Series 10018-191

Thermal Stability

Introduction

Fuel thermal stability has become a fuel property of increasing importance as engine designers have turned to the problems of the SST and higher Mach Number aircraft. For years, the ASTM-CFC Fuel Coker has been relied upon to indicate whether or not a fuel had a passable thermal stability rating, but has always been acknowledged to have serious problems of precision and meaning. Despite the many coker modifications and substitutions which have been advanced, the problem of a suitable thermal stability test has still not been solved, while the need for such a test has become more imperative.

Also, in the development of multi-Mach Number aircraft fuels, a thermal stability test appropriate for research-type application is needed. In constrast to the qualitative nature of the coker test, what is needed is a device which will quantitatively measure fuel deposition tendency. Unfortunately, fuel thermal stability is not a physico-chemical property, but is strongly related to environmental conditions. It is difficult, therefore, to conceive of a test which would yield stability data without some dependence upon the particular apparatus used.

The purpose of this work is to delineate a few of the environmental factors which can influence the precision of coker ratings. Some of these are controlled variables such as temperature, pressure, test duration, and fuel flow rate; but other factors such as metal exposure, history of the fuel and tube surface preparation may play a significant role.

Finally, we are concerned with the subject of coker tube deposit rating, which is probably the most serious unresolved deterent to repeatable, reproducible, and meaningful coker deposit ratings.

Experimental

The thermal stability work referred to in this report has been performed with a fuel coker similar in principle to the Standard ASTM Coker, but modified for research purpose to operate at temperatures up to 950°F and pressures up to 500 psig. In its present form, it operates on 150 ml of fuel, and normally on the recycle mode. It will be referred to herein as the SD/M-7 or the SD Fuel Coker. A detailed description of the basic apparatus can be found in Reference 10. The present modification utilizes the pump only for fuel circulation; static pressure is imposed by gas pressure.

Factors Which Influence Fuel Coker Deposit Ratings

Although the coker test is simple in concept, in practice it is complex. Small changes in controlled variables and fuel purity can and do influence test sensitivity, which explains the difficulty commonly experienced in obtaining good repeatability and reproducibility although rigorous attention to detail at the hands of a skilled operator can produce better results. Temperature and pressure are of course controlled variables, and temperature inaccuracy has been identified as a source of poor test repeatability between laboratories. The effect of pressure has received little attention.

Temperature and Pressure

We have investigated the sensitivity of the SD/M-7 Coker test to temperature and pressure variations with three fuels: Decalin, SHELLDYNE, and SHELLDYNE-H. In these test, temperatures were varied as widely as 275 to 850°F, and pressures from 150 to 400 psig. Both temperature and pressure were varied simultaneously, and the results were subjected to regression analysis.

No correlation was found with pressure, even though both pure liquid state and boiling operating conditions variously existed. Both the maximum deposit code and total code ratings could be expressed as simple linear functions of temperature, with a precision generally as good as the reproductibility of the test. Equations 1, 2, and 3 are the expressions for predicting the maximum code (MCR) ratings for Decalin, SHELLDYNE, and SHELLDYNE-H, respectively, at temperature T (°F) while Equations 4, 5, and 6 are the corresponding expressions for the total code (TCR).

Decalin:	MCR = (T-503)/38.7	(1)
SHELLDYNE:	MCR = (T-571)/12	(2)
SHELLDYNE-H:	MCR = (T-585)/42	(3)
Decalin:	TCR = (T-565)/15.4	(4)
SHELLDYNE:	TCR = (T-575)/1.6	(5)
SHELLDYNE-H:	TCR = (T-575)/7.3	(6)

From these relationships, it is interesting to note that the temperature errors required to produce a 1/4 maximum code number difference would be 10° for Decalin, 10° for SHELLDYNE-H, but only 3° for SHELLDYNE. $T_{2.5}$ breakpoint temperatures (the temperature at which the maximum deposit code is 2.5) for the three fuels, predicted by the equations, are 600, 600, and 690°F for Decalin, SHELLDYNE, and SHELLDYNE-H, respectively. Since the deposit ratings are considered good to ±1/2 code number, these ratings might then be given as 600 ± 20°, 600 ± 6°, and 690 ± 21°. It is evident that no correlation exists between the thermal stability ratings of these fuels and their temperature sensitivities (or thermal stability temperature coefficients).

The agreement of predicted values with the experimental data from which they were derived is shown in Tables 94, 95, and 96 and in Figure 55.

In connection with the correlation studies with temperature and pressure, the test fluids from the coker runs were, in some cases, subjected to light absorption measurements at 500 mu. The increase in light absorption over that obtained with the original base fuel was determined, and an attempt was made to correlate these increases with coker tube ratings. However, this attempt was a complete failure, as will be seen by the data in Table 94: no correlation was found for either maximum or total tube ratings.

However, the spread in Δ percent light absorbed values was not very large. This was a consequence of choosing a wavelength which would put the light absorptions for Decalin, SHELLDYNE, and SHELLDYNE-H all on the same scale. While this selection spread the readings for SHELLDYNE and SHELLDYNE-H the readings for Decalin were compressed into the 0-10 percent range. A value

Table 24. COMPARISON OF SO FUEL COKER RATINGS WITH VALUES PREDICTED BY CORRELATION EQUATIONS

Decalin

Run	Pressure, psig	Temperature, °F	Preheater Tube Code Ratings		Δ Percent[b] Light Absorbed
			Experimental	Predicted	
51	150	550	1/ 5.5	1/ 13	-
52	150	550	1.5/ 10	1/ 13	-
54	150	550	1/ 5.5	1/ 13	-
196	250	750 (boiling)	6/ 15	6.5/24.5	-
221	250	850 (SC)[a]	6/ 19	8/ 30	-
222	250	850 (SC)	6.5/ 33	8/ 30	-
227	250	750 (boiling)	6/ 35	6.5/24.5	-
228	250	750 (boiling)	6/ 14	6.5/24.5	-
232	250	725 (boiling)	5.5/ 21	5.5/ 23	-
233	250	675	5/ 37	4.5/ 20	-
236	250	575	1.5/ 12	2/14.5	-
252	250	275	0/ 0	0/ 0	-
262	250	625	3.5/ 20	3/ 17	-
263a	250	625	4/ 29	3/ 17	-
263b	250	625	3.5/ 26	3/ 17	-
284	150	650 (boiling)	3.5/ 26	4/18.5	-
285	150	600	3/20.5	2.5/15.5	-
286	150	600	2.5/16.5	2.5/15.5	-
320	150	675 (boiling)	5/ 28	4.5/ 20	1.3
345	150	600	3/17.5	2.5/15.5	-
347	150	600	2.5/13.5	2.5/15.5	1.4
348	150	600	2/10.5	2.5/15.5	0.6
352	150	600	2/ 15	2.5/15.5	1.9
355	150	600	2.5/ 12	2.5/15.5	1.3
369	400	550	2/ 11	1/ 13	-
370	400	600	2/ 13	2.5/15.5	10.1

a) SC = supercritical.
b) 500 millimicron wavelength.

(Continued)

Table 9b (Contd). COMPARISON OF SD FUEL COKER RATINGS WITH VALUES PREDICTED BY CORRELATION EQUATIONS

Run	Pressure, psig	Temperature, °F	Preheater Tube Code Ratings		Percent Light Absorbed
			Experimental	Predicted	
372	150	550	1/ 6.5	1/ 13	11.0
375	150	550	2/11.5	2/ 13	4.6
376	400	550	1.5/ 9.5	2/ 13	4.4
381	150	700 (boiling)	6/27.5	5/21.5	1.5
382	150	700 (boiling)	6/ 21	5/21.5	2.9
319	150	600	2.5/11.5	2.5/ 15	10.5
325	150	625	2.5/ 19	3/ 17	3.9
327	150	600	2.5/13.5	2.5/ 15	0.9
330	150	600	2/12.5	2.5/ 15	1.0
332	150	600	2/ 14	2.5/ 15	1.0
334	150	600	3/20.5	2.5/ 15	3.5
338	150	600	2/ 17	2.5/ 15	-
340	150	600	2/ 12	2.5/ 15	-
341	150	600	3/ 18	2.5/ 15	-
342	150	600	2/ 8.5	2.5/ 15	-
349	150	600	2/ 12	2.5/ 15	-
350	150	600	2/12.5	2.5/ 15	-
351	150	600	2/ 14	2.5/ 15	-
379	150	600	2/14.5	2.5/ 15	-
380	150	600	3/ 13	2.5/ 15	-

Table 95. COMPARISON OF SD/M-7 FUEL COKER RATINGS WITH VALUES PREDICTED BY CORRELATION EQUATIONS

SHELLDYNE

Pressure, psi	Temperature, °F	Tube Code Ratings		ΔPercent[a] Light Absorbed
		Experimental	Predicted	
150	575	0.5/ 3	0.5/ 0	-
150	600	3/ 21	2.5/15.5	-
150	600	2/12.5	2.5/15.5	-
150	625	3.5/ 26	4.5/ 31	-
150	625	5.5/ 38	4.5/ 31	-
150	650	6/37.5	6.5/46.5	31.1
150	675	8/ 64	8/ 62	49.6

a) 500 millimicron wavelength.

Table 96. COMPARISON OF SD/M-7 FUEL COKER RATINGS WITH VALUES PREDICTED BY CORRELATION EQUATIONS

SHELLDYNE

Pressure, psi	Temperature, °F	Tube Code Ratings		ΔPercent[a] Light Absorbed
		Experimental	Predicted	
150	625	1.5/ 11	1/ 7	-
150	675	1.5/ 8	2/ 14	-
150	700	3/22.5	2.5/ 17	-
150	700	2/12.5	2.5/ 17	36.7
150	700	2.5/19.5	2.5/ 17	72.8
400	700	3.5/ 21	2.5/ 17	31
150	775	4/ 23	4.5/27.5	-
150	775	5/ 32	4.5/27.5	95

a) 500 mμ wavelength.

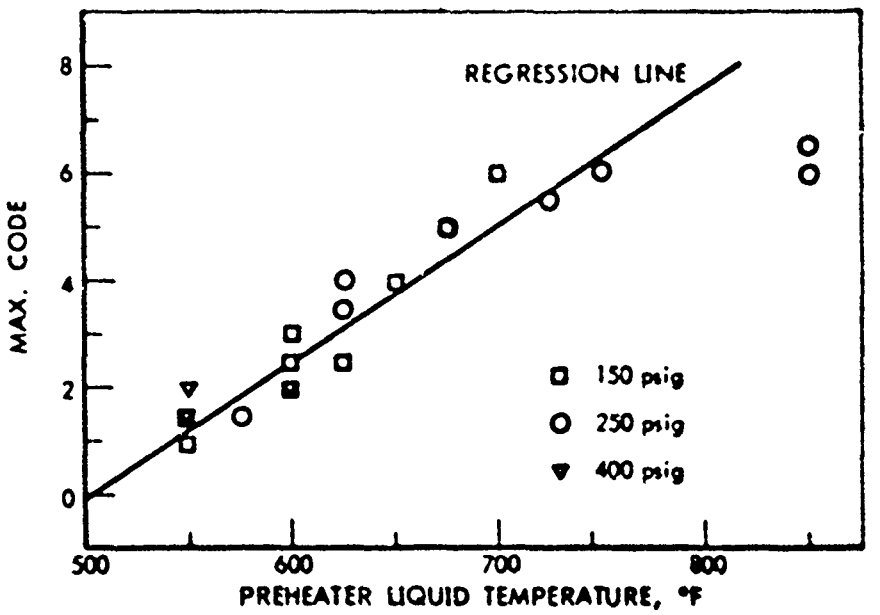

Figure 55. SD/M-7 FUEL COKER RATINGS OF DECALIN

of 350 mu would probably have given better sensitivity for Decalin, and perhaps deserves another look before the hypothesis of a possible correlation of tube rating with light absorption is tossed out. The outlook is not optimistic, however, since failure was also experienced in our attempt to relate existent gum from Decalin coker samples with tube ratings. The agreement between light absorption and existent gum was also poor, as shown in Table 7".

Since heavy tube deposits would reduce the existent gum and reduce also the increase in light absorption due to oxidation, it is not unreasonable to find a lack of correlation between these measurements. The gum molecular weight and state of agglomeration would of course influence all three measurements, and conceivably in different ways. An additional factor is the deposit fallout in the cooler zones of the coker, which would effect light transmission and gum determinations, but not coker tube ratings.

Temperature and Time

The correlations of Equations 1 through 6 apply only for 5-hour tests. We have also investigated the time-temperature tradoff relationship of thermal stability in the SD Coker, using a high quality jet fuel (RAF 159-60; described in Table 98). Time was varied over a period of 1 to 4 hours and temperature, from 600 to 675°F.

Regression analysis of data obtained from these tests provided Equations 7 and 8 for maximum and total code ratings, which are seen to contain interaction terms between time and temperature.

$$MCR = (T-573)/14 \quad (7)$$
$$TCR = -0.0784\,T + (0.0404\,T - 24.75)\,t + 59.9 \quad (8)$$

T = Preheater Temperature, °F
t = Test Duration, hours.

As may be expected, code ratings increase with both time and temperature. The agreement of (7) and (8) with the experimental data is shown in Table 99 and Figure 56. If the reasonable liberty is taken to extrapolate (7) and (8) to 5 hours, we then obtain expressions of MCR and TCR for RAF 159-60 similar to (1) through (6):

$$MCR = (T-573)/14 \quad (9)$$
$$TCR = (T-516)/8.1 \quad (10)$$

If a constant temperature of 600°F is assumed, Equation (7) becomes

$$MCR = (t - 1.4)/3.33 \quad (11)$$

We see, then, from (9) and (11) that when the preheater temperature is constant, the maximum code rating is linear with time, and that when the time is constant, maximum code is linear with temperature. This is true over the ranges of time and temperature used and for the fuel tested, but might not hold for long periods of time, as suggested by the time effect comparison up to 20 hours shown by Shayeson.[25]

However, analysis of (7) suggests that for small changes, time and temperature might be meaningfully interchanged. For example, with the present fuel, if the test time were shortened from 5 to 2 hours, the compensating

Table 97. COMPARISON OF JP FUEL COKER RATINGS WITH VALUES OF EXISTENT GUM[a] OBTAINED ON COKER EFFLUENT DECALIN

Coker Run Number	Coker Temperature, °F	Tube Ratings	Δ Percent Light Absorbed	Gum, mg/dl
319	600	2.5/11.5	10.5	45
320	675	5/ 28	1.3	25
325	625	2.5/ 19	3.9	15
372	550	1/ 6.5	11.0	45
382	700	6/ 21	2.9	0
Decalin Base Stock	-	-	0.0[b]	0.4

a) Obtained by Steam Jet Gum Method, ASTM D381-60 (450°F)
b) The fresh Decalin stock was used as the reference liquid; therefore, it is defined as zero light absorption.

Table 98. DESCRIPTION OF JET FUEL RAF-159-60

Properties			
Grav ASTM D287, °API	50.7	Water Tol, F-791, 5251, Interface Rating	1
Distillation, ASTM D86, °F		Sulfur, D1266, %w	0.0007
I.B.P.	359	Mercaptan Sulfur, D1323, %w	nil
5%	403	Corrosion, Cu Strip, D130, 2 hr at 212°F	1B
10%	407	Aromatic Content, D1319, %v	0.8
20%	410	Bromine No. D1159	0.7
30%	413	Naphthalenes, F791, 3704T, %v	nil
40%	418	Smoke Point, D1322, mm	35
50%	423	Luminometer No., D1740	100
60%	428	Existent Gum, D381, mg/dl	1
70%	436	16-hr Potential Gum, D873, mg/dl	2
80%	450	Net Heat of Combustion, Btu/lb	
90%	471	ASTM D240 (Paar 2600 Modified)	18,909
95%	496	NBS 5917	18,886
E.P.	533	Hydrogen, D1018, %w	14.9
Residue, %	1.5	Copper, mg/liter	<0.02
Loss, %	0.5	Nitrogen, ppm	<5
Flash Point, TOC, D55, °F	164	Basic Nitrogen, ppm	<0.5
Freezing Point, D1477, °F	-32	Peroxide No., D-1563	<0.04
Color Saybolt, D15	30+	Water Separometer Index, Severity 15	99
Viscosity, D445:		Light Transmission, % at 425 mμ	100
at 100°F	1.81	Sediment, mg/gal, 0.45 micron	
at 0°F	6.75	Average	4.6
at -30°F	12.9	Range, Eight Determinations	1.8-9.8
Aniline Pt, °F	182	Other	
Aniline-Gravity Constant	9227	Paraffins, %v Mass Spec	80
		Naphthenes, %v Mass Spec	19

Table 99. TIME-TEMPERATURE EFFECTS ON THE SD/M-7 COKER RATINGS OF RAF-159-60

Pressure: 150 psig

Test Duration, hours	Temperature, °F	Preheater Tube Ratings, Max./Total	
		Experimental	Predicted
2	600	1/ 13	1/ 12
4	600	1.5/ 12	1.5/ 11
3	625	2/ 9	2.5/12.5
2	675	3.5/14.5	3.5/ 12
1	675	2/ 8.5	2/ 9.5

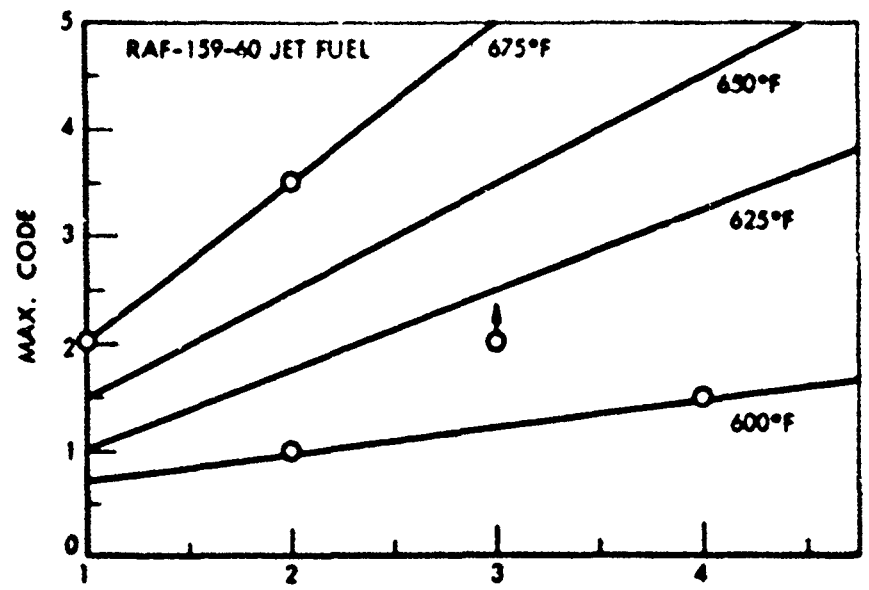

Figure 56. SD/M-7 COKER RATINGS AS A FUNCTION OF TIME AND TEMPERATURE

temperature increase required would be from 608 to 630°F, or 22°, to give the same max. code rating. It is interesting to look at (7) assuming that a 1 % code number actual change might change the observed rating by 1/2 max. code, then holding one independent variable constant at some arbitrary value while observing the rate of change of the other. When this is done, we find that for the RAF 159 fuel and 600°F, the minimum detectable time change is 50 minutes, but this increases to 10 minutes at 700°F. Similarly, when the time is held constant at 5 hours, the minimum detectable temperature change is 4°, which changes to 13°F at 1 hour.

Although applied to only three fuels, this study suggests the important conclusion that the same results might be obtained from coker tests by simply running for a fraction of the present 5 hours, but at a slightly higher temperature. By so doing, two runs per shift instead of one might be possible. As an example, it was found that Decalin, when run at 675°F, gave the same max. code rating at 2-1/2 hours as it did at 600°F and 5 hours.

Fuel Flow Rate

Flow is not a critical factor in coker operation, but we have explored it in the JFD Coker with both Decalin and methylcyclohexane (MCH). The results we report and the conclusions drawn are somewhat peculiar to the recycle flow system used, and the size of the fuel complement enters into the results, as will be shown.

When Decalin was run in a 125 ml amount for 2-1/2 hours at 600°F, a 2-1/2 lb/hr flow gave a more severe rating than did the standard 6 lb/hr, as shown in Table 100. Also, the deposits tended to be shifted further toward the inlet end with the lower flow rate, as would be expected due to heat transfer rates. These results show that the flow rate could be in error as much as 0.5 lb/hr before an effect on max. code would be discernible, which is to say that the flow rates could be set at 6.0 lb/hr ± 8 percent, or 2.5 lb/hr ± 20 percent.

The total effective residence time in the preheater tube is about the same for both flow rates in a recycle system, since although the residence time per pass is 15 seconds for 6.0 lb/hr Decalin flow and 36 seconds for 2.5 lb/hr, the same particle of fuel goes through the preheater 36/15, or 2.4 as many times at 6.0 lb/hr. Therefore, for the present case, the residence time per pass is more important than total residence time. In a once through system such as the Standard ASTM Coker, the total and per pass residence times are identical, and deposit code rating would again be expected to show the same relative relationship to flow rate. With fuels which contain trace amounts of very low thermal stability materials, the once through flow system can have the effect of having more unstable material exposed per test at the higher flow rate, whereas unstable materials in such a fuel tend to be reacted out in a few passes in the recycle mode.

However, with larger fuel compliments total residence time may become controlling in the recycle coker, as was shown by the following tests. Here total test time was doubled to 5 hours and the volume of Decalin increased by a factor of three (Table 101). Under these conditions, the effect of flow rate over the range of ca 3 to 12 lb/hr disappeared. A similar result was obtained with MCH at 3 and 6 lb/hr.

Table 100. EFFECT OF DECALIN FLOW RATE ON DEPOSIT RATINGS

Preheater Temperature: 600°F
Run Time: 2-1/2 hours
Decalin: 125 ml

Flow, lb/hr	Tube Rating, Max./Total	Deposit Rating Profile by Inches												
		13	12	11	10	9	8	7	6	5	4	3	2	1
6.0	2.5/15.5	0	0	0	0	.5	0.5	1.0	2	← 2.5 →				
6.0	2/ 17	0.5	0.5	0.5	0.5	.5	1.0	1.5	← 2 →					
2.5	4/32.5	1.0	2.5	0.5	2.0	.5	2.0	4.0	4	4.0	3	3	3.0	2
2.5	4/28.5	0.5	0.5	0.5	1.0	.5	3.0	3.5	4	3.5	3	4	3.5	2

Table 101. EFFECT OF DECALIN AND MCH FLOW RATES ON DEPOSIT RATINGS

Preheater Temperature: 550°F
Run Time: 5 hours
Decalin: 365 ml

Flow, lb/hr	Tube Rating, Max./Total	Deposit Rating Profile by Inches												
		13	12	11	10	9	8	7	6	5	4	3	2	1
Decalin														
3.0	3/ 20	0.5	0.5	0.5	1.0	1.0	1.0	1	1.5	2.0	3.0	3	3	2.0
6.0	3/18.5	0	0	1.0	1.0	1.0	1.0	1	1.0	1.5	2.0	3	3	3.0
11.7	3.5/ 19	0	0	0.5	0.5	1.0	1.0	1	1.0	2.0	2.5	3	3	3.5
MCH														
3.0	2/10.5	0	0	0	0.5	0.5	0.5	1	1.5	1.0	1.5	2	1	1.0
6.0	2/ 10	0	0	0	0	0	0	1	1.0	2.0	2.0	2	1	1.0

From the comparison shown in Table 122 at low fuel volume, it now becomes evident that another trade-off providing equal tube ratings is the simultaneous reduction of flow rate and total test time. This is so at least with the very pure Decalin fuel and the recycle mode of operation.

Metal Environment

Besides immediate Fuel Coker control factors, handling and preparation of the test fuel are important, and can be dominant factors in rating precision and reproducibility. Regardless of the care that is taken to avoid adventitious materials, however, normal contact of fuels with metal environments can have important effects. Spectrophotometric analysis of fuels in our laboratories has shown that iron and copper contents of fuels, as received, may be as high as 20 and 100 ppb, respectively. The latter amount of copper is more than sufficient to reduce thermal stability in some fuels. The coker pump itself can be a source of metal contamination, and we have found, for example, large differences in wear rates of the Zenith pump in the SD/M-7 Fuel Coker with fuels of different viscosity and lubricity properties.

To determine the extent of this problem and the effect of particular metals, a series of test were run in which Decalin was first percolated through a silica gel column, and then shaken with a powdered metal for a minimum period of 7 hours. The ratio of metal to Decalin was ca 5 grams/liter. The powdered metal was then filtered out and the Decalin introduced directly into the coker. In addition, some tests were run in which the fuel was also constantly recycled through a bed of the same metal throughout the test. In all cases, a twin run was made in which 240 ppm metal deactivator (MDA; N,N'-disalicylidene-1,2-propanediamine) was added after filtration.

The metals tested included Fe, Cu, Ni Cr, Zn, Pb, and 316-stainless steel. All runs were at 600 or 625°F. Results are shown in Table 103.

As shown, only copper gave a clearly deleterious effect, amounting to an increase in max. code of 3 numbers. (Ratings above 4 were obtained using a scale extension commonly applied to lacquer ratings on piston skirts. Although not linear with the ASTM color code, it gives a better idea of relative deposit amounts than simply calling all ratings above 4, 4+.)

The addition of MDA in the 240 ppm amount (0.214 g/liter) improved Decalin max. ratings by about 1 number in some cases, i.e., clear Decalin, and Decalin plus Cu or Zn, but this was only in the 600°F runs. No benefits from MDA occurred at higher temperatures, and with clear Decalin, MDA was harmful at 625 and 675°F.

Apparently, the chelating action of MDA with metal is responsible for the improvements in Decalin ratings at 600°F, but this must largely occur during the early cycles, since MDA is not stable above about 540°F. However, the MDA chelates would be expected to be stable at higher temperatures. As temperature is increased, the MDA would eventually be expected to decompose and actually contribute to thermal instability of the fuel, which seems to be in harmony with the 625 and 675°F ratings shown in Table 103. At high temperature, use of a more stable chelating compound is indicated.

Table 102. TRADE-OFF IN FLOW RATE AND TEST DURATION FOR EQUAL RATINGS

Preheater Temperature: 600°F
Decalin: 125 ml

Test Conditions	Tube Rating, Max./ Total	Deposit Rating Profile by Inches												
		13	12	11	10	9	8	7	6	5	4	3	2	1
2.5 lb/hr; 2.5 hours	4/32.5	1.0	2.5	.5	2.0	.5	3.0	4.0	4.0	4.0	3	3	3.0	2
	4/28.5	0.5	0.5	.5	1.0	.5	3.0	3.5	4.0	3.5	3	4	3.5	2
6.0 lb/hr; 5 hours	4/27	0.5	0.5	.5	0.5	.5	3.5	2.0	2.5	3.0	3	3	3.5	4

Table 103. EFFECTS OF METAL ENVIRONMENT ON THERMAL STABILITY OF DECALIN (F-1.0) WITH AND WITHOUT METAL DEACTIVATOR

Coker Run	Temp, °F	Metal Pre-equil	Metal Re-equil	MDA Added, g/liter	Tube, Max./ Total	Filter, Δ% Hg
285, 286, 314, 315, 316, 346, 352, 355	600	-	-	-	2.5/17	1.0
255, 262 263a,263b	625	-	-	-	3/23	0.0
294	650	-	-	-	3.5/26	2.9
329	675	-	-	-	5/28	0.2
287	600	-	-	0.0046	2.5/12	0.0
295	600	-	-	0.214	1.5/10	0.8
294	625	-	-	0.214	4/16	0.7
295	675	-	-	0.214	6.5/16	0.4
288	600	Fe	-	-	2.5/12	0.0
349, 350	600	Fe	Fe	-	2.5/16	0.0
304	600	Fe	Fe	0.214	2.5/ 8	0.0
351	600	Cu	-	-	2.5/11	0.0
353, 354	600	Cu	Cu	-	5.5/37	0.0
291	600	Cu	Cu	0.214	4/22	1.5
327, 334	600	Ni	Ni	-	3/17	0.0
317, 333	600	Ni	Ni	0.214	3/14.5	0.0
308	600	Cr	Cr	-	2.5/21	0.8
310.	600	Cr	Cr	0.214	2.5/18	4.8
319	600	Zn	Zn	-	2/12	0.4
292, 318	600	Zn	Zn	0.214	1/10	1.5
313, 325	625	Zn	Zn	-	3/23	1.3
296, 301, 302, 311, 329	625	Zn	Zn	0.214	3/18	0.6
338	600	Pb	Pb	-	2.5/21	0.0
337	600	Pb	Pb	0.214	2.5/21	0.0
332	600	316SS	316SS	-	2.5/18	0.0
331, 321	600	316SS	316SS	0.214	2.5/13	2.0

Tube Surface Preparation

The occasional observation that a scratch on the tube surface may lead to heavier deposits along that line led us to wonder how critical surface preparation procedures might be. Moreover, a recent report[26] on the preparation of JFTOT tubes that dry abrasives significantly increased thermal ratings over those obtained with the standard A-1 polish further piqued our interest. Electropolishing has also been reported to increase preheater tube deposits.[27]

We decided to look at the effect of polishing agents, and also to see what effect the degree of polishing might have on coker ratings. Two fuels were selected for these tests: Decalin, for 600°F, and SHELLDYNE-H, for 700°F. A large backlog of ratings was already available on these fuels with the A-1 polish, which increased their reliability as reference standards. Polishing agents investigated included two dry abrasives, two liquid polishes, one waxy polish containing an abrasive, and one dry abrasive made into a paste with Decalin. These are shown together with test results in Table 10A.

Overall, the differences in Decalin ratings were not large. The two dry alumina abrasives did produce higher ratings (3.5/26-27) than did A-1 polish (2.5/12.5-15), and both of the alumina polishes produced surfaces which were not quite as mirror-like as can be obtained with A-1. However, the latter fact may not be important, since the rather coarse Rayosol polish, which produces a fresh surface resembling code 1, gave ratings in excellent agreement with A-1. The larger total code obtained with Rayosol was due to the diffuse appearance of the metal substrate in low deposit or deposit-free areas.

Similarly, no significant effect was found between new tube code ratings of "0" and "0.5" with the same A-1 polish. However, liquid polishes gave generally lower deposit ratings.

In contrast to Decalin, SHELLDYNE-H produced a distinctly lower deposit rating for a highly polished tube (code "0") than for the less polished surface (code "0.5").

Thus, different fuels may have different sensitivities to surface roughness, and it is clearly important that the tube surface be carefully prepared by a reproducible method.

Tube Deposit Rating Methods

Besides the inherent weaknesses of the coker test itself, the strictly qualitative nature of the color code rating method often casts complete doubt on comparative ratings. Deposit colors sometimes do not correspond at all to the yellow-tan shades of the color comparator; sometimes the deposits are transparent, sometimes they are opaque. One never really knows how thick they are.

The necessity of having a thermal stability test for research purposes which will provide quantitative relative measurements of the deposits laid down has led us to explore several different methods of deposit rating. Included among these are: 1) direct heat transfer coefficient measurement;

Table 10b. INFLUENCE OF POLISH TYPE AND FRESH TUBE FINISH ON TUBE RATINGS

Fuel	Polish	"Fresh" Tube Rating, Code	Deposit, Max./Total	Temp, °F
Decalin	A-1	0	2.5/12.5	600
Decalin	A-1	0.5	2.5/15	600
Decalin	Raycool	1	2.5/21.5	600
Decalin	Silicon Carbide/Decalin Paste	0.5	3/16	600
Decalin	Tripoly (fine; rouge dispersed in a waxy base)	0	3/16	600
Decalin	Gamma Alumina No. 3 (dry)	0-0.5	3.5/26	600
Decalin	Alumina No. 40-6430AB (dry)	0-0.5	3.5/27	600
RJ-5[a)]	A-1	0	2/5.5	700
RJ-5[a)]	A-1	0.5	2.5/18	700

a) SHELLDYNE-H.

2) combustion of the deposit, followed by absorption of the product gases; 3) radiative methods; 4) solvent dissolution and gum determination. These will be reviewed briefly relative to their strong and weak points.

Direct Heat Transfer Coefficient Measurements

The advantage of this method is that it gets right at the property of interest. Indeed, all other methods may be regarded as simply being indicative of what the relative reduction in heat transfer coefficient might be.

In our efforts to measure heat transfer coefficient changes due to coker deposits and artificial acrylic lacquer "deposit" films, we found that coatings above 0.1 mil and above code 4 were necessary. Only if the severity of the coker test were greatly increased would it be possible to practically apply this approach directly to coker tubes, which would almost certainly involve a higher temperature or a longer test than the standard 5 hours with the ASTM Coker. The cleverly designed Minex II tester is purported to be capable of accomplishing this in a 10 to 15 hour test.[25] (More recently the time for a test has been lowered to 5-6 hours, but at a higher temperature.)

Complete Combustion of Tube Deposits

The combustion method involves conversion of the deposit to CO_2 and H_2O, followed by either absorption and weighing, or by gas chromatographic detection. It is assumed that sulfur and nitrogen can generally be neglected, and that in fact, CO_2 determination will be sufficient. In our own tests, we have measured H_2O as well, since this procedure permits us to determine the C/H ratio of the deposit.

Figure 57 shows schematically the apparatus used for determination of deposits on coker tubes. The coker tube is placed in a heated shell so as to form an annular space through which air is passed. The effluent from the combustion zone is passed through a cupric oxide bed which operates at 1600°F, where conversion of CO to CO_2 occurs. CO_2 and H_2O are then separately absorbed and gravimetrically determined.

Polystyrene "deposits" were used to determine the precision of the method, as shown in Table 105. Recovery was generally found to be within 5 percent, provided adequate oxygen flow rate and time is provided to complete the reaction.

The combustion method was found adequate for the rating of coker tube deposits; however, certain drawbacks do exist.

First, the method is not rapid in its present form, considerable time being required for handling and weighing. While these factors can be improved, a further disadvantage is that the approximately 1000°F temperature required for combustion damages the tube, possibly rendering it unsuitable for further coker runs.

Sensitivity of the method is limited mainly by the ability to avoid contamination via the air or from other adventitious organic substances. All traces of fuel and rinse solvents must of course be removed.

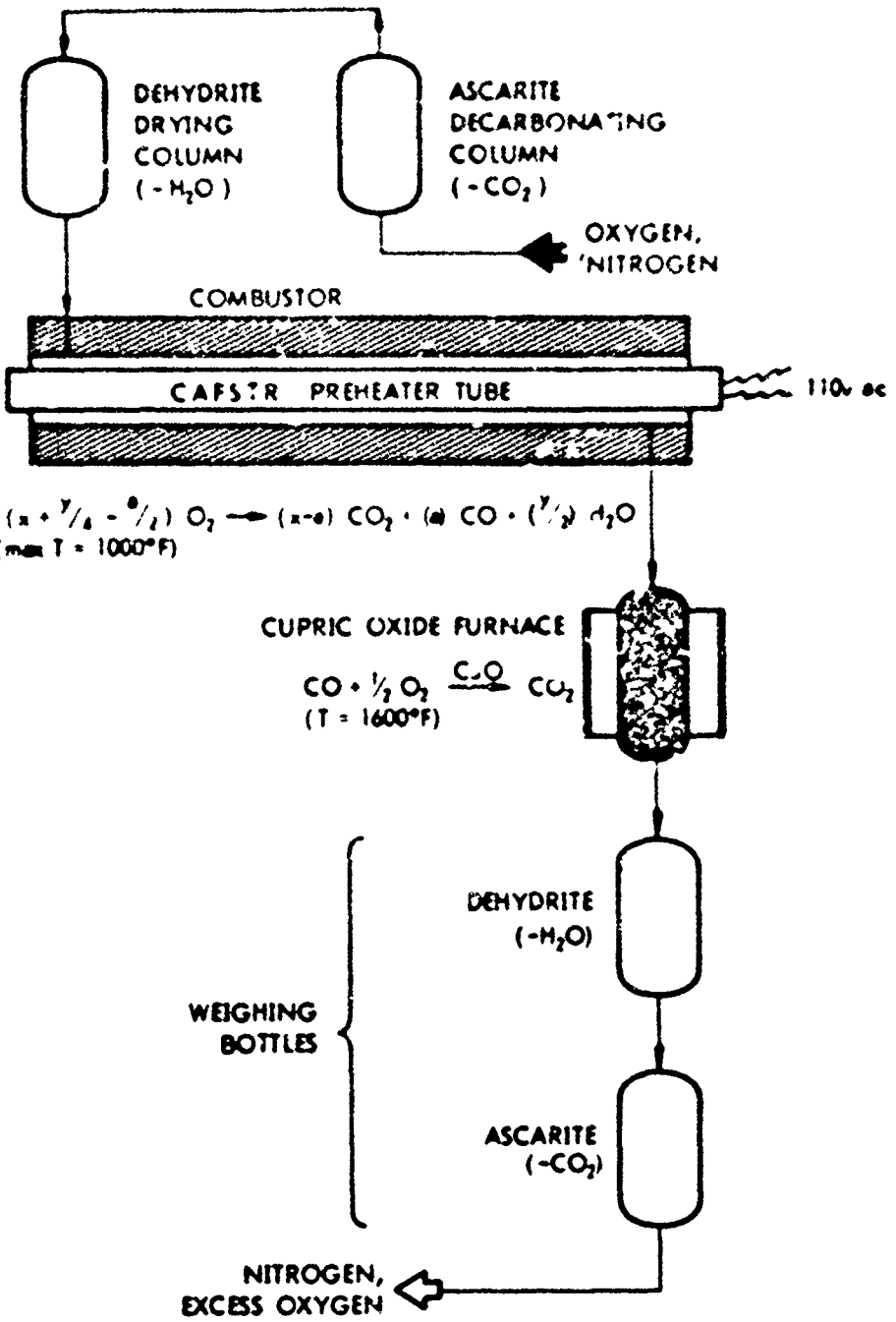

Figure 57. COMBUSTION TUBE RATOR DESIGN

Table 105. COMBUSTION RATINGS OF POLYSTYRENE "DEPOSITS"

Tube Wall Temp, °F	Gas		Deposit		Est. Max. Code Rating	Percent[a] Deposit Recovered
	Flow, ml/min	O_2, %	Wt, g	Average Thickness, mil		
1000	350	77	.0348	.083	8	104
1000	250	28	.0144	.034	8	96
1000	250	28	.0043	.01	5	107
1000	250	46	.0105	.025	8	105
1100	250	46	.0142	.034	8	100
1000	200	48	.0365	.087	8	69

a) Calculated from CO_2 and H_2O recovery.

A variant in the combustion method which circumvents the tube damage problem is the substitution of ozone for part of the oxygen. However, this approach has not yet proved completely successful. The difficulty has arisen from the amount of time required to remove the deposits, and the stringent requirement of almost perfect purity of the oxygen necessary to avoid error.

A critical factor appears to be temperature. If the temperature is too high, the ozone decomposes too fast; if the temperature is too low, the reaction rate with the deposit is too slow. In our experimental setup, a tube temperature of about 200°F appears to be near optimum. At this temperature, however, nearly two hours flow, with flow conditions of 0.025 ft^3/min. and 80 mg O_3/liter, are required to completely remove a code 4 deposit. After this exposure there still remains a white powdery film, believed to be metal oxides, but not proven. The origin of the oxide film is uncertain, since it extends far beyond the area of visible deposits observed prior to the ozone treatment. The material could, of course, originate from the fuel and the pump, but in two tests where a brass thermocouple shield was inserted through the outer wall of the oxidation chamber, copper was transferred to the surface of the coker tube. This suggests that ozone is capable in some way of volatilizing a metal and then depositing it again, perhaps after critical partical sizes have been attained. Thus, the metal film observed could partially result from transfer from other metal parts of the deposit removal system.

At the flow conditions cited above, about 85 liters of oxygen containing a total of about 6.8 g ozone will have passed over the coker tube. Perhaps a design which would provide greater turbulence would result in a more efficient utilization of the ozone and a shorter time to accomplish the deposit removal, since this amount of ozone is many times greater than is needed to burn off a maximum of perhaps 0.2 mg of deposits (at code 4). A reduced time and total flow is of course desired. For example, at the flow conditions described, impurity levels in the oxygen which would cause a rating error equivalent to 1/2 code number or more would only have to exceed 0.6 ppm CO_2, 1.5 ppm H_2O, or 0.5 ppm CH_4. If the equipment design can be suitably altered, the importance of gas stream impurities might be greatly reduced by reduction in the amount of oxygen required. However, the limitation may be a very slow reaction rate of ozone with the deposits, in which case ozone may simply prove to be impractical. Some further investigation of this approach is warranted.

In addition to the use of combustion with the SD Coker tubes, we have also experimented with the combustion method on the small (Alcor) JFTOT fuel tester tubes. Here, although the amounts of deposits are smaller, the entire tube can be combusted in a closed vessel and the CO_2 determined by either infrared or gravimetric analysis of the product gas. Sensitivity in this instance is even more favorable than that with the larger tubes since the amount of oxygen required is comparatively small, and impurities in the oxygen are of negligible importance. Moreover, the smaller tubes are less expensive and can be expended after each run.

We have rated the deposits on a series of five such tubes which were obtained from the ALCOR Corporation. Each had been run on a turbine fuel and had a max. code rating of 4 or over. We rated these tubes visually along each cm of its total 6 cm length, recording both the max code and the integrated visual rating. The tubes were then rated by the beta-backscattering technique discussed in the next section of this report. Finally,

each tube was sectioned into 1 cm lengths and the deposit thickness determined by the combustion method. Figures 58 through 62 show the comparison of the visual and combustion rating profiles, where the maximum deposit level was assigned a value of 1.0 on a relative deposit level scale. It can be seen that the visual profile generally follows the combustion quite well, although tubes No. 1 and 4 show some marked disagreements and demonstrate how the visual method can give some misleading results. This assumption that the combustion rating is more correct than the visual is intuitive, but also is in agreement with the results from the beta-backscattering method, as shown in comparison of the total deposits of the five ALCOR tubes (Figure 63). Here it may be seen that the combustion and beta-backscattering methods always agree as to the relative total amounts of deposits, and that the visual ratings may deviate in either direction from the true quantitative amount. These data illustrate the deficiencies of the standard visual method of rating tubes. On the basis of the agreement between the combustion and back-scattering method we have designed and received authorization for the construction of a prototype β-ray back-scattering device.

Radiative Methods

Two methods of radiative deposit rating have been considered. First of these is the beta-radiation back-scattering technique, which we have already mentioned as being effective in the rating of the small TOT tube deposits.

This method involves placing the tube in a partial vacuum and irradiating it with a soft beta source such as ^{63}Ni, while simultaneously measuring the back-scattered beta particles. The tube was scanned longitudinally along representative sides, and the back-scattering compared with that from the clean tube. Calibration is achieved by means of a film of known thickness of polymeric material. Details of the method are elaborated in the Appendix.

Sensitivity of the method proved adequate to detect the equivalent of half an ASTM code number, but revealed very poor correlation with visual ratings, as was shown in Figures 58-63, and as is shown again now in Table 106. This fact provides additional evidence for the great need to quantify coker deposit ratings. Comparison between the three methods of rating coker tubes, visual, combustion and β-ray, are shown in Table 107.

Infrared offers a further possible method of deposit rating. However, inquiry made to manufacturers of infrared equipment has led to the conclusion that light coker deposits are too thin for detection by infrared absorption. There is the possibility that differences in emissivities of the bare metal and film coated surfaces might provide a basis for infrared detection.

Our only attempt with infrared involved heating the coker tube to about 600°F in a totally dark room, and then photographing it with type 413 Polaroid infrared film. At this temperature, a 3-minute exposure was required to record any kind of an image at all, but the deposit area could not be distinguished. We are informed that more sensitive detectors are available, but this approach appears very expensive.

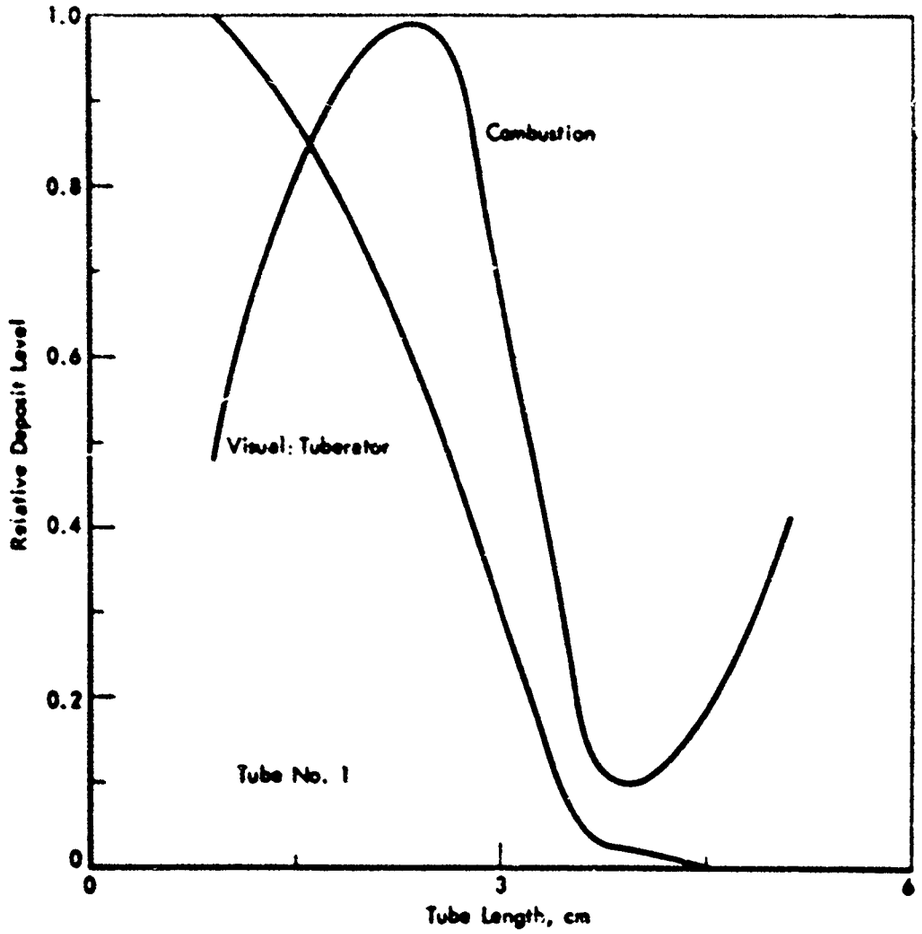

Figure 58. COMPARISON OF DEPOSIT PROFILES
Combustion vs Visual Ratings

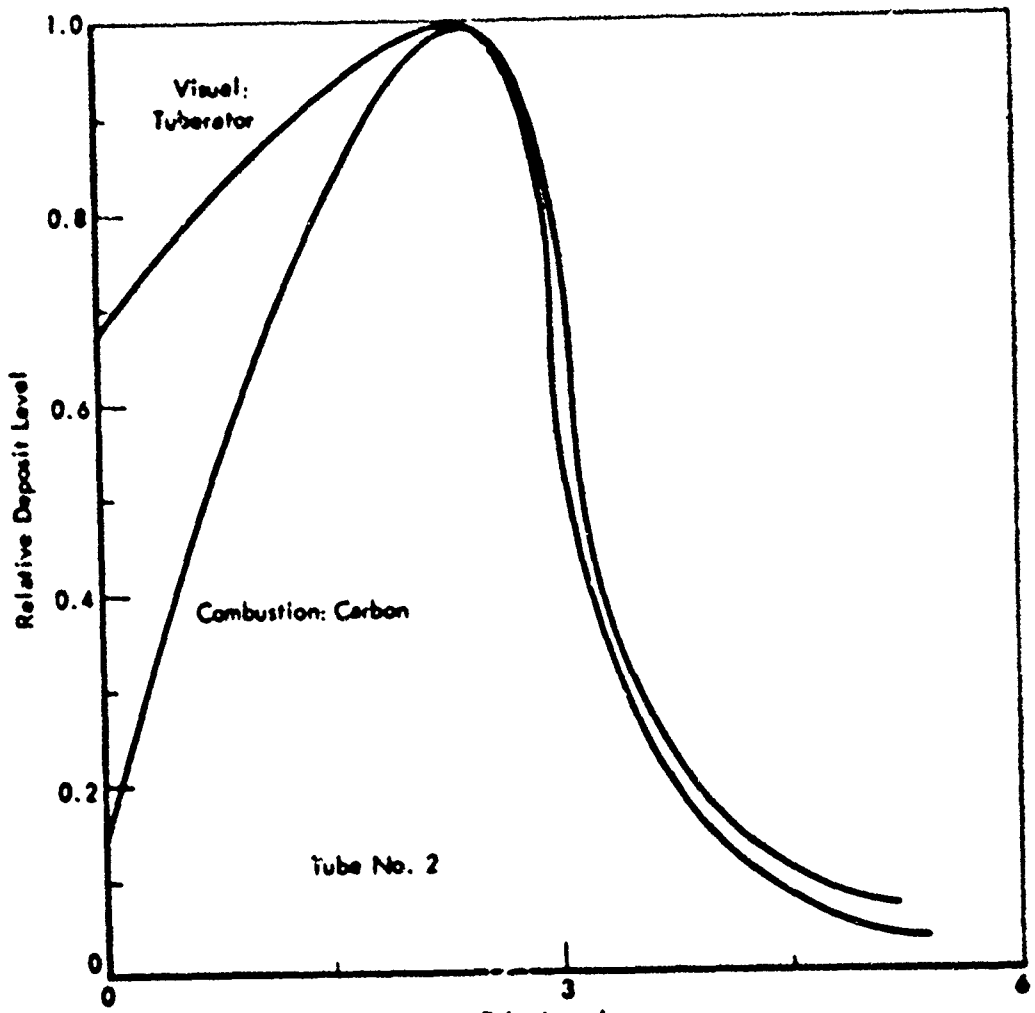

Figure 59. COMPARISON OF DEPOSIT PROFILES
Combustion vs Visual Ratings

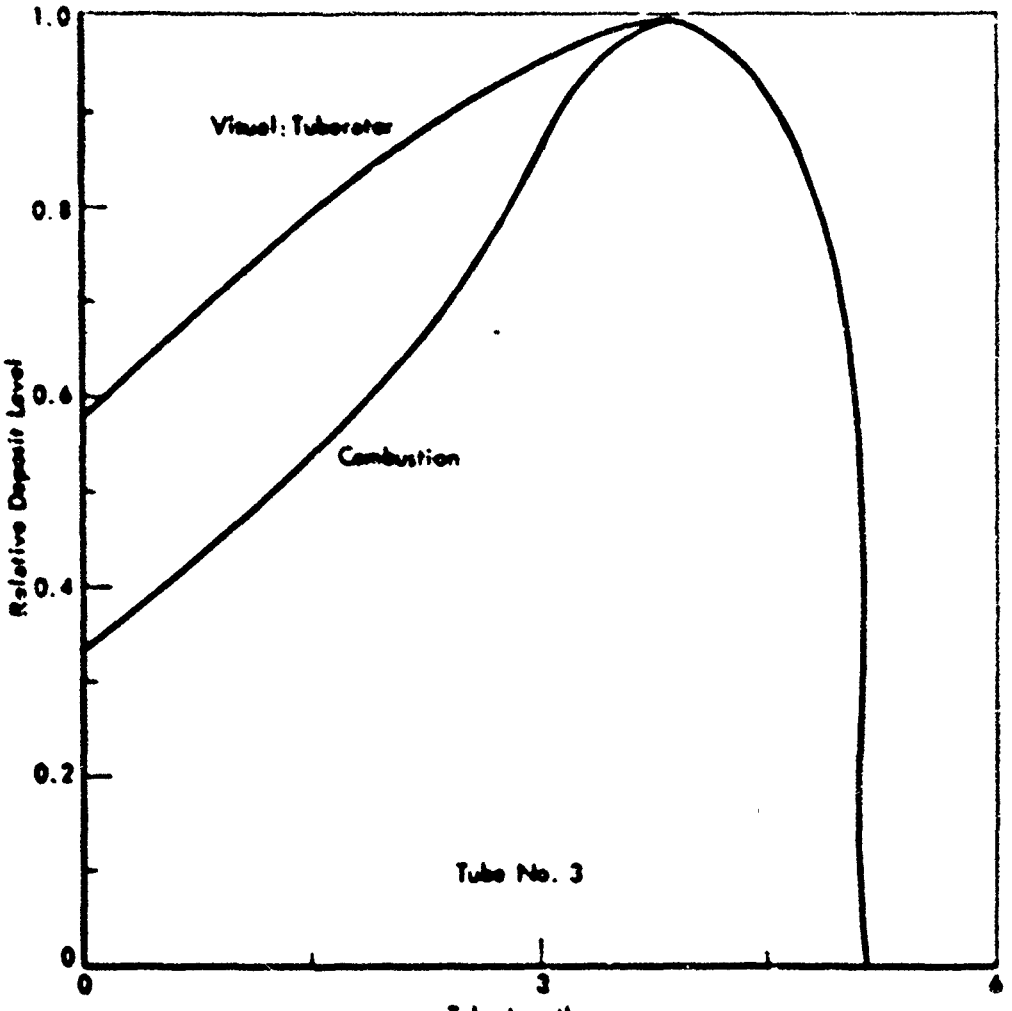

Figure 60. COMPARISON OF DEPOSIT PROFILES
Combustion vs Visual Ratings

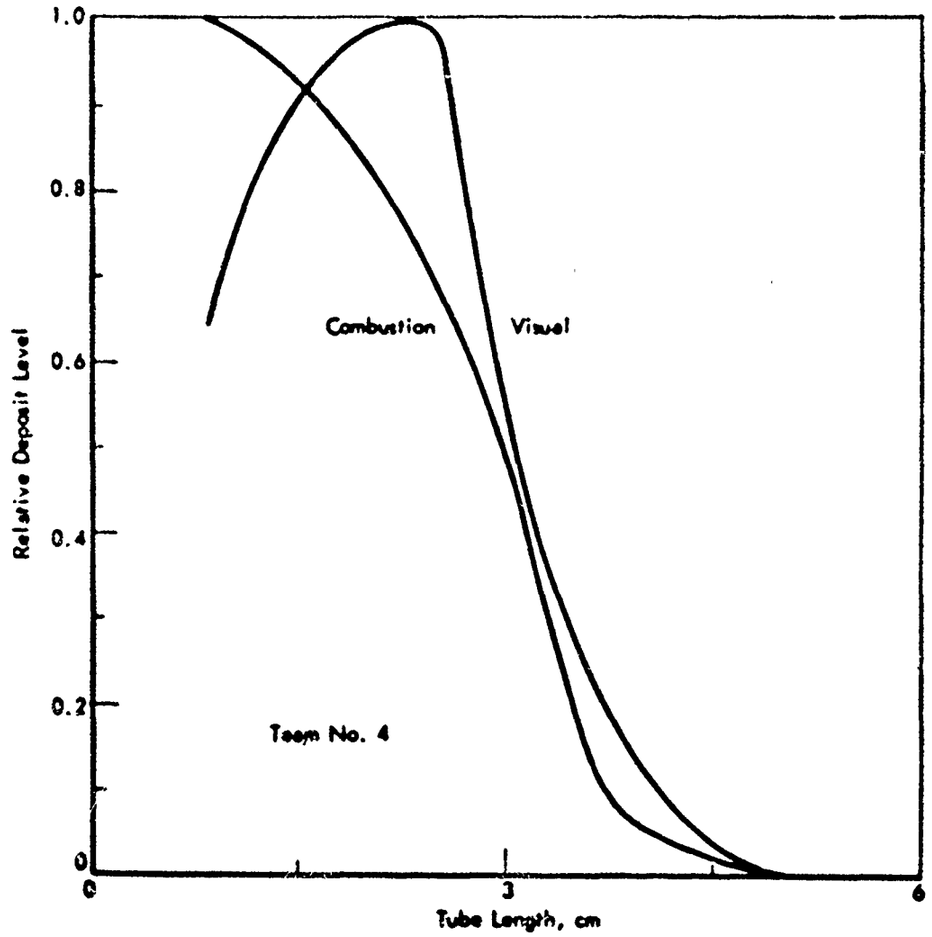

Figure 61. COMPARISON OF DEPOSIT PROFILES:
Combustion vs Visual Ratings

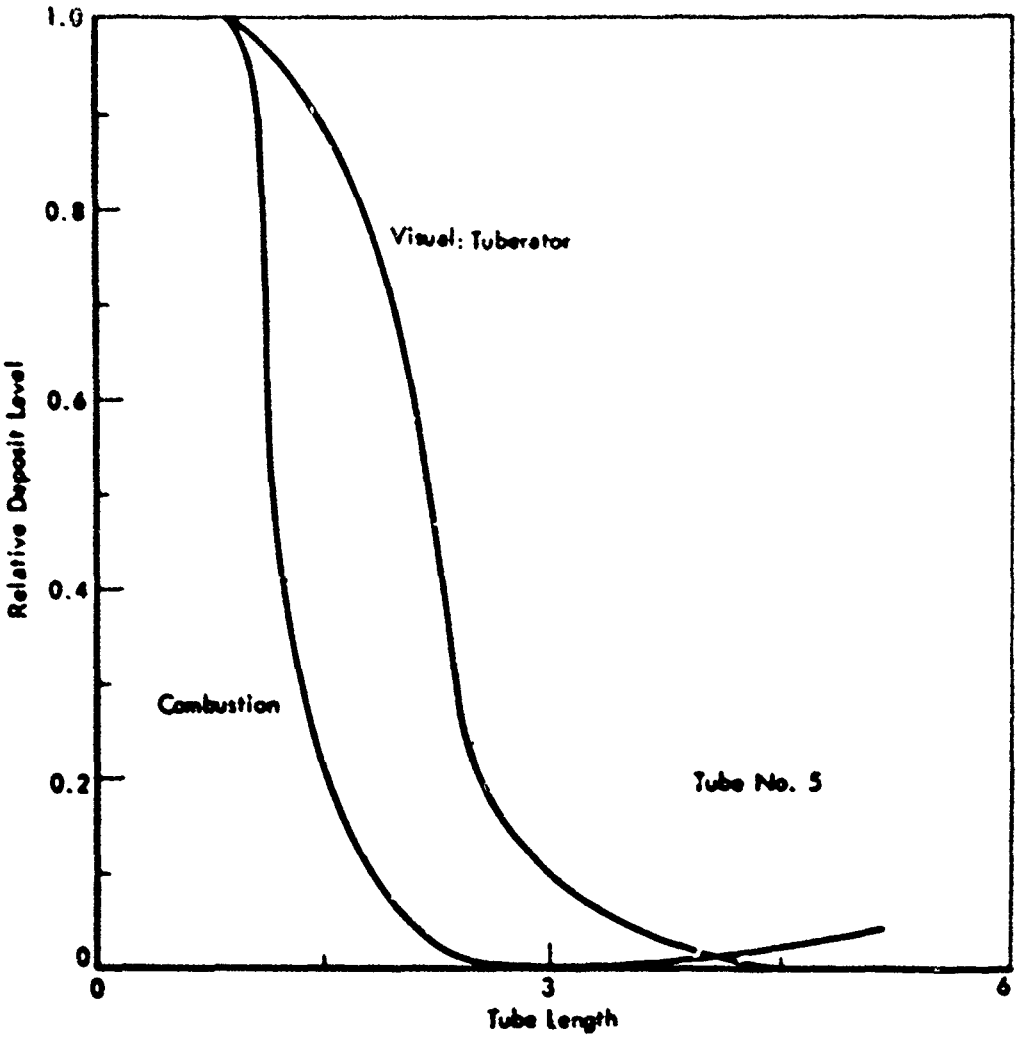

Figure 62. COMPARISON OF DEPOSIT PROFILES
Combustion vs Visual Ratings

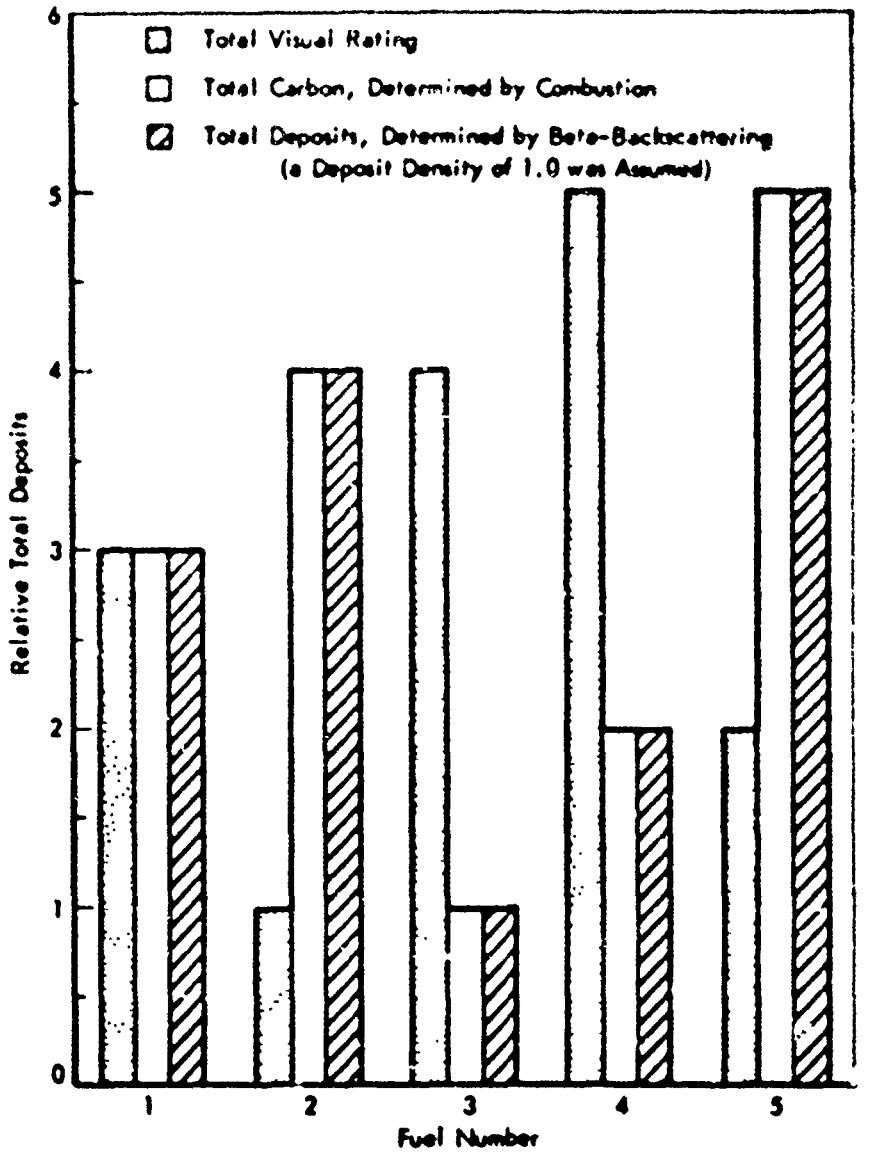

Figure 63. COMPARISON OF TUBE DEPOSIT RATING METHODS

Table 106. COMPARISON OF BETA BACK-SCATTERING WITH VISUAL RATINGS OF JT8D TUBE DEPOSITS

Tube	Beta Count Decrease, Counts/sec	Maximum Thickness		Width by Beta, cm	Area, Å x cm	Width, Visual, cm	Visual Code	
		Å	mils				Max	Avg[a]
1	85	5000	0.02	3.5	6000	3.3	5	1.3
2	70	4500	0.018	4.0	7000	4.4	4	2.0
3	20	1200	0.005	3.5	1500	5.8	4	2.3
4	50	3000	0.012	4.0	4000	3.9	6.5	2.6
5	125	8000	0.032	2.5	6000	3.25	6.5	1.4

a) Weighted average.

Table 107. COMPARISON OF THREE DEPOSIT RATING METHODS-EXAMINATION OF FIVE TUBES FROM THE ALCOR "JFTOT" THERMAL STABILITY TEST RIG BY COLORATOR, COMBUSTION AND BETA-BACKSCATTER

Tube No.	Total Deposits µg C			Relative Ratings			Relative Rating Order of Tubes		
	Visual[a]	Comb.	Beta-[b]	Visual	Comb.	Beta-	Visual	Comb.	Beta
1	72	58	79	.64	.29	.96	3	3	3
2	58	104	80	.52	.52	.97	5	2	2
3	104	25	18	.32	.12	.22	2	5	5
4	112	27	46	1.0	.14	.56	1	4	4
5	72	200	82	.64	1.0	1.0	4	1	1

a) For comparison purposes, color code ratings were assigned the following values: Code 1 = 45 µg; Code 2 = 90 µg; Code 3 = 135 µg on the basis of best present knowledge. The code ratings are weighted averages for the entire tube surface.

b) Beta-backscattering thickness measurements were converted to weights by assuming a deposit density of 1.0 and calculating a weighted average for the entire tube surface.

Solvent Deposit Removal

Coker deposits might conceivably be removed and weighed, but are difficult to scrape off mechanically without removing some metal as well. We therefore thought of trying the idea of dissolving the deposit into a suitable solvent, and then determining the deposit level by running a gum determination on the solvent.

Since past experience had shown that coker tube deposits are generally not very soluble, particularly if they are of the resinous, adherent type, we used a heated shell into which the coker tube could be inserted. About 50 ml of solvent was required to submerge the tube, and the temperature of the solvent was raised to 100°C (or less, if the pressure reached 200 psig).

As will be seen from the summary of results shown in Table 108, only N,N-dimethylformamide came even close to doing a complete job of removal. A second treatment with DMF sometimes completed the deposit removal, as nearly as could be detected visually, but more often left a patchy light stain. Again, the method was found time consuming, about 2 hours being required for best results.

Summary of Deposit Rating Methods

Several additional approaches to quantitative deposit rating have been considered, utilizing such techniques as measuring capacitance or conductance: measurement of the UV, Visible, or x-ray absorption; oxygen plasma burning; and microwave spectroscopy. Some appear to be prohibitively expensive; others, insufficiently sensitive.

Of those tried, the combustion and beta back-scattering approaches appear most promising. Table 109 summarizes the estimated minimum deposit detection levels for the methods discussed, which shows that all except direct heat transfer coefficient determination have sufficient sensitivity for coker tube deposit application.

Beta back-scattering appears to be the simplest and quickest test, and it appears that the assumption is safe that the deposit consists almost entirely of carbon and hydrogen. Most other elements which are likely to be found in the deposit will tend to cause a slight error in the direction of indicating that the film is thinner than it really is. Thus, elements such as O, S, Fe, Pb, Cu, etc., which are commonly found in fuels, if they become part of the deposits, would increase back-scattering and make the deposit look a little thinner to the instrument. This effect is roughly proportional to the atomic number and the concentration of the element. Although every tube metal - even different aluminum alloys - would require recalibration, this could be done by cleaning a small section of the tube before rating. Table 110 gives an estimated indication of the extent of the effect of impurities.

It would probably be worthwhile to have available film approximating in composition and thickness a typical deposit for calibration purposes.

Table 108. SOLVENT DEPOSIT REMOVAL TESTS

Solvent	Temp, °C	Press., psig	Time, hr	Tube Rating	
				Before	After
Morpholine	100	27	2	4+	7.5
2-Nitropropane	90	200	1	3.5	4.5
Tetrahydrofuran (THF)	100	170	1	3.5	3.5+
Hexylene Glycol Diacetate	50	190	1	3.5	4.5
N,N-Dimethyl Formamide	100	32	3/4	3.5	3.5
DMF (2nd Consecutive exp.)	100	225	1	3.5	0
DMF	100	28	1	4.0	1.0
DMF (2nd Consecutive)	100	25	2	1.0	0
DMF	142	180	1	4.0	3.0
1/3 DMF + 2/3 THF	90	190	1	3.5	3.5
1/2 DMF + 1/2 Morpholine	100	90	1	4.0	7.5
Shell Solutizer Solution[a)]	100	25	1	2.0	3.5
Sulfolane	100	6	1	2.5	2

Solvents which had no effect: Dimethyl sulfoxide, Phorone, Piperidine, Diacetone Alcohol, Amyl Acetate, Propyl Alcohol, sec-Butyl Alcohol, Methylene Chloride, Acetone, Methyl Ethyl Ketone, Toluene, Freon-II, Mesityl Oxide.

a) 6 N KOH, 3.1 N KIO3.

Table 109. ESTIMATED MINIMUM DETECTION LEVELS FOR FIVE DIFFERENT COKER TUBE RATING TECHNIQUES

Rating Method	Average Deposit Thickness,[a] mil	Total Deposit Weight, mg	Approx Max Color Code Equivalent[b]
ASTM Color Code	0.002	0.2	1.0
Heat Transfer Coefficient	0.25	26	8
Combustion	0.003	0.3	1.0
Beta Back-Scattering	0.003	0.3	1.0
Solvent Removal	0.003	0.3	1.0

a) Maximum deposit thicknesses are usually several times the average thickness.
b) Assuming Max Code = 2 x Average Code.

Table [illegible] ESTIMATED ERRORS IN BETA BACKSCATTERING MEASUREMENTS OF DEPOSIT THICKNESSES DUE TO NON-CARBON ELEMENTS

Assumed Composition of Deposit	%w non CH	Error in Deposit Thickness, %
CH	--a)	--a)
CH_2	7, H	-2.0
$CHO_{.25}$	23.5, O	+1.5
$CHS_{.05}$	11.0, S	+3.5
$CHFe_{.01}$	4.1, Fe	+2.5
$CHPb_{.001}$	1.4, Pb	+3.1

a) CH was taken as the reference composition.

Thermal Stability of Dimethanodecalin and RJ-4 Fuel

As a part of a continuing program of rating thermal stabilities of candidate endothermic fuels, dimethanodecalin and RJ-4 fuel (Tetrahydromethylcyclopentadiene dimer, obtained from Esso Research and Engineering Company, and designated TH Dimer Ramjet) were tested in the SD/M-7 coker. Results of these tests are compared in Table 111 with similar results for SHELLDYNE-H and Decalin.

Table 111. THERMAL STABILITY OF DIMETHANODECALIN AND RJ-4 FUEL IN THE SD/M-7 COKER AT 150 PSIG

Run No.	Test Fuel	Density, g/ml (68°F)	Preheater Temp., °F	Preheater Tube Ratings, Max./ Total Cokes
397	Dimethano-Decalin	1.01	600	3.5/27.5
(composite)	Decalin	0.876	600	2.5/15
389	RJ-4	0.918	550	2/12
390	RJ-4	0.918	600	2/12.5
391	RJ-4	0.918	650	3.5/20.5
(composite)	SHELLDYNE-H	1.072	750	2.5/15.5

From the data, RJ-4 has an estimated breakpoint of about 625°F, whereas that of dimethanodecalin would be about 575°F. By comparison, SHELLDYNE-H and Decalin[29] have breakpoints of 750 and 600°F, respectively. However, the result on dimethanodecalin is on the basis of a small, old sample which, though refrigerated, could have deteriorated in the ten years since it was made. It will therefore be necessary to confirm the present results with a fresh sample.

Effect of Decalin Impurities on Coker Ratings

When 30 drums of RAF-161-60 Decalin were purified recently,[18] the silica gel treatment removed appreciable amounts of color bodies and produced a water white product from the original material which had a strong yellow treatment prior to treatment. Existent gum and particularly fuel coker ratings were improved.

Following the silica gel treatment, the gel was drained, washed with n-hexane, and eluted with acetone. The recovered extract was then water washed and vacuum flashed to remove the acetone and hexanes. When the product was cooled to -2°F, a crystalline substance separated out, leaving a dark brown-black liquid. The crystalline phase by itself melts at a temperature above 70°F, however.

We were interested in learning what the active ingredient responsible for the poor coker ratings of the untreated Decalin might be, since its presence at a concentration of 1000 ppm or less was surprisingly harmful. Erdco Coker ratings of Decalin before and after silica gel treatment are shown in Table 112.

Table 112. EFFECT OF DECALIN IMPURITIES ON COKER RATINGS

Coker	Fuel	Temp, °F	Pressure, psi.	Tube Ratings
Erdco	Decalin, "as received"	500 600	250 250	2/ 5 4/23.5
"	Decalin, silica gel treated	625	250	3/ 20
SD/M-7	Decalin + 1% Xylene desorbate	550	150	2/12.5
"	Decalin + 1% liquid desorbate	550	150	2/ 12
"	Decalin + 1% total desorbate	550	150	4/23.5
"	Decalin, silica gel treated	660 625	150 150	2/ 12 3/ 17

SD Coker runs were made on reconstituted blends of purified Decalin with the total extract, the crystalline phase, and the liquid phase. Results of these tests are also shown in Table 112. Curiously, neither the crystalline nor the liquid phase were very harmful to coker ratings separately; but the total extract was harmful, though less so than expected from the original "as received" Decalin ratings of the Erdco Coker.

Two explanations seem possible for the apparently lighter reconstituted ratings. First is the possibility that some harmful impurity was adsorbed from the Decalin which was not desorbed by the acetone. The second, and more probable, is that we are seeing a true difference in the way the SD Coker and the Erdco Coker rate a fuel where the deposits are due to an almost trace component. Thus, the deposit in the Erdco test derives from about 6.8 g impurities (3 lb/hr x 453.6 g/lb x .001), whereas the deposit from the SD test comes from only about 0.3 g impurities (350 ml x .883 g/ml x .001). However, when the pure silica gel treated Decalin is being tested, the Erdco and the SD Cokers agree very well indeed (see Table 112). This comparison is in agreement with earlier predictions concerning similarities and differences of the two cokers.[34]

We are unable to explain the apparent synergistic effect of combining the liquid and crystalline impurities removed from the Decalin, however. Some work will be done in the future, involving further separation of the impurities.

New Equipment for Thermal Stability Testing

To broaden the scope and understanding of the thermal stability problems of endothermic jet fuels we have recently purchased from ALCOR, Inc. a Phillip's 5-ml Bomb Apparatus Assembly. This equipment has now been assembled and will be used for occasional correlation tests with the Erdco and SD Fuel Cokers.

We have also constructed another small stainless steel bomb for development studies on a new thermal stability test. The concept of the test is to accumulate deposits on finely divided metal or catalyst particles of very high surface area. It is hypothesized that, among other factors, the deposition tendency is dependent on surface area, surface roughness, and it should be possible to reduce both test time and sample size. The hope would be to develop a thermal stability test which would be rapid and simple, yet would reflect the deposit forming tendency of the fuel as reflected by the coker test, or better still by the engine itself.

We propose to accomplish this by adding the suitable metal and fuel to the bomb, expose it to temperature in the presence of oxygen, then remove the metal particles, wash and dry them, and determine the deposit weights. The latter might be performed either by combustion or gravimetrically.

Two previous bombs were built for this purpose. The first, constructed of aluminum, failed by seizure of the threads at the end of a test. The second, made of stainless steel, had an inadequate seal which leaked under pressure. The present bomb is also constructed of 316 SS, but is equipped with a crown seat. A nickel bursting disk also serves as a soft gasket to insure a perfect seal. The bursting disk is designed to rupture

at 1006 psi and 500°F. Total volume of the bomb is 3.55 ml. The bomb itself is 1" OD x 2-3/8" long; overall length including the head is 3". In operation the bomb will be dropped into a snugly fitting hole in a previously heated aluminum block 4" in diameter and 2-1/2" thick. After some time (perhaps one hour) the bomb will be pulled out of the block, quenched and opened. The bomb will also contain a small Teflon-coated stirring magnet which will be rotated during the test.

In a typical projected experiment with Decalin, for example, the following situation might exist:

Initial contents of the bomb:

0.79 g Decalin (= 0.89 ml)

0.1 ml of finely divided metal stirring magnet

ca 2.15 ml of O_2 at 1 atm pressure

At 500°F the liquid Decalin will constitute 0.76 g (1 ml) of the total amount, and the total pressure will be 89.1 psig.

The apparatus is completely set up for testing, with suitable temperature controller, and candidate metals and/or catalysts are being prepared for initial tests. Powdered metals including Fe, Cu, 304 and 316 stainless steel, Ni, and Zn are being reduced in a hydrogen blanketed furnace and will be tried first.

Modifications to the SD Fuel Coker

As was previously described, the Zenith pump in the present SD Coker system serves only to meter the fuel and to recirculate it. Since the pump is of a volumetric type, the flow rate is determined with an electronic counter which reads in terms of an rpm the rotation of the pump drive gear. (Total pressure is supplied by the sparge gas.) With the present Type-2 Zenith pump the speed is ca 43 rpm for delivery of 6 lb/hour fuel flow (depending upon the exact fuel density), which makes possible the control of flow to within ±0.5 percent (2 counts in 430) once the proper count rate has been established. This is done for each new fuel at the beginning of a run by measuring the time required to collect 50 ml (since the pump is volumetric, the number of counts is always the same: 429-431 cpm). The precision of the flow control system thereafter is dependent on the assumption that the pressure drop across the pump remains relatively constant, which is true unless abnormally high filter plugging develops. When there is no filter plugging, the pressure developed by the pump is just the small system flow resistance amounting to a few inches of water pressure drop. Generally, the small build-up of pressure drop during a run has an insignificant effect on pump slippage or efficiency.

However, with the electronic monitoring system alone, once the run is in process it has been impossible to get a direct flow measurement (because the entire recycle flow system is under system pressure). On rare occasions where extreme filter plugging occurred, reduced flow became apparent when reduced preheater power requirements were observed, in which case the run was either terminated or the pump speed was compensated to restore normal power requirements.

To remedy this problem we have now installed a Fischer-Porter Model 10A3665A Rotameter with a stainless steel ball. The rubber seals were replaced with Teflon, and all surfaces in contact with the fuel are either stainless or Teflon. The rotameter can be safely operated to 500 psig and is equipped with a safety shield. Although the scale can be read to .05 on a 0 to 25 spread, we only use the rotameter as a visual flow monitor. If the flow were to deviate significantly from the control setting, pump speed would be varied to restore it.

Filter Pressure Differential

The present SD Fuel Coker requires about 350 ml per test. This requirement is largely due to the Foxboro d/p cell used for measuring filter pressure drop. Since experimental fuels are frequently in short supply, we have decided to reduce this requirement to an absolute minimum by replacing the d/p cell with a Model PL280TC-15-350 Statham Differential Pressure Transducer. The present double pen Brinton ΔP and P recorder will be replaced with a Model UR5 Statham Analog Readout and 0-600 psig Duragage. All metals are stainless steel. The transducer is good for 1000 psig static pressure and ranged for 15 psig maximum differential pressure. There is provision for a large differential overpressure safety margin.

Equilibration gas sparging will be accomplished in a separate sparge and disengagement tube. (Currently, re-equilibration is being accomplished via a bubbler in one side of the d/p cell.) But even with this tube it is hoped to be able to get by with as little as 125 ml per test.

Tube Surface Preparation

Recent work by R. M. Schirmer[35] has shown that deposits form preferentially at the ragged edges of scratches on the tube surface, suggesting that surface roughness may not only affect the appearance of the tube with respect to visual rating, but the actual amount of deposits formed as well. We have therefore determined to exercise increased care in the preparation of the tube surfaces, and have installed a new lathe in the lab to assist in the accomplishment of this aim. The convenient location of the lathe will also result in time savings over the use of shop lathes as well as reducing the possibility of contamination.

Coker Tube Surface Temperature Measurements

The formation of the tube deposits is believed to be more closely related to surface temperatures than to the liquid bulk temperature. Therefore, as a further aid to the interpretation of coker data, we have begun ordering coker tubes with a chromel/alumel thermocouple installed on the inner surface of the tube wall. However, presently this is just for observation purposes, and the preheater temperature control is on the preheater fluid effluent, in the conventional way.

Electron Microscopic Examination of a Plugged Filter

Because of their purity, almost none of the candidate endothermic fuels are limited in thermal stability by filter plugging. Another reason for this absence of filter plugging is that often the temperatures in the

preheater and filter are above the boiling point and the fuel passes through the filter as a vapor.

When filter plugging does occur, there is often some doubt as to whether the test fuel is the source of the solid matter, or whether the fuel loosened some debris or deposits from the system not removed in cleaning. Also, there is a question as to whether plugging is due to fuel oxidation or to adventitious impurities introduced with the fuel.

We were stimulated by the excellent work of R. M. Schirmer on the morphology of fuel deposits[35] to scan a coker filter under the electron microscope in search of clues for filter plugging. The filter is a conventional 5 micron (nominal) pore size, sintered stainless steel construction. Photographs were taken of a filter from a run with SHELLDYNE at 625°F and 150 psig where the ΔP had increased to ca 50" Hg; that is, the filter was almost completely plugged. Under these conditions the SHELLDYNE would be mainly in the liquid condition. The instrument used for this work was a Japan Electron Optical Laboratories Scanning Electron Microscope, and the sample was first given a thin gold overlay before scanning. Photographic results are shown in Figure 64, a-e at magnifications of 100x, 500x, 1000x, 5000x, and 10,000x.[a]

The large round mounds in the center of a and b Figure 64, are granules of the stainless steel filter, overlayed with an apparently congealed deposit. An enlargement of the structure of this deposit is shown in c and d of Figure 10. The shot in e at 10,000x is the edge of one of the holes shown in c and d. It was the molten deposit which almost totally sealed off the filter. The large resinous looking chunks of material in b appear to be broken off from some place else in the system and then carried in the stream to the filter. Other forms of debris and unidentified particles are observable in a, probably partly from the original fuel.

a) Photographs were taken by R. G. Meisenheimer of the Analytical Department.

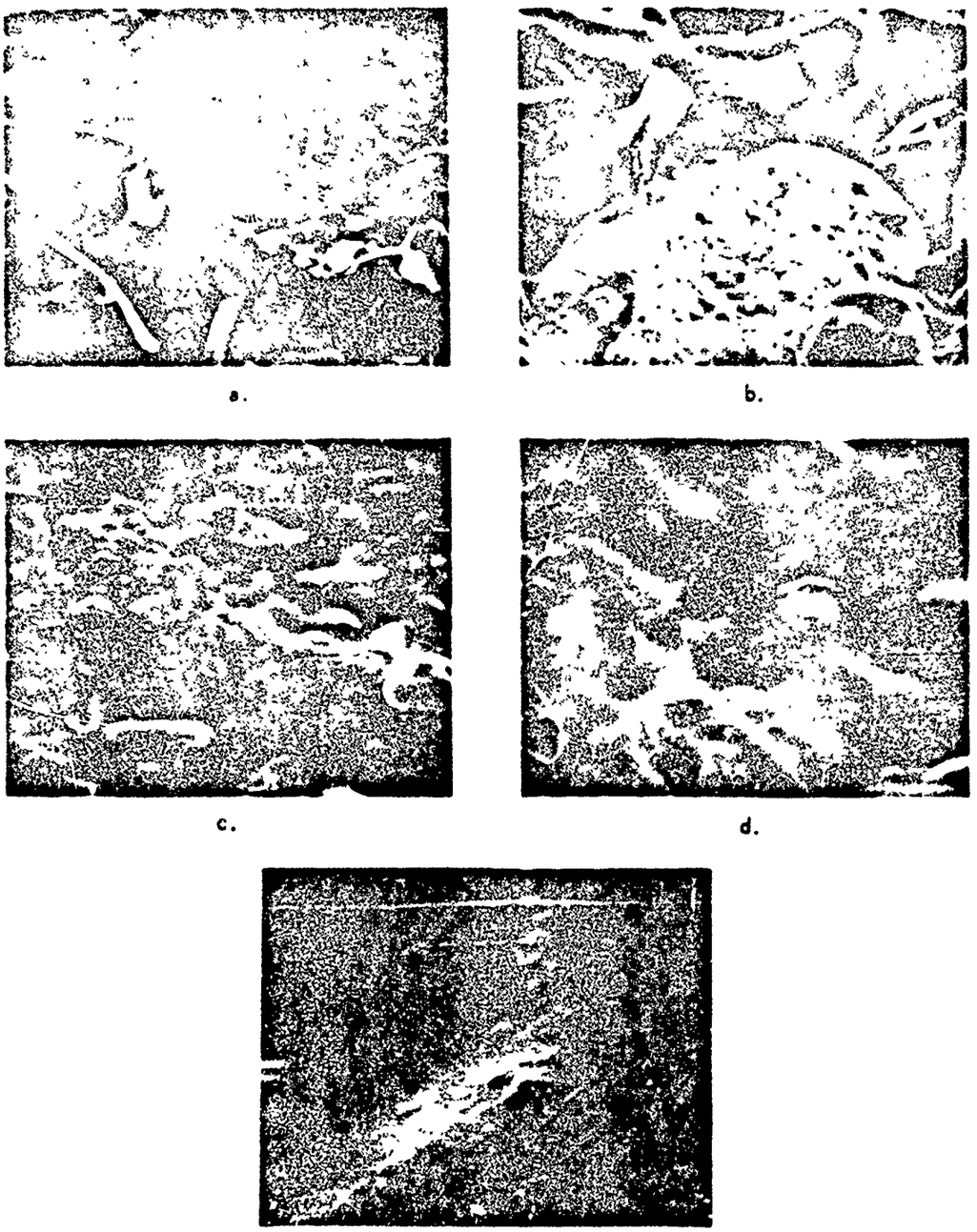

a.

b.

c.

d.

e.

Figure 64. ELECTRON MICROSCOPIC EXAMINATION OF A PLUGGED FILTER

64987

Model of a Regenerative Heat Exchanger for Missile Application

Development of a Heat Transfer Correlation

One of the near term applications of Air Force programs on vaporizing and endothermic fuels involves utilization of supersonic combustion ramjet engines for powering missiles. Present plans contemplate using only the latent and sensible heat capacity of the fuel for cooling the engine. Under the current contract the behavior of candidate fuels are being investigated both analytically and experimentally.

In order to arrive at the optimum design of experimental equipment a one-dimensional computer model has been developed to be used in predicting the effect of geometric and experimental variables on heat transfer and profiles of pressure and temperature. Fuel is assumed to flow through a cylindrical heat exchanger and absorb heat prior to injection into the combustion chamber. The computer program predicts the pressure and temperature profiles of the fuel. Past calculations[16] have shown the need for an improved correlation in predicting film heat transfer coefficients in the liquid phase and critical region. Current work is directed toward developing a correlation based on data from the FSSTR.

Experimental film heat transfer coefficients were determined in the following manner. Data from the FSSTR consisted of the initial pressure and temperature of the fuel, fuel mass flux, heat flux profile along the wall, and outside wall temperatures at various points. Inside wall temperatures were determined from the conduction equation through a cylindrical wall. The fuel pressure and bulk temperature at various points were determined by using the computer model for the heat exchanger. The temperature differences between the inside wall and bulk fluid were used along with the heat flux to determine the experimental heat transfer coefficients.

Regression analysis was used to determine the effect of different variables on the heat transfer coefficient. The heat transfer coefficient was cast as a Nusselt number based on fluid properties at either the bulk, average film, or wall temperature. The variables were combined into dimensionless groups: Reynolds number, Prandtl number, and ratios of viscosity, density, and temperature.

The experimental data correlated were recorded during the high heat flux runs with MCH in the 26.5 mil diameter tube. Heat fluxes varied from 2×10^5 to 6×10^6 Btu/ft^2-hr and mass flow rates from 31 to 77 lb/hr. MCH conditions were 628 to 955 psia and 80 to 636°F (mostly subcritical). Inside wall temperatures varied from 162 to 813°F.

The only significant variables were found to be the Reynolds and Prandtl numbers. The fluid properties at a mean film temperature provided the best correlation.

$$Nu_f = 0.000595\ Re_f^{1.091 \pm 0.021} Pr_f^{0.729 \pm 0.027} \qquad (1)$$

where Nu = Nusselt number
Re = Reynolds number
Pr = Prandtl number

Subscript f refers to fluid properties at the mean film temperature

$$T_f = \frac{T_b + T_w}{2} \tag{2}$$

where T_f = mean film temperature
T_b = mean bulk temperature
T_w = inside wall temperature

The viscosity, density and temperature ratios did not improve the correlation significantly. The effect of axial distance was negligible.

The correlating equation is plotted in Figure 65. The data have very little scatter about this equation; much less than about the standard correlations[28] shown in Figures 66 and 67.

$$Nu_f = 0.023\ Re_f^{0.8} Pr_f^{0.4} \tag{3}$$

$$Nu_b = 0.023\ Re_b^{0.8} Pr_b^{\frac{1}{3}} \left(\frac{\mu_b}{\mu_w}\right)^{0.14} \tag{4}$$

where μ = fluid viscosity

and subscripts b and w refer, respectively to the fluid properties at the mean bulk temperature and the inside wall temperature. The errors associated with the correlations are listed in Table 113. The derived correlation has by far the best agreement with the experimental data and their slope. The Dittus-Boelter correlation is not far from the experimental data, but Figure 66 indicates that the slope for the correlation, which is a combination of the exponents on Re_f and Pr_f, has the wrong value. For the Sieder-Tate correlation both the curve and its slope differ appreciably from the experimental data. Hence the derived correlation is more suitable for estimating heat transfer coefficients. Current heat transfer data for Decalin and SHELLDYNE-H are being analyzed to check the correlation for other hydrocarbons and modify it if necessary.

Table 113. HEAT TRANSFER CORRELATIONS AND ERRORS

Correlation	Log Standard Error
Derived	0.092
Dittus-Boelter	0.235
Sieder-Tate	0.372

Reaction Kinetics of Decalin Dehydrogenation

Development of a Kinetic Model

Dehydrogenation of naphthenes is the most promising endothermic reaction for fuel cooling. Currently MCH and Decalin are the fuels studied most extensively of these fuel condidates which undergo dehydrogenation.

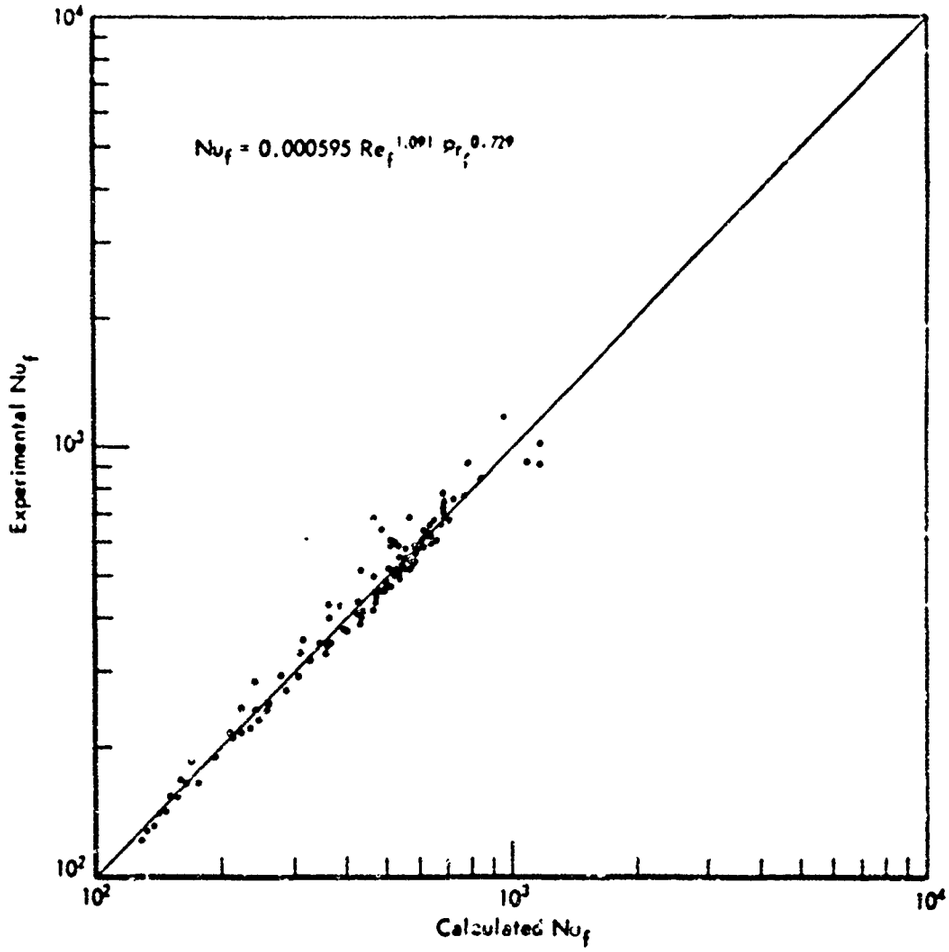

Figure 65. HEAT TRANSFER CORRELATION DERIVED BY REGRESSION ANALYSIS FOR MCH

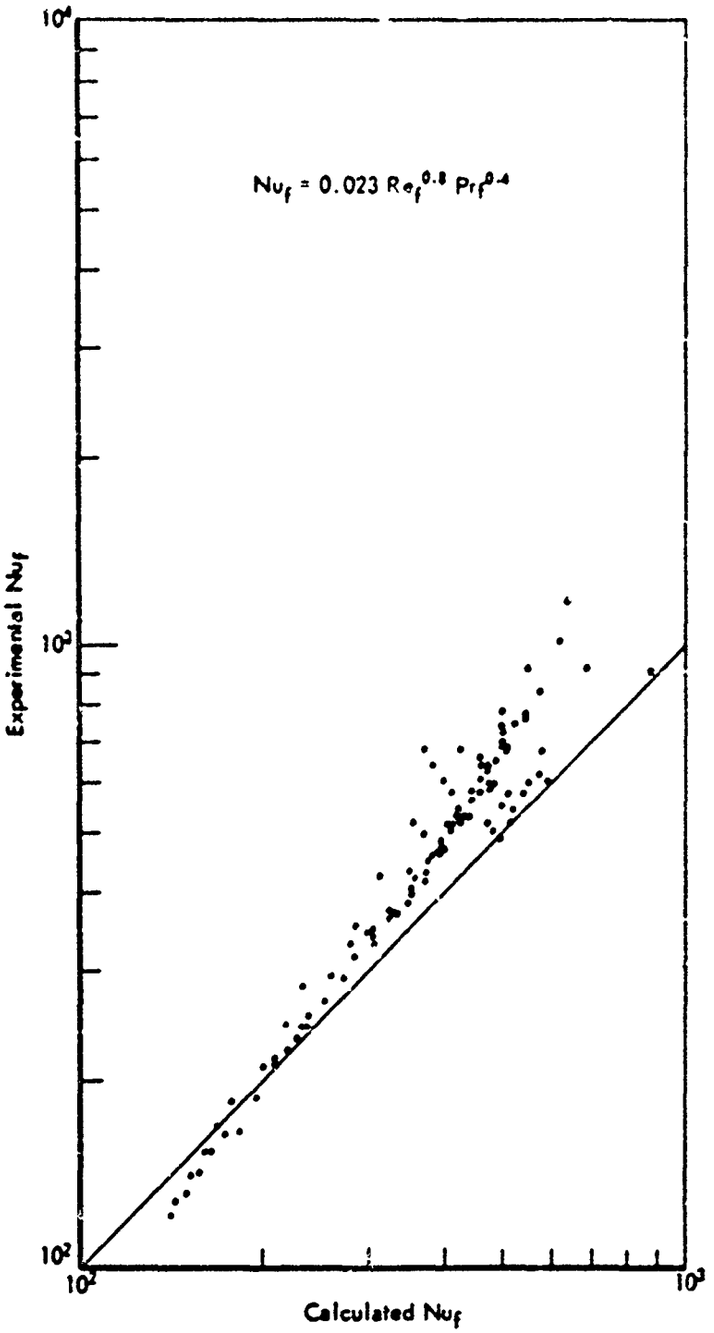

Figure 66. DITTUS-BOELTER HEAT TRANSFER CORRELATION FOR MCH

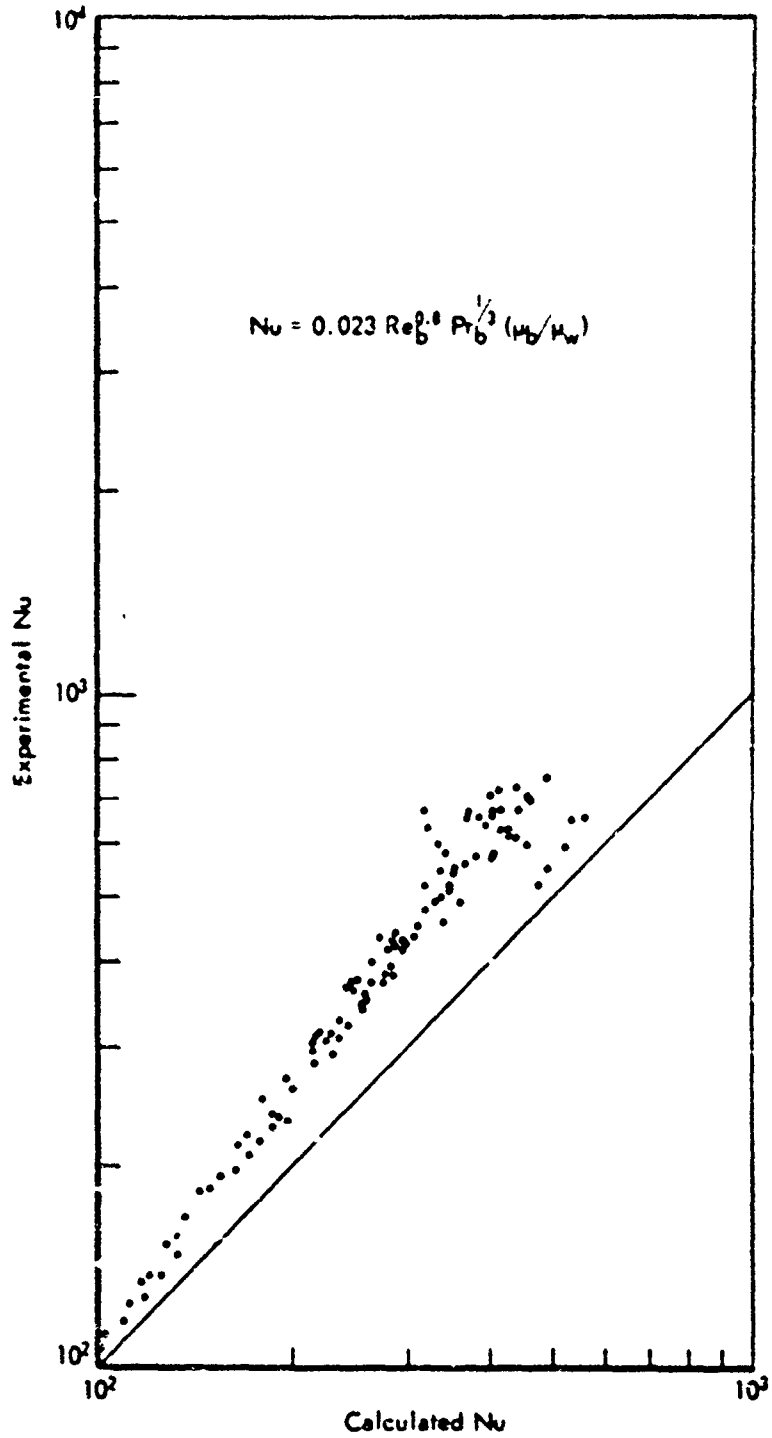

Figure 67. SIEDER-TATE HEAT TRANSFER CORRELATION FOR MCH

The dehydrogenation reaction for MCH has been investigated sufficiently that its kinetic behavior can be predicted.[10] More recently an analysis has been attempted on bench scale data for Decalin dehydrogenation in order to determine a kinetic model for this reaction.

The dehydrogenation of MCH is a single reaction step, MCH forming toluene and hydrogen. However, the dehydrogenation of Decalin is more complex. Decalin is composed of two isomers of cis- and trans-form. These isomers both dehydrogenate and isomerize at significant rates. The dehydrogenation proceeds by two steps from each isomer to form the intermediate tetralin, along with hydrogen, and the final product naphthalene, also with hydrogen. A diagram of the reaction system is shown below:

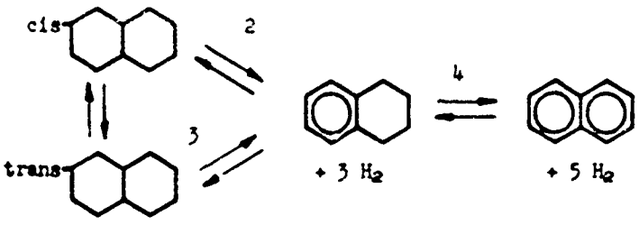

Reaction System for Decalin Dehydrogenation

Bench-scale data were available for pressures of 10 to 25 atm and temperatures of 667 to 791°F. Feeds were composed of Decalin and tetralin and varied in composition. Some feeds consisted of each isomer and tetralin in almost pure form. Other feeds were mixtures of these components in various ratios.

A kinetic model with steps first order in the hydrocarbon was applied to the data.

$$\frac{dc_{cD}}{dt} = -(k_1 + k_2)C_{cD} + k_{-1}C_{tD} + k_{-2}P_H^3C_T \qquad (5)$$

$$\frac{dc_{tD}}{dt} = k_1C_{cD} - (k_{-1}C_{tD} + k_3C_{tD}) + k_{-3}P_H^3C_T \qquad (6)$$

$$\frac{dc_T}{dt} = k_2C_{cD} + k_3C_{tD} - (k_{-2}P_H^3 + k_{-3}P_H^3 + k_4)C_T + k_{-4}P_H^2C_N \qquad (7)$$

$$\frac{dc_N}{dt} = k_4C_T - k_{-4}P_H^2C_N \qquad (8)$$

where C_I = concentration of species I
k_j, k_{-j} = rate coefficients for forward and reverse rates of step j
t = time

and the literal subscripts indicate the following hydrocarbons:

cD = cis-decalin
tD = trans-decalin
T = tetralin
N = naphthalene
H = hydrogen

Since the thermodynamics of the system are well known, the reversible reaction steps can be included in the kinetic parameters. Also, the dehydrogenation to naphthalene is equilibrium limited at the lower reaction temperatures. Arrhenius type rate coefficients were assumed for each forward step:

$$k_j = A_j \exp\left(-\frac{B_j}{RT}\right) \tag{9}$$

where A_j, B_j = rate parameters
R = universal gas constant
T = absolute temperature

The rate coefficient is then given by

$$k_{-j} = \frac{k_j}{K_j} \tag{10}$$

where K_j = equilibrium constant for step j

and

$$K_j = \exp\left(-\frac{\Delta H_j}{RT} + \frac{\Delta S_j}{R}\right) \tag{11}$$

where the equilibrium parameters are

ΔH_j = enthalpy of reaction for step j
ΔS_j = enthropy of reaction for step j

The model was fitted by regression analysis. The four reactions and rate equations reduced to three independent ones. Errors in predicted conversions for the three independent reactions were used to determine an error sum of squares; this was minimized to determine the kinetic parameters.

The results of the regression analysis are given in Table 114 as kinetic parameters for each reaction step. Equilibrium parameters for each step are also given. The temperature coefficients for steps 2 to 4 are high if these are considered as activation energies. For the dehydrogenation of tetralin this is much higher than what would be expected for such a strained molecule. An explanation for these high values can be found in the fact that the minimum error sum of squares was not well defined. The two kinetic parameters for each step were highly coupled and could be varied such that the sum of squares was somewhat insensitive to the change. The degree of coupling between each pair of parameters can be reduced if data could be obtained over a wider temperature range. The coupling is also due to inaccuracy in the data. Calculated parameters for a kinetic model are always sensitive to errors in the experimental data. However, conversions predicted

Table 114. EQUILIBRIUM AND KINETIC PARAMETERS FOR DECALIN DEHYDROGENATION

Equilibrium Constants: $K_j = \exp(-\Delta H_j/RT + \Delta S_j/R)$
Rate coefficient of foward step: $k_j = A_j \exp(-B_j/RT)$
Rate coefficient of reverse step: $k_{-j} = k_j/K_j$

Reaction Step j	Units of K_j	Equilibrium Parameters		Kinetic Parameters	
		$[10^{-3}\ (\Delta H_j/R)]$ °R	$(\Delta S_j/R)$	A_j, hr^{-1}	$10^{-3}\ (B_j/R)$, °R
1. cD ⇄ tD	None	-2.82	-0.31	323	0.4
2. cD ⇄ T + $3H_2$	Atm^3	48.33	52.20	272	67.9
3. tD ⇄ T + $3H_2$	Atm^3	51.15	52.51	110	57.9
4. T ⇄ N + $2H_2$	Atm^2	26.91	28.93	2840	27.7

by a kinetic model are rather insensitive to errors in the model, if the reaction conditions are within the range of experimental conditions used to gather data for the model. In view of this, the above model for Decalin dehydrogenation should only be used for pressures and temperatures in the range of those used in the experiments and should not be extrapolated beyond those conditions. It is intended to apply the model here developed to the analysis of FCSTR results on Decalin, using the packed bed reactor model developed for MCH by substituting the appropriate Decalin physical properties for those of MCH and writing subroutines for the Decalin kinetic model to be substituted for the MCH kinetic model subroutines.

Physical Properties Estimation

Considerable improvement has been made in the physical properties calculation. Properties for Decalin and JP-5 jet fuel have been calculated and are listed in Tables 137 to 144 of the Appendix.

The Decalin properties are those for an equimolal mixture of the two isomers. Properties of the mixture and the pure isomers are very similar with the greatest exception being the liquid viscosity at low temperatures. E.g., Table 115 shows that trans-Decalin has a viscocity 2.4 times that of cis-Decalin at -40°C. However, the mixture is not far from either pure component viscosity. These converge rapidly as the temperature increases, and there is very little difference at higher temperatures. Because of the close similarity in properties, the equimolal mixture properties probably can be used for those of any mixture or pure component of Decalin.

Table 115. VISCOSITY OF SATURATED LIQUID

Temperature, °C	Viscosity, cp		
	trans-Decalin	Equimolal Decalin Mixture	cis-Decalin
-40	9.98	15.30	23.5
-20	5.38	7.57	10.66
0	3.25	4.30	5.68
20	2.14	2.70	3.41
40	1.504	1.838	2.25
60	1.114	1.328	1.584
80	0.861	1.008	1.180
100	0.688	0.795	0.918
120	0.565	0.647	0.740
140	0.475	0.540	0.614
160	0.404	0.459	0.522
180	0.342	0.393	0.452
200	0.290	0.340	0.399

Pseudocritical methods were used to calculate most of the physical properties. First the vapor pressure and enthalpy of vaporization were determined at subcritical temperature. Then ideal gas properties were calculated over the full range of temperatures. Next correlations were used to

correct for the effect of pressure to obtain real gas properties. Liquid phase and dense phase correlations: some of these were semitheoretical, others were empirical and required experimental data. Sufficient data were available in the scientific literature to determine Decalin properties. Data for JP-5 were furnished by the Florida Research and Development Center of Pratt and Whitney Aircraft. Equations used for estimating properties are described below.

Gas Properties

1. The compressibility factor was determined by the Redlich-Kwong-Ackerman equation of state:[29]

$$Z = Z_{RK} + Z_1 + \omega Z_2 \tag{12}$$

where Z = compressibility factor
Z_{RK} = compressibility factor calculated by the Redlich-Kwong equation of state
ω = acentric factor
Z_1, Z_2 = generalized functions of reduced pressure and temperature

The Redlich-Kwong equation of state is[30]

$$\left[P + \frac{a}{T^{\frac{1}{2}}V(V+b)}\right](V-b) = RT \tag{13}$$

where P = absolute pressure
T = absolute temperature
V = volume
R = universal gas constant
a, b = functions of critical pressure and temperature

The Redlich-Kwong-Ackerman equation of state is a generalized correlation which gives an accurate value for the compressibility factor.

2. The specific heat at constant pressure for an ideal gas was determined by the group contribution method of Rihani-Doraiswamy:[31]

$$c_p^{\circ} = a + bT + cT^2 + dT^3 \tag{14}$$

where c_p° = ideal gas specific heat
a, b, c, d = parameters determined by the addition of group contributions and correction factors

The effect of pressure on specific heat was determined by differentiation of the pressure effect on enthalpy.

3. The enthalpy for an ideal gas was found by integration of the ideal gas specific heat.

$$H^{\circ} - H^{\circ}_{T_0} = \int_{T_0}^{T} c_p^{\circ} dT \tag{15}$$

where H^o = ideal gas enthalpy
T^o = reference temperature

The pressure effect was calculated by a modified form of the Redlich-Kwong equation of state:[32]

$$H - H^o = (H - H^o)_{RK}(1 - \omega F) \tag{16}$$

where H = enthalpy of real gas
H^o = enthalpy of ideal gas
$(H - H^o)_{RK}$ = pressure effect on enthalpy as calculated by the Redlich-Kwong equation of state
F = generalized function of reduced temperature

The Redlich-Kwong equation of state for enthalpy is

$$(H - H^o)_{RK} = PV_{RK} - RT + \frac{3a}{2RT^{\frac{1}{2}}} \ln\left(\frac{V_{RK}}{V_{RK} + b}\right) \tag{17}$$

where V_{RK} = volume calculated by Equation (15).

4. The <u>entropy</u> of an ideal gas was calculated from the specific heat by

$$S^o - S^o = \int_{T_o}^{T} \left(\frac{C_{pO}}{T}\right) dT \tag{18}$$

where S^o = ideal gas entropy

The real gas entropy was determined from the enthalpy and Gibbs free energy:

$$S = \frac{H - G}{T}$$

where S = entropy
G = Gibbs free energy

5. The <u>Gibbs free energy</u> of an ideal gas was determined from the enthalpy and entropy by rearrangement of Equation (19). The real gas free energy was calculated by

$$G - G^o = RT \int_0^P \left(\frac{Z-1}{P}\right) dP \tag{19}$$

where G^o = Gibbs free energy of an ideal gas
R = universal gas constant
P = pressure
Z = compressibility factor

6. The ratio of specific heats and the specific heat at constant volume were determined by

$$\gamma = \frac{c_p}{c_v} \tag{20}$$

$$c_v = c_p + T\left(\frac{\partial V}{\partial T}\right)_P^2 \left(\frac{\partial P}{\partial V}\right)_T \tag{21}$$

where γ = ratio of specific heats
c_v = specific heat at constant volume
$\left(\frac{\partial V}{\partial T}\right)_P, \left(\frac{\partial P}{\partial V}\right)$ = derivatives determined from the Redlich-Kwong equation of state

7. The sonic velocity was determined by

$$u_s = V\left[-\frac{\gamma}{M}\left(\frac{\partial P}{\partial V}\right)_T\right]^{\frac{1}{2}} \tag{22}$$

where u_s = sonic velocity
M = molecular weight

8. The Joule-Thomson coefficient was calculated by

$$\mu_{JT} = -\frac{1}{c_p}\left(\frac{\partial H}{\partial P}\right)_T \tag{23}$$

where μ_{JT} = Joule-Thomson coefficient
$\left(\frac{\partial H}{\partial P}\right)_T$ = derivative determined from the modified Redlich-Kwong equation of state

9. The ideal gas viscosity was estimated by the Stiel-Thodos corresponding states correlation.[33,34]

$$\mu^o = 3.40 \times 10^{-6}\, a\, T_r^{0.94} \qquad T_r \leq 1.5 \tag{24}$$

$$\mu^o = 1.778 \times 10^{-6}\, a(4.58\, T_r - 1.67)^{5/8} \qquad T_r > 1.5 \tag{25}$$

where μ^o = ideal gas viscosity, cp
T_r = reduced temperature

$$a = \frac{M^{1/2} P_c^{2/3}}{T_c^{1/6}}, \quad \frac{(atm)^{2/3}}{(^oK)^{1/6}} \tag{26}$$

The Jossi-Stiel-Thodos correlation,[33,30] based on reduced density was used to determine the viscosity of a real gas:

$$\mu = \mu^{o} + 1.10 \times 10^{-6}\, a[\exp(1.584\ \rho_r) - 1] \quad \rho_r < 0.26 \tag{27}$$

$$\mu = \mu^{o} + 10^{-6}\, a[2.312 \exp(1.079\ \rho_r) - 2.5] \quad 0.26 < \rho_r < 1.53 \tag{28}$$

$$\mu = \mu^{o} + 10^{4}\, a(0.10230 + 0.023364\ \rho_r + 0.058533\ \rho_r^{2} - 0.040758\ \rho_r^{3} + 0.0093324\ \rho_r^{4}) \quad 1.53 < \rho_r < 3 \tag{29}$$

where μ = viscosity, cp
ρ_r = reduced density
a = parameter defined by Equation (26).

10. The thermal conductivity of an ideal gas was estimated from the ideal gas viscosity by a correlation that includes a polyatomic correction:[32]

$$k^{o} = \frac{\mu^{o}}{M}\ 0.0234345 \left(\frac{c_p{}^{o}}{R}\right) + 0.013055 \tag{30}$$

where k^{o} = ideal gas thermal conductivity, cal/cm-sec-°F
μ^{o} = ideal gas viscosity, cp

The pressure effect on the thermal conductivity was determined by the Stiel-Thodos dense gas correlation:[37]

$$k = k^{o} + 14.0 \times 10^{-8} \left(\frac{a}{MZ_c{}^{5}}\right) \left[\exp(0.535\ \rho_r) - 1\right] \quad \rho_r < 0.5 \tag{31}$$

$$k = k^{o} + 13.1 \times 10^{-8} \left(\frac{a}{MZ_c{}^{5}}\right) \left[\exp(0.67\ \rho_r) - 1.069\right] \quad 0.5 < \rho_r < 2.0 \tag{32}$$

$$k = k^{o} + 2.976 \times 10^{-8} \left(\frac{a}{MZ_c{}^{5}}\right) \left[\exp(1.155\ \rho_r + 2.016)\right] \quad 2.0 < \rho_r < 2.8 \tag{33}$$

where k = thermal conductivity, cal/cm-sec-°K
Z_c = critical compressibility factor
a = parameter defined by Equation (26)

Liquid Properties

The liquid properties were estimated only for a saturated liquid phase.

1. The vapor pressure was calculated by the Frost-Kalkwarf-Thodos correlation:[38]

$$\ln p_v = a + \frac{b}{T} + c \ln T + \frac{dp_v}{T^{2}} \tag{34}$$

where p_v = vapor pressure
a,b,c,d = parameters determined by linear regression of experimental vapor pressures and the critical pressure.

2. The enthalpy of vaporization was estimated by the Watson equation:[39][40][41]

$$\Delta H_v = a(T_c - T)^{0.38} \tag{35}$$

where ΔH_v = enthalpy of vaporization
a = parameter determined by linear regression of experimental data

At high temperature the enthalpy of vaporization may be estimated by the Pitzer-Chen correlation:[42]

$$\frac{\Delta H_v}{T_c} = \frac{T_r(7.90\ T_r - 7.82 - 3.088 \ln P_{vr}}{1.07 - T_r} \tag{36}$$

where ΔH_v = enthalpy of vaporization, cal/gmole
T_c = critical temperature, °K
p_{vr} = reduced vapor pressure

3. A choice of equations was available for calculating the density. The Francis equation can be used for low temperatures:

$$\rho = a + bT + \frac{c}{d - T} \tag{37}$$

where a,b,c,d = parameters determined by multiple regression of experimental densities

At higher temperatures where experimental values are not available the density can be calculated by the Guggenheim equation:[32]

$$\rho_r = 1 + a(1 - T_r)^{1/3} + b(1 - T_r) \tag{38}$$

where a,b = parameters determined by equating densities and their first derivatives from Equations (37) and (38) at some temperature.

The Bradford-Thodos correlation[43] is an alternative to either or both of the above equations:

$$\rho_r = 1 + a(1 - T_r) + b(1 - T_r)^2 + c(1 - T_r)^{0.38} \tag{39}$$

where a,b,c = parameters determined by multiple regression of experimental data

4. The specific heat at constant pressure was determined by differentiation of Equation (36) and subtraction from the specific heat of the saturated gas:

$$c_{PL} = c_{PG} - \frac{d(\Delta H_v)}{dT} \tag{40}$$

5. The enthalpy was found by the difference between the enthalpy of the saturated gas and the enthalpy of vaporization:

$$H_L = H_G - \Delta H_v \tag{41}$$

6. The viscosity was calculated by the Giriialco equation[44] at low temperat ~es:

$$\ln \mu = a + \frac{b}{T} + \frac{c}{T^2} \tag{42}$$

where a,b,c = parameters determined by linear regression of experimental viscosities

Equation (42) gives substantially the same correlation as ASTM D341-39 viscosity-temperature chart. At higher temperatures the Jossi-Stiel-Thodos dense phase correlation, Equations (28) and (30), was used to predict viscosities.

7. The thermal conductivity was estimated by the Robbins-Kingrea correlation[45] at low temperatures:

$$K_L = \frac{10^{-3}\, c_p}{\Delta S^*} (88.0 - 4.94\ H) \left(\frac{0.55}{T_r}\right)^N \rho^{4/3} \tag{43}$$

where K_L = liquid thermal conductivity, cal/cm-sec-°K
c_p = liquid heat capacity, cal/gmole-°K
ρ = liquid density, gmole/cm^3
H,N = Robbins-Kingrea parameters
ΔS^* = modified Everett entropy of vaporization, cal/gmole-°K

$$\Delta S^* = \frac{\Delta H_{vb}}{T_b} + R \ln \left(\frac{273}{T_b}\right) \tag{44}$$

where ΔH_{vb} = enthalpy of vaporization at the normal boiling point
T_b = normal boiling point, °K

At temperatures near the critical point the Stiel-Thodos correlation, Equations (32) to (34), was sometimes used.

The Prediction of Autoignition Temperatures of Jet Fuels and of Pure Naphthenes

A fuel property of interest to aircraft engine designers, but one which is frequently not available, is the spontaneous ignition or autoignition temperature (AIT), defined as the lowest temperature at which the fuel will autogenously ignite.

Unfortunately, this temperature is not a pure physico-chemical property of the fuel, but is influenced by the particular experimental apparatus employed in its determination. Most generally, this is done by introducing the fuel dropwise into a container at a controlled temperature.

In addition to the physical and chemical properties of the fuel, the AIT is influenced by pressure, type and condition of the wall surface, and size and shape of the combustion chamber. However, AIT's determined in the same or similar apparatus serve as a useful index to combustion performance, re-ignition characteristics, and flame-out tendencies. Perhaps because the AIT's of jet fuels fall within reasonably narrow limits, they are not included as a part of standard fuel specifications.

The AIT of a fuel may be expected to depend upon both its volatility, which influences the formation of a combustible mixture, and upon its reactivity with oxygen. These considerations led to an attempt to correlate AIT with Flash Point (FP), which is generally taken as a measure of volatility and with the lower limit of combustion, defined as the percent hydrocarbon in the limiting ignitable fuel/air mixture (LL).

To test this relationship, a regression analysis of AIT with FP and LL data for several jet fuels (JP's) and fuel oils was attempted. SHELLDYNE-H was included because of a special interest in this hydrocarbon, and to see if a material of this type would correlate with other commercial fuels relative to AIT, FP, and LL properties. The following equation was found to give an excellent fit of the experimental data:

$$AIT = 1625\,(LL - 0.6659)^2 - 4.065 \times 10^3\,(FP - 144.5)^2 + 464.7 \qquad (45)$$

As shown in Table 116, the agreement between experimental and predicted AIT values is excellent. Unfortunately, however, LL and FP data are not always available for fuels and hydrocarbons of interest. We have therefore endeavored to express AIT in terms of other properties which might be more available.

Since FP and LL can be estimated[28] from such properties as heat of combustion, q_n, (Btu/lb), molecular weight, M, normal boiling point, t_n (°F), and ASTM 10 percent slope, s, it was decided to substitute the expressions for these estimates directly into (45):

$$AIT = 1625\,(1.87 \times 10^6/q_n \times M - 0.06695)^2 - 4.065 \times 10^{-3}\left(t_n - \frac{86.5}{0.142 + \frac{212}{t_n + 460}} - 0.04\sqrt{s} - 144.5\right) \qquad (46)$$

Predictions based on (46) are also tabulated in Table 116, but were found generally less satisfactory than those from (45), and in some instances to be rather poor.

In a third attempt, a correlation of AIT was run directly with t_n, q_n, M and s. This regression yielded (47), from which estimates of AIT were found to be as good or better than those from (45) (Table 116).

$$AIT = (1/q_n)(10{,}700 - 296{,}800/q_n + 105.4 \times 10^4/M) + 0.9863\,t_n - 7.817/s \qquad (47)$$

where q_n is now net heat of combustion in Btu/lb x 10^{-3}.

Table 116 summarizes all the results plus the experimental data from which the correlation equations were derived.

Table 116. PREDICTION OF AUTOIGNITION TEMPERATURES OF FUELS FROM PROPERTIES

Fuel	LL	FP	s	M	q_n	AIT			
						Experimental	Eq. (45)	Eq. (46)	Eq. (47)
JP-3	0.9	22	4.5	112	18,710	495	493	486	495
JP-4	0.9	3	4.7	125	18,678	472	472	452	475
JP-5	0.59	138	2.5	169	18,522	475	474	475	472
No. 1 F.O.	0.62	130	2.6	174	18,595	469	467	477	471
No. 2 F.O.	0.52	156	4.0	198	18,476	496	499	493	496
No. 4 F.O.	0.45	240	3.8	206	17,967	505	503	474	505
SHELLDYNE-H	0.5[illegible]	225	0.2	184	17,893	455	457	429	455

An attempt to find a similar relationship to predict the AIT of pure naphthenes has been only partially successful. In this instance, a regression analysis study relating AIT to boiling point, net heat of combustion, molecular weight, and the lean limit of combustion resulted in a standard error of estimate of 33°F, which is a magnitude error of about 6 percent. In constrast, autoignition temperatures for wide boiling range fuels above were good to within 1 percent. The best fit correlation equation for naphthenes is as follows:

$$AIT = 8.388 \times 10^{-4}(Q_n - 18,321)^2 + 188.93\ LL^2 - 0.01704\ M^2 + 2.076\ t_n - 111.38 \quad (48)$$

where Q_n = net heat of combustion, Btu/lb
LL = lean combustion limit, percent fuel in air
M = molecular weight
t_n = normal boiling point, °F

The agreement of the estimates from Equation (48) are shown in Table 117.

The regression was run on the first twelve compounds, all data being from the literature.[47)48)49)] SHELLDYNE-H autoignition temperature was predicted rather poorly, indicating that it does not behave like a typical naphthene. The experimental value for SHELLDYNE-H was determined at Emeryville.

It is most probable that the agreement between experimental and predicted AIT values shown in Table 117 is limited more by the inconsistency of the experimental data than by an actual inability of the selected variables to predict ignition temperatures, the data having come from a variety of different sources and experimenters. However, we had wondered if systematic errors, such as with increasing molecular weight, might be involved. To the contrary, the AIT Residuals (prediction deviations from experimental) showed no consistent pattern when plotted versus M, and the scatter about the 45° line for the plot of experimental versus predicted values gave a random pattern (Figure 68).

If data in sufficient quantity could be obtained from a single apparatus, no doubt a good correlation could be obtained. We hope to do some further work on this problem in the future, extending it to other hydrocarbon types.

Combustion Studies

Equipment Modifications

In the last annual report we included a considerable amount of data on a number of high molecular possible fuel candidates such as SHELLDYNE, SHELLDYNE-H DMD and so forth. In order to get sufficient hydrocarbon into the reaction zone for these high molecular weight materials it was necessary to heat the tube and the storage bottle etc. up to 80°C, which was the limit of the capability of the heating system that we then had on the tube. This was somewhat marginal from the standpoint of the vapor pressure of the components of interest. When the heating system burned out, we took advantage of the

Table LII. ESTIMATES OF AUTOIGNITION TEMPERATURES OF PURE NAPHTHENES[a]

Naphthene	Q_n, Btu/lb	LL, %	M, mol wt	t_L, °F	Autoignition Temp, °F	
					Experimental	Estimate
Cyclo-C_3	18,254	2.41	42.08	-29	928	941
Cyclo-C_5	18,825	1.5	70.13	121	725	650
Cyclo-C_6	18,676	1.31	84.16	176	518	572
Et-Cyclo-C_4	18,516	1.2	84.16	159	414	415
Me-Cyclo-C_5	18,768	1.33	84.16	161.26	614	565
Me-Cyclo-C_6	18,642	1.20	98.18	213.68	545	544
Et-Cyclo-C_5	18,730	1.1	98.18	218	504	543
Et-Cyclo-C_6	18,661	0.95	112.21	269.4	504	519
Decalin	18,324	0.74	138.25	382	482	455
Di-Et-CH	18,650	0.75	140.27	344	468	487
Bi-CH	18,400	0.65	166.3	460.4	473	481
Di-Me-Decalin	18,238	0.69	166.3	455	433	416
SHELLDYNE-H	17,983	0.56	184	510	455	583

a) From Equation (48).

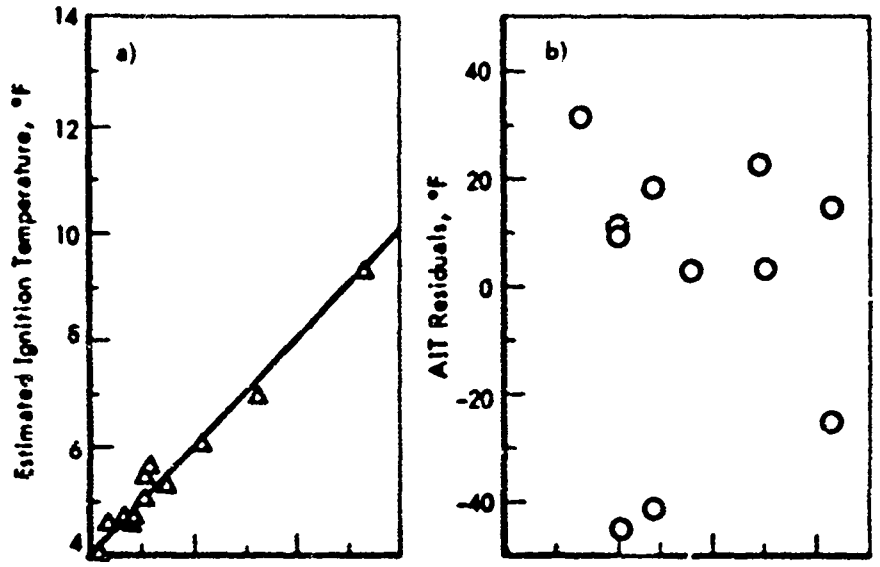

Figure 68. IGNITION TEMPERATURES OF NAPHTHENES
a) Agreement of Estimates with Experimental Values
b) AIT Residuals as a Function of Molecular Weight

situation and improved the thermal capability of the system when we re-worked it so that we could raise the ambient temperature to 150°C. Because of the thermal expansion of the tube under these conditions, it was necessary to "float" the downstream end of the tube along with the infrared detection system and the pressure pick up in order to avoid misalignment as the tube heated up. It was also necessary, for other reasons, to replace the indium antimonide infrared detector. We also have had the tube re-rated from a pressure standpoint so that we could investigate the pressure region up to 100 psi. Although some test runs have been done with the new system, completely satisfactory operation has not yet been achieved, and we have no new data at the higher temperature and pressure conditions that can be usefully discussed.

Oxidative Reaction Rates[a)]

One matter of considerable interest is the rate at which fuels combust in a supersonic flow field since this will affect engine dimensions critically. Accordingly the data we have obtained in the past on two hydrocarbons of widely different characteristics, n-octane and SHELLDYNE-H, were analyzed from this point of view.

In the examination of the post-ignition appearance of CO_2 it was found that the initial rate of appearance (over at least the first 100-300 μsec) following ignition may be described by:

$$R = k(C^* - C)$$

where C^* is the ultimate (total combustion) concentration of CO_2 and C, the current value. The rate constant, k, was found to be relatively insensitive to temperature, with an activation energy of about 7 kcal/mole or less; and has a value of 10^3 sec^{-1} in the middle of the temperature range studied (ca 2000°F). No significant effect of oxygen concentration on this rate was found. Data obtained for CO_2 formation from n-octane are shown in Figure 69. The most significant observation here is the low activation energy for post-ignition combustion. The indication is that combustion proceeds at a rate nearly independent of temperature, after ignition, and that a matter of several milliseconds will be required for relatively complete combustion. It should be pointed out that these results are limited to quite lean mixtures, however; hence the conclusion may not be safely extrapolated to near stoichiometric conditions. Also, the effect of pressure in the reaction has not been adequately explored.

Similar, but more limited, data are shown for SHELLDYNE-H in Figure 70. Although the data points are quite scattered the rate of combustion and the temperature coefficient appear to be of the same order of magnitude as for n-octane. This suggests that, as thought by Orr[53)] and Levinson,[52)] the initial reaction of both hydrocarbons involves thermal cracking to olefins and hydrogen. The rate determining step for oxidation is considered to be

$$H + O_2 \longrightarrow OH + O \qquad (50)$$

a) We are pleased to acknowledge the assistance of our colleagues, Drs. B. E. Anshus and J. O. L. Wendt, in connection with this and the subsequent section.

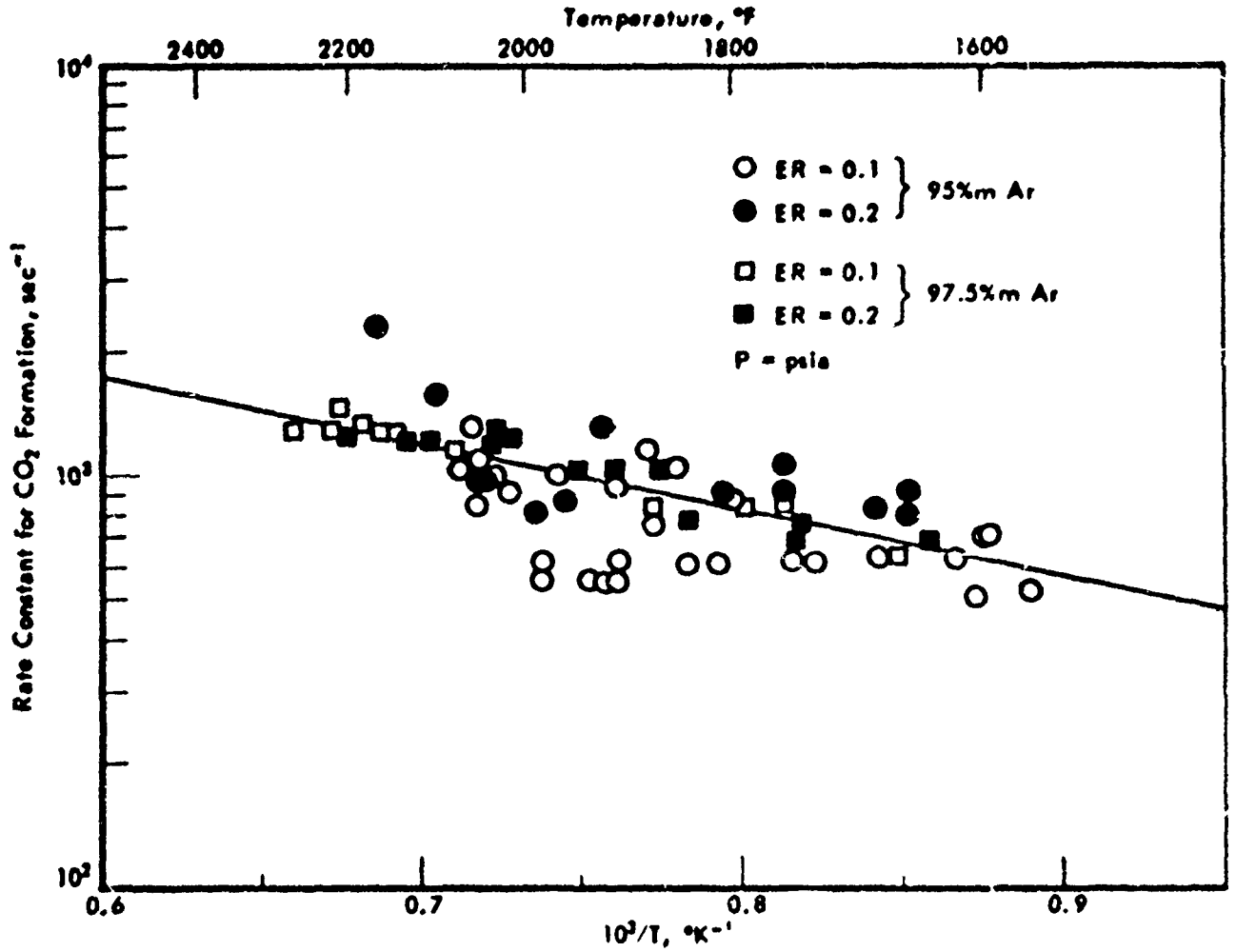

Figure 69. RATE COEFFICIENTS FOR POST-IGNITION APPEARANCE OF CO_2 IN n-OCTANE-OXYGEN-ARGON

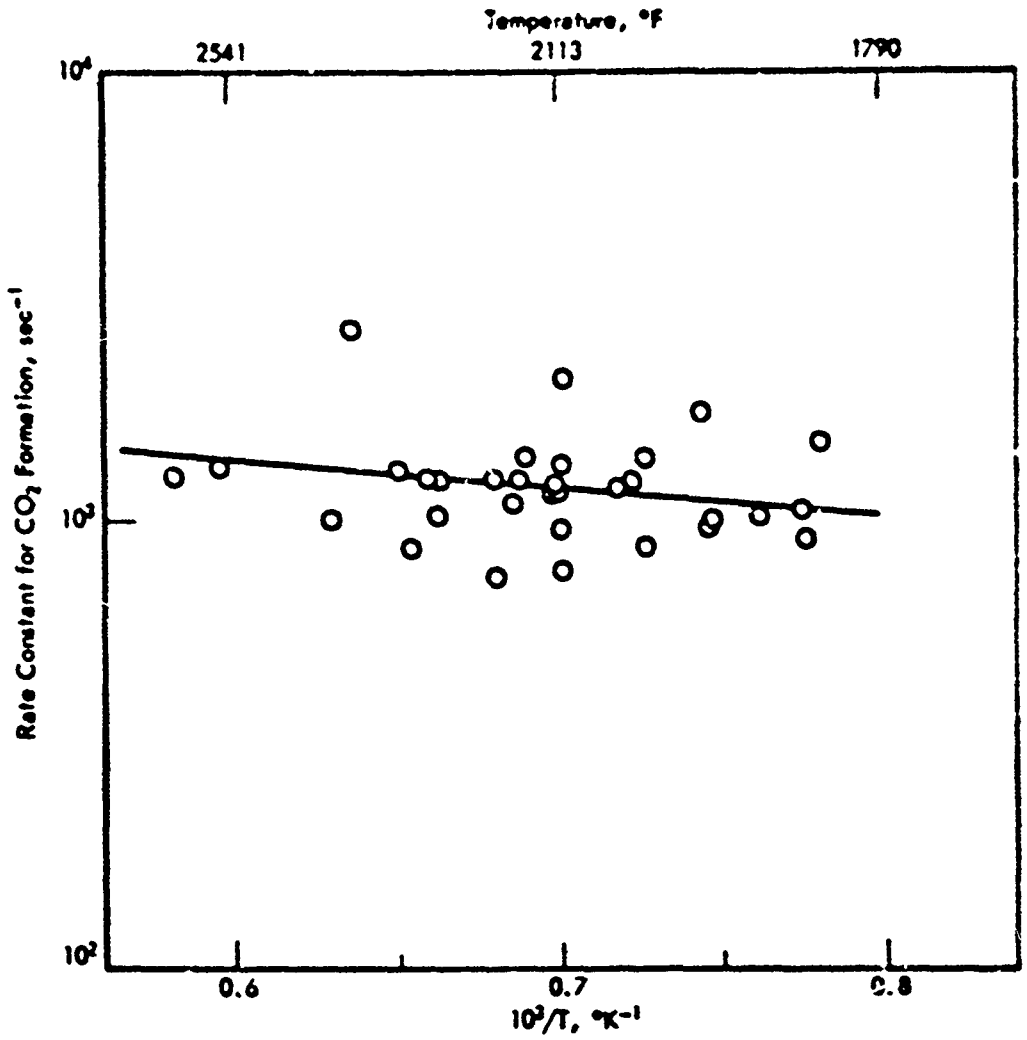

Figure 70. RATE COEFFICIENTS FOR POST-IGNITION APPEARANCE OF CO_2 FOR SHELLDYNE H-OXYGEN-ARGON

with the H atoms being produced either directly from cracking of the hydrocarbon or by the reactions of

$$H_2 + O_2 \longrightarrow 2\,OH \qquad (51)$$

$$OH + H_2 \longrightarrow H_2O + H \qquad (52)$$

The rate constant for (50) is quoted to be 5×10^3 sec^{-1} at about 1800°F which is reasonably close to the observed rate of oxidation of the hydrocarbons. Since the hydrocarbon cracksate would influence the rate by reacting with free H it seems reasonable that two hydrocarbons of such diverse structure could crack to fragments of similar characteristics. We plan to do some additional work on this and similar systems with improved instrumentation and under extended pressure conditions, obtaining data also under a greater variety of conditions and with oxidation catalysts present.

Attenuation in the Shock Tube

Because of the demonstrated sensitivity of ignition delay correlations on the assumed attenuation coefficient, and since we had no basis for the assumption other than what others had measured on other shock tubes,[51] it was decided to measure attenuation on our shock tube so that a reliable attenuation rate could be established.

The shock tube was set up with three thin film heat gages at points A, B, and C of Figure 71 to measure two velocities. Timers were wired to read times for shock passage from A to B and from A to C with the distances between these points were accurately measured. The velocities of passage from A to B and from B to C were then calculated and fitted into the exponential attenuation model[51] to calculate an attenuation coefficient A'. The model says that

$$\frac{(M_s^2 - 1)_2}{(M_s^2 - 1)_1} = \exp\left(-A'\frac{X}{D}\right)$$

where M_s is the Mach number, X is length from point 1 to point 2, and D is tube diameter.

An experimental program was designed to gain information about the scatter in replications and the effect of shock strength and tube pressure on attenuation coefficient. Three replications were done at each of five P_1, P_4/P_1 positions (for nomenclature, see reference 50) to gain the necessary information. The results are tabulated in Table 118 along with the values of A, the attenuation coefficient based on hydraulic radius of the tube. With this data a correlation of attenuation coefficient versus P_1 and P_4/P_1 may be made, but it should be kept in mind that the influence of the variance may be quite significant. The correlation is $A' = 0.00436 - 0.0000457\ P_1 + 0.0000698\ (P_4/P_1)$. Some experiments measuring both ignition delay and shock attenuation have been made but the data has not been reduced as yet.

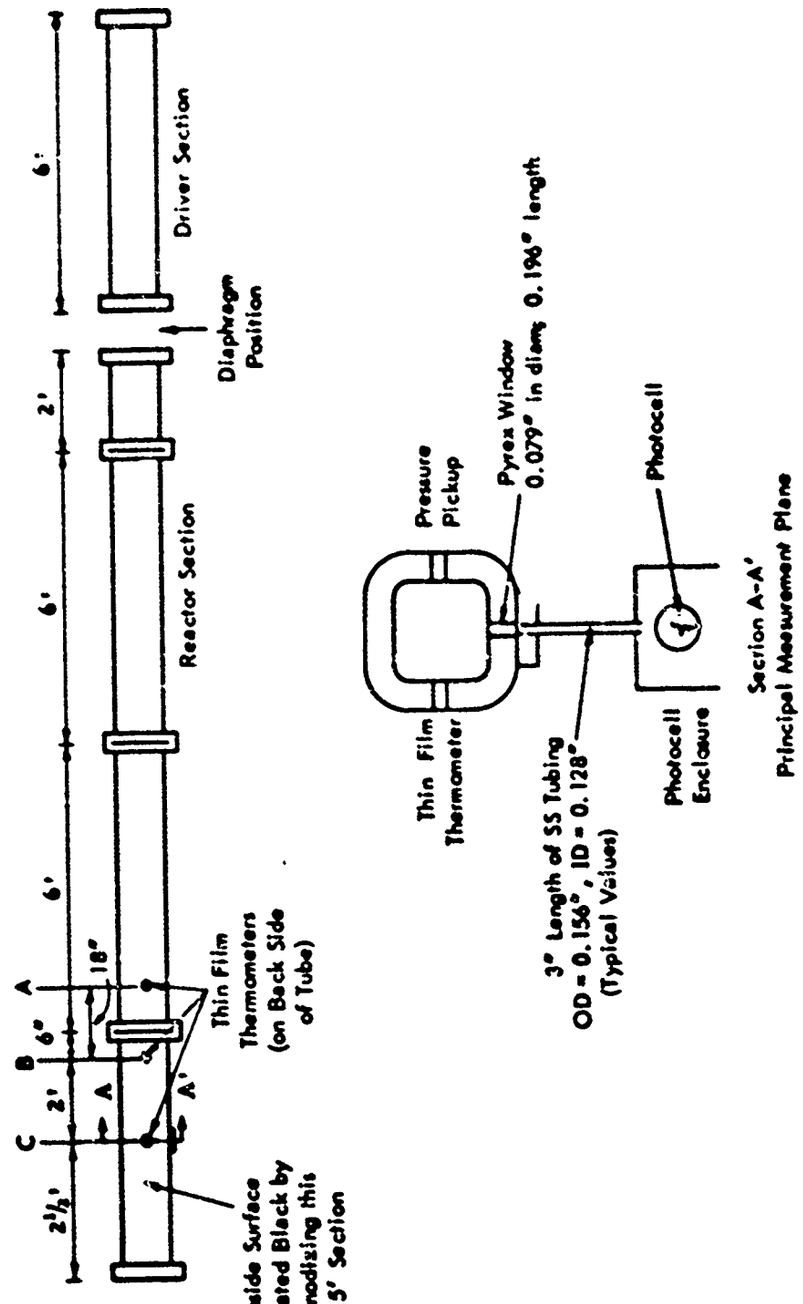

Figure 71. LAYOUT OF SHOCK TUBE SHOWING POSITIONS OF INSTRUMENTS
Not to Scale

61145

Table 118. REPLICATION OF ATTENUATION MEASUREMENTS

P_1 = initial pressure in shock tube
P_4 = initial pressure in driver
V_A = coefficient of variance

P_1, mm Hg	P_4/P_1	Experimental		Calculated, A x 10^3
		A' x 10^3	V_A^2 x 10^6	
40	60.7	2.78	33.7	0.70
40	100	6.25	131	1.56
100	60.7	3.94	16.5	.99
100	100	3.26	59.1	.82
70	80.35	5.56	390	1.39

Present Status and Future Projections

I. A recent calculation of the amount of cooling required by a supersonic combustion ramjet engine at Mach 8 indicated a requirement of ca 1900 Btu/lb. Although this was on the basis of simplifying assumptions the result does reinforce our conviction that useful cooling should be available for engines operating into this speed range through endothermic reactions. We will continue to generate or accumulate data bearing on this aspect of the problem.

II. Varieties of reactions of fuels and catalysts have been examined using the recently developed pulse reactor. This reactor has a number of advantages, including practically isothermal conditions and much greater flexibility with respect to the time required for carrying out an experiment and the nature of the reaction environment. Since the amount of fuel required for carrying out an investigation is trivial (1 µl/experiment) it allows us to examine exotic fuels without any substantial monetary expenditure. Present studies have indicated that the rate of reaction of Decalin in the pulse reactor is greater by a factor of approximately 200 than in the bench scale reactor and probably thus comes closer to the rate that might be expected with a very finely dispersed catalyst. The much smaller difference observed between various catalysts in the pulse reactor suggests that it may be possible to greatly reduce the amount of catalytic metal in the catalyst and still achieve equivalent reactivity.

The pulse reactor has also been used to study the possibility of increasing the rate of thermal cracking quantitatively under low temperature conditions. A large number of possible free radical generating compounds have been tested and rate increases of several fold have been observed at ca 800°F. Since these also are "integral" catalysts this type of investigation will be continued.

III. Additional information on the relation between pore size of catalysts and their stability has been determined with respect to the MCH-Pt/Al_2O_3 catalyst system. Results confirm those previously observed with Decalin and indicate that generally speaking greater catalyst stability is associated with small pore diameter. The one exception noted may be associated with pore size distribution. Since one of the important problems we must face in the future is the development of catalysts of high thermal stability, observations of this sort are important in pointing the direction to proceed.

IV. Laboratory facilities for the study of the thermal reaction of candidate fuels have been improved to include the possibility of operation up to 1500 psi. In studies up to 1000 psi the observation that the rate of thermal reaction of MCH and Decalin is independent of pressure confirms that the reaction is first order to this pressure limit. There is some indication of changes in product distribution as a result of increasing pressure, particularly coke formation. Further experimentation will be required to isolate the effects of the pressure and contact time.

V. Examination of bicycloheptane under both thermal and catalytic conditions points up the desirability of utilizing this bridge ring type structure because of its high thermal stability but also the problems in

achieving high heat sink availability. Both BCH and DMD are less reactive thermally but apparently will not dehydrogenate over the present Pt/Al_2O_3 catalyst used. Since upwards of 2000 Btu/lb are theoretically possible by endothermic reaction of this type of compound, the possibility of utilizing different types of catalysts will be examined.

VI. Continued fruitful experimentation has proceeded in connection with catalysts for the dehydrogenation of candidate fuel materials. Areas of experimentation embrace three types of catalysts: conventional bed, reactor tube wall, and dispersed phase.

VII. The possibility of achieving an improved catalyst of the conventional form has had considerable attractiveness since this would allow a reduction in the amounts of catalyst used for the bringing about of the reaction and hence reduce both the weight and pressure drop occasioned by the presence of the catalyst. Under the present program we have now obtained or prepared and generally examined 827 catalysts. For the first time we have achieved a non-platinum containing catalyst which seems to be the equal to the reference catalyst in reactivity and selectivity although the particular catalytic element involved in this case is somewhat restricted in availability and high in price. The fact that this improvement was achieved by pretreatment of the support lends encouragement to the idea of making some improvements with catalysts having cheaper catalytic elements. Similarly, improvements in platinum catalysts by modification of the support have been achieved.

VIII. Activity in the area of wall catalysts is continuing to be focused on the problem of increasing adhesion. Methods here include pretreatment of the tube wall by sandblasting and acid treatment as well as precoating with various materials and by various means. Although no evidence of spalling was encountered in FSSTR runs with two different catalyst lined tubes, the runs were not particularly long. Initial tests of the two lined reactor tubes in the FSSTR indicated that this mode of application indeed has considerable promise. Operation was possible at a space velocity of 8,590 with 35% conversion of MCH to toluene without significant pressure drop. Experiments indicate that the stability of the catalyst could be a problem since, even though production of toluene per gram of platinum per hour was about 4 times that in a comparable packed bed reactor, the catalysts showed signs of deactivation towards the end of the experiment. Methods of improving the thermal stability of the catalyst under these application conditions will continue to be studied in the future.

IX. Results achieved with a variety of integral catalysts have been encouraging in that some activity has been observed with quite a number of materials tested even though conversion and selectivities have not been high. The implication is that this sort of catalytic activity is not a unique property of a single element and that the activity of the catalyst is a function of the particular structure in which the element exists. This suggests that continued experimentation will have a reasonable chance for success and that it may be possible to tailor additive molecules which will have sufficient activity. Because of the possibility of achieving a great simplification of the mode of application experiments in this direction will be continued.

X. One of the most active granular catalysts to be produced under our catalyst development program (Shell 113) has been directly compared in the FSSTR to the R-8 catalyst usually employed. Under similar operating conditions, with MCH, yields were 3-1/2 percent higher at 30°F lower exit temperature. Indications of deactivation which occurred at the highest temperatures again suggest the necessity of continuing to work for the improvement in the thermal stability of our catalysts.

XI. Decalin has been dehydrogenated for the first time in the FSSTR, again using the Shell 113 catalyst. Based on present analyses reactivity was comparable to that observed with MCH and, on that score, Decalin should prove to be a satisfactory endothermic fuel candidate. As observed in bench scale experiments Decalin caused more rapid catalyst deactivation than did MCH.

XII. We are in the midst of the study to determine the nonreactive cooling capability of four different fuels of widely different properties: MCH, Decalin, SHELLDYNE-H, F-71. While this study is being done in anticipation of the possibility of utilizing a fuel of one of these types for cooling missiles, the information will have applicability in other types of applications where nonreactive fuel cooling is utilized and also in the preliminary portion of an endothermic cooling system. The first portion of this study under low severity conditions (i.e., high heat flux but relatively low wall temperature) has been completed and all four fuels will be tested under conditions of high wall temperature as well as high heat flux. All of the heat transfer information being gathered in the operation of the mini-FSSTR is being utilized for the construction of the regenerative heat exchanger model. Data obtained utilizing MCH as a fluid has been correlated at heat fluxes up to 6×10^6 Btu/hr/sq ft. Excellent correlation was obtained with the equation $Nu = 0.000595\ Re^{1.091} \times Pr^{0.729}$, being much better than with either the Dittus-Boelter or the Sieder-Tate equations. As more information is obtained in the operation of the mini-FSSTR, both with different tube diameters and different fuels, it will be examined in a similar way. The correlations are being made available on computer.

XIII. After attempting for some time, without success, to adapt the kinetic form representing the reaction for the dehydrogenation of MCH to the similar reaction with Decalin, we have developed a kinetic model with first order steps in the hydrocarbon. Coefficients representing the rate parameters in the equation have been calculated from bench-scale data by regression analysis. The kinetic model has been reduced to a computer program which will be fitted as a subroutine into the existing packed-bed reactor program which will then be utilized to analyze the data obtained for the dehydrogenation of Decalin in the FSSTR.

XIV. We continue to study the thermal stability of interesting fuels in a manner related to the customary (coker) method of rating fuels for thermal stability. We recently derived correlations for Decalin with respect to temperature, pressure and light transmission changes. We found by regression analyses that our SD Coker data correlates well with temperature but pressure within the range of experimentation had no effect and the changes of color during the test were not correlatable with the rated thermal stability. We have found that titanium apparently induces more deposit formation than does aluminum. This coupled with the recent observation of the dependence of

thermal cracking rates on tube composition points out the necessity for giving critical attention to the materials of construction of heated fuel systems. Further demonstration of the complexity of this phenomenon (if such be needed) is provided by the observation of the synergy exhibited by the two fractions of deposit inducing materials separated from Decalin. Experiments designed to improve our understanding of the general phenomenon of thermal stability and the reliability of the equipment that we have available for study will be continued.

XV. The possibility of achieving more significant data with respect to thermal stability for different endothermic and missile fuels has hinged on the possibility of establishing a more critical and significant rating method for tubes used in the SD Coker and the CAFSTR. Various methods of determining the amount of deposit on the tube have been evaluated both analytically and experimentally. At the present time, we consider the more promising methods to be combustion, utilizing either pure oxygen or ozone, and beta-ray backscattering. On the basis of favorable results with a "bread board", model of the beta-ray backscattering apparatus we proceeded with the design and have received authorization for the construction of a prototype model. This is intended to accept tubes either from Erdco or SD cokers, the CAFSTR or the small Alcor or Erdco JFTOT tubes.

XVI. We maintain a continuing effort to accumulate physical and transport properties for all fuels and products of interest in this investigation and to improve the methods of arriving at such data. An improved version of our method of calculation is given in the present report together with the properties derived from a 50-50 mixture of the two isomers of Decalin, JP-5 and preliminary values for SHELLDYNE-H. Similar values will be calculated for other fuels in the future.

XVII. Not much additional data on combustion has been obtained in the current year but work has gone forward on the upgrading of our shock tube to enable it to handle fuels of higher molecular weight. The entire tube can now be thermostated to 150°C and the operating pressure can be raised to 100 psi. The higher temperature of operation necessitated the provision of a sliding platform for carrying the free end of the tube and its associated instruments. In an attempt to achieve greater precision in our measurements an experimental value of the attenuation coefficient was determined.

XVIII. By utilizing the slope of the CO_2 concentration versus time curves from shocking oxidations we have been able to get some indication of the rate of oxidation of hydrocarbons in the shock tube. Comparison of these values between normal octane and SHELLDYNE-H indicates that the rates of oxidation are about equal and both have similar low energies of activation. This emphasizes the desirability of studying the effects of additives for increasing the rate of oxidation under such conditions.

REFERENCES

1. Grenleski, S. E. and Billing, F. S., J. of Aircraft 5, 59 (1968).

2. Detra, R. W. and Hidalgo, H., "Generalized Heat Transfer Formulae and Graphs", Report 72, March 1960, Avco-Everett Research Lab, Everett, Massachusetts.

3. Marks, L. S., Mech. Eng. Handbook, 5th Ed., pp. 247-250, McGraw-Hill, New York, 1951.

4. Stepka, F. S., "Considerations of Turbine Cooling Systems for Mach 3 Flight", NASA TN D-4491 (1969).

5. Aihara, Y., AIAA Journal 6, 2187 (1968).

6. De-Riva, I. and Urrutia, ibid., p. 2095.

7. Catton, I., Hill, D. E., and McRae, R. P., ibid., p. 2084.

8. Panton, R. and Oppenheim, A. K., ibid, p. 2071.

9. Anderson, J. D. Jr., ibid., p. 2216.

10. "Vaporizing and Endothermic Fuels for Advanced Engine Application", Technical Documentary Report No. APL-TDR-64-100, Part I. Contract No. AF 33(657)-11096, Shell Development Company, September, 1964.

11. Ibid, Part II, September 1965.

12. Dugger, G. L., "Comparison of Hypersonic Ramjet Engines With Subsonic and Supersonic Combustion. Combustion and Propulsion - Fourth AGARD Colloquim", pp. 84-109, Pergamon Press, 1961.

13. Hesse, W. J. and Mumford, N. V. S., "Jet Propulsion for Aerospace Applications", pp. 382-406, Pitman Publishing Corp., 1964.

14. Kays, W. M., "Convection Heat and Mass Transfer" (Preliminary Printing), Stanford University.

15. Keenan, J. H. and Kaye, J., "Gas Tables", John Wiley and Sons., Inc., 1961.

16. "Vaporizing and Endothermic Fuels for Advanced Engine Application", Technical Documentary Report AFAPL-TR-67-114, Part II, Contract No. AF 33(615)-3789, Shell Development Company, September 1968.

17. Weber, R. J. and MacKay, J. G., "An Analysis of Ramjet Engines Using Supersonic Combustion", NACA TN4386, Washington, September 1958.

18. "Vaporizing and Endothermic Fuels for Advanced Engine Application", Technical Documentary Report AFAPL-TR-67-114, Part I. Contract No. AF 33(615)-3789, Shell Development Company, October 1967.

REFERENCES (Contd-1)

19. "Vaporizing and Endothermic Fuels for Advanced Engine Application", Technical Documentary Report No. APL-TDR-64-100, Part III. Contract No. AF 33(657)-11096, Shell Development Company, September 1966.

20. Fabuss, B. M. et al, "Research on the Mechanism of Thermal Decomposition of Hydrocarbon Fuels", ASD-TDR 63-102, Part II, Contract No. AF 33(647)-8193, Monsanto Research Corp., October 1964.

21. Satterfield, C. N. and Sherwood, T. K., "The Role of Diffusion in Catalysis", Wesley-Addison Publishing Company, Reading, Massachusetts, 1963.

22. Wheeler, A., "Advances in Catalysis. III", 250, Academic Press. New York, 1951.

23. Spenadel, L. and Boudart, M., J. Phys. Chem. 64, 204 (1960).

24. Burggraf, F. and Shayeson, M., "A New Small-Scale Method for Measuring Fuel Thermal Stability", Paper presented to International Automotive Engineering Congress, Detroit, Michigan, January 11-15-, 1965.

25. Shayeson, M. W., "Thermal Stability Measurements of Fuels for the U.S. Supersonic Transport Engine", General Electric Company, Paper presented at the ASME 14th Annual International Gas Turbine Conference and Product Show, March 9-13, 1969, Cleveland, Ohio.

26. Personal communication from Al Hundere to A. C. Nixon.

27. Whisman, M. L. and Ward, C. C., Storage Stability of High Temperature Fuels, Part II, "The Effect of Storage Upon Thermally Induced Deposition of Labeled Fuel Components", Technical Report AFAPL-TR-68-32, Part II, March 1969.

28. Knudsen, J. G. and Katz, D. L., "Fluid Dynamics and Heat Transfer", pp. 394-395, McGraw-Hill, New York, 1958.

29. Redlich, O., Ackerman, F. J., Gunn, R. D., Jacobson, M., and Lau, S., Ind. Eng. Chem. Fundamentals 4, 369 (1965).

30. Redlich, O. and Kwong, J. M. S., Chem. Rev. 44, 233 (1949).

31. Rihani, D. N. and Doraiswamy, L. K., Ind. Eng. Chem. Fundamentals 4, 17 (1965).

32. Lundberg, G. W., Technical Information Record No. 155, Shell Development Company, Emeryville (Feburary 1968).

33. Stiel, L. I. and Thodos, G., A.I.Ch.E. J. 7, 611 (1961).

34. Stiel, L. I. and Thodos, G., A.I.Ch.E. J. 8, 229 (1962).

REFERENCES (Contd-2)

35. Jossi, J. A., Stiel, L. I., and Thodos, G., A.I.Ch.E. J. 8, 59 (1962).

36. Stiel, L. I. and Thodos, A.I.Ch.E. J. 10, 275 (1964).

37. Stiel, L. I. and Thodos, G., A.I.Ch.E. J. 10. 26 (1964).

38. Frost, A. A. and Kalkwarf, D. R., J. Chem. Phys. 21, 264 (1953).

39. Gambill, W. R., Chem. Eng. 64, 12, 261 (1957).

40. Gambill, W. R., Chem. Eng. 65, 1, 159 (1958).

41. Watson, K. M., Ind. Eng. Chem. 35, 398 (1943).

42. Chen, N. H., J. Chem. Eng. Data 10, 207 (1965).

43. Bradford, M. L. and Thodos, G., Can. J. Chem. Eng. 46, 277 (1968).

44. Girifalco, L. A., J. Chem. Phys. 23, 2446 (1955).

45. Robbins, L. A. and Kingrea, C. L., Hydrocarbon Processing and Petrol. Refiner. 41, 5, 133 (1962).

46. Barnett, Henry C. and Hibbard, Robert R., "Properties of Aircraft Fuels", Technical Note 3276, National Advisory Committee for Aeronautics, Lewis Flight Propulsion Laboratory, Cleveland, Ohio (August, 1956).

47. The Associated Factory Mutual Fire Insurance Companies, "Properties of Flammable Liquids, Gases and Solids", Ind. Eng. Chem., 32, No. 6, June, 1940, pp. 880-884.

48. Jackson, Joseph L., "Spontaneous Ignition Temperatures of Pure Hydrocarbons and Commercial Fluids", NACA RM E50J10, 1950.

49. Dunstan, Nash, Brooks, and Tizard, "Science of Petroleum", Vol. IV, pp. 2970-5, Oxford, England, Oxford University Press, 1938.

50. Bradley, J. N., "Shock Tubes in Chemistry and Physics", John Wiley and Sons, Inc., New York, 1962.

51. Emrich, R. J. and Wheeler, D. B., Jr., "Wall Effects in Shock Tube Flow", Physics of Fluids 1, 14 (1958).

52. Levinson, G. S., "High-Temperature Preflame Reactions of n-Heptane", Combustion and Flame 9(1), 63 (1965).

53. Orr, C. R., "Combustion of Hydrocarbon Behind a Shock Wave", 9th Symposium on Combustion, Cornell U., Aug. 1962, p. 1034, Academic Press, New York.

REFERENCES (Contd-3)

54. Nixon, A. C. and Henderson, H. T., "Thermal Stability of Endothermic Heat-Sink Fuels", I and EC Product Research and Development, 5, March, 1966, pp. 87-92.

55. Schirmer, R. M., "Morphology of Deposits in Aircraft Fuel Systems, Phillips Petroleum Company Research Division Report 5029-68R, August, 1968.

56. Rhodes, J. R., "Composition and Coating Thickness Testing Using Radioisotope Techniques", AERE-R4457 (1963).

57. Clayton, C. G. and Cameron, J. F., "A Review of the Design and Application of Radioisotope Instruments in Industry", IAEA Symposium on Radioisotope Instruments in Industry and Geophysics, Warsaw, 1965.

58. Tittle, C. W., "How to Compute Absorption and Backscattering of Beta Rays", Nuclear Chicago Corp., Technical Bulletin No. 8, 1960.